Efficacy of Clonal Progenitor Cells from Dental Pulp and Bone Marrow to Regenerate Craniofacial Mineralised Tissue Structures

A Thesis Completed in Fulfilment of the Requirements for the Degree of

Doctor of Philosophy (PhD)

Cardiff University

2014

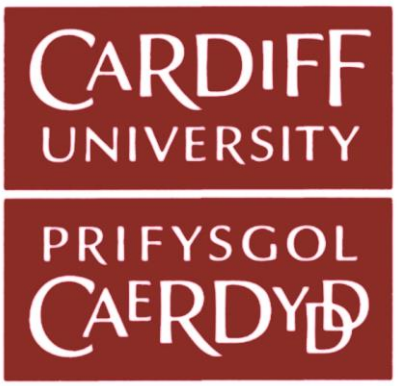

Jodie Harrington, BSc Hons, PGCert

Tissue Engineering and Reparative Dentistry

School of Dentistry

Cardiff University

Wales, UK

"You never really understand a person until you consider things from his point of view... Until you climb into his skin and walk around in it."

spoken by Atticus Finch

written by Harper Lee, To Kill a Mockingbird

Acknowledgments

To my principal supervisor, Professor Rachel Waddington, I sincerely appreciate your advice, guidance and feedback, which provided me with a foundation to develop as a researcher. To Professor Alastair Sloan, for his guidance and insightful contributions to my PhD project. You both provided the opportunities that spurred and enabled the completion of this thesis. And to the Medical Research Council (MRC) who afforded me with a Capacity Building Studentship to begin my postgraduate studies and research career.

Praise goes to all technical staff of the Tissue Engineering and Reparative Dentistry Theme, who every day share their knowledge and skill, which propagates lab life and is often taken for granted. My gratitude goes to Dr Nafiseh Badiei, Swansea University Institute of Life Science, for her patience and expertise in scanning electron microscopy.

I would like to thank all Mineralised Tissue Group members, previous and present, for making the ‘team’ what it is, of which I am humbled to be a part: to John and Jess for their simultaneous entertainment and wisdom, Amr for being a supportive colleague and friend, Yati for lightening the PhD rollercoaster ride, Abeer for ensuring I am well and fed, and Fraser and Rachel who alongside myself experienced the “joys” of tissue culture life!

My friends Sarah ‘Diffy’, and Carly ‘Patsy’, for all the years, fun times and sad times, I hope your love and understanding for me is as much returned to you.

And Kelly ‘Dudette’, for all the Undergraduate, PhD, and life stories we’ve shared, they will never be forgotten and always treasured.

I also want to remember a friend passed, Ashley Ducey; who knew what was held for our little selves or where our souls would travel. May the journey continue, until we meet once again.

My Aunt and Uncle, Tess and Bill Herbert, your constant solidarity for me in all that I have done cannot be repaid. For your love and help (food, car wash, and University digs moving), and open home for me, even when unannounced, I am truly blessed.

To all other friends and family, and others unnamed, I am thankful for you being a part of my life and shaping my person.

By no means least, I am eternally grateful to my mum and dad, Ann and Gerald Harrington, for the numerous ways that they have encouraged me in all that I have done. I honour and dedicate this thesis to them both, who have no boundaries to their love and support, patience and understanding; particularly on those occasions when I was late or even absent due to beckoning lab commitments. This thesis surely would not have been possible without you both, and is as much your achievement as mine.

Awards and Publications

Chapters 3 and 4 have been presented and awarded, and accepted for publication:

2012 **Cardiff Institute of Tissue Engineering and Repair, Best Poster**

http://www.cardiff.ac.uk/citer/%5bhidden%5dresources/CITER%20News%2020th%20Edition%20March%202013.pdf

2014 **Quantification of Clonal Heterogeneity of Mesenchymal Progenitor Cells in Dental Pulp and Bone Marrow**

Connective Tissue Research Journal (Harrington et al., 2014).

Summary

The current clinical choice for bone regeneration is autologous bone grafts from the iliac crest. The associated drawbacks, however, in terms of morbidity and low cell number following tissue harvest, have led to search for alternative stromal cell sources in conjunction with native tissue matrix components. For mineralised tissue engineering, alternative to mesenchymal bone marrow stromal cells (BMSCs), mesenchymal dental pulp stromal cells (DPSCs) have been proposed due to high colony formation and differentiation potential. Understanding which stromal population is exemplar for rapid and effective regeneration is paramount, and central to efficient bone regeneration is providing the optimal microenvironment to the characterised stem cells.

This thesis compared clonal BMSCs that formed few and large colonies, with DPSCs that formed many small colonies. Comparison of clonal differentiation along adipogenesis, chondrogenesis, with particular attention on their capacity for osteogenic formation, showed BMSCs were multipotent, while DPSCs only displayed uni- and bi- potency (osteogenic inclusive). Neither VCAM1 nor MCAM mesenchymal marker expression related to differentiation capacity.

Stromal clones exposed to whole-protein tissue matrix extracts from bone (BME) and tooth (TME), found *in vitro* mineralisation by BMSCs and DPSCs with TME, but mineralisation by DPSCs only with BME. BMSC and DPSC clones were also assessed on bone- and tooth- slabs to replicate *in vivo* injury of fracture and caries, respectively. BMSCs and DPSCs displayed proliferation and differentiation on tissue-slabs, but BMSCs did not attach to tooth-slab, which was probable of tissue differences in supportive extracellular proteins.

In summary, results indicated BMSCs are more primitive stromal cells closely related to the mother stem cell, while DPSCs are more lineage committed and are suggestive of transit-amplifying cells; indicative of their *in vivo* roles, that is, bone is remodeled constantly and tooth responds to injury only. While much research is still required, DPSCs and their matrix-proteins potentially offer an easily accessible and viable alternative for craniofacial bone reconstruction.

Abbreviations

AcOH	Acetic acid
ACS	American Chemical Society
ASC/SSC	Adult/Somatic Stem Cell
BAG-75	Bone-Acidic Glycoprotein-75
BCA	Bicinchoninic Acid
BME	Bone Matrix Extract
BMP	Bone Morphogenic Protein
BMSC	Bone Marrow Stromal Cell
BSA	Bovine Serum Albumin
BSP	Bone Sialoprotein
Ca^{2+}	Calcium
CBFA1	Core Binding Factor Alpha1 subunit protein (AKA RUNX2)
CD	Cluster of Differentiation
CDK	Cyclin-Dependent Kinase
cDNA	Complementary DNA
C/EBPα	CCAAT/Enhancer Binding Protein (C/EBP), alpha
CFE	Colony Forming Efficiency
CFU-F	Colony-Forming Unit-Fibroblastic
CO_2	Carbon Dioxide
Ct	Cross Threshold
ddH_2O	Double Distilled Water
DAPI	4',6-Diamidino-2-Phenylindole
DFPC	Dental Follicle Progenitor Cell
DMP1	Dentin Matrix Protein-1
DMSO	Dimethyl Sulfoxide
DNA	Deoxyribonucleic Acid
dNTP	Deoxyribonucleotide Triphosphate
DPP	Dentin Phosphoprotein
DPSC	Dental Pulp Stromal Cell
DSP	Dentin Sialoprotein
DSPP	Dentin Sialophosphoprotein

ECM	Extracellular Matrix
EDTA	Ethylenediaminetetraacetic acid
EGF	Epidermal Growth Factor
EGFR	Epidermal Growth Factor Receptor
ERK	Extracellular signal-Regulated Kinase
ESC	Embryonic Stem Cell
FABP4	Fatty Acid Binding Protein 4
FAK	Focal Adhesion Kinase
FGF	Fibroblast Growth Factor
FGFR	Fibroblast Growth Factor Receptor
FITC	Fluorescein Isothiocyanate
FZD	Frizzled
GAG	Glycosaminoglycan
GFAP	Glial Fibrillary Acidic Protein
GSM	Germ Stem Cell
H_2O_2	Hydrogen Peroxide
H&E	Haematoxylin and Eosin
HCl	Hydrochloric acid
HLA	Human Leukocyte Antigen
HMDS	Hexamethyldisilazane
HRP	Horseradish Peroxidase
IBMX	3-isobutyl-1-methylxanthine
IDPSC	Immature Dental Pulp Stem Cell
IFNγ	Interferon Gamma
IGF	Insulin-like Growth Factor
IGFBP	Insulin-like Growth Factor Binding Protein
IGFR	Insulin-like Growth Factor Receptor
IL	Interleukin
ISCT	International Society for Cellular Therapy
LPL	Lipoprotein Lipase
LRP	Low-density Lipoprotein Receptor-related Protein
MAPK	Mitogen-Activated Protein Kinase
MCAM	Melanoma Cell Adhesion Molecule

Mg^{2+}	Magnesium
MHC	Myosin Heavy Chain
MMP	Matrix Metalloproteinase
MSC	Mesenchymal Stromal Cell
MSX	Msh Homeobox
MTT	Thiazolyl Blue Tetrazolium Blue
NaOH	Sodium Hydroxide
NF	Neurofilament
PAGE	Polyacrylamide Gel Electrophoresis
Pax	Paired box
PBS	Phosphate Buffered Saline
PCNA	Proliferating Cell Nuclear Antigen
PCR	Polymerase Chain Reaction
PDGF	Platelet Derived Growth Factor
PDL	Population Doubling Level
PDLSC	Periodontal Ligament Stem Cell
PI3K	Phosphoinositide 3-kinase
PPARγ	Peroxisome Proliferator-Activated Receptor gamma
PG	Proteoglycan
PTPRC	Protein Tyrosine Phosphatase, Receptor type, C
qPCR	Quantitative Polymerase Chain Reaction
RNA	Ribonucleic Acid
RT	Reverse Transcription
RUNX2	Runt-related transcription factor 2 (AKA CBFA1)
SCAP	Stem Cell from Apical Papilla
SDS	Sodium Dodecyl Sulphate
SE_{mean}	Standard Error (of the mean)
SEM	Scanning Electron Microscopy
SHED	Stem Cells from Human Exfoliated Deciduous Teeth
SLRP	Small Leucine-Rich Proteoglycan
SM	Smooth Muscle
SMAD	SMA and MAD Related Family
SOX2	SRY (Sex Determining Region Y)-box 2

Spp1	Secreted phosphoprotein 1
TA	Transit-Amplifying
TBS	Tris Buffered Saline
TGFβ	Transforming Growth Factor β
TLR	Toll-like Receptor
TMB	3,3',5,5'-Tetramethylbenzidine
TME	Tooth Matrix Extract
TNF	Tumour Necrosis Factor
UV	Ultra Violet
VCAM1	Vascular Cell Adhesion Molecule 1
WISP1	WNT1-induced Signalling Protein 1
Wnts	Wingless

Units of Measurement

%	Percentage
bp	Base Pairs
°C	Degrees Celsius
Cm	Centimetre
cm^2	Centimetres squared
g	Gravitational Acceleration
M	Mole
mA	Milliampere
mb	Millibar
mg	Milligram
mL	Millilitre
mm	Millimetre
mM	Millimole
nm	Nanometre
µg	Microgram
µL	Microlitre
µM	Micromole
rpm	Revolutions Per Minute

v/v	Volume/Volume
w/v	Weight/Volume

Contents

Chapter 1

Background Introduction

Within the literature, the term stem cell is often used incorrectly for adult mesenchymal cells, which should be referred to as stromal cells (Horwitz et al., 2005) until they have been fully characterized by colony unit formation, surface marker expression, proliferation capacity, and differentiation potential (Dominici et al., 2006). Within the adult, mesenchymal stromal cells have two key characteristics of self-renewal and multi-differentiation potency, and serve to replace tissues during normal homeostasis or cells lost following injury (Hombach-Klonisch et al., 2008). Mesenchymal stromal cells are a vital tool in the fields of tissue engineering and regenerative medicine, as well as wound healing, and as such would enhance repair of craniofacial tissues and significantly benefit current clinical treatments for dental/periodontal disease, paradontopathies, malformations, trauma, and post cancer, which is lacking (Miura et al., 2006). The use of stromal cells in conjunction with an appropriate bio-scaffold is seen as the future for regenerative medicine and thus it is paramount to understand the intimate relationship that stromal cells share with their niche microenvironment.

Mesenchymal bone marrow stromal cells (BMSCs) are the “gold standard” tissue source for regenerative medicine, against which other mesenchymal stromal cells are compared due to their colony formation, proliferation, and differentiation abilities (Prockop, 1997, Pittenger et al., 1999, Gronthos et al., 2003). Bone marrow stromal cells can differentiate along multiple lineages that

typically include osteogenic, chondrogenic, and adipogenic, and in addition myelosupportive stroma, myogenic, and neurogenic lines. There are complications, however, associated with obtaining bone marrow stromal cells, such as pain and secondary-morbidity at collection site following the procedure, and a low harvest number of cells (Huang et al., 2009). As such, it is becoming increasingly apt to find an alternative tissue source, and understanding what stromal cell population is best suited to bring about rapid and effective regeneration of several related tissues is a major issue. Dental pulp stromal cells (DPSC) were first isolated and introduced as a potential source for tissue engineering by Gronthos *et al.*, 2000. Mesenchymal DPSCs are proposed as a viable option due to their adherence to culture plastic, expression of mesenchymal markers, and ability to form multiple cell lineages *in vivo* and tissue like structures *ex vivo* (Gronthos et al., 2000, Gronthos et al., 2002), which satisfied the minimal criteria for mesenchymal stromal cells (Dominici et al., 2006) (see Adult Mesenchymal Stromal Cells). In addition, the growth factors and genes that influence osteogenesis were also evident in contributing to odontogenesis, which suggests that despite the distinct origins of these mesenchymal stromal cells (Komada et al., 2012), they share similar molecular pathways involved in proliferation and differentiation (Shi et al., 2001).

Extensive research has focused on growth factors to promote bone formation *e.g.* bone morphogenic proteins (BMPs), but costly supra-physiological levels are required for clinical use (Fan et al., 2013a). The extracellular matrix is hypothesised to regulate niche signalling by provision, storage and/or

compartmentalisation of growth factors and cytokines that are indispensable for both cell proliferation and differentiation (Riquelme et al., 2008). The proteoglycans decorin and biglycan belong to the small-leucine rich protein (SLRP) family and play important roles in the development of osteoid. Biglycan and decorin are conjugated to dermatan sulphate or chondroitin sulphate glycosaminoglycans, with two and one glycosaminoglycan chains respectively (Mecham, 2001). During bone formation, dermatan sulphated biglycan was present during phases of proliferation and differentiation, and chondroitin sulphated biglycan was present at onset of mineralisation (Waddington et al., 2003b). Within the tooth, dermatan sulphated decorin was associated with early matrix deposition and maturation, while chondroitin sulphated decorin presents during matrix mineralisation (Waddington et al., 2003a). Moreover biglycan was implicated as a coregulator of growth factors such as FGF2 (Hou et al., 2007) and TGFβ (Chen et al., 2002), which are important factors for progenitor proliferation and mineralisation. As such, we have specific interest in the influence of extracellular matrix proteins on stromal cell proliferation, and differentiation, with particular attention to osteogenic capacity. Here, *in vitro* bone formation of stromal cells within 2-Dimensional *in vitro* cultures to assess the role of extracellular matrix proteins in controlling stem cell behaviour, with a view to producing novel bioactive scaffolds. As in conjunction with the stromal cells, a bio-scaffold can act as a matrix where cells can adhere and reside by mimicking the native niche microenvironment, and importantly the matrix protein itself influences the behaviour of unspecialised and non-differentiated stromal cells.

In this thesis, the focus was to compare the properties of bone marrow and dental pulp stromal cells. For each source, the proliferative capacity and gene expression will be characterised. The differentiation potential of clonal populations will be analysed along the lineages of adipocytes, chondrocytes, and osteocytes. Clonal populations will be observed in the presence of extracellular matrix proteins and within a 2-Dimensional culture tissue-slab model, to investigate the novel role and influence that extracellular matrix proteins have on stromal cell proliferation and osteogenic differentiation. Thus, the goal is to increase understanding of how the niche microenvironment controls stromal cell survival, proliferation, and differentiation, and whether the dental pulp can prove an alternative source for cell-based tissue engineering.

Stem Cell Overview

Within the literature, it is has been highlighted that the use of the terms ‘stem’ and ‘progenitor’ cells are often inter-changed and the rigorous definitions abandoned. Emphasis of such classification, underscores the need for repeated culture-assays to continuously assess cells for ‘stem’ and ‘progenitor’ criteria (Seaberg and van der Kooy, 2003), which may not be practically feasible. To this end, a simplistic definition of a stem cell (“mother”) would be having unlimited self-renewal capacity and multi-potent differentiation ability, and a progenitor cell (“progeny”) as having limited proliferation and potency *i.e.* restricted differentiation potential (Pittenger et al., 1999). In addition, stromal cells are often termed progenitors, before they have been characterised and classified as stem cells. Stem cells are unique cells with two essential characteristics of self-renewal and potency. Self-renewal is the

generation of an identical daughter cell and occurs either by symmetric or asymmetric division. Symmetric division produces two identical daughter cells. Whereas asymmetric division produces one cell identical to the first and another, more differentiated daughter cell. As such, the self-renewal of stem cells can occur at a single cell or progeny population level to maintain the stem cell population (Spradling et al., 2001). Stem cell potency refers to the ability of stem cells to produce diverse cell types *via* differentiation, and as a result generate tissues and organs (Sell, 2004). In humans, there are four main classes of stem cell potency: 'totipotent' or 'omnipotent' cells differentiate into a range of cells that are present in all tissues, but are limited to blastomeres of the early-stage morula and consequently differentiation capacity is difficult to prove experimentally. 'Pluripotent' cells differentiate into a range of phenotypes across several tissues *e.g.* embryonic stem cells. 'Multipotent' cells differentiate into a range of phenotypes only within a specific tissue *e.g.* the haematopoietic system. 'Oligopotent' cells differentiate into a few descendent phenotypes e.g. lymphoid or myeloid cells. Finally, 'unipotent' cells only differentiate into its own closely related phenotype within a single tissue *e.g.* fibroblast cells (Knoepffler et al., 2007).

Stem cells are present during development, but also throughout adulthood, reserved for when the body experiences damage and requires repair, or during normal cell replacement as part of homeostasis. There are three main classes of stem cell: germ stem cell (GSM), embryonic stem cell (ESC), and adult/somatic stem cell (ASC/SSC). As such, stem cells in the adult are referred to as progenitors, or an intermediate precursor, in order to refrain from

the more generic term or entity ‘stem cell’ that can imply pluripotent embryonic stem cells (Fuchs et al., 2004). As cells responsible for repair, this thesis will focus on adult stromal cell progenitors. Within many different organs of the body *e.g.* bone marrow, brain, and liver, stromal cells infrequently divide to generate transient-amplifying cells, which act to divide and rapidly expand cell numbers to produce more mature progeny (Reya et al., 2001). In adults, the hierarchical division and differentiation of stem cell progenitors permits amplification of mature cell numbers from a single progenitor (figure 1.1) and minimises possible DNA replication mutations in the genome of these long-lived cells (Reya et al., 2001, Riquelme et al., 2008).

Adult Mesenchymal Stromal Cells

Adult progenitors are found in tissues of the bone marrow, the blood stream, cornea and retina, dental pulp, blood vessels, skeletal muscle, liver, skin, gastrointestinal tract, pancreas, spinal cord and brain (Sell, 2004), but this list is not an exhaustive one. Adult progenitors are self-renewing, clonogenic, are multipotent or pluripotent in nature, and show characteristics of plasticity, although it is unclear by which process this occurs *e.g*. de-differentiation, trans-differentiation, epigenetic factors, and/or cell fusion. In addition, the use of adult progenitors for tissue regenerative medicine overcomes ethical and tumorigenic issues associated with embryonic stem cells, and immuno-rejection problems by sourcing cells from the patient themselves (Hombach-Klonisch et al., 2008).

Adult progenitors are cells known as mesenchymal stromal cells that have enormous therapeutic potential, which has generated considerable interest throughout the biomedical disciplines for use in tissue engineering medicine. Due to the varied tissue sources and different methodologies used for isolation, expansion, and characterisation of mesenchymal stem cells, it is sometimes difficult to directly compare and contrast studies in the field of stem cell science. To address this issue the International Society for Cellular Therapy (ISCT) reported “minimal criteria” to define mesenchymal stem cells because of inconsistent definitions used among investigators, which is crucial to ensure progress in human cell therapy (Dominici et al., 2006). From the report, the Mesenchymal and Tissue Stem Cell Committee of the ISCT proposed three criteria to define human mesenchymal stem cells used in laboratory-based investigations, and recognise that standards may need revision as new data arise. Briefly, the three criteria proposed are adherence to plastic, expression of specific surface antigens, and multipotent differentiation. Although it is recognised that recommendations may not apply in non-human systems, as other species antigen expression is not entirely characterised, the criteria are a standard on which mesenchymal stem cells should be based. The first criterion is that mesenchymal stem cells must be plastic-adherent when being maintained with standard culture conditions in tissue culture flasks. The adherence of mesenchymal stem cells to plastic is a well described property (Colter et al., 2000), and while they can be maintained without adherence using highly specific culture conditions (Baksh et al., 2003), these cells would need to demonstrate adherence to be considered as true mesenchymal stem cells. The second criterion states ≥95% of the

mesenchymal stem cell population should express specific surface antigens CD73 (an ecto 5' nucleotidase), CD90 (Thy-1), and CD105 (endoglin), as measured using flow cytometry. There is recognition however, that there are a vast number of other mesenchymal markers. In addition, cells should lack expression or be ≤2% positive for haematopoietic antigens CD45 (pan-leukocyte marker), CD34 (endothelial cells and primitive haematopoietic progenitors), CD14 or CD11b (both for monocytes and macrophages), CD79α or CD19 (B-cell markers) and HLA class II (human leukocyte antigen that can be expressed by mesenchymal stem cells when stimulated with IFNγ, interferon gamma). Only one out of two markers for macrophages and B-cells need to be tested. For the third and final criterion, mesenchymal stem cells must be capable of differentiating into osteoblasts, chondroblasts, and adipocytes, using *in vitro* differentiating conditions from standard published protocols or even commercially available kits. Osteoblast differentiation is demonstrated using alizarin red to detect calcium deposits, or von Kossa staining to quantify mineralisation. Chondroblast differentiation can be shown by alcian blue staining for glycoproteins or immunohistochemical detection of collagen type II. While Oil Red O staining for lipids can demonstrate adipocyte differentiation most readily. Abiding by the minimal set of criteria stated above allows for uniform characterisation of mesenchymal stromal cells and facilitation of more direct comparisons within the scientific literature (Dominici et al., 2006), that can lead to defining tissue sources are harbouring true stem cells for regenerative medicine.

Mesenchymal Bone Marrow Stromal Cells

Mesenchymal stromal cells are found in many tissues throughout the adult body, and follows from early works by German pathologist Cohnheim, who studied wound repair in the 1860s. The initial discovery of clonogenic fibroblast precursors, CFU-F (Colony-Forming Unit-Fibroblastic), was in bone marrow, spleen and thymus of adult mice (Friedenstein et al., 1976), and were subsequently characterised in human bone marrow as fibroblast colony-forming cells (Castro-Malaspina et al., 1980). These bone marrow CFU-F cells became later referred to as mesenchymal stem cells or marrow stromal cells (MSCs), in order to be distinguished as non-haematopoietic tissue stem cells (Prockop, 1997). Bone marrow mesenchymal stem cells are the most studied cells of mesenchymal origin, and are found in long bones along with haematopoietic stem cells, and endothelial stem cells. BMSCs are the “gold standard” for tissue engineering medicine and against which other mesenchymal stem cell populations are characterised (Pittenger et al., 1999, Gronthos et al., 2003). The repertoire of mitogenic factors required for bone marrow progenitor proliferation is not entirely known, but those known to be important are PDGF, EGF, FGF2, TGFβ, and IGF1 (Bianco et al., 2001). Bone is a large repository of many growth factors that provides a rich microenvironment for the cells contained within (Kamura et al., 2010). The extracellular matrix serves as a reservoir for growth factors by presenting extracellular binding molecules, as with FGF2 (Brunner et al., 1993). The turnover of bone involves numerous cytokines and chemokines that are released during remodelling as a means for osteoblast and osteoclast communication. In addition, the specialised microvasculature of the bone

marrow allows for ease of cells to pass in and out of blood (Bussard et al., 2008).

BMSCs have a great ability for *ex vivo* expansion up to approximately 40 population doublings before senescence occurs, which is not a state of terminal differentiation because cells remain capable of osteogenic differentiation (Bruder et al., 1997). An array of cell surface markers have been observed for bone marrow progenitors, which include STRO-1 (bone marrow stromal cell and erythroid precursor marker), CD73, CD90, CD105, CD146 (MCAM), Oct4 and Nanog (pluripotent stem cell markers). Bone marrow progenitors are absent for CD14, CD34, CD45, and HLA-DR. BMSCs were highlighted as a population of heterogeneous cells with different morphologies, and gene and protein expression profiles (Huang et al., 2009). Compared to heterogeneous cell populations, purified clonal populations are reported to only undergo proliferation of >20 population doublings in a small proportion of clones (Gronthos et al., 2003). The heterogeneity in morphology, function, and growth of bone marrow cells is evidence of the difficulty in identifying a phenotypic fingerprint of mesenchymal stromal cells (Bianco et al., 2001) and supports the notion of stromal hierarchy due to limited potential of some CFUs where others show multipotent differentiation (Owen and Friedenstein, 1988). Within the mesenchymal stem cell field, it is well known that bone marrow stromal cells can differentiate along multiple lineages that typically include osteogenic, chondrogenic and adipogenic, and in addition myelosupportive stroma, myogenic, and neurogenic lines. There are complications, however, associated with obtaining bone marrow stromal cells, such as pain and

secondary-morbidity at collection site following the procedure, and a low harvest number of cells, and as a result alternative sources of mesenchymal stem cells have been sought after (Huang et al., 2009). One such source that has attracted much attention is mesenchymal dental pulp stromal cells (DPSCs), which is discarded as biomedical waste following tooth extraction. Dental pulp stromal cells were first identified from human adult dental pulp and compared to bone marrow stromal cells *in vitro* and *in vivo* by Gronthos *et al*., 2000.

Mesenchymal Dental Pulp Stromal Cells

Dental tissue is specialised and the mineralised matrices of enamel and dentin do not undergo continuous remodelling as does bone tissue. Bone remodels slowly throughout post-natal life, and may indicate that dental stromal cells have restricted differentiation potency compared to bone marrow stromal cells (Gronthos et al., 2000). Dentin is formed by odontoblasts that differentiate from the ectomesenchymal cells of the dental papilla that later becomes the pulp, following interaction with epithelial cells of the inner enamel organ, during a process known as dentinogenesis. Odontoblasts are of neural crest origin that are recognized morphologically as tall columnar cells with an eccentric nucleus and long processes that align at the outer edge and throughout the dentin. Odontoblasts produce an organic matrix that subsequently becomes mineralised (Ten Cate, 1994). The formation of enamel is by ameloblasts and is known as amelogenesis, which is induced by dentinogenesis. Ameloblasts are of ectodermal origin, which differentiate from the inner dental epithelium following elongation and polarization (Ten Cate, 1994) (figure 1.2). So dental

stromal cells are responsible for forming the special mineralised matrices that constitute the tooth (Gronthos et al., 2000). Although progenitors do not remodel the tooth, cells present in the adult pulpal tissue induce reparative dentin to form a loosely organised mineralised matrix to serve as a protective barrier for dental pulp following trauma from mechanical damage, chemicals or disease processes (Smith et al., 1995). The dental mesenchyme is referred to as ectomesenchyme due to its early developmental association with neural crest cells (Lumsden, 1988) that are a group of multipotent cells that derive from the ectoderm, which are collectively responsible for forming epidermal tissues and the nervous system during embryogenesis. As such, dental stromal cells are proposed to have greater potential for differentiating along a neural lineage compared to other mesenchymal stromal cells (Huang et al., 2009).

The clonogenic capacity of dental pulp stromal cells was first recognised by Gronthos *et al*., 2000 who found the colony-forming efficiency and proliferation rate of dental pulp was higher than whole-bone marrow progenitors. The report states, however, that colony forming efficiency of bone marrow progenitors devoid from haematopoietic cells was 10-fold higher than whole-bone marrow and thus is fairly equivalent to dental pulp progenitors, but they did not publish these data. In addition, the report finds the cell surface and protein marker phenotypes of dental pulp and bone marrow stromal cells was quite similar and indicated that both are heterogeneous cell populations. Some of the markers present were CD44, integrin β1, VCAM1, collagen types I and III, osteonectin, and FGF2, in all cell populations, while αSM actin, MCAM, Spp1

(osteopontin), and alkaline phosphatase were in a subset of the heterogeneous population. Exceptions were osteocalcin that was present in all dental pulp cells but only in a subset of bone marrow cells, and BSP that was not present in dental pulp but was present in a subset of cells in bone marrow. Absent markers included CD14, CD34, CD45, MYOD, neurofilament, collagen-II, and PPARγ (Gronthos et al., 2000), which comprised a set of minimal criteria markers for defining mesenchymal stromal cells (Dominici et al., 2006). In addition, odontoblast marker DSPP was absent in dental pulp stromal cells, which suggested they had an undifferentiated phenotype (Gronthos et al., 2000). Bone marrow stromal cells also demonstrated low level presence of dentin markers DSPP and DSP (Qin et al., 2002). In addition to dental pulp stromal cells (DPSC), other so-termed dental progenitors include stem cells from human exfoliated deciduous teeth (SHED) (Miura et al., 2003), periodontal ligament stem cells (PDLSCs) (Seo et al., 2004), stem cells from apical papilla (SCAP) (Sonoyama et al., 2006), and dental follicle progenitor cells (DFPCS) (Morsczeck et al., 2005). Similar to other post-natal stromal cells, these cell populations display mesenchymal stem cell properties, which include self-renewal and multi-lineage differentiation similar to that of bone marrow mesenchymal stromal cells (Huang et al., 2009).

Bone Marrow and Dental Pulp Mesenchymal Stromal Cells Control Extracellular Matrix Production

At *in vitro* level, a heterogeneous DPSC population can differentiate into osteocytes, chondrocytes, adipocytes, neurocytes, and myocytes, like that attributed to BMSCs (Huang et al., 2009). High-level alizarin red-positive

calcium nodules were reported to demonstrate osteoblast differentiation of heterogeneous DPSCs but deposits were sparse throughout a single mineralised layer, in contrast to BMSCs that formed calcified deposits within extensive sheets of adherent cells (Gronthos et al., 2000). Differentiation of DPSCs to adipocytes correlated with expression of the early adipogenic marker PPARγ2 and late adipogenic marker lipoprotein lipase, and DPSC-derived neurocytes expressed neural precursor marker nestin and GFAP (Gronthos et al., 2002). Myogenic differentiation gave elongated myoblast-like phenotype but no multinucleate cells, and demonstrated presence of early myocyte marker MYOD1 and the late differentiation marker MHC (Zhang et al., 2006). Myogenic fusion was possible, however, when human dental pulp was co-cultured with a murine myocyte line, C2C12, to form myotubes (Laino et al., 2006). Differentiation of BMSCs along the chondrogenic lineage was seen by alcian blue staining of cells among an organised extracellular matrix containing collagen-II and many sulphated proteoglycans (Zhang et al., 2006). It must be noted, however, that there were occasions when DPSCs failed to differentiate into adipocytes, chondrocytes, and myoblasts (Zhang et al., 2006). This failure was suggested to be due to the heterogeneous cell types that constituted the dental pulp, due to stem cell hierarchy, and also because *in vitro* culture systems do not offer an architectural tissue model to determine complete developmental potential and formation (Gronthos et al., 2000).

When a human heterogeneous DPSC population was expanded *ex vivo* and transplanted *in vivo* with HA/TCP (hydroxyapatite/tricalcium phosphate) powder into immunocompromised mice, dentin and pulp-like structures

formed. The dentin was akin to primary dentin, as opposed to the disorganised matrix that is characteristic of reparative dentin (Gronthos et al., 2000). The dentin structures comprised an ordered collagen matrix, predominantly collagen-I, perpendicular to a differentiated odontoblast-like layer of cells. Odontoblast-like cells extended cytoplasmic processes into a dentinal matrix that had an interface with a pulp-like tissue, which was infiltrate with blood vessels and nerve fibres, but they failed to produce active haematopoietic marrow and adipogenesis (Gronthos et al., 2000, Gronthos et al., 2002). In addition, the dentin laid down can thicken over time (Batouli et al., 2003). Corresponding BMSCs formed distinct lamellae bone on the HA/TCP conjugate surface with collagen fibres and differentiated osteoblasts aligning parallel to bone-forming surfaces, while differentiated osteocytes became entombed within bone matrix. In addition, the bone matrix surrounded interstitial tissue and was infiltrate with a sinusoid network that resembled a marrow-like organ, and unlike DPSCs, BMSCs showed areas of haematopoiesis and adipocyte accumulation (Gronthos et al., 2000, Gronthos et al., 2002). The formation of these organ-like structures, however, are chimeric tissues formed by dynamic and interactive processes between both the transplanted progenitor cells and host microenvironment (Batouli et al., 2003).

Heterogeneous multi-colonies stromal cells derived from deciduous teeth were capable of *ex vivo* expansion and have achieved >140 population doublings (Miura et al., 2003), whereas BMSCs achieved 30-45 population doublings (Bruder et al., 1997), and they showed consistent capacity for proliferation and

regeneration of dentin *in vivo* (Gronthos et al., 2000). The majority of single cell derived colonies/clones, *i.e.* 80%, was reported to only proliferate up to 20 population doublings. As such, only the approximate 20% of DPSCs that proliferated beyond 20 population doublings were able to be analysed for their *in vivo* developmental potential (Gronthos et al., 2002). The single-cell derived colonies that did proliferate beyond 20 population doublings were able to form *ex vivo* dentin-pulp like structures containing organised collagen fibres, similar to heterogeneous multi-colony derived DPSCs (Gronthos et al., 2000), but a third of single-cell clones only formed low to moderate amounts of dentin (Gronthos et al., 2002). This suggested DPSC have subset populations that differ in their ability for odontogenesis due to different proliferative capacities and developmental potentials, which was a property originally attributed to that of BMSCs (Owen and Friedenstein, 1988).

Regarding other tooth-associated stromal cells, SHED proliferated faster than DPSCs and BMSCs (SHED>DPSC>BMSC) (Huang et al., 2009) and showed a capacity of >140 population doublings (Miura et al., 2003). SHED have also been termed immature DPSCs (IDPSCs) following findings that cells expressed embryonic and pluripotent markers Oct4 and Nanog, and were positive for stage-specific embryonic antigens SSEA-3 and -4, and tumour recognition antigens TRA-1-60 and TRA-1-81 (Kerkis et al., 2006). Both SHED/IDPSC showed capacity for osteogenic, chondrogenic, adipogenic, neurogenic, myogenic, and odontogenic differentiation (Miura et al., 2003, Kerkis et al., 2006). SHED was positive for a variety of neural markers, and formed aggregate and sphere-like clusters, which in conjunction with high

proliferative capacity was analogous to neural stem cells. *In vivo* studies show SHED formed DSPP-positive odontoblast-like cells in association with a dentin-like structure, but did not form a dentin-pulp like complex (Miura et al., 2003). Stromal cells from deciduous teeth (SHED) and permanent teeth (DPSC) both demonstrated ability to differentiate into osteoblasts, chondrocytes and adipocytes (Govindasamy et al., 2010), which satisfied minimal mesenchymal stem cell requirements (Dominici et al., 2006). SHED exhibited greater capability to differentiate along osteogenic and adipogenic lineages and in addition were capable of forming odontoblasts and hepatocytes. Compared to DPSCs, the proliferation rate of SHED was higher and expression of pluripotent markers Oct4, SOX2 and Nanog was >2 fold higher, which suggested these cells are of more primitive origin. Conversely, DPSCs showed higher expression of neuroectoderm markers Pax6 and nestin, and higher neurosphere formation with better ability to form neuron-like cells expressing NF and GFAP. Both stromal cell types showed propensity for neuronal lineage, but SHED retained plasticity over the same amount of passages as DPSC, which lost plasticity and commited toward neuronal lineage (Govindasamy et al., 2010). As such, dental progenitors are mesenchymal stromal cells that share close origins with the neural crest, which probably relates to their higher neurogenic potency compared to bone marrow progenitors (Huang et al., 2009).

Gene Expression and Growth Factors of Mesenchymal Stromal Cells Influence Extracellular Matrix Production

The gene expression profiles of DPSCs and BMSCs were similar for >4000 genes, and among those encoded genes for collagen types III and V, non-collagenous components of the extracellular matrix (osteopontin, osteonectin, matrix gla-protein, decorin, biglycan, and alkaline phosphatase) and cell adhesion molecules (VCAM1, CD44, integrins β1, αv2, αv, and β3). These similarly expressed gene marker molecules are functionally associated with initiating mineralisation and bone homeostasis, and also influence dentinogenesis (Shi et al., 2001). The gene expression profiles were an accurate representation of those proteins detected by immunohistochemical analyses of pulp and marrow progenitors (Gronthos et al., 2000), which included growth factors implicated as strong osteogenic promoters and in mineralised matrix formation (IGF1, PDGF, FGF2, TGFβ, BMP2, BMP4, and BMP7) (Shi et al., 2001). Shi *et al*., 2001 also reported human dental pulp and bone marrow progenitors expressed low levels of two CBFA1 isotypes, CBFA1 type I and II, although it was unclear if the low levels represented that which was only expressed in a subset of the cell population. The transcription factor CBFA1 was a specific osteoblast regulatory molecule, but seemed to be an important factor for normal tooth development as CBFA1-null mice displayed arrested tooth development (D'Souza et al., 1999), in addition to lack of bone formation (Komori et al., 1997) and. Human CBFA1 gene mutations caused manifestation of cleidocranial dysplasia syndrome that was associated with skeletal abnormalities and delayed tooth development (Otto et al., 1997). Other transcription factors, MSX1 and MSX2, were expressed in dental pulp

and bone marrow progenitors at high and low levels respectively, and so the MSX gene family may act as regulators in odontogenesis and osteogenesis (Shi et al., 2001). Evidence of MSX regulation include phenotypic observations in MSX1-deficient mice and MSX1 human mutations of craniofacial abnormalities such as cleft palate and tooth development failure (Satokata and Maas, 1994), while MSX2-deficient mice showed delay in bone growth and ossification, concomitant with CBFA1 downregulation (Ducy, 2000). In addition, TGFβ signals controlled proliferation of chondrocytes and prevented premature cartilage/bone differentiation, and loss of TGFβ signals cause diminished MSX2 expression, but not MSX1. Specifically, the TGFβ2 isoform was suggested to mediate MSX2 expression that was critical for cranial development (Hosokawa et al., 2007). Of interest, enhanced expression of MSX2 prevented osteoblast differentiation and extracellular matrix mineralisation, and stimulated cells to harbour a state of proliferation (Dodig et al., 1999, Liu et al., 1999). Only a few genes were expressed differently between pulp and marrow progenitors, which included IGF2 and IGFBP7, while no genes were exclusively expressed by either cell population. The expression profiles between dental pulp and bone marrow functionally demonstrated that pulp progenitors have a higher proliferative capacity compared to marrow progenitors, due to increased expression of CDK6, a cell-cycle specific kinase, and the mitogen IGF2 (Shi et al., 2001), which was supported by the *ex vivo* expansion capacity of >140 population doublings by SHED (Miura et al., 2003). Specifically, IGF2 may contribute to steady-state conditions of the tooth and dental pulp microenvironment by preventing dentin de-mineralisation (Finkelman, 1992). Conversely, IGFBP7 may contribute to

the lower proliferation rate of bone marrow progenitors (Shi et al., 2001), as the IGFBPs are implicated in the suppression of growth rate and cellular senescence (Kato, 2000). Even though there were genes expressed differently between dental pulp and bone marrow stromal cells, the majority were expressed similarly, which indicated similar molecular pathways involved in both tooth development and bone formation (Shi et al., 2001). The dissimilar pathways, however, of dentinogenesis and osteogenesis allowed for active haematopoiesis by bone marrow and not dental pulp progenitor transplants *in vivo*, likely due to elevated FGF2 and MMP-9 (Batouli et al., 2003). In addition, different gene profiles and molecular pathways exist between native osteoblasts and osteoblasts derived from human pulp stem cells (ODHPSC), which may explain the histological differences observed in the bone-like tissues formed (Carinci et al., 2008).

Odontoblasts and osteoblasts both expressed several mineralised matrix proteins as stated above (Gronthos et al., 2000). The potent regulators involved in bone formation were implicated as promoters in development of odontoblasts *e.g.* TGFβ, BMP2 and BMP4 (Nakashima et al., 1994, Shiba et al., 1998). In addition, other growth factors that influenced osteoblast cells also regulated odontoblast precursor proliferation and differentiation, which included FGF2, PDGF, EGF, IGF1, TNFα and ILβ1 (Kettunen et al., 1998, Shiba et al., 1998, Onishi et al., 1999). Taken together, the biochemical pathways shared by dental pulp and bone marrow progenitors were very similar in the differentiation of pulp progenitors into odontoblasts and marrow progenitors into osteoblasts (Gronthos et al., 2000). Of note, dental pulp and

bone marrow progenitors originate from highly vascular tissues, and both expressed markers for smooth muscle and endothelium. Based on developmental biology, studies have suggested that several different stem cell types may originate from the developing blood vessels (Bianco and Cossu, 1999), with evidence that bone progenitors have a close relationship to pericytes of outer surface vasculature (Doherty et al., 1998). Even though dental pulp and bone marrow progenitors shared similar cell surface and protein marker profiles, and regulatory factors, dental pulp differed significantly in its proliferation capacity and developmental potential *in vitro*, and upon transplantation *in vivo* their representative tissues distinctly mimicked their native microenvironments (Gronthos et al., 2000).

Extracellular Matrix Components Control Stromal Cell Progenitors

Connective tissue stroma and the associated extracellular matrix (ECM) organisation are vitally important to normal functioning of the human body, as evidenced by the array of pathologies known because of mutations within connective tissues. The ECM and its associated molecules are an integral component of a stem cell niche by way of creating a microenvironment and architecture that is favourable for survival and propagation of progenitors, in addition to acting as a substrate anchor. The ECM is hypothesised to regulate niche signalling by provision, storage and/or compartmentalisation of growth factors and cytokines that are indispensable for both cell proliferation and differentiation. In addition, other ECM components such as proteoglycans and collagen-I are thought to modulate growth factor and cytokine accessibility as well as other signalling molecules (Riquelme et al., 2008). Hence, the following

sections highlight the roles of those structural and/or signaling molecules of importance to stromal cell progenitors, with many in common between BMSCs and DPSCs.

Small Leucine-Rich Proteoglycans

The small leucine-rich proteoglycans (SLRPs) are relatively small and generally <150kDa including their glycosaminoglycan (GAG) chains, compared to other proteoglycans. SLRPs are a group of molecules with a similar structural motif known as the leucine-rich repeat (LRR). Other structural features include, a highly variable N-terminal domain that may have GAG chains attached or even sulphated tyrosine residues, a cluster of four-cysteines, and a disulphide bond at the C-terminal (figure 1.3). They tend to have more leucine and other aliphatic-hydrophobic amino acids than most other proteins. The common features may allow similar functions of the SLRP, by binding the same molecules on the cell surface and in the extracellular matrix. The SLRP gene and protein structures, however, suggest the members have been structurally diverged for a long time (Neame and Kay, 2000). SLRPs interacted with a number of cytokines, which included TGFβ, BMP4, WISP1, von Willebrand factor, PDGF and TNFα, leading to the modulation of a diverse range of biological functions. SLRPs also engaged signalling receptors, which included TLRs, IGF1R, EGFR, LRP1, integrin α2β1, and c-Met. Thus, SLRPs can act as direct triggers for signal transduction, to modulate cell growth, proliferation, differentiation, survival, adhesion, and migration (Merline et al., 2009).

Biglycan and decorin are both members of the SLRP family. The core protein of decorin is ~38kDa and has a single chondroitin or dermatan sulphate GAG chain at its N-terminus. Decorin has heterogeneous GAG chain sizes and as such, the secreted proteoglycan ranges in molecular weight between 100 and 250kDa. The core protein of biglycan is 45kDa, and harbours two chondroitin or dermatan sulphate GAG chains at the N-terminus. The GAG chains are also heterogeneous and give a proteoglycan weight range between 200-350kDa (figure 1.4) (Mecham, 2001).

Proteoglycans Regulate Cellular Behaviour

Biglycan and decorin were highly expressed in bone, and displayed spatially restricted gene expression patterns and proteoglycan localisation (Bianco et al., 1990). Clinical conditions involving low biglycan levels caused short stature in Turner syndrome patients because they lack an X chromosome, whereas patients with high biglycan levels have increased limb length due to additional X chromosomes (Vetter et al., 1993, Ameye and Young, 2002). The importance of decorin and biglycan *in vivo* is clear from targeted deletion of the genes in mice (reviewed Ameye and Young, 2002). In single-deletion of biglycan, mice developed a phenotype of osteoporosis and failed to achieve a peak bone mass, causing significantly short femurs, due to low osteoblast numbers and low activity (Xu et al., 1998). Lack of biglycan *in vitro*, caused a rapid decrease of bone marrow progenitors with age due to a decrease in proliferation and an increase in apoptosis, and biglycan knock-out showed a decrease in response to exogenous TGFβ and synthesis of collagen-I. Taken together, these features contributed to the osteopenic phenotype observed *in*

vivo (Chen et al., 2002). In addition, altered phenotype in tooth mineralisation caused a broader predentine/dentine interface and dramatic enamel increase, which suggested biglycan normally exerts negative feedback (Goldberg et al., 2003). The important relationship shared by stromal cell progenitors and their microenvironment was observed from the different histological characteristics between bone-like tissue formed by normal osteoblasts and osteoblasts derived from human pulp cells (ODHPSC). Although seemingly the same morphological cell, the different genetic profiles displayed between the two osteoblasts, and as a result most probably the proteins expressed, led to formation of different tissues (Carinci et al., 2008).

The influence that the ECM component proteoglycans have on stromal cells is evident from the mineralisation processes involved in both bone and dentine. Such mineralised matrices typically harboured chondroitin sulphate substituted proteoglycans, whereas soft connective tissues *e.g.* skin and ligament contained dermatan sulphated glycosaminoglycans (Waddington et al., 2003b). Proteoglycans in their non-glycosylated forms have also been identified in human skin (Fleischmajer et al., 1991), human intervertebral disc (Johnstone et al., 1993), human cartilage (Johnstone et al., 1993, Theocharis et al., 2002), and predentine (Waddington et al., 2003a). It is, however, unclear if non-glycosylated proteoglycans are simply presence of the core-protein alone or because of degradation, hence these structurally different molecules may contribute alternative functions. In teeth, various proteoglycan pools are suggested to extend from predentine to dentine, which includes the predentine/dentine interface. Dermatan sulphate conjugated biglycan and

decorin were predominantly present in the predentine, while chondroitin sulphate conjugated proteoglycans dominated the predentine/dentine and was the only glycosaminoglycan present in dentine. Catabolism of biglycan and decorin within predentine suggested that glycosaminoglycan degradative products may contribute bioactivity, whereby dermatan sulphate may act to inhibit mineralisation, and conversely chondroitin sulphate could control and/or promote mineralisation (Waddington et al., 2003a) having the capacity to bind five-fold more calcium than dermatan sulphate (Embery et al., 1998). The role of glycosylated biglycan and decorin in the developing osteoid is becoming more apparent. Dermatan sulphated decorin was associated with early matrix deposition and maturation, while chondroitin sulphated decorin presented during matrix mineralisation. Dermatan sulphated biglycan was expressed during phases of proliferation, whereas chondroitin sulphated biglycan was expressed at onset of mineralisation (Waddington et al., 2003b). Biglycan bound active TGFβ but not as effectively as its non-glycosylated form, which had higher activity. This suggested conjugated glycosaminoglycans could hinder growth factor interaction with the core protein (Hildebrand et al., 1994). Recombinant forms of chondroitin sulphate conjugated decorin promoted collagen fibrillogenesis, as did the core protein itself, although there was a delay in initial fibril aggregation. Conversely, recombinant biglycan did not influence collagen fibrillogenesis. These recombinant proteoglycans also bound hydroxyapatite predominantly through glycosaminoglycan chains and inhibited crystal growth, with greater inhibition by core proteins alone. As such, both proteoglycans regulated mineralisation, whereby biglycan had a more prominent role due to higher hydroxyapatite affinity (Sugars et al., 2003).

Biglycan Regulates Cellular Proliferation and Differentiation

Among the multitude of functions performed by SLRPs, they have a role in regulating cellular proliferation, but only a limited number of studies have addressed the specific role of biglycan in regulating proliferation. Up to now, TLR2 and TLR4 were identified as the signalling receptors of biglycan (Merline et al., 2009). Biglycan was suggested to favour proliferation during osteoblast development (Waddington et al., 2003b), and proliferation of vascular smooth muscle cells by CDK2- and p27- dependent pathways (Shimizu-Hirota et al., 2004). Opposed to its proliferative capacity, biglycan also had anti-proliferative effects. In pancreatic cancer, biglycan induced G1 arrest, thereby inhibiting the proliferation of tumour cells. This inhibition was associated with upregulated CDK inhibitor p27, downregulated cyclin A and PCNA, and decreased Ras and ERK activation (Weber et al., 2001). Biglycan has been shown to inhibit proliferation of BMSCs, which can be abrogated by WISP1 (Inkson et al., 2009). Interestingly, WISP1 rescued diminished osteogenic differentiation in the absence of biglycan. Biglycan also influenced cellular differentiation, and was shown to control osteoblast differentiation by modulating BMP4 (Chen et al., 2004b). Biglycan was a critical component in organising the niche of tendon stem/progenitor cells, and its absence affected tendon progenitor differentiation by modulating BMP signalling (Bi et al., 2007). Taken together, biglycan may regulate proliferation in a cell-specific manner *via* specific receptor and signalling pathways, or by an indirect and unidentified mechanism. Thus, more research is required to understand biglycan-mediated signalling, and its influence in cellular processes such as proliferation and differentiation (Merline et al., 2009).

Dermatan Sulphate Biological Activity

Proteoglycans within bone and tooth harbour sulphated glycosaminoglycans. An interesting notion is that the glycosaminoglycan, dermatan sulphate, may have a specific cell signalling role and may be responsible for biological actions (Akita et al., 2008). As the core protein of biglycan, along with the glycosaminoglycan chains, influenced tissue remodelling and mineralisation in tooth (Waddington et al., 2003a) and bone (Waddington et al., 2003b). From the literature, more evidence is reported on decorin rather than biglycan. In matrix organisation, following chemical insult of mouse skin, decorin increased in molecular size by increasing dermatan sulphate rather than protein core size during post-inflammation. These dermatan sulphate filaments orientated in an orthogonal fashion to collagen fibrils and extended into enlarged interfibrillar gaps between collagen fibrils, which indicated the important role of dermatan sulphate in extracellular matrix organisation in wound healing (Kuwaba et al., 2001). Proteoglycans such as biglycan are identified as coregulators in FGF signalling (Hou et al., 2007). Studies show that *in vitro* proteoglycans from wound fluid bound to multiple components within the cellular microenvironment and were functionally active during wound healing processes. Among present proteoglycans was decorin, and a large proportion of glycosaminoglycans was dermatan sulphate that bound FGF2 (Turnbull et al., 1992), which supports to FGF2 mediated cell proliferation *via* FGFR1 (Penc et al., 1998). In addition, FGF2 was the major factor released *via* ERK signalling pathways upon damage of articular cartilage by cutting or enzymatic degradation, which supports an extracellular sequestered store (Couchman et al., 1984), influencing tissue remodelling (Vincent et al., 2002) by preferentially activating

FGFR1 (reviewed Ellman et al., 2008). As well as a functional role in wound healing, the dermatan sulphate molecule itself may have a role in reparative processes as opposed to deleterious effects during inflammation. Dermatan sulphate, unlike heparin sulphate and chondroitin sulphates A and C, rapidly activated NF-κB (nuclear factor kappa B), and induced surface and soluble ICAM1 (intercellular adhesion molecule 1) following direct cell activation at physiological wound concentrations *in vitro* and *in vivo*. The aforementioned activation and induction, however, did not involve TNFα or IL1 that normally contribute to pro-inflammation, but was facilitated by other unknown autocrine factors. This suggested a beneficial upshot considering NF-κB has a variety of advantageous biological functions, which include ICAM1 cascade and transmigration of leukocytes that defend against infection at sites of injury. It has been speculated, however, that dermatan sulphate may contribute towards dermal disease processes that induce ICAM1 (Penc et al., 1999), as well as other pathological diseases (reviewed Malavaki et al., 2008). Hence, dermatan sulphate is an important glycosaminoglycan that needs further elucidation to its role in proliferation and differentiation of mesenchymal progenitors.

Transforming Growth Factor β Superfamily and Bone Morphogenic Proteins

TGFβ is a superfamily that includes at least thirty-four members, which constitute growth and differentiation factors (Dimitriou et al., 2005). The BMPs belong to the TGFβ superfamily and strongly influence osteoprogenitor differentiation, although osteogenesis does occur in BMP-deficient mice

(Deschaseaux et al., 2009). The BMPs modulate bone formation, whereby positive osteogenesis was regulated by BMP2, BMP6, BMP7, and BMP9, and activity was inhibited by BMP3. Signalling by BMP/TGFβ was transduced through type I and II serine/threonine kinase receptors (Chen et al., 2004a). The ligand-receptor complexes acted through the transcriptional modulator SMAD proteins (Wan and Cao, 2005). SMADs were critical mediators for TGFβ signalling, but BMP2 could activate pathways that are Smad-independent. Such pathways included MAPK that had distinct regulatory roles in alkaline phosphatase and osteocalcin (Lai and Cheng, 2002). Following injury of articular cartilage BMP2 was upregulated, and SMAD1 and SMAD5 underwent phosphorylation, which may possibly have a reparative role (Dell'Accio et al., 2006).

Fibroblast Growth Factor Polypeptide Family

The FGF gene family includes twenty-three members that bind variously to the seven FGF tyrosine kinase receptors, the FGFRs (Su et al., 2008), and are well known for their roles in embryogenesis and angiogenesis (Kim et al., 1993), and wound healing (Shirakihara et al., 2011). The FGF polypeptide family play critical roles in the regulation of endochondral and intramembranous ossification. FGFR1 was expressed by hypertrophic chondrocytes, and signalling had stage-specific effects on the maturation of osteoblasts. FGFR1 acted by stimulating osteoprogenitor differentiation, or arresting differentiated osteoblast maturation (Jacob et al., 2006). In osteoblasts, FGF -2, -9 and -18 are thought to bind FGFR1. FGF -9 and -18 expression was seen in the perichondrium/periosteum, and were thought to

predominantly influence embryonic skeletogenesis (Huang et al., 2007). At post-natal stages, FGF2 was expressed by periosteal cells and osteoblasts, and mesenchymal stromal cells from FGF2-null mice failed to mineralise *in vitro* (Montero et al., 2000). The addition of FGF2 to bone marrow progenitors improved their proliferation potential and maintained their differentiation potential (Delorme et al., 2009). Signalling *via* FGF2/FGFR and its effects on migration and proliferation of cells such as vascular endothelia has been apparent for some time (Yoshida et al., 1996). The downstream signalling pathways involved in such processes, however, are not well known. One activated pathway of migration signalling was the PI3K family, found in corneal endothelial cells (Lee and Kay, 2003), and bone and soft tissue tumour cells (Kamura et al., 2010). In this case, PI3K was motile specific and did not involve its other pathways in stimulating proliferation and survival. During the migration of such cells, the PI3K pathway reorganised the actin cytoskeleton that altered cell morphology and allowed motility (Kamura et al., 2010). FGF2 was also known to stimulate epithelial to mesenchymal transition, which was important during development, wound healing and tissue repair (Shirakihara et al., 2011), and was implicated in tumour metastasis (Lee and Kay, 2003). FGFR2 was expressed by reserve chondrocytes and was down-regulated in proliferating chondrocytes. FGFR2 splice variants were tissue-specific, and mesenchymal FGFR2C forms were activated by FGF -2, -4, -6, -8, and -9. FGFR3 and its physiological ligand FGF18, regulated proliferating chondrocyte growth and differentiation, and bone density and cortical thickness in differentiated osteoblasts (Ornitz, 2005).

Platelet Derived Growth Factor Signalling

PDGF is an extracellular factor that has three biologically active isoforms, composed of polypeptide chains PDGF-A and PDGF-B. PDGF-BB inhibits osteogenic differentiation, which decreases mRNA levels and activity of alkaline phosphates. PDGF binding occurs through dimerisation of two receptors (αPDGFR and βPDGFR), which formed three distinct patterns (αα, αβ, and ββ) (Arvidson et al., 2011). Mesenchymal stromal cells expressed both forms of receptor. The nature of signalling in these cells was not clear, but PDGF signalling was important in various cell functions *e.g.* cell growth and division. Depleting the βPDGFR gene in mesenchymal bone marrow stromal cells decreased mitogenic activity and migration, but enhanced osteogenic differentiation, as shown by increased alkaline phosphatase activity, osteocalcin, BMP2, RUNX2 and osterix (Tokunaga et al., 2008). Although pharmacological inhibition of PDGFR decreased PDGF-BB-induced proliferation in mesenchymal stromal cells, but had no influence on osteoblast differentiation (Kumar et al., 2010).

Insulin-like Growth Factor Signalling

The IGF family has two secreted forms of growth factor, IGF1 and IGF2, which bind the two receptors, IGF1R and IGF2R. IGF stimulated osteoblasts and bone matrix deposition, which favoured collagen and non-collagenous protein synthesis. Osteoblasts expressed both IGF forms and showed similar biological activities, but IGF1 was more potent (Giustina et al., 2008). IGF1 appeared to correlate with bone mesenchymal stromal cell recruitment and proliferation at implant sites, while IGF2 correlated with differentiation and

mineralisation (Prisell et al., 1993). Studies using animal models showed that IGF was essential for normal formation, growth, and maintenance of bone (Arvidson et al., 2011).

Wnt Signalling Pathway

Wnts (wingless) are a large family of secreted proteins that bind membrane-spanning frizzled (FZD) receptors, and are involved in many cellular processes, such as cell growth, differentiation, function, and death. Wnts signal through canonical and non-canonical pathways. The canonical pathway involves complexes of Wnt proteins, FZD, and low-density receptors, LRP5 or LRP6 (Arvidson et al., 2011). Much evidence indicated the canonical pathway was critical in bone formation and expression of osteoblast specific markers (Westendorf et al., 2004, Jackson et al., 2005). Binding of Wnt proteins to FZD/LRP5/6 complexes inhibited GSK3 (glycogen synthase kinase 3) activity that blocked phosphorylation of β-catenin and prevented its ubiquitin-degradation, which led to nuclear translocation and interaction with T-cell factor/lymphoid enhancer family of transcription factors (Fujita and Janz, 2007). β-catenin appears to be required for directing bipotential osteochondro-progenitors toward a specific lineage. Whereby β-catenin/T-cell factor 1 complex enhanced expression and activity of osteogenic promoter RUNX2, and low β-catenin levels caused mesenchymal stromal cells to be directed along chondrogenesis (Day et al., 2005).

Epidermal Growth Factor

EGF receptors, ErbB1-4, activate intrinsic kinases that are widely expressed by many cell types, which include epithelial and mesenchymal lineages. EGF receptors have five genetically distinct ligands, which include EGF, TGFα (transforming growth factor α), amphiregulin, HB-EGF (heparin-binding EGF), and other virally encoded factors. The EGF receptors have pleiotropic cell responses, which include cell proliferation, differentiation, and migration, as well as homeostatic functions (Wells, 1999). EGF is a prototypical mitogen shown to enhance BMSC motility and proliferation in human (Krampera et al., 2005), but not rat (Tamama et al., 2006). EGF has also been shown to enhance osteogenic differentiation, whereas PDGF did not (Kratchmarova et al., 2005). To the contrary, other reports show EGF alone does not induce differentiation, or alter osteogenic, adipogenic, and chondrogenic differentiation processes (Tamama et al., 2006). These contradictions are possibly due to the different actions of soluble and tethered forms of EGF (Tamama et al., 2010).

β1 Integrins

Integrins are the receptors providing structural links between a cells cytoskeleton and the ECM, which allows for oriented division of the cell. Integrins also assist growth factor receptors by enhancing signal transduction in such processes as cell proliferation, apoptotic protection and motility (Kuwada and Li, 2000, Comoglio et al., 2003, Riquelme et al., 2008). In addition, with integrins being most likely responsible for spatial positioning within a stem cell niche, integrins may well influence downstream cellular

signals and play a key role in niche maintenance (Riquelme et al., 2008). The importance of integrins as cell adhesion receptors during development and matrix organisation is well described (Barczyk et al., 2010). Primitive cells were specifically isolated by their high expression of surface β1 integrins (Jones et al., 1995, Gandarillas and Watt, 1997, Zhu et al., 1999). This was *via* rapid focal adhesion to the extracellular matrix (ECM) protein fibronectin, as opposed to transit amplifying cells, which express lower levels of β1 integrins (Adams and Watt, 1991, Jones and Watt, 1993). The terminal differentiation of keratinocytes has been shown to be associated with a decrease in the fibronectin-specific α5β1 integrin receptor and precedes a loss in fibronectin-adhesion (Adams and Watt, 1990, Hotchin et al., 1995). Furthermore, interaction of fibronectin with α5β1 integrin has the ability to suspend terminal differentiation (Watt et al., 1993). In addition, when fibronectin was present within the matrix, decorin and biglycan were shown to regulate specific gene signals that possibly contribute to remodelling of tissues in such processes as morphogenesis and wound healing, as well as disease states (Huttenlocher et al., 1996).

Gene Markers of Mesenchymal Stem Cells

In addition to the markers for “minimal criteria” in defining mesenchymal stem cells, research is uncovering other markers that identify BMSCs and DPSCs. As Shi *et al*., (2001) report, however, the gene expression profiles of DPSCs and BMSCs are similar for >4000 genes. Added to this, is the heterogeneity of both progenitor cell types, which can make it difficult to distinguish between them. Nevertheless there were two differentially expressed gene markers,

IGF-2 and IGFBP-7, between each progenitor source that plays an important role for mesenchymal stromal cells (Shi et al., 2001).

FGFR1 (CD331) was important for bone development and osteoblast maturation (Jacob et al., 2006). In addition, FGFR1 was important in orchestrating epithelial-mesenchymal transition (EMT) and mesoderm morphogenesis, which involved cell migration and patterning, by controlling Snai1 expression (Ciruna and Rossant, 2001). The importance of FGFR1 and Snail1 during development was illustrated in their absence, by craniofacial abnormalities *e.g.* cleft palate. FGFR1 was implicated in human congenital defects (Carinci et al., 2007), and animal models (Trokovic et al., 2003). Snai1 was implicated in murine craniofacial defects (Murray et al., 2007). Interestingly, FGF2 is a main activator of FGFR1, and was suggested to have a regulatory role in the expression of decorin and biglycan (Bodo et al., 1999). Snai1 was also involved in EMT, and important in differentiation of embryonic epithelia to mesenchymal cells. Interestingly, Snai1 was induced by TGFβ2, and mediated endogenous EMT (Kokudo et al., 2008).

The adhesion molecules MCAM (CD146) and VCAM1 (CD106) were both present in BMSCs (Halfon et al., 2011) and DPSCs (Gronthos et al., 2000). MCAM is a vascular/endothelial lineage marker (Filshie et al., 1998), and dental pulp and bone marrow progenitors originate from highly vascular tissues. This marker is of interest as studies have suggested that several different stem cell types may originate from the developing blood vessels (Bianco and Cossu, 1999), and could localise the stem cell niche within these tissues. VCAM1 is critical in MSC mediated immunosupression, which is a vital

component for translation therapy to be used in a clinical setting (Ren et al., 2010).

RUNX2 (Cbf1a) is a key transcription in osteoblast differentiation, and is a member of the RUNX transcription factor family, which were abundantly expressed in calcified cartilage and bone (Lian et al., 2004). In addition, RUNX2 was suggested to be involved in dental development, influencing cell growth and differentiation (Xuan et al., 2010). RUNX2 is a transcription factor for Spp1 (Osteopontin) (Nakashima et al., 2002), which was suggested to be important for cell anchoring (Reinholt et al., 1990). Osteopontin was expressed by BMSCs and DPSCs (Gronthos et al., 2000), and in bone osteopontin was reported to be an important factor in osteoblast differentiation and development during bone remodelling (Sodek et al., 1995).

Embryonic markers Nanog and SOX2 will be investigated by gene expression, as an indication of pluripotency of the DPSCs and BMSCs. Nanog was important in the self-renewal of ESC (Loh et al., 2006), and SOX2 generated inducible pluripotent stem cells (Takahashi et al., 2007). These embryonic markers were reported to be expressed by BMSCs and DPSCs (Janebodin et al., 2011). Lastly, mesenchymal stromal cells should be negative for CD14, CD34, and PTPRC (CD45), which are markers for monocytes/macrophage, haematopoietic, and leukocyte lineages, respectively (NIH Stem Cell Guidelines).

Research Aims

An increasing amount of literature on mesenchymal stromal cells, from *in vitro* and *in vivo* studies, is shedding light on dental pulp as a potential alternative cell source for use in tissue regenerative medicine. The vast majority of reports on both dental pulp and bone marrow stromal cells, however, uses multi-colony stromal cell progenitors as opposed to single-cell derived clones. This thesis seeks to better understand the potential of dental pulp stromal cells, and the continued use of bone marrow stromal cells for tissue engineering, and to investigate the influence of extracellular matrix proteins on stromal cell proliferation and mineralisation. The aims are:

I. Characterise primitive bone marrow and dental pulp mesenchymal stromal cells, from fibronectin-adherence assay, by comparing colony-formation and proliferation capacity of isolated clonal colonies, and quantify stem cell marker expression of clones during culture expansion.
II. Examine differentiation capacity of characterised mesenchymal stromal cell clones along adipogenic, chondrogenic, and osteogenic lineages.
III. Observe influence of whole bone- and tooth- extracellular matrix protein extracts on proliferation and osteoinduction of selected mesenchymal stromal cell clones.
IV. Investigate proliferation and differentiation of selected mesenchymal stromal cell clones on bone and tooth tissue-slabs, to assimilate fracture and caries, respectively.

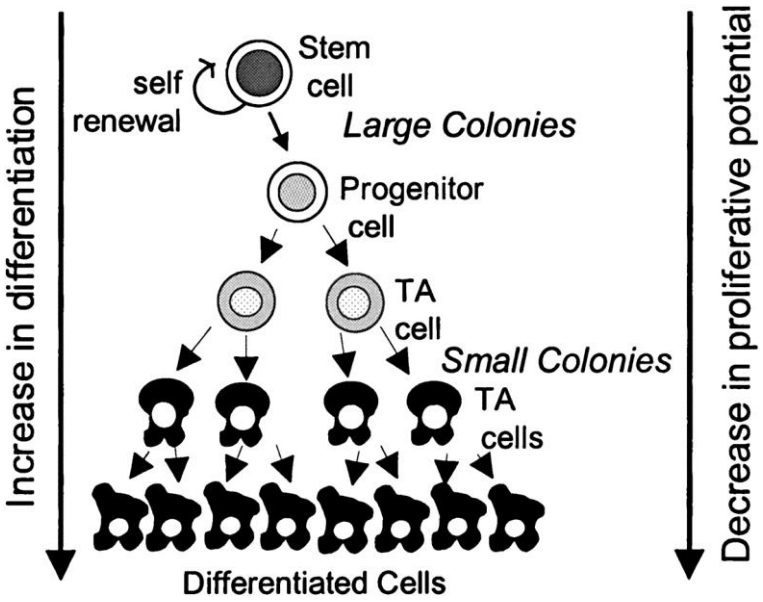

Figure 1.1: Hierarchy of stem cell differentiation showing possible relationship to large and small colonies. Stem cells are able to self-renew and replace themselves, or differentiate to give rise to committed progenitors. These progenitors proliferate and give rise to more differentiated transit amplifying (TA) cells, which rapidly proliferate and finally differentiate to produce a large number of terminally differentiated functional cells with no capacity for proliferation. It is postulated that large colonies are initiated by putative stem/progenitor cells and the small colonies are initiated by putative TA cells. Taken directly from (Chan et al., 2004).

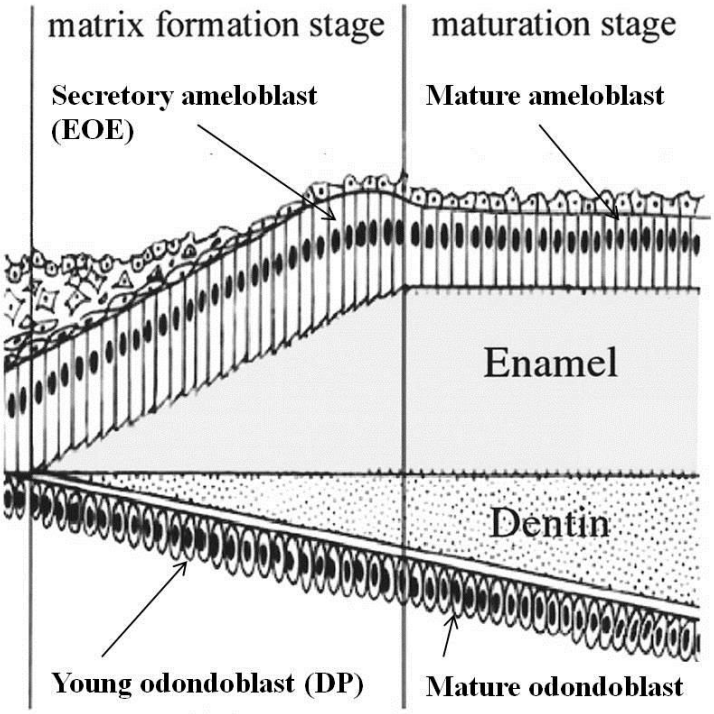

Figure 1.2: Schematic of developing tooth involving odontoblasts and ameloblasts. Odontoblasts differentiate from ectomesenchymal cells of the dental papilla, which later becomes the pulp, following interaction with inner enamel organ epithelial cells. Odontoblasts are of neural crest origin and form dentin during a process known as dentinogenesis, which is the tissue layer below enamel. Odontoblasts are tall columnar cells with an eccentric nucleus and long processes that aligns with dentin. Ameloblasts are of ectodermal origin and form enamel during amelogenesis, which is induced by dentinogenesis. Ameloblasts differentiate from the inner dental epithelium following elongation and polarization (Ten Cate, 1994). EOE, enamel organ epithelia layer; DP, dental papilla. Adapted from (Nagano et al., 2003).

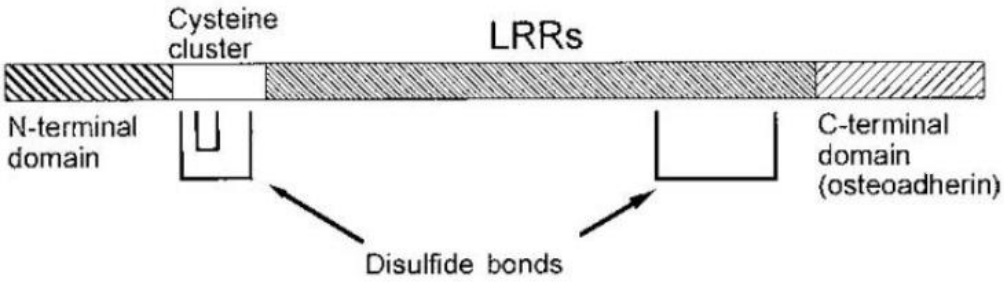

Figure 1.3: A generic structure representing small leucine-rich proteoglycans (SLRPs). SLRPs all possess features which include: an N-terminal domain, followed by a 4-cysteine-cluster region that harbours a 3 amino acid group Cys-X-Cys. Following the cysteine-cluster region, are a variable number of leucine-rich repeats, which has a disulphide bond at its C-terminal. In addition, osteoadherin has a C-terminal extension. Sourced from (Neame and Kay, 2000).

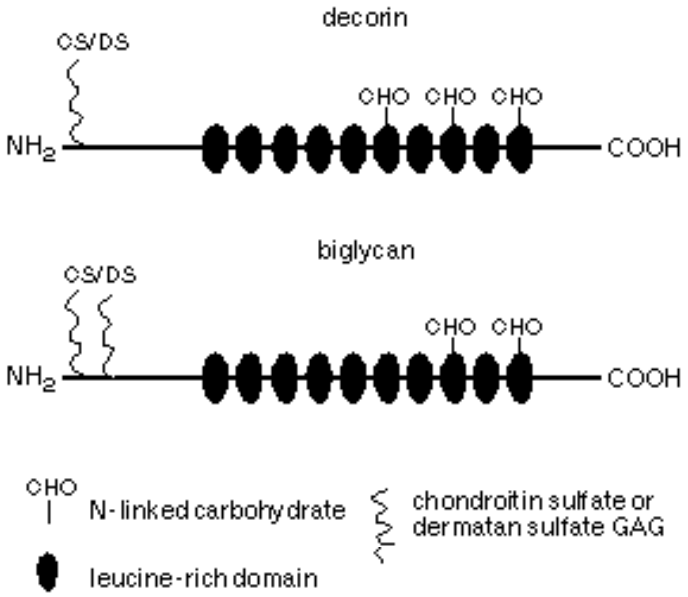

Figure 1.4: Domain maps of decorin and biglycan from the small leucine-rich proteoglycan family. The core protein of decorin is ~38kDa with a single chondroitin or dermatan sulphate glycosaminoglycan (GAG) chain at its N-terminus. Decorin GAG chains are heterogeneous and the molecular weight ranges between 100 and 250kDa. The core protein of biglycan is 45kDa, with two chondroitin or dermatan sulphate GAG chains at the N-terminus. Biglycan GAG chains are also heterogeneous and range between 200-350kDa. CS, chondroitin sulphate; DS, dermatan sulphate. Adapted from (Mecham, 2001).

Chapter 2

Materials and Methods

2.1 Primary Bone Marrow and Dental Pulp Cell Culture

All animals were handled and sacrificed in accordance with Code of Practice for the Humane Killing of Animals Under Schedule 1 to the Animals (Scientific Procedures) Act 1986. Upper and lower incisors, and femoral bones, were dissected from 21-28 day old male Wistar rats. The incisors and bones were collected in αMEM (with ribonucleasides and deoxyribonucleosides; Invitrogen) with 10% antibiotic-antimycotic ($1x10^3$ units/mL penicillin G, 1mg/mL streptomycin sulfate, and 2.5µg/mL amphotericin B; Sigma-Aldrich, Inc). Dental pulp was extirpated, chopped by hand on a glass slide using a scalpel, and digested with 4mg/mL collagenase/dispase (Roche) for 45 minutes at 37^{o}C. Digested pulp was filtered through a 70µm nylon cell strainer (BD Falcon) with 9mL αMEM with 1% antibiotic-antimycotic (working medium) and centrifuged at 1800rpm for 5 minutes. The cell pellet was suspended in 1mL of working medium and the number of viable cells counted using Trypan Blue solution (Sigma-Aldrich, Inc).

Bone marrow was prepared using a Histopaque-1077 (Sigma-Aldrich, Inc) medium to facilitate isolation and recovery of the mononuclear cell layer containing progenitor cells. Marrow was collected in 1mL working medium by opening and brushing the bones with a disposable 2mm micro-applicator brush (MICROBRUSH® International). Marrow was suspended in working medium with an equal volume to the pellet, and centrifuged at 1800rpm for 5 minutes. Histopaque was allowed to come to room temperature and the marrow with

working medium was layered onto an equal volume of histopaque, and centrifuged at 1800rpm in a swing-bucket for 30 minutes at room temperature. The mononuclear layer of cells (second from the top) was then recovered and counted as above.

Fibronectin plates were prepared at 10µg/mL (fibronectin from human plasma; Sigma-Aldrich, Inc) reconstituted in PBS (phosphate buffered saline, with 1mM calcium and 1mM magnesium), and used with 1ml fibronectin/PBS (Ca^{2+} and Mg^{2+}) per well in 6-well plates. The recovered pulp and marrow cells were seeded at 4000 cells/cm^2 in 1mL culture medium into each well of coated plates, immediately after removing fibronectin/PBS solution. Cells were then incubated at 37^{o}C for 20 minutes to select for the fibronectin adherent, α5/β1 integrin-positive primitive cell populations. After 20 minutes incubation, non-adherent cells were aspirated and unattached cells were rid with several PBS washes. A volume of 2mL fresh culture medium was added and plates were incubated. Culture medium consisted of αMEM supplemented with 20% Fetal Bovine Serum (FBS) (EU Approved, South American origin, Invitrogen), 1% antibiotic-antimycotic, and 100µM L-ascorbic acid 2-phosphate (both Sigma-Aldrich, Inc). Culture medium was changed every two days. Cells were incubated at 37^{o}C in a 5% CO_2 atmosphere. All tissue culture plastic consumables were SARSTEDT or Greiner Bio-One, unless specified.

Mycoplasma testing was routinely conducted every two weeks and if found positive cells were treated with 10µg/mL Ciprofloxin antibiotic (Claris Lifescience UK Ltd) for 2 weeks until tested negative. If infection persisted cells underwent BM Cyclin treatment (Roche) for 2 weeks, after which cells were

either cultured as normal if mycoplasma negative, or disposed of if mycoplasma positive.

2.2 Colony-Forming Efficiency and Population Doubling Level

Within each well the numbers of clonal colonies (>32 cells) were counted on days 3, 6, 10 and 12, and considered as a proportion of the total number of cells at 24 hours, to calculate the colony forming efficiency (CFE) (Dowthwaite et al., 2004). All cells and colonies attached in each well were counted manually by viewing in a serpentine configuration using an Olympus CK2 inverted microscope with stage. On day 12, the number of cells in each individual colony was counted, and then isolated using a cloning ring, and treated with a proteolytic and collagenolytic enzyme StemPro® Accutase® (Invitrogen) as follows. The 6-well plate was washed with PBS, each individual colony was isolated using a cloning ring with petroleum jelly smeared around the lower rim, and incubated at room temperature with 150µL StemPro® Accutase® for 5 minutes. Alternatively, dental pulp clones were positively "picked" to ensure isolation of large or close proximity colonies. Cells were recovered and plated into a well of a 96-well plate and culture expanded. When approximately 80% confluent, cells were passaged with StemPro® Accutase® (Invitrogen), counted using 0.4% trypan blue solution (Sigma-Aldrich, Inc) to calculate passage cell number, and the population doubling level (PDL) as a proportion to original number of cells within the colony at isolation ($PDL=(\log_{10}(24\text{ hour cell count})-(\text{total cell number reseeded}))/\log_{10}(2)$). Passaged cells were reseeded at the density $4x10^3$ cells/cm^2. All dental pulp clones (except DP 2.7) were culture expanded by doubling surface area alone

for the first four passages, after which culture expansion proceeded in the normal way of seeding at $4x10^3$ cells/cm^2. Cells were continually propagated and underwent cryopreservation using 1:10 dimethyl sulphoxide (DMSO) (Invitrogen)/FBS when sufficient cells were gained. Cryopreserved cells were decreased to -80^oC in isopropanol before transferring to liquid nitrogen for storage until required for future use.

2.3 Mycoplasma Testing for Polymerase Chain Reaction

Mycoplasma testing used the VenorGeM Mycoplasma Detection Kit for Conventional PCR standard protocol (Cambio, manufactured by Minerva Biolabs). Briefly, 100µL of culture medium supernatant was used from cell cultures at approximately 80% confluency. The sample was incubated at 95^oC for 5 minutes, centrifuged to pellet cellular debris, and 2µL of culture medium supernatant used for PCR in a final volume of 25µL containing kit master-mix. Cycling conditions used for PCR was one cycle at 94^oC for 2 minutes, and thirty-nine cycles at 94^oC for 30 seconds, 55^oC for 30 seconds, and 72^oC for 30 seconds. Products were separated using 2% agarose/ethidium bromide gels and captured using UV light. Bands are seen at 191bp for negative sample, and 270bp for positive sample. Negative control used RNA free water, and positive control used DNA template.

2.4 β-Galactosidase Stain for Cell Senescence

Cell senescence was measured as a percentage of β-Galactosidase staining using the manufacturer protocol for Senescence Cells Histochemical Staining kit (Sigma-Aldrich, Inc). Briefly, cells seeded at $4x10^3$ cells/cm^2 were cultured

for 48 hours in culture medium, and the β-Galactosidase stain was used overnight without CO_2 at 37ºC. The number of positive cells out of 100 was counted from at least four random fields of view, to give an average percentage.

2.5 Reverse Transcription and End-Point Polymerase Chain Reaction for Colony Clones

Total RNA was extracted from $1.15x10^3$ cells seeded at $4x10^3$ cells/cm^2 grown to 90% confluence, at the time-points shown in table 2.1. The extraction used RNeasy Mini Kit and QIAshredder (Qiagen) as per manufacturer protocols. Quantity and purity of RNA was determined by 260/280nm absorbance. Firstly, 500ng of total RNA was denatured with 1µL random primer, added to nuclease-free water for a final volume of 15µL, and run at 70ºC for 5 minutes. The reverse-transcription (RT) negative control did not contain sample RNA. Secondly, cDNA was transcribed by adding the 15µL of denatured RNA to an RT reaction mix to produce a final volume of 25µL sample cDNA. Each sample RT reaction mix contained: 5µL 5x MMLV Reaction buffer, 1.25µL 10mM dNTPs, 0.6µL RNasin, 1µL MMLV enzyme, and 2.15µL nuclease-free water, for a total volume of 10µL. The RT 25µL final volume was run at 37ºC for 1 hour. The polymerase chain reaction (PCR) reagents used for each 24µL reaction contained: 5µL 5x buffer, 0.5µL 10mM dNTPs, 2µL 3µM primers (forward and reverse), 1µL 25mM magnesium chloride, 0.25µL Taq polymerase, and 13.25µL nuclease-free water. To the 24µL PCR reaction mix, 1µL cDNA was added for a final volume of 25µL. The PCR negative control did not contain sample cDNA. All reagents used were Promega. Thermo cycler

(G-Storm, Gene Technologies Ltd., Software V3.3.0.0) conditions used were: heated lid at 110ºC, 95ºC for 5 minutes, and thirty-five cycles of 95ºC for 1 minute, primer specific annealing temperature for 1 minute, and 72ºC for 1 minute, and a final cycle of 72ºC for 10 minutes. Primer sequences were designed using online internet National Centre for Biotechnology Information (NCBI) Primer-BLAST software unless specified, see table 2.2. The control reference gene used was β-actin. Products were separated using 1% or 2% agarose/ethidium bromide (Promega) or Safeview DNA Stain (NBS biologicals) gels, and captured using UV light.

2.6 Quantitative-Polymerase Chain Reaction of Colony Clones

Total RNA was extracted and cDNA synthesised as for end-point PCR. cDNA was diluted 1:10 with nuclease-free water. For each reaction the qPCR reagents used were 2µL 3µM primers (forward and reverse), 5µL diluted cDNA sample, 10µL Precision MasterMix pre-mixed with SYBR green (Primer Design Ltd), and 1µL RNA-free water, for a final volume of 20µL. All samples were triplicated in Bright White 96-well plates (Primer Design Ltd). Real-time quantitative-PCR runs were conducted on ABI Prism 7000 Sequencing Detection System and ABI Prism 7000 SDS Software V1.0. Reaction conditions were one cycle of 95ºC for 10 minutes, and forty cycles of 95ºC for 15 seconds, 55ºC for 30 seconds and 72ºC for 30 seconds. Primer sequences were designed by OligoArchitect Primer and Probe Design Solutions (Sigma-Aldrich, Inc) unless specified, see tables 2.3, 2.4, and 2.5. The control reference gene used was β-actin. Products were separated and captured as for end-point PCR to confirm product band. Statistical analyses were

conducted using one-way ANOVA with Tukey test and statistical package GraphPad InStat v3.06. Statistical values were defined as * = P<0.05 (significant), ** = P<0.01 (very significant), *** = P<0.001 (extremely significant).

2.7 Mesenchymal Stromal Cell Differentiation

Assessment of MSC differentiation potential was investigated for three lineages: adipocytes, chondrocytes, and osteoblasts. Differentiation potential was investigated for three clonal populations from both tissue sources: bone marrow and dental pulp. These same three clonal populations from both tissue sources at mid PDL (see table 2.1) underwent analysis hereon in.

2.7.1 Adipogenic Differentiation Media

For adipogenesis cells were seeded at $10x10^3/cm^2$ and fed with 10% serum culture medium (see 2.1 Primary Bone Marrow and Dental Pulp Cell Culture) until virtually 100% confluent (*NB* cells need to be tightly packed). Differentiation media consisted of two treatments referred to as induction and maintenance. Adipogenic induction medium consisted of 1µM dexamethasone (Sigma-Aldrich, Inc) dissolved in ethanol (Genta Medical, UK), 0.5mM 3-isobutyl-1-methylxanthine (IBMX) in dissolved dimethyl sulfoxide (DMSO) (both Sigma-Aldrich, Inc), 10µg/mL dissolved insulin (Sigma-Aldrich, Inc) dissolved in hydrochloric acid (HCl) (Fisher Scientific), and 100µM indomethacin (Sigma-Aldrich, Inc) dissolved in methanol (Fisher Scientific). Adipogenic maintenance medium contained 10µg/mL insulin dissolved in HCl only. At 100% confluency (day 1), adipogenic differentiation was started for a

total 21 days. Media change schedule as follows: induction (days 1 and 4), maintenance (day 7), induction (days 9 and 12), maintenance (day 15), and induction (day 17). Photographs were taken on days 1, 7, 15, and 21, and finally specimens were processed on day 21. Media stock solutions were vortexed to give a precipitate-free solution and 0.22µm filter sterilised before storing at -20^{o}C until use. Adipogenic components were thawed, mixed, and added to 10% serum culture medium (final concentrations stated above), and vortexed for thorough dissolution immediately before each change. Control was 10% serum culture medium alone, and was fed alongside adipogenesis treatment. Cells were cultured using 32mm #1 glass round cover slips (VWR International Ltd) in 3x9.6cm^2 wells for total RNA extraction, and 13mm #1 glass round cover slips (VWR International Ltd) in 2cm^2 wells for neutral lipid staining.

2.7.2 Adipogenic Differentiation Marker Expression Analysis

Total RNA was extracted from 28.8x10^5 cells seeded at 10x10^3 cells/cm^2 after 21 days in culture, for adipogenic expression detection using quantitative PCR, see markers in table 2.4 (see 2.6 Quantitative-Polymerase Chain Reaction of Colony Clones). Total RNA was analysed from three samples: before differentiation at mid PDL (see table 2.1), and 21-day non-adipogenic and adipogenic differentiation media (see 2.7.1 Adipogenic Differentiation Media).

2.7.3 Adipogenic Differentiation Neutral Lipid Detection

Two culture groups were set up for neutral lipid analysis: 21-day non-adipogenic medium and 21-day adipogenic differentiation medium. Cells were

fixed and probed using HCS LipidTOX™ Green neutral lipid stain as per manufacturers protocol (Invitrogen). Briefly, cells were washed twice with PBS, fixed with 4% PFA for 10 minutes at room temperature, washed thrice with PBS, and stained with LipidTOX™ diluted 1:200 in PBS for 30 minutes. Lastly, glass cover slips were counter-stained with DAPI Vectashield Hard-Set Mounting Medium (Vector Labs) and inverted onto SuperFrost microscope slides (Thermo Scientific Gerhard Menzel). Nuclear DAPI and green-lipid fluorescence was observed at 373nm/456nm and 490nm/520nm wavelengths, respectively, using Olympus Provis AX70 microscope with Nikon ACT-1 v.2.63 software.

2.7.4 Chondrogenic Differentiation Media

Chondrogenesis was assessed using StemMACS ChondroDiff Media as per manufacturers protocol (Miltenyi Biotech Ltd.). To the ChondroDiff Media 1% antibiotic-antimycotic (Sigma-Aldrich, Inc) was added. Working aliquot volumes were stored at -20^{o}C, and thawed immediately before use. Cells were seeded at 2.5x10^{5} with either 1mL non-chondrogenic 10% serum culture medium (see 2.1 Primary Bone Marrow and Dental Pulp Cell Culture) or 1mL ChondroDiff Media, in 15mL polypropylene tubes with loosely capped lids for air circulation. A minimum two tubes for each specimen with non-chondrogenic and chondrogenic media was set up. Tubes were centrifuged at 150*g* for 5 minutes at room temperature before and after each media change. Media was changed every three days and formed pellets were collected for processing on day 24. An additional two tubes for both media were set up for RNA extraction,

however, neither RNeasy Mini Kit with QIAshredder (Qiagen) nor TRI Reagent® (Sigma-Aldrich, Inc) could recover total RNA for PCR.

2.7.5 Chondrogenic Differentiation Pellet Tissue Histology

Following 24 days, formed pellets were washed with PBS and transferred to a universal tube containing 20mL 3.7% formalin/PBS fixative for a minimum 24 hours with gentle agitation. After fixing, pellets were transferred to tissue paper and dabbed with haematoxylin for easy identification, wrapped up within the tissue paper by folding edges several times and put in embedding cassettes for automatic processing (Leica ASP300S). This automation dehydrated samples through 90%, 95%, and 100% ethanol concentrations, washed by xylene immersion, and soaked in molten paraffin wax. Specimens were then manually embedded in paraffin wax (Leica EG1150H) and stored in darkness at room temperature until use. Paraffin embedded samples were microtomed (Leica SM2400), and 5µm sections collected on SuperFrost poly-L-lysine coated microscope slides (Thermo Scientific Gerhard Menzel) and incubated overnight in a drying oven at 60^{o}C (BINDER). Mounted sections were stored in a sealed dark box until use.

2.7.6 Chondrogenic Differentiation Immunohistological Analysis

Chondrogenic pellet sections (see 2.7.5 Chondrogenic Differentiation Pellet Tissue Histology) underwent haematoxylin and eosin (H&E) staining for nuclear and cytoplasmic components for extracellular matrix observation, which was conducted by automation (Shandon Linistain). A series of xylene, graded ethanol and water submersions, deparaffinised and rehydrated

samples. Samples were then stained with haematoxylin, and Scott's tap water, and washed with 1% acid alcohol. Lastly samples were stained with eosin, dehydrated in ethanol, and washed in xylene. Sections were fixed and sealed with cover slips using DPX mounting medium (CellPath, UK).

In addition, chondrogenic pellet sections were examined for collagen type II. Tissue sections were deparaffinised with xylene for 10 minutes, rehydrated in a series of 90%, 70%, 60%, and 40% ethanol for 5 minutes each, and washed with TBS (tris buffered saline) for 5 minutes. Endogenous peroxidase was quenched with 1% v/v H_2O_2 (30% weight in H_2O; Sigma-Aldrich, Inc) in methanol for 40 minutes, and washed in TBS for 5 minutes. Sections were enzymatically treated with 1mg/mL pepsin peptidase (porcine gastric mucosa; Sigma-Aldrich, Inc), 0.1M AcOH and 0.5M NaCl in TBS (pH 2-3) at 37^{o}C for 1 hour, washed in TBS for 5 minutes (enzyme deactivation), followed by treatment with 1mg/mL type I-S hyaluronidase (bovine testes; Sigma-Aldrich, Inc) in TBS at 37^{o}C for 1 hour, and another wash in TBS for 5 minutes. Sections were blocked in 1% BSA fraction V (Fisher Scientific Bioreagent) in TBS for 30 minutes and incubated in 2µg/mL primary antibody collagen type II (mouse CIIC1 supernatant; Developmental Studies Hybridoma Bank) in 1% BSA/TBS, overnight at 4^{o}C. Isotype control used 2µg/mL normal mouse IgG (sc-2025; Santa Cruz Biotechnology, Inc), and antibody exclusion control was 1% BSA/TBS only. Next day, sections were washed three times in TBS for 5 minutes, incubated with 4µg/mL secondary antibody goat anti-mouse IgG-HRP (SC-2005; Santa Cruz Biotechnology, Inc) for 1 hour at room temperature, and washed three times in TBS for 5 minutes for a final time. Peroxidase substrate was developed by 30 minutes incubation with 2mg/mL

AEC (3-Amino-9-ethylcarbazole; Sigma-Aldrich, Inc) in DMF (N,N-Dimethylformamide; Sigma-Aldrich, Inc), with 10mL 10x imidazole buffer solution (1M NaCl, 0.2M citric acid.xH_2O, and 1M imidazole ACS reagent; all Sigma-Aldrich, Inc), plus 80mL ddH_2O, activated by addition of 20µL H_2O_2 (30% weight; Sigma-Aldrich, Inc). Sections were mounted using 10% v/v glycerol/TBS (Sigma-Aldrich, Inc), overlaid with 22x22mm #1 glass square cover slips (VWR International Ltd), and sealed with varnish. All images were captured using Olympus Provis AX70 microscope with Nikon ACT-1 v.2.63 software.

2.7.7 Osteogenic Differentiation Media

For osteogenesis, cells were seeded at $4x10^3/cm^2$ and fed with 10% serum culture medium (see 2.1 Primary Bone Marrow and Dental Pulp Cell Culture) for 5 days. On day 5, osteogenic differentiation medium was started for 21 days. Media was changed every two days, and specimens were collected on day 23 for analysis. Osteogenic medium consisted of 10µM dexamethasone (Sigma-Aldrich, Inc) and 10mM β-glycerophosphate, 0.22µm sterile filtered, in 10% serum culture medium. Non-osteogenic used 10% serum culture medium alone. Cells were cultured using 32mm #1 glass round cover slips (VWR International Ltd) in $3x9.6cm^2$ wells for total RNA extraction, and 13mm #1 glass round cover slips (VWR International Ltd) in $2cm^2$ wells for protein imuunocytochemistry and alizarin red staining.

2.7.8 Osteogenic Differentiation Marker Expression Analysis

Total RNA was extracted from $1.15x10^5$ cells seeded at $4x10^3$ cells/cm^2 after 23 days in culture, for osteogenic expression detection using end-point product and quantitative PCR, in table 2.5 (see 2.5 Reverse Transcription and End-Point Polymerase Chain Reaction for Colony Clones and 2.6 Quantitative-Polymerase Chain Reaction of Colony Clones). Total RNA was analysed from three samples: before differentiation at mid PDL (see table 3.1), and 23-day non-osteogenic and osteogenic differentiation medium (see 2.7.7 Osteogenic Differentiation Media).

2.7.9 Osteogenic Differentiation Alizarin Red Staining

To assess mineralisation of cultured cells, alizarin red S (Sigma-Aldrich, Inc) was used to stain calcium ion deposits within the extracellular matrix. Samples were washed twice with PBS, exposed to 2% w/v alizarin red S/ddH_2O (pH 4.2, 0.5% ammonium hydroxide) for 4 minutes at room temperature with gentle agitation, and washed thrice with ddH_2O or until wash solution was clear of red. Samples were allowed to air dry before acquiring images using Nikon Eclipse TS100 with a Canon P1234 camera.

2.7.10 Osteogenic Differentiation Immunocytochemistry

Cells were washed twice with PBS, fixed in ethanol for 30 minutes, and blocked with 1% BSA/TBS solution for 30 minutes at room temperature. Osteopontin primary goat polyclonal IgG antibody (P-18) (sc-10593; Santa Cruz Biotechnology, Inc) was incubated using 4µg/mL in 1% BSA/TBS for 1 hour at room temperature. Isotype control used 4µg/mL normal goat IgG (sc-2028;

Santa Cruz Biotechnology, Inc), and antibody exclusion control was 1% BSA/TBS only. Cells were washed twice with TBS for 5 minutes, and incubated with 4µg/mL secondary antibody rabbit anti-goat IgG-FITC (sc-2777; Santa Cruz Biotechnology, Inc) in 1% BSA/TBS for 1 hour at room temperature, and lastly washed thrice in TBS for 5 minutes. Glass cover slips were counter-stained with DAPI Vectashield Hard-Set Mounting Medium (Vector Labs) and inverted onto SuperFrost microscope slides (Thermo Scientific Gerhard Menzel). Nuclear DAPI and green-lipid fluorescence was observed at 373nm/456nm and 490nm/520nm wavelengths respectively, using Olympus Provis AX70 microscope with Nikon ACT-1 v.2.63 software.

2.8 Mineralised Tissue-Slab Preparation and Culture

Male Wistar rats, 21-28 days old, were dissected for long-bones from femur, tibia, and fibula, and for tooth lower and upper incisors. Extracted bones and teeth were rid of all external soft tissues, had ends sawed to leave tissue-shaft chamber and were sectioned longitudinally using an IsoMet® low speed saw with a wafering blade 15HC (BUEHLER). Sections were cut two or three times to produce tissue-slabs of 4-5mm length. The internal chamber of tissue-slabs were cleaned of connective-tissues with a disposable 2mm micro-applicator brush (MICROBRUSH® International) and PBS, and placed in 10% antibiotic-antimycotic (Sigma-Aldrich, Inc) in PBS on ice for use immediately, or at -80^{o}C for storage. Within an ABS Class 2 Cabinet (Bioquell UK Ltd), tissue slabs were dabbed dry and placed into a 96-well plate (SARSTEDT) with adhesive carbon tape (Agar Scientific), and immediately seeded with cells at 16x10^{3} cells/cm^{2} in culture medium. Following two days incubation, cell-seeded

tissue-slabs were washed thrice with ddH_2O for 10 minutes, and fixed with 2.5% glutaraldehyde (25% EM grade; Agar Scientific) overnight at 4^oC. Fixed cell-seeded tissue-slabs were then taken for antibody detection or scanning electron microscopy (SEM) analysis. Control tissue-slabs had no cells seeded with culture medium.

2.9 Mineralised Tissue-Slab Antigen Detection

Following fixation of cell-seeded tissue-slabs in 2.5% glutaraldehyde (25% EM grade; Agar Scientific) overnight at 4^oC, endogenous peroxidase was quenched with 1% v/v H_2O_2 (30% weight in H_2O; Sigma-Aldrich, Inc) in TBS for 30 minutes. Slabs were washed twice with TBS and a third time for 5 minutes, before permeabilising with 0.1% Trition-X 100 (Sigma-Aldrich, Inc) in TBS for 15 minutes. Slabs were blocked with 1% BSA/TBS solution for 30 minutes at room temperature, before incubating with proliferating cell nuclear antigen (FL-261) primary rabbit polyclonal IgG antibody (sc-7907; Santa Cruz Biotechnology, Inc) at 4µg/mL in 1% BSA/TBS for 1 hour at room temperature. Isotype control used 4µg/mL Rabbit (DA1E) mAb IgG XP® (#3900; Cell Signaling Technology, Inc), and antibody exclusion control was 1% BSA/TBS only. Slabs were washed twice with TBS for 5 minutes, and incubated with 80ng/mL secondary goat anti-rabbit IgG-HRP antibody (sc-2004; Santa Cruz Biotechnology, Inc) in 1% BSA/TBS for 1 hour at room temperature. Slabs were washed thrice in TBS for 5 minutes, and lastly incubated with TMB (3,3',5,5'-Tetramethylbenzidine; eBioscience, Inc) for 13 minutes, and washed twice with TBS for 5 minutes. Images were immediately captured using Zeiss Axiovert 200M microscope with Improvision® OpenLab™ v4.0.3 software.

2.10 Mineralised Tissue-Slab Scanning Electron Microscopy

Following fixation in 2.5% glutaraldehyde (25% EM grade; Agar Scientific) overnight at 4^{o}C, cell-seeded tissue-slabs were washed thrice with ddH_2O for 10 minutes, and dehydrated in ethanol for 10 minutes each concentration: 30%, 50%, 70%, 80%, 90%, and 95%. The final concentration of 100% ethanol was thrice for 20 minutes. Lastly, samples were exposed to 50% hexamethyldisilazane (HMDS) (Fisher Scientific) in ethanol for 10 minutes, and 100% HMDS twice for 15 minutes and a third time for evaporation overnight. Tissue-slab samples were affixed to 1.2mm aluminium stubs with adhesive carbon tape (both Agar Scientific), gold sputter-coated for 1 minute 20 seconds (15nm/minute at 30mA with 3cm spacing) in an argon gas chamber at 3mb (Edwards Sputter Coater S150B), and viewed under SEM (Hitachi 4800 S, Hitachi High-Technologies Pte Ltd., Singapore).

2.11 Mineralised Tissue Whole-Protein Extraction and Dialysis

Rat bone and tooth tissues were prepared as in section 2.8 Mineralised Tissue-Slab Preparation and Culture, up to point of culture. Next, prepared tissues were separately snap-frozen in liquid nitrogen and powdered with a Freezer/Mill® 6750 (SPEX CertiPrep) for 1 minute at rate 10. Powdered tissue was immediately collected with 10-20mL of 4^{o}C-cold 10% tri-sodium ethylenediaminetetraacetic acid (EDTA) buffer in ddH_2O with 10mM NaOH (both Fisher Scientific) (pH 7.45, AcOH), and put into 33mm width cellulose membrane dialysis tubing (>12kDa cut-off) (Sigma-Aldrich, Inc). Tubing contents was dialysed for 5 days in 10% EDTA buffer with 10mM NaOH, and

3 days in protease inhibitor solution (0.5mM iodoacetic acid, 0.5mM benzamidine, and 0.1mM N-ethylmaleimide) at 4^{o}C with magnetic stirrer for continuous agitation. Dialysed contents was spun at 1600rpm for 30 minutes at 4^{o}C to rid non-soluble proteins, supernatant collected in fresh tubing and dialysed a final time in ddH_2O for a day. Dialysed supernatant was subsequently lyophilised (Edwards Freeze Dryer Modulyo), and referred to as bone matrix extract (BME) and tooth matrix extract (TME).

2.12 Bicinchoninic Acid Protein Assay

Lyophilised protein was suspended in 1-2mL TBS until completely dissolved and kept on ice. Protein concentration was analysed using BCA Protein Assay Kit as per manufacturer protocol (Pierce® Thermo Scientific). Briefly, 25 µL of each protein sample was added to 200µL working reagent alongside BSA standards (20-2000µg/mL) in triplicates and mixed thoroughly on plate shaker for 30 seconds. The plate was incubated at 37^{o}C for 30 minutes, brought to room temperature, and colorimetric absorbance read at 562nm using SPECTROstar Omega plate reader v3 and MARS data analysis software v2.41 (BMG LABTECH). Absorbencies were blank corrected and averaged, and protein concentration calculated using standard curve and polynomial (order 4) equation with Microsoft® Excel® 2013 package.

2.13 Metabolism Assay with Thiazolyl Blue Tetrazolium Bromide

Cells were seeded in 10% culture medium (with or without protein) at $2.8x10^3/cm^2$, $5.7x10^3/cm^2$, $11.4x10^3/cm^2$, $17.1x10^3/cm^2$, or $22.8x10^3/cm^2$, in triplicate wells of a 96-well plate (SARSTEDT) for 1, 2, 3, 5, or 7 days period

of time, before addition of 5mg/mL MTT (Sigma-Aldrich, Inc) in fresh 10% medium for 5 hours. Next, MTT and medium solution was removed and replaced with dimethylsulfoxide (DMSO) for 30 minutes, and colorimetric absorbance was read at 570nm using SPECTROstar Omega plate reader v3 and MARS data analysis software v2.41 (BMG LABTECH). Blank served as MTT in medium without cells. Absorbencies were blank corrected and averaged to plot metabolism over culture time-period. Statistical analyses were conducted using two-way ANOVA and Instat3 statistical package v3.06.

2.14 Sodium Dodecyl Sulphate – Polyacrylamide Gel Electrophoresis

BME and TME protein samples were run in duplicate for Coomassie Brilliant Blue R (Sigma-Aldrich, Inc) and Silver Stain Kit analyses. An amount of 10µg protein sample was lyophilised (Edwards Freeze Dryer Modulyo), mixed with 15µL Laemmli sample buffer (62.5mM Tris-HCl (pH 6.8), 2% SDS, 10% glycerol, 0.5% bromophenol blue, 2.5% β-mercaptoethanol (14.3M)), vortexed for 30 seconds, and centrifuged for 2 minutes at 2.5*g*, 4^{o}C. Protein samples (10µg) were boiled for 5 minutes and centrifuged again. Protein samples were run on 1mm precast polyacrylamide gels (4-15% Mini-PROTEAN® TGX™; Bio-Rad Laboratories, Inc), at 200V for 40 minutes, alongside Kaleidoscope™ Prestained Standard (Bio-Rad Laboratories, Inc). Gel lanes containing standard and protein samples were isolated with a scalpel and subsequently stained.

2.15 Coomassie Brilliant Blue R Protein Staining

Protein sample SDS-PAGE gels were immediately stained using 20% v/v Coomassie Brilliant Blue R (0.25% w/v in 50% v/v methanol; Sigma-Aldrich, Inc), 35% v/v methanol and 10% AcOH v/v for 30 minutes at room temperature. The gel was de-stained using 5% v/v methanol and 7.5 v/v AcOH for 30 minutes and further overnight at room temperature, with constant agitation. Gels were finally washed with ddH_2O to rid all excess coomassie and images were captured using a 3-Megapixel digital camera.

2.16 Protein Silver Stain Kit

A Silver Stain was conducted to detect proteins <100ng, as per manufacturer instructions (Thermo Fisher Scientific, Inc). Briefly, protein sample SDS-PAGE gels were fixed overnight with 50% v/v ethanol and 5% v/v AcOH at room temperature. Gels were washed with ultrapure water (Nanopure Diamond™, Barnstead) five times, each for 20 minutes with agitation. Gels were incubated with Silver working solution for 30 minutes, rinsed in ddH_2O for 20 seconds, incubated in Reducer working solution for 5 minutes, rinsed in ddH_2O for 5 seconds, and lastly incubated in Stabiliser working solution for 40 minutes. Images were captured using a 3-Megapixel digital camera.

Table 2.1: RNA extraction time-points for gene marker expression detection. Tissue: BM, bone marrow; DP, dental pulp; and individual specimen identity. Clone: specific clone name. PDL, population doubling level. Day: *in* vitro culture time. Stage: E, earliest; M, mid; L, late; LR, later.

Tissue	Clone	Passage	PDL	Day	Stage
BM i	1.4	8	12	35	E
		11	16	47	M
		19	32	82	L
		23	42	96	LR
BM i	2.6	7	8	40	E
		16	17	87	M
		23	30	102	L
		31	41	125	LR
BM ii	3.1	10	11	71	E
		15	18	89	M
		25	33	116	L
		30	41	128	LR
DP i	2.7	13	11	128	E
		20	20	161	M
		26	33	179	L
		31	44	191	LR
DP iii	E11	9	10	151	E
		12	19	172	M
		17	32	205	L
		21	41	224	LR
DP iv	F2	7	10	62	E
		11	16	85	M
		18	31	111	L
		23	42	129	LR

Table 2.2: End-point PCR primer sequences, annealing temperature, and cycle number for gene marker expression detection during culture expansion. Special annealing temperature for SOX2: 94°C for 10 minutes, forty cycles of 98°C for 10 seconds, 55°C for 30 seconds and 72°C for 1 minute, and lastly 72°C for 7 minutes.

Official Symbol	Official Full Name	Synonym	Primer Sequence	Annealing Temperature °C	Product Length bp	Designer
Actb	Actin, beta	β-Actin	F: 5'- TGAAGATCAAGATCATTGCTCCTCC-3' R: 5'- CTAGAAGCATTTGCGGTGGACGATG-3'	55/62	108	Sigma-Aldrich, Inc
Ptprc	Protein tyrosine phosphatase, receptor type, C	CD45	F: 5'- CTCACCACACTCACGGCTGCTCCCAGCG-3' R: 5'- GCAGGGCCATTTCGTTGCACCCTCCCAA-3'	62	887-1010	Author
Fgfr1	Fibroblast growth factor receptor 1	CD331	F: 5'- GCCAACAAGACCGTGGCCCTGGGCAGCA-3' R: 5'- TCGGCCAACACCACCTGCCCGAAGCAGC-3'	62	701	Author
Mcam	Melanoma cell adhesion molecule	CD146	F: 5'- GCAGCGCCACGGGTGTGCCAGGAGAGG-3' R: 5'- CCCCACTGTGGTGCTTCTGGGCGGGCT-3'	62	900	Lee CP (Cardiff University)
Msx2	Msh homeobox 2	MSX2	F: 5'- CTTACAGAAACCCAGGTCAAA-3' R: 5'- AGCACAGGTCTATGGAAGG-3'	62	200	Sigma-Aldrich, Inc
Nanog	Nanog homeobox	Nanog	F: 5'- GGGGATTCCTCGCCGATGCCTGCCGTT-3' R: 5'- GGGATACTCCACCGGCGCTGAGCCCTT-3'	55	477	Lee CP (Cardiff University)
Snai1	Snail family zinc finger 1	Snail	F: 5'- GCGAGCTGCAGGACGCGTGTGTGGAGT-3' R: 5'- CGGCAAAGGCACGGTTGCAGTGGGAGC-3'	62	597	Lee CP (Cardiff University)

Sox2	SRY (sex determining region Y)-box 2	SOX2	F: 5'- CAGCATGTCCTACTCGCAGCA -3' R: 5'- GGAACTGGCCTCGGACTTGA -3'	Special	82	(Nozaki and Ohura, 2011)
Vcam1	Vascular cell adhesion molecule 1	CD106	F: 5'- TCCACACTGACGCTGAGCCCTGTGGGTG-3' R: 5'- CTCCGGCATCCTGCAGCTGTGCCTTGCG-3'	62	898	Author
Nt5e	5' nucleotidase, ecto	CD73	F: 5'- TCCCGCGGCTGCTACGGCACCCAAGTG-3' R: 5'- ACCTTGGTGAAGAGCCGGGCCACGCCG-3'	62	204	Alraies A (Cardiff University)
Thy1	Thy-1 cell surface antigen	CD90	F: 5'- CCTGACCCGAGAGAAGAA-3' R: 5'- TGAAGTTGGCTAGAGTAAGGA-3'	55	125	Sigma-Aldrich, Inc
Eng	Endoglin	CD105	F: 5'- CGGTCTCCAGCTGCGGTGGTGGGCTCC -3' R: 5'- CACTGCCACCACGGGCTCCCGCTTGCT-3'	62	896	Lee CP (Cardiff University)

Table 2.3: qPCR primer sequences for quantification of gene marker expression during culture expansion.

Official Symbol	Official Full Name	Synonym	Primer Sequence	Annealing Temperature °C	Product Length bp	Designer
Actb	Actin, beta	β-Actin	F: 5'-TGAAGATCAAGATCATTGCTCCTCC-3' R: 5'-CTAGAAGCATTTGCGGTGGACGATG-3'	55	108	Sigma-Aldrich, Inc
Mcam	Melanoma cell adhesion molecule	CD146	F: 5'-TTCACAAGGAGAGGCAGATA-3' R: 5'-TTGCTCTTACACAGGAACATC-3'	55	163	Sigma-Aldrich, Inc
Msx2	Msh homeobox 2	MSX2	F: 5'-CTTACAGAAACCCAGGTCAAA-3' R: 5'-AGCACAGGTCTATGGAAGG-3'	55	200	Sigma-Aldrich, Inc
Vcam1	Vascular cell adhesion molecule 1	CD106	F: 5'-GAGACTTGAAATGCCTGTGAA-3' R: 5'-CAATCTGAGCGAGCGTTT-3'	55	128	Sigma-Aldrich, Inc

Table 2.4: Adipogenic qPCR primer sequences for quantification of gene marker expression.

Official Symbol	Official Full Name	Synonym	Primer Sequence	Annealing Temperature °C	Product Length bp	Designer
Actb	Actin, beta	β-Actin	F: 5'-TGAAGATCAAGATCATTGCTCCTCC-3' R: 5'-CTAGAAGCATTTGCGGTGGACGATG-3'	55	108	Sigma-Aldrich, Inc
Adipoq	Adiponectin, C1Q and collagen domain containing	Adiponectin	F: 5'-GAATCATTATGACGGCAGCAC-3' R: 5'-CTTGGAGCCAGACTTGGTCTC-3'	55	224	(Ding et al., 2013)
Cebpa	CCAAT/enhancer binding protein (C/EBP), alpha	C/EBPα	F: 5'-GGGAGAACTCTAACTCCCCCAT-3' R: 5'-CTCTGGAGGTGGCTGCTCATC-3'	55	82	Unknown
Cfd	Complement factor D	Adipsin	F: 5'-CCGATGTCCTGCAGCAACT-3' R: 5'-GTCCCTGCGGTTGCTCTCT-3'	55	119	(Searfoss et al., 2003)
Fabp4	Fatty acid binding protein 4, adipocyte	FABP4	F: 5'-GGAATTCGATGAAATCACCCC-3' R: 5'-TGGTCGACTTTCCATCCCACT-3'	55	104	(Georgiou et al., 2012)
Lpl	Lipoprotein lipase	LPL	F: 5'-AGGTCAGAGCCAAGAGAAGCA-3' R: 5'-GGAGTAGGTTTTATTTGTGGCG-3'	55	215	(Li et al., 2012)
Pparg	Peroxisome proliferator-activated receptor gamma	PPARγ	F: 5'-GGAAGCCCTTTGGTGACTTTATGG-3' R: 5'-GCAGCAGGTTGTCTTGGATGTC-3'	55	174	(Ji et al., 2009)

Table 2.5: Osteogenic end-point detection and quantitative PCR primer sequences for gene marker expression.

Official Symbol	Official Full Name	Synonym	Primer Sequence	Annealing Temperature °C	Product Length bp	Designer
Actb	Actin, beta	β-Actin	F: 5'-TGAAGATCAAGATCATTGCTCCTCC-3' R: 5'-CTAGAAGCATTTGCGGTGGACGATG-3'	55	108	Sigma-Aldrich, Inc
Bglap	Bone gamma-carboxyglutamate (gla) protein	Osteocalcin	F: 5'-AAGCCCAGCGACTCTGAGTCT-3' R: 5'-CCGGAGTCTATTCACCACCTTACT-3'	55	75	(Korkalainen et al., 2009)
Ibsp	Integrin-binding sialoprotein	BSP	F: 5'-CAGAAAGAGCAGCACGGTTG-3' R: 5'-CCTCGTAGCCTTCATAGCCA-3'	55	173	(Li et al., 2012)
Runx2	Runt-related transcription factor 2	Cbfa1	F: 5'-GCCACCTTCACTTACACCCC-3' R: 5'-CGCTGACGAAGTACCATAGTAGAG-3'	55 (end-point)	171	(Li et al., 2012)
Sp7	Sp7 transcription factor	Osterix	F: 5'-GCTTTTCTGTGGCAAGAGGTTC-3' R: 5'-CTGATGTTTGCTCAAGTGGTCG-3'	55 (end-point)	136	(Georgiou et al., 2012)
Sparc	Secreted protein, acidic, cysteines-rich	Osteonectin	F: 5'-CCTGTGGAGCTGCTGGCCCGAGACTTTG -3' R: 5'-CAGTGGGGCCAGCTCCGTGTGGGACAGGTA-3'	55	132	(Suzuki et al., 2002)
Spp1	Secreted phosphoprotein 1	Osteopontin	F: 5'-TCCAAGGAGTATAAGCAGAGGGCCA-3' R: 5'-CTCTTAGGGTCTAGGACTAGCTTGT-3'	55	200	(Kawashima et al., 1999)

Chapter 3

Characterisation of Bone Marrow and Dental Pulp Mesenchymal Stromal Cell Clones

3.1 Introduction

Over the past few decades there has been increasing focus upon autologous adult mesenchymal progenitor stromal cells for use in tissue engineering and regenerative medicine, from sources such as bone marrow (Pittenger et al., 1999), dental pulp (Zhang et al., 2006), adipose tissue (Zuk et al., 2002), cartilage (Peng et al., 2008), muscle (Jackson et al., 2011) and umbilical cord blood (Zhang et al., 2011), due to their multi-potent differentiation ability along adipogenic, chondrogenic and osteogenic lineages. Since their isolation from bone marrow stroma (Friedenstein et al., 1976), bone marrow stromal cell (BMSC) progenitors have become the “gold” standard source for tissue engineering applications, and comparison of other mesenchymal sources (Prockop, 1997). Owing to morbidity associated with their collection and low cell-harvest, however, alternative sources have been sought (Huang et al., 2009). Dental pulp stromal cell (DPSC) progenitors are a proposed alternative source of mesenchymal progenitors due to their self-renewing capacity, displayed high clonogenicity and proliferation, and similar immuno-phenotype compared to BMSCs (Gronthos et al., 2000). In addition, DPSCs displayed capacity for multi-lineage differentiation potential (Gronthos et al., 2002). The focus, in this chapter, is to assess how the standard BMSC and alternative DPSC tissue sources compare, and how they can contribute to bone-tissue regeneration, specifically for the orofacial region due to congenital abnormality

and following trauma or tumor resection, which is an unmet clinical need (as reviewed (Mao and Prockop, 2012)).

As with BMSCs (Gronthos et al., 2003), DPSC colonies can be isolated and propagated at a clonal level, albeit limitedly. DPSCs displayed heterogeneity in their proliferative abilities, with 80% having displayed less than 20 population doublings, and only a limited number of clones successfully propagated to more than twenty population doublings for characterisation; of which only 67% were capable of abundant ectopic dentin formation (Gronthos et al., 2002). Bone marrow tissue is also heterogeneous in nature, with high proliferation and multipotential differentiation displayed by an unidentifiable phenotype-subset of BMSC progenitor clones, while other clones are lineage restricted (Satomura et al., 2000). Likewise, BMSCs displayed less than 20 population doublings in 83% of clones, and 54% of which form mineralised bone tissue (Gronthos et al., 2003). Such clonogenic features, could identify a “pure” population of mesenchymal stromal cell progenitors and lead to characterisation, by way of a favorable “fingerprint”, which thus far remains elusive (Bianco et al., 2001). Such heterogeneity amongst stromal cell clones highlights the hierarchical nature of stem cells and progenitors, in adult somatic tissues: within this model, clones that form large colonies are closely related to the mother stem cell and could be considered as multipotent progenitor cells, and clones that form smaller colonies are further-down the stem cell hierarchy and could be considered as lineage-restricted transit-amplifying (TA) cells (Chan et al., 2004) (see Chapter 1, figure 1.1). Clonal analysis is paramount, due to mesenchymal stromal cell (MSC) population heterogeneity

that suggests only 20-30% of the total cell population is truly multipotent, with the remaining population representing bi- or uni- potential, which are non-distinguishable by morphology or MSC marker expression (Abdallah and Kassem, 2012). Further, heterogeneous MSC populations from the bone marrow and dental pulp displayed very similar immuno-phenotypes (Huang et al., 2009) and only a few differentially expressed genes out of 4000 (Shi et al., 2001), which underlines need for analysis of tissue sources at a clonal level.

Isolation of MSC clones, for the majority, is accomplished by plastic adherence, as defined by the minimal criteria of mesenchymal stem cells (Dominici et al., 2006). Alternative techniques, however, use isolation on the basis of cell-surface markers, but showed cells with similar capabilities (Gronthos et al., 2003). Within this thesis, fibronectin adherence was used to select for stem cells progenitors expressing the α5/β1 integrin receptor (Dowthwaite et al., 2004), which were highly clonogenic and proliferative, compared to lower-expression by transit-amplifying cells (Jones and Watt, 1993). This has led to successful isolation of clones at a high efficiency, following protocol optimisation, and lends reliability of such a technique for analysis of clones from homogeneous tissue sources.

This research chapter focus and aims are to compare the stem cell characteristics of BMSCs against DPSCs using clonal populations, rather than whole tissue, so as to better characterise and phenotype these progenitor tissue sources: analysing clonogenicity by colony forming efficiency (CFE),

proliferation by population doubling level (PDL), and cell-surface marker phenotype by observing and quantifying specific marker expression.

3.2 Materials and Methods

Bone marrow and dental pulp stromal cell clones were isolated from 21-28 day old male Wistar rats, using fibronectin adherence (see 2.1 Primary Bone Marrow and Dental Pulp Cell Culture). The colony forming efficiency (CFE) was analysed by counting colonies up to 12 days *in vitro* and calculated as a proportion of the original cell number seeded. The CFE was analysed using three set parameters, based on seeding density and serum concentration: 4000 cells/cm^2 in 10% serum, 2000 cells/cm^2 in 20% serum, and 4000 cells/cm^2 in 20% serum. Successfully isolated clones were culture expanded *in vitro* to observe proliferation potential (see 2.2 Colony-Forming Efficiency and Population Doubling Level). Three progenitor clones from each tissue source were further analysed and characterised. Following culture expansion, up to approximately 40 population doublings, the six progenitor clones had their *in vitro* growth curve replicative ability analysed, by culturing and expanding progenitors a second time, following cryopreservation. During culture expansion total RNA was isolated at defined time-points (see table 2.1), to assess presence and maintenance of stem cells markers using end-point PCR and quantitative PCR (see sections 2.5 Reverse Transcription and End-Point Polymerase Chain Reaction for Colony Clones, and 2.6 Quantitative-Polymerase Chain Reaction of Colony Clones). In addition, cell senescence was monitored during culture by blue β-Galactosidase staining (see 2.4 β-Galactosidase Stain for Cell Senescence).

3.3 Results

3.3.1 Progenitor Colonies from Bone Marrow and Tissues Dental Pulp

Single-cell progenitor colonies (>32 cells) formed successfully on fibronectin for both tissues sources. Figure 3.1 shows typical morphological appearance of clonal colonies from dental pulp and bone marrow, 12 days post-seeding. Progenitors from both tissue types appeared healthy with haloed edges. Cells had a rounded appearance at the centre of the colony and a more flattened and spread shape at the border where the colony was expanding. Bone marrow formed larger cell-compact colonies harbouring higher cell numbers compared to dental pulp. On average, by day 12 post-isolation and seeding, bone marrow formed colonies with an average $3.3x10^3$ cells, whereas dental pulp formed colonies $<1.5x10^3$ cells. Based on the total number of cells seeded and fibronectin-formed colonies at day 12, the percentage of progenitor cells from each source was calculated as <0.0001% and <0.001% for bone marrow and dental pulp (*n*=3), respectively.

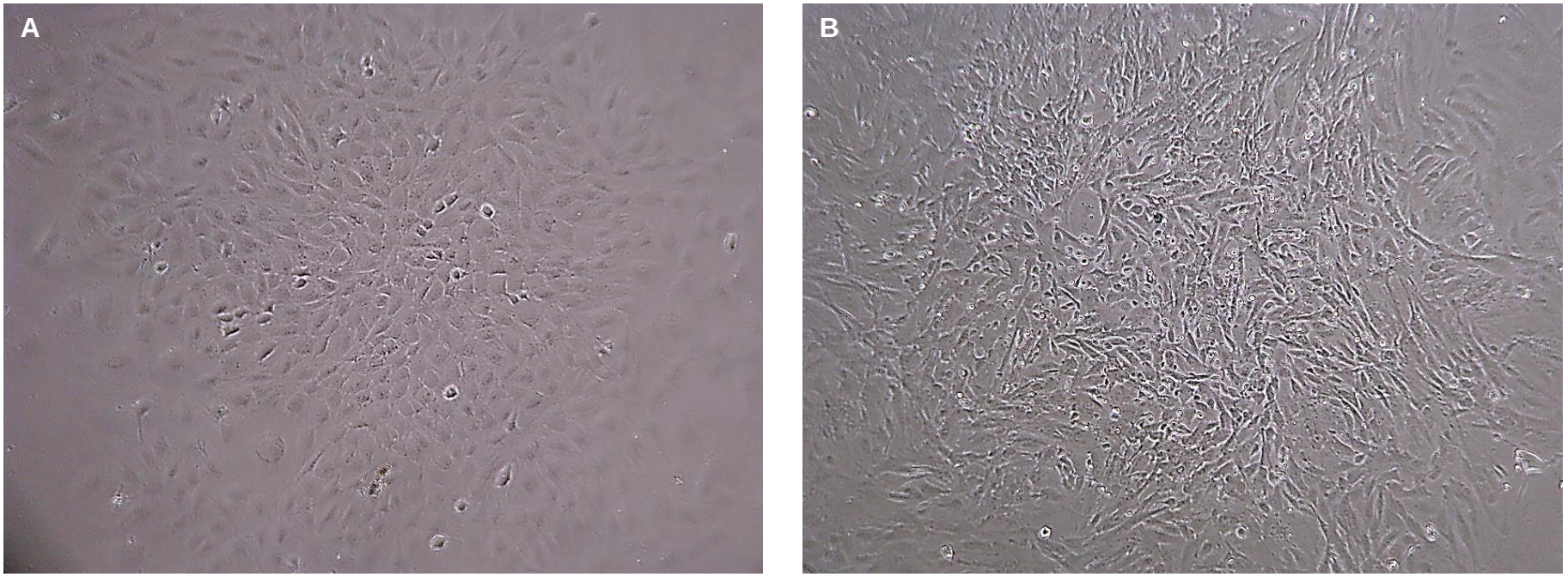

Figure 3.1: Representative phase micrographs of high-density colony for dental pulp (A) and bone marrow (B) mesenchymal progenitors 12 days post-seeding. Morphological appearance of progenitors appeared healthy with haloed edges. Cells had a rounded appearance at the centre of the colony, and a more flattened and spread-shape at the border where the colony was expanding.

3.3.2 Colony-Forming Efficiency of Bone Marrow and Dental Pulp Progenitors

The overall average colony forming efficiency (CFE) of dental pulp progenitors was twelve times greater than bone marrow progenitors over the twelve-day culture period (figure 3.2). At the three seeding densities and serum concentrations set, dental pulp formed higher colony numbers compared to bone marrow. Optimal colony formation occurred when cells were seeded at 4000 cells/cm^2 in 20% serum. At 4000 cells/cm^2 in 10% serum the bone marrow failed to form any colonies. Using the optimal seeding density and serum concentration, the CFE of dental pulp and bone marrow, was 0.088±0.033 and 0.007±0.006 at day 12 (*n*=3), respectively (figure 3.2).

The statistical analysis of CFE for bone marrow and dental pulp tissue during twelve-day *in vitro* culture following isolations is detailed in figure 3.3 (see legend). No significant differences existed between bone marrow for all cell seeding density and serum concentration parameters set. Only by day 10, did the CFE of dental pulp progenitors become significantly higher than bone marrow progenitors ($P<0.05$), which became extremely significant by day 12 ($P<0.001$). Likewise, only by and after 10 days culture was a significant difference ($P<0.05$) between dental pulp progenitor parameters evident, which became extremely significant by day 12 ($P<0.001$) (figure 3.3). As such, a 12 day culture period is required to achieve maximum CFE.

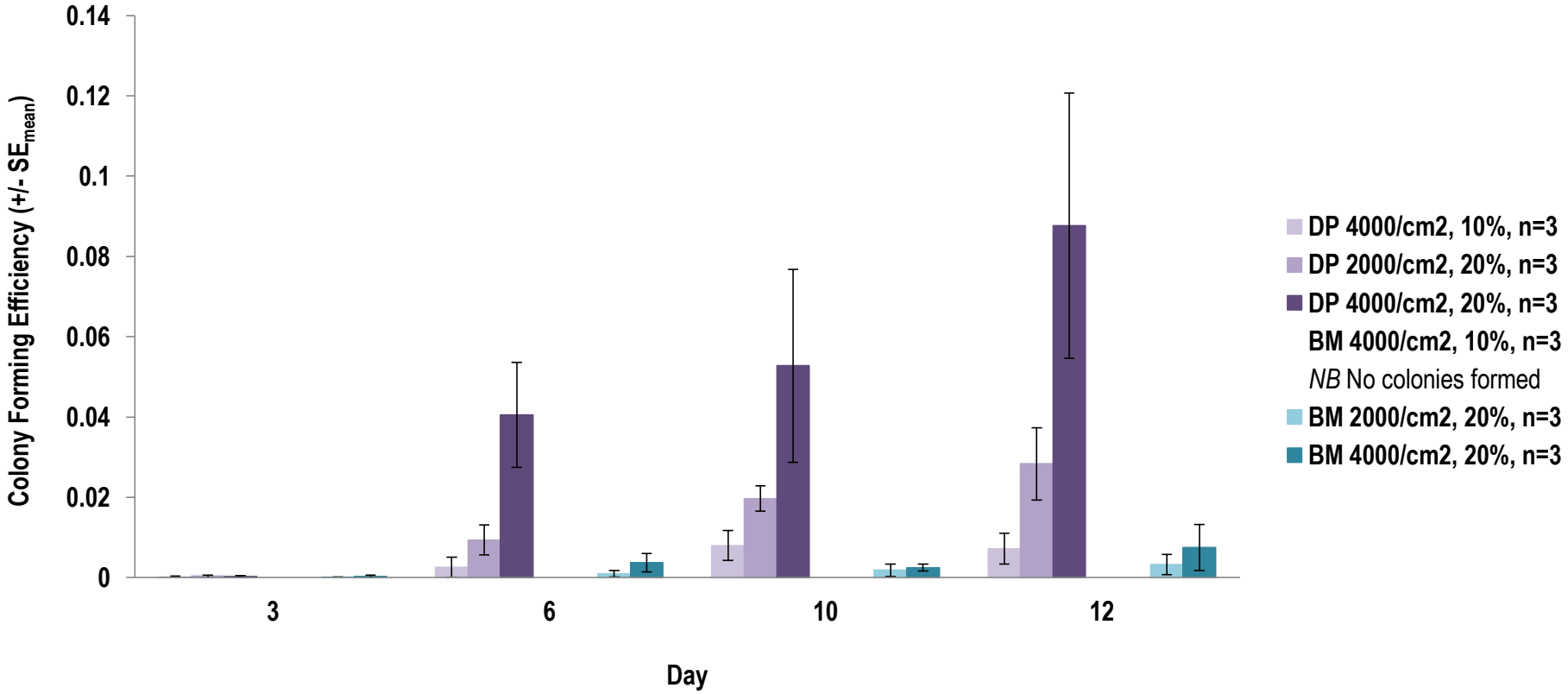

Figure 3.2: The colony forming efficiency (CFE) of bone marrow and dental pulp tissue isolations during twelve-day *in vitro* culture. Dental pulp progenitors formed more colonies compared to bone marrow progenitors and the overall average CFE of dental pulp was thirteen times greater than bone marrow across twelve-days culture for each parameter set: $4x10^3$ cells/cm^2 in 10% serum, $2x10^3$ and $4x10^3$ cells/cm^2 in 20% serum. For bone marrow seeded at 4000 cells/cm^2 in 10% serum, colonies failed to form. The optimal CFE occurred at 4000 cells/cm^2 in 20% serum. Statistical analysis in figure 3.3.

		Day 3						Day 6						Day 10						Day 12					
		DP 4x10^3 in 10% FBS	DP 2x10^3 in 20% FBS	DP 4x10^3 in 20% FBS	BM 4x10^3 in 10% FBS	BM 2x10^3 in 20% FBS	BM 4x10^3 in 20% FBS	DP 4x10^3 in 10% FBS	DP 2x10^3 in 20% FBS	DP 4x10^3 in 20% FBS	BM 4x10^3 in 10% FBS	BM 2x10^3 in 20% FBS	BM 4x10^3 in 20% FBS	DP 4x10^3 in 10% FBS	DP 2x10^3 in 20% FBS	DP 4x10^3 in 20% FBS	BM 4x10^3 in 10% FBS	BM 2x10^3 in 20% FBS	BM 4x10^3 in 20% FBS	DP 4x10^3 in 10% FBS	DP 2x10^3 in 20% FBS	DP 4x10^3 in 20% FBS	BM 4x10^3 in 10% FBS	BM 2x10^3 in 20% FBS	BM 4x10^3 in 20% FBS
Day 3	DP 4x10^3 in 10% FBS				na						na					*	na					***	na		
	DP 2x10^3 in 20% FBS				na						na					*	na					***	na		
	DP 4x10^3 in 20% FBS				na						na					*	na					***	na		
	BM 4x10^3 in 10% FBS										na						na						na		
	BM 2x10^3 in 20% FBS				na						na						na						na		
	BM 4x10^3 in 20% FBS				na						na						na						na		
Day 6	DP 4x10^3 in 10% FBS				na						na						na					***	na		
	DP 2x10^3 in 20% FBS				na						na						na					***	na		
	DP 4x10^3 in 20% FBS				na						na						na					*	na		
	BM 4x10^3 in 10% FBS				na												na						na		
	BM 2x10^3 in 20% FBS				na						na						na						na		
	BM 4x10^3 in 20% FBS				na						na						na						na		
Day 10	DP 4x10^3 in 10% FBS				na						na						na					***	na		
	DP 2x10^3 in 20% FBS				na						na						na					***	na		
	DP 4x10^3 in 20% FBS				na	*	*				na	*					na	*					na		
	BM 4x10^3 in 10% FBS				na						na												na		
	BM 2x10^3 in 20% FBS				na						na						na						na		
	BM 4x10^3 in 20% FBS				na						na						na						na		
Day 12	DP 4x10^3 in 10% FBS				na						na						na					***	na		
	DP 2x10^3 in 20% FBS				na						na						na					***	na		
	DP 4x10^3 in 20% FBS				na	***	***				na	***	***				na	***	***				na	***	***
	BM 4x10^3 in 10% FBS				na						na						na								
	BM 2x10^3 in 20% FBS				na						na						na						na		
	BM 4x10^3 in 20% FBS				na						na						na						na		

Figure 3.3: Statistical analysis of colony forming efficiency of bone marrow and dental pulp tissue isolations during twelve-day *in vitro* culture. By day 12, the CFE of dental pulp progenitors seeded at $4x10^3$ cells/cm^2 in 20% serum, was significantly (P<0.001) higher than bone marrow progenitors at 3, 6, 10 and 12 days seeded at $2x10^3$ cells/cm^2 and $4x10^3$ cells/cm^2 in 20% serum. In addition, by day 12, the CFE of dental pulp progenitors seeded at $4x10^3$ cells/cm^2 in 20% serum, was significantly (P<0.05) higher than dental pulp progenitors at all seeding and serum concentrations on days 3 and 6, and significantly (P<0.001) higher than $4x10^3$ cells/cm^2 in 10% serum and $2x10^3$ cells/cm^2 in 20% serum on days 10 and 12. * = P<0.05, ** = P<0.01, *** = P<0.001. na, no colonies.

3.3.3 Population Doubling of Bone Marrow and Dental Pulp Progenitor Clones

Once isolated the bone marrow and dental pulp clones were culture expanded and population doubling levels (PDLs) were recorded (figure 3.4 and 3.5). The isolation of bone marrow clones was initially more successful than dental pulp, with ~54% of bone marrow clones successfully propagated, as opposed to <10% of dental pulp clones. Each growth line represents a progenitor clone and each symbol a passage point, with a total eight BMSC clones isolated, and a total ten DPSC clones. Whereas DPSCs had a higher colony forming efficiency, the population doubling level of DPSC clones was on average 1.5 times slower than BMSCs. In addition, the population doubling levels of DPSCs was more variable compared to BMSCs. The fastest proliferating clone for bone marrow was progenitor BM 1.4 that reached PDL 42 by 96 days, and the slowest was BM 1.2 that reached PDL 36 by 174 days, with clones achieving PDL 40 within an approximate 84 day range (figure 3.4). For DPSCs, the fastest proliferating clone was DP A4 that reached PDL 41 by 114 days, and the slowest was DP C5 that reached PDL 41 by 245 days, with all clones achieving PDL 40 within an approximate 131 day range (figure 3.5). To note, isolated clonal BMSCs are capable of up to 61 PDLs in 149 days (figure 3.6). An additional two clones, BM 2.1 and BM 2.6, were allowed to propagate further before cryopreservation, and achieved PDL 65 in 189 days and PDL 54 in 145 days, respectively. Speculatively, if allowed to propagate, all other isolated clones would have probably reached this higher PDL, as none showed signs of decreased PDL or senescence (figure 3.7). Most clones, however,

were halted in culture upon achieving a PDL of 40, as progenitors of primitive age was desirable to use for analysis herein.

All clones appeared to go through a period of plateau between days 40 and 163, but following this period, clones continued to increase their population doubling level. During culture, clones remained healthy (figure 3.7A), however, for clones that displayed an intermittent plateau of PDL <0.5 a week, a β-galactosidase stain (figure 3.7B) was conducted and levels were determined as <2% of the total population. Lack of staining excluded the possibility of senescence, particularly as population doubling levels proceeded to increase following plateau (figures 3.4 and 3.5).

Once a minimum of $1.3x10^6$ cells was achieved, each progenitor clone was cryopreserved for later use. Following highlight of such an intriguing feature of plateau growth patterns, the reproducibility of progenitor proliferation profiles was analysed. Three clones from each tissue source were chosen and were additionally propagated to establish a second proliferation curve, for comparison to the initial PDL growth curve. The progenitor clones (within this thesis these six clones were analysed herein, see table 2.1), were thawed following cryopreservation. Progenitor clones from bone marrow (figure 3.8) and dental pulp (figure 3.9) displayed remarkably similar proliferation curves following cryopreservation compared to their original proliferation curve following isolation. Progenitor clone DP F2, produced a virtually identical second PDL growth curve as for the initial PDL profile. While, the second PDL for progenitor clones BM 1.4, BM 3.1, and DP E11, produced a strikingly similar growth curve that mirrored the initial PDL achieved, albeit at a somewhat lower rate. Interestingly, the second PDL growth profile for progenitor clone DP 2.7,

followed an almost identical growth profile from the beginning of the second PDL curve at day 132 until day 155, after which point the second PDL curve proceeded as other clones at a mirrored lower rate. For progenitor clone BM 2.6, however, the second PDL overtook the initial PDL growth profile following intersection at day 97, and thereafter proceeded at a rate above the original, reaching PDL 40 by 136 days compared to PDL 39 by 145 days for the initial PDL. Nevertheless, over the 66 day period, the second growth curves reproduced, only deviated by 15% from the initial PDL growth profile. In essence, for every clone from each tissue source, both PDL growth profiles were very similar and lends support to culture conditions' reproducibility and efficiency for cell maintenance, following generation of sufficient cell numbers for cryopreservation.

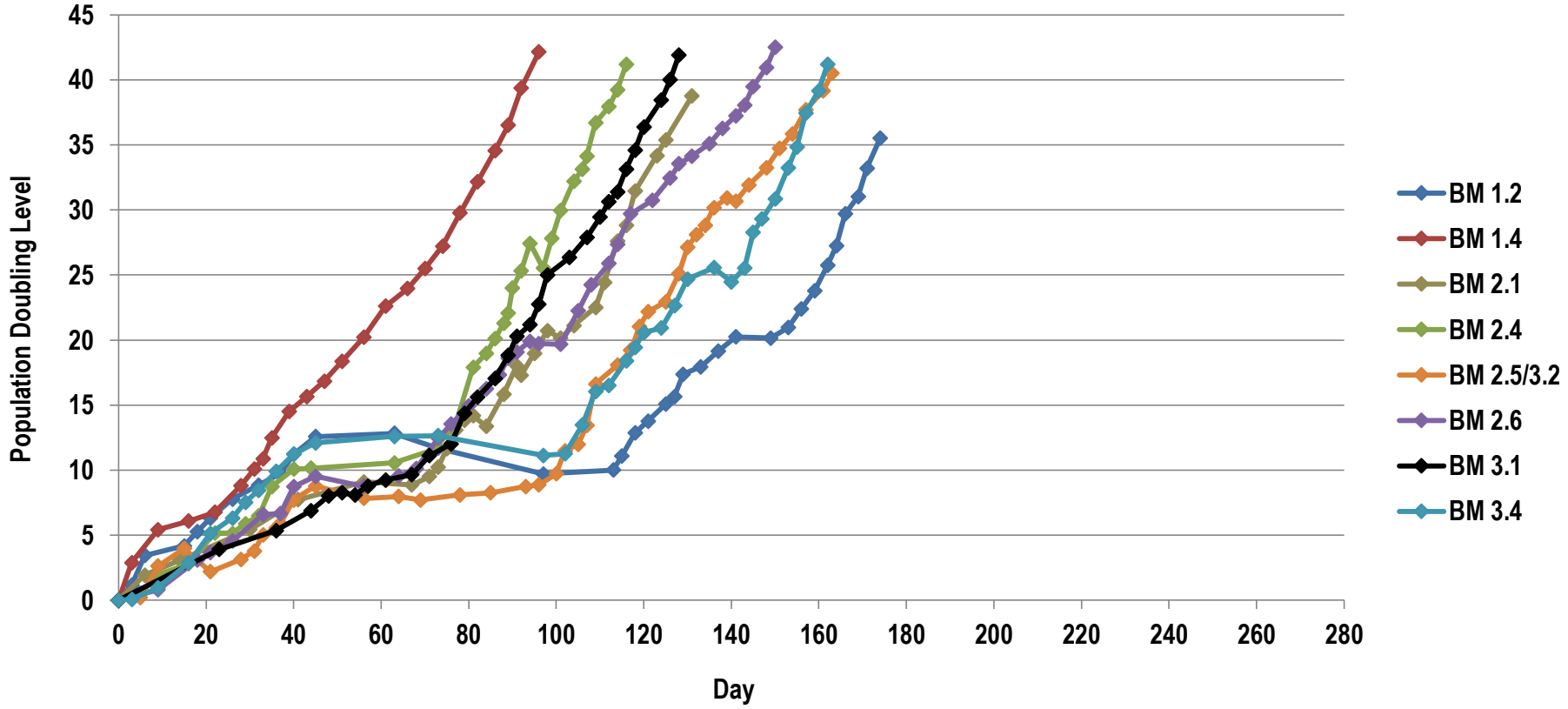

Figure 3.4: Population doublings of bone marrow progenitor clone colonies during *in vitro* culture. Bone marrow clones were successfully propagated for ~50% of colonies isolated, up to PDL 40. All clones except one, BM 1.4, displayed a plateau period between days 40-113, however, successively clones continued to expand during *in vitro* culture. On average progenitor clones reached PDL 40 within 142 days. Each line represents a progenitor clone and each symbol a passage point. BM, bone marrow; #.#, progenitor clone identity.

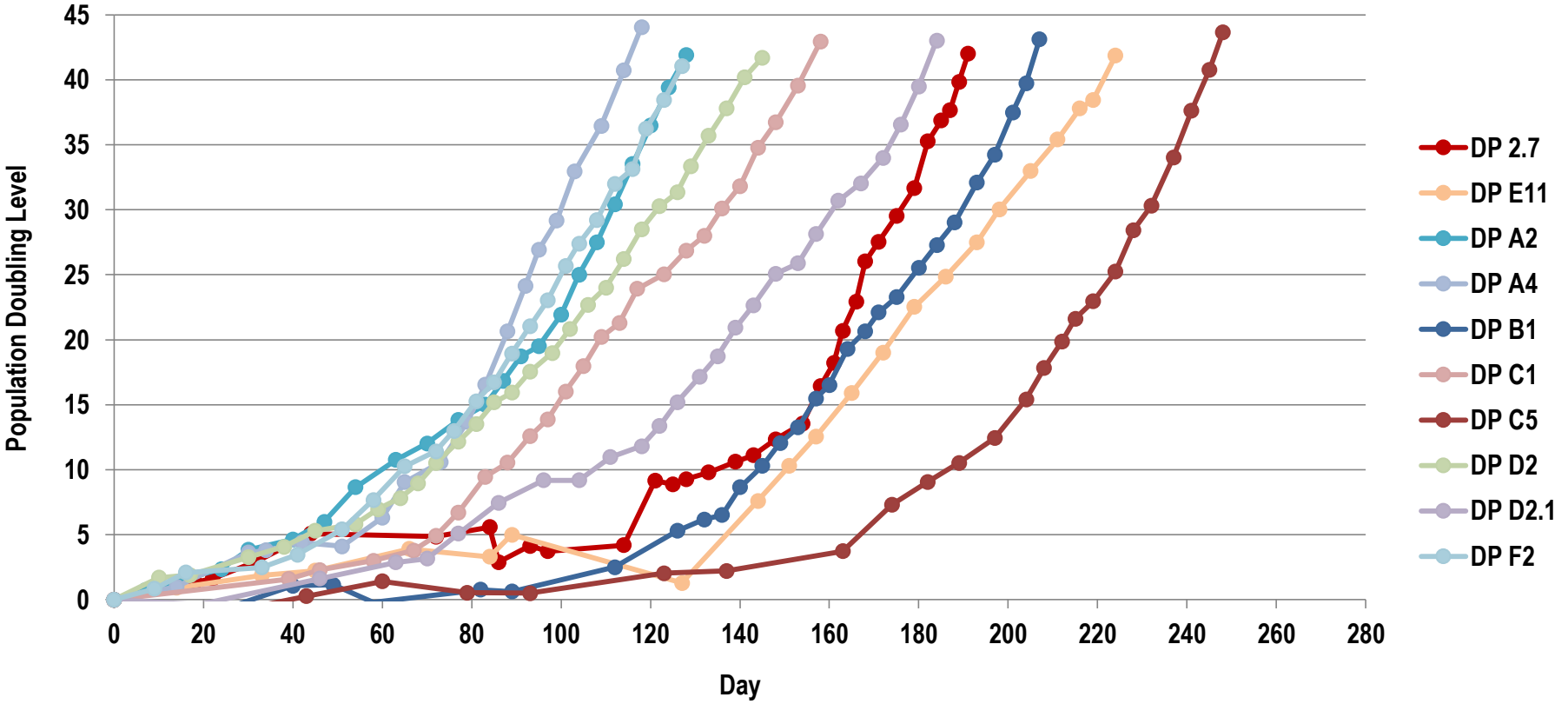

Figure 3.5: Population doublings of dental pulp progenitor clone colonies during *in vitro* culture. Dental pulp clones were successfully propagated for <10% of colonies isolated, up to PDL 40. More than half of the clones successfully isolated, displayed a plateau period between days 40-163, however, successively clones continued to expand during *in vitro* culture. On average progenitor clones reached PDL 40 within 171 days. Each line represents a progenitor clone and each symbol a passage point. DP, dental pulp; #.# or letter #.#, progenitor clone identity.

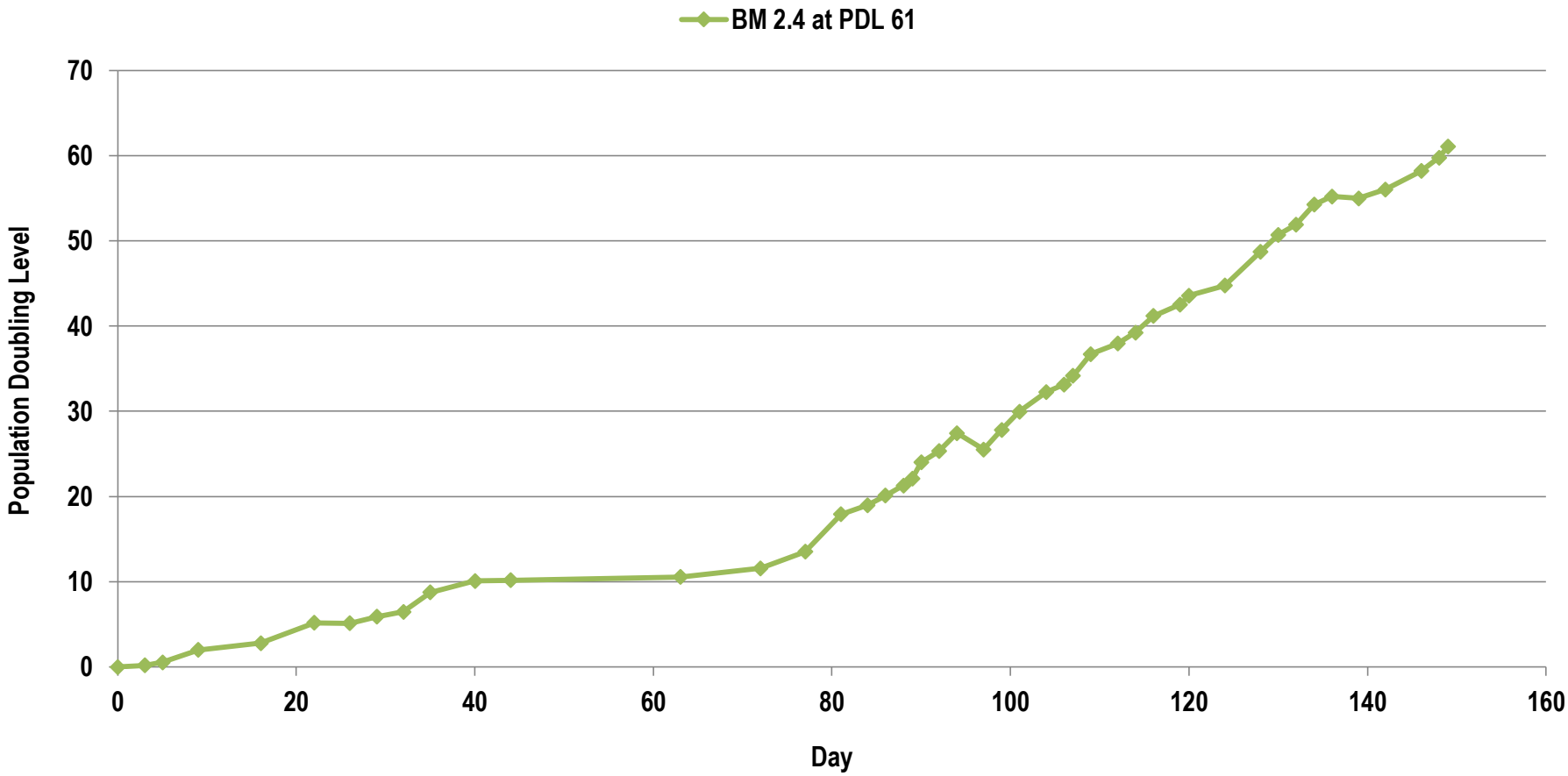

Figure 3.6: Population doublings of progenitor clone BM 2.4 during *in vitro* culture. The bone marrow clone successfully propagated up to PDL 61 in 149 days, which was three times more than that reported by others. The clone was halted in culture at PDL 61 as progenitors of immature age was desirable for use herein.

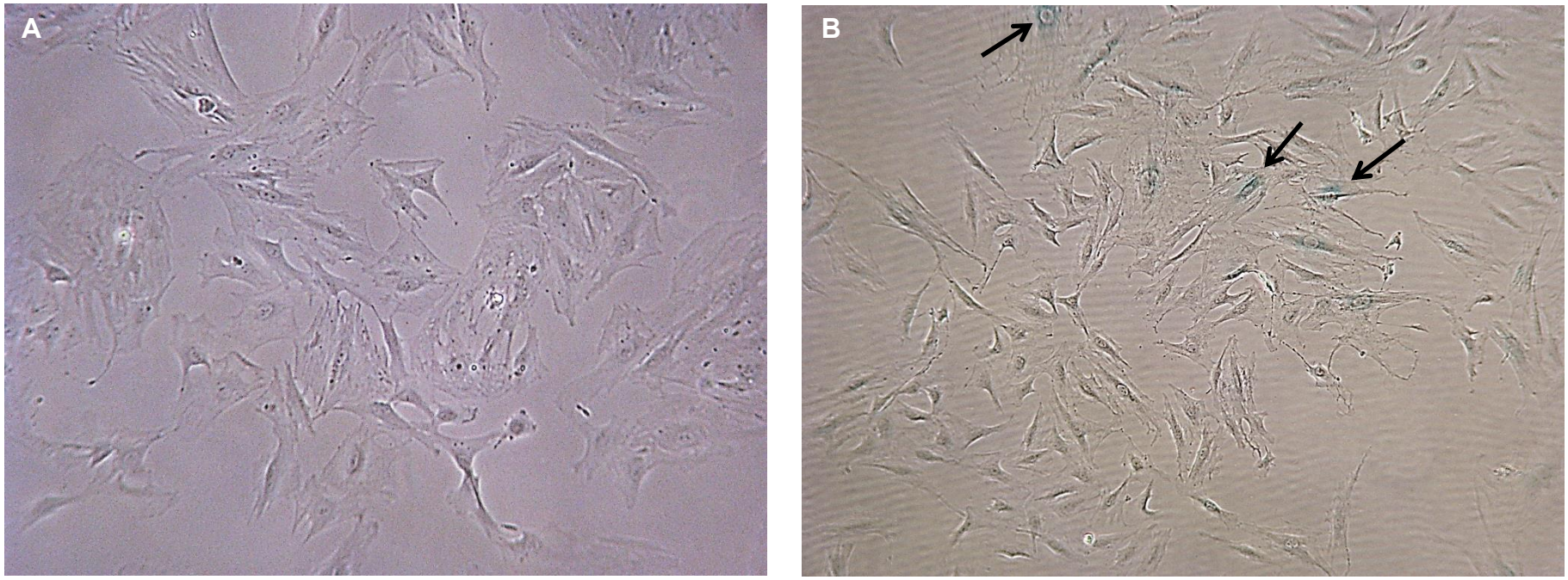

Figure 3.7: Representative micrographs of a typical progenitor clone (A) and after β-galactosidase staining (B). β-galactosidase staining was weak and <2% of progenitor populations. This excluded cell senescence during population doubling plateau in clones, which displayed a PDL of <0.5 per week (see figures 3.4 and 3.5). β-galactosidase was seen as blue staining within cells (arrows in B).

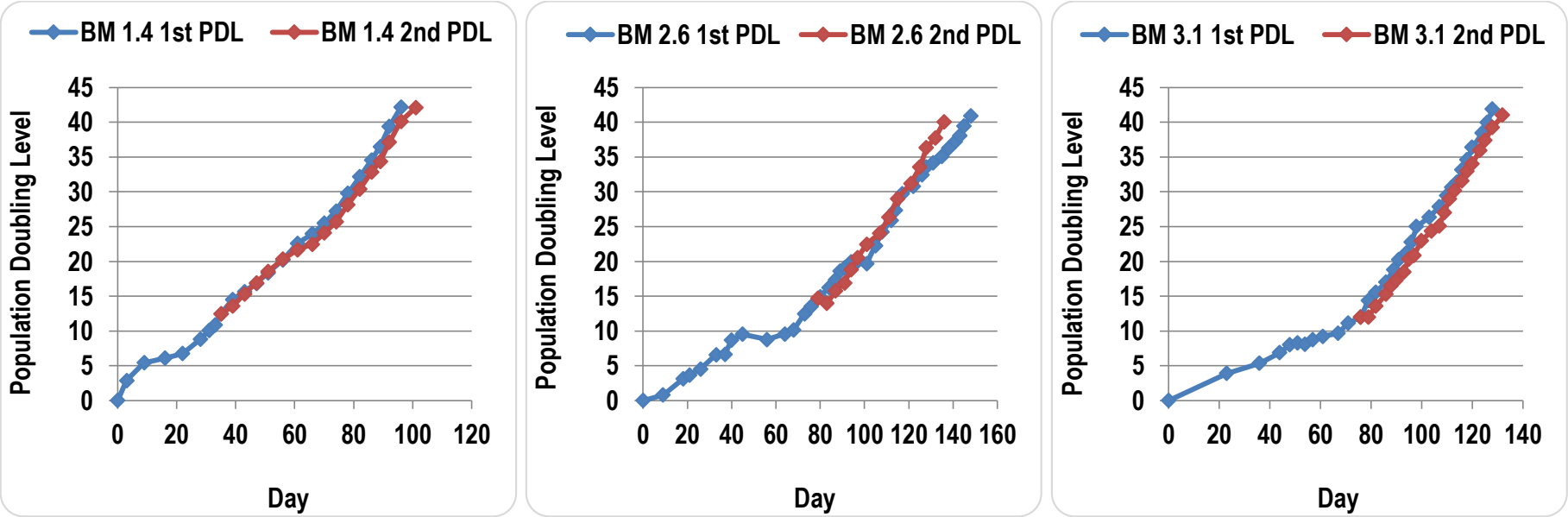

Figure 3.8: Progenitor clones BM 1.4, BM 2.6, and BM 3.1 during *in vitro* culture expansion displayed strikingly similar proliferation curves following cryopreservation for 20 months, 12 months, and 1 month, respectively. The two PDL profiles shown are: following isolation and continual primary culture up to ~40 PDLs (blue), and the same clone having been cryopreserved, thawed, and re-seeded in standard culture conditions (red). BM 1.4, first PDL was 42 in 96 days and second PDL was 42 in 101 days, cultured from day 35. BM 2.6, first PDL was 40 in 136 days and second PDL was 41 in 148 days, cultured from day 79. And BM 3.1, first PDL was 42 in 128 days and second PDL was 41 in 132 days, cultured from day 76.

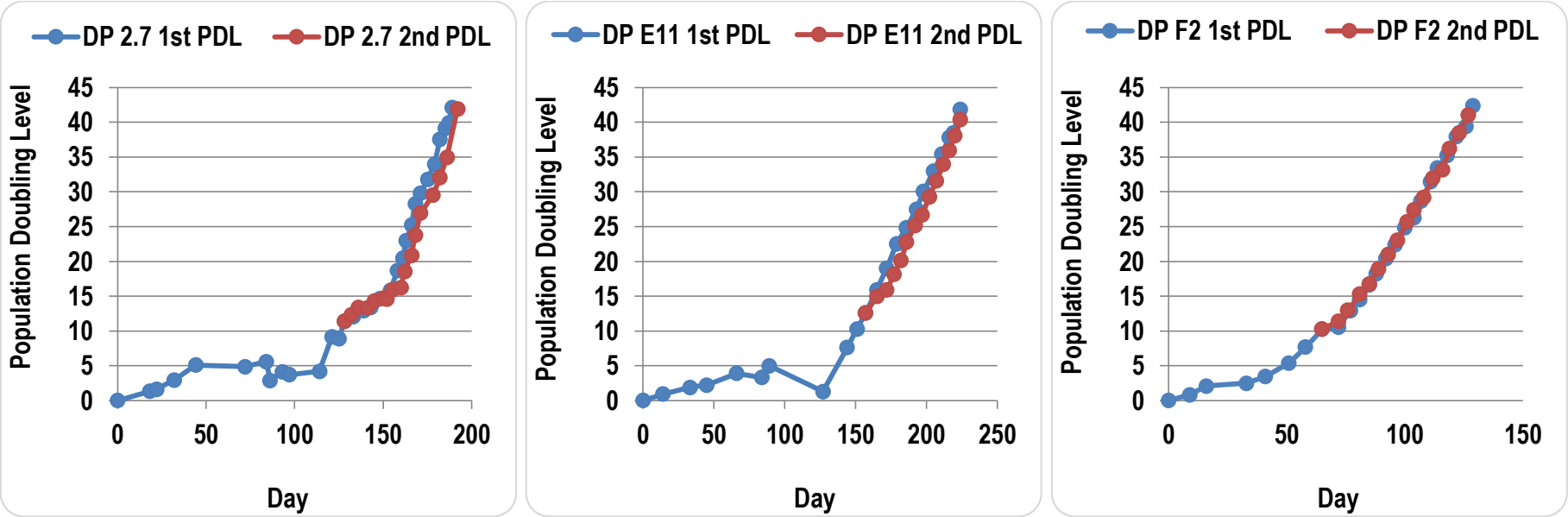

Figure 3.8: Progenitor clones DP 2.7, DP E11, and DP F2 during *in vitro* culture expansion displayed strikingly similar proliferation curves following cryopreservation for 5 months, 18 days, and 10 days, respectively. The two PDL profiles shown are: following isolation and continual primary culture up to ~40 PDLs (blue), and the same clone having been cryopreserved, thawed, and re-seeded in standard culture conditions (red). DP 2.7, first PDL was 42 in 189 days and second PDL was 42 in 192 days, cultured from day 128. DP E11, first PDL was 42 in 224 days and second PDL was 40 in 224 days, cultured from day 157. And DP F2, first PDL was 42 in 129 days and second PDL was 41 in 127 days, cultured from day 65.

3.3.4 Culture Expansion Morphology

Micrographs of all six progenitor clones was qualitatively assessed visually, during *in vitro* culture at earliest, mid, late, and later PDL time points (see table 2.1). For bone marrow and dental pulp progenitors, representative micrographs showed that at the four defined time-points, during the period of forty PDLs in culture, the morphological appearance of clones remained unchanged. Progenitor clones maintained their individual cell-pattern, with clearly distinguished nuclei, cell bodies and borders. Bone marrow progenitor clones had a characteristic cobble-stone appearance and were similar to each other (figure 3.14). Dental pulp progenitor clones DP 2.7 and DP E11, had a more stellate characteristic, while DP F2 displayed a rather dendritic appearance (figure 3.15).

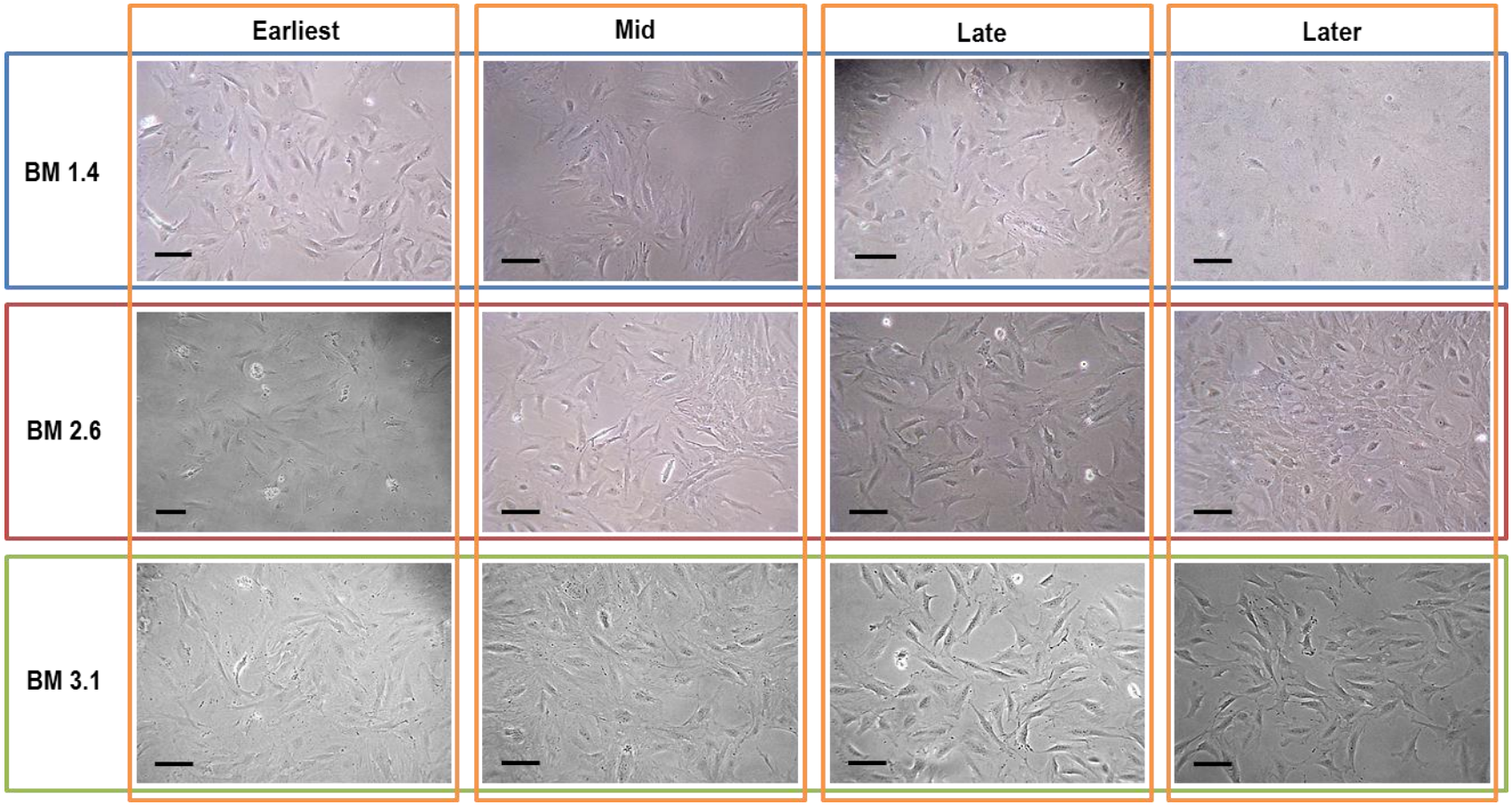

Figure 3.14: Representative micrographs of bone marrow clone progenitors during *in vitro* culture at earliest, mid, late, and later PDL time points. For the period of forty PDLs in culture, the morphological appearance of clones remained unchanged with clearly distinguished nuclei, cell bodies and borders (see main text for details). Scale bar, 100µm.

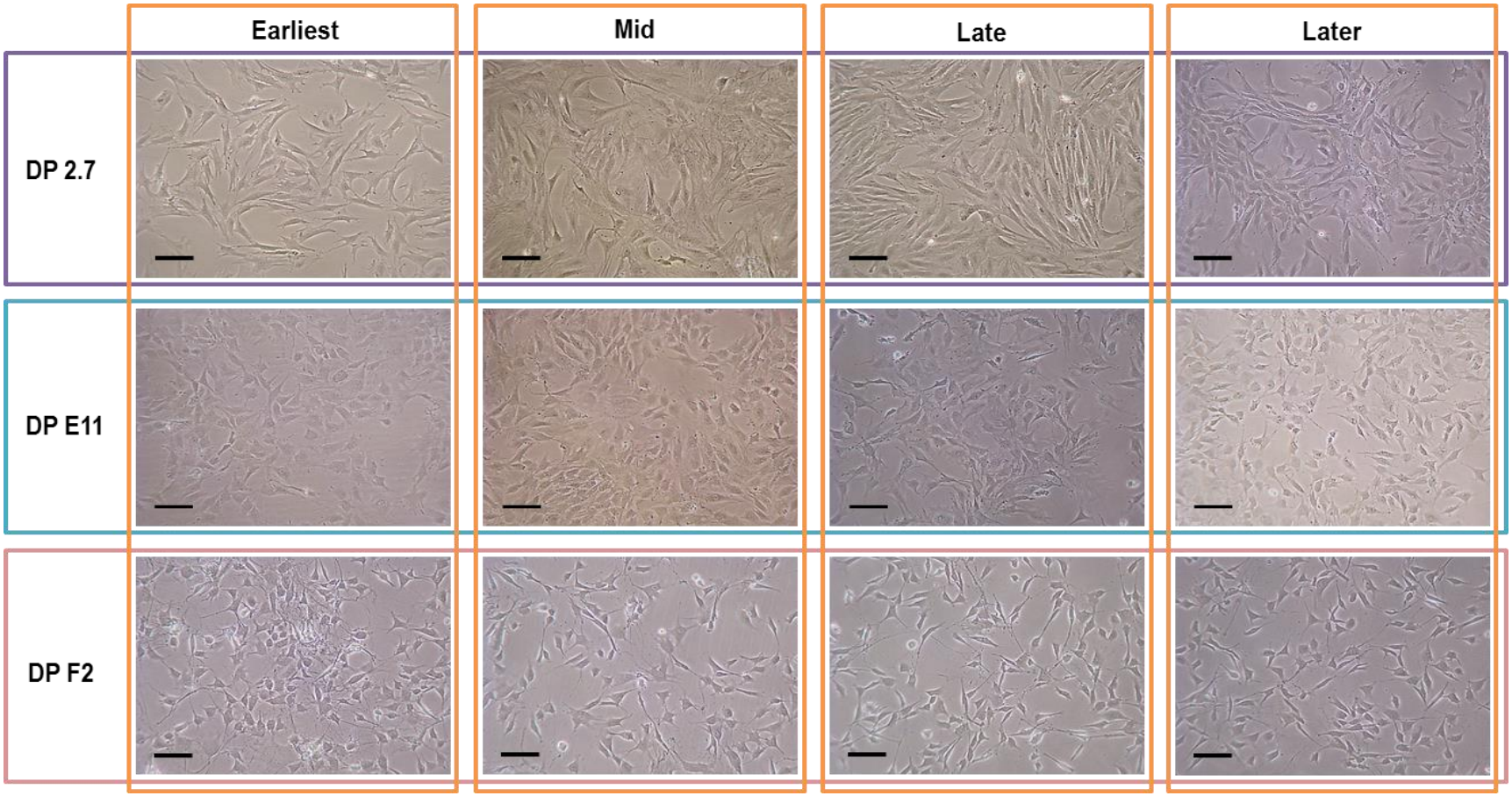

Figure 3.15: Representative micrographs of dental pulp clone progenitors during *in vitro* culture at earliest, mid, late, and later PDL time points. For the period of forty PDLs in culture, the morphological appearance of clones remained unchanged with clearly distinguished nuclei, cell bodies and borders (see main text for details). Scale bar, 100μm.

3.3.5 End-point PCR Gene Expression Levels of Bone Marrow and Dental Pulp Progenitor Clones

During culture-expansion, for the three clones from each tissue source, total RNA was extracted and end-point PCR conducted to establish gene marker expression, at four defined population doubling levels (see table 2.1). Due to limitations, end-point PCR was used as a product absence/presence technique to establish gene marker expression before proceeding with quantitative-PCR. The reference gene used was β-actin for 35 cycles, following amplification cycle increments to identify the geometric exponential phase (very specific reaction efficiency), as a rationale to decrease band-intensity variability and increase band precision (figure 3.16, yellow box). End-point PCR revealed that β-actin reference gene remained consistent during *in vitro* culture expansion over 40 population doubling levels, and absence of hematopoietic marker, PTPRC (CD45) (figure 3.16).

For defined mesenchymal stem cells, the minimal criteria triplicate markers CD73, CD90 and CD105, were present in all clonal progenitors over their culture period. FGFR1 and MSX2 markers, appeared to be consistently expressed during culture. Likewise, Snai1 and Nanog, was expressed by all progenitors from both tissue sources during culture. VCAM1 and MCAM markers displayed the most variability over the four defined PDLs, as-well-as different intensities between tissue sources, and between clones from the same tissue source. For example, clones BM 3.1, DP E11, and DP F2, showed no band for VCAM1. A second example marker, MCAM, was absent for clone DP F2, and displayed different intensities at the four PDLs for clones DP 2.7 and DP E11, while all three bone marrow clones appeared consistent. The

only marker that seemed the exception between tissue sources was SOX2, with all three bone marrow progenitor clones showing a band, which was absent in all three dental pulp progenitor clones.

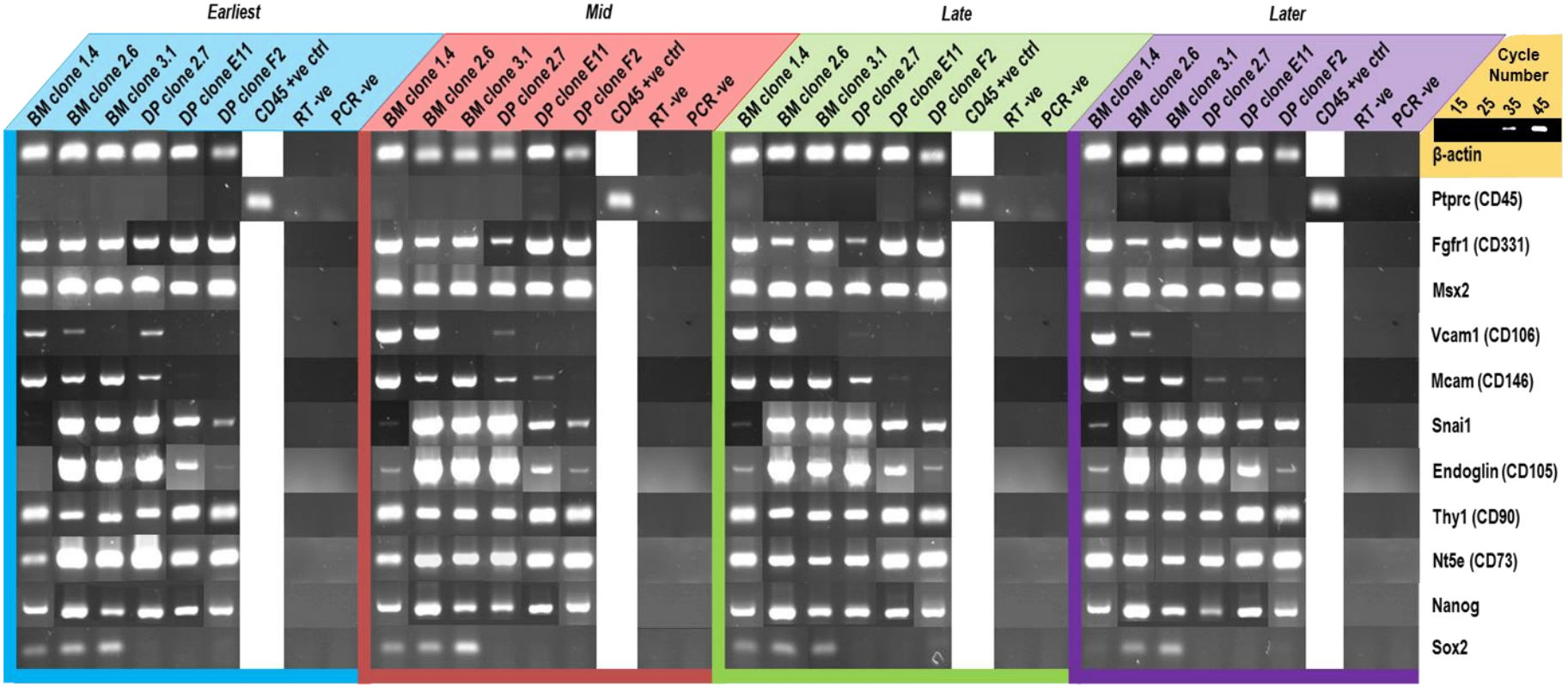

Figure 3.16: Collated end-point PCR of gene marker expression for bone marrow and dental pulp progenitor clones at defined in vitro PDLs. Reference marker β-actin was consistently expressed throughout culture and haematopoietic marker CD45 was negative. Minimal-defined MSC triplicate markers CD73, CD90, and CD105 were consistently expressed. Other markers varied in banding intensity e.g. VCAM1 and MCAM, and as such qPCR analysis was subsequently conducted (see figures 3.18-3.19). For β-actin, a band first appeared at cycle 35 (yellow box), which indicated geometric phase of PCR (increased band intensity precision). Earliest PDL, 7-12; Mid PDL, 16-20; Late PDL, 30-33; and Later PDL, 41-44 (see table 2.1). Spleen positive control.

3.3.6 qPCR Gene Expression Levels of Bone Marrow and Dental Pulp Progenitor Clones

Within this chapter, for each progenitor clone, the gene expression levels were quantified by consistently setting the same Ct (cross threshold) value within the geometric phase for the β-actin reference gene, against which genes of interest were compared as a percentage. In addition, only those genes with a dissociation curve peak at a single melting temperature was considered as specific expression for analysis. Using relative quantification, bar graphs represented gene expression levels as a percentage of reference gene β-actin Ct value, which acted as a reliable and specific control. A cDNA dilution assay was conducted that proved reliability of β-actin, due to overlapping and proportional Ct values, and decreased cDNA band intensities (see figures 3.17A and 3.17B).

qPCR was analysed for the three bone marrow (figure 3.18) and three dental pulp (figure 3.19) progenitor clones, at population doubling levels shown in table 2.1. Expression of MCAM for all clones, was either extremely low or not present during culture expansion *e.g.* for BM 3.1 earliest and later PDLs MCAM was not detected. VCAM1 was expressed in two bone marrow clones and one dental pulp clone, and each gave a completely different expression pattern. The overall trend for MSX2, was decreased expression with *in vitro* culture. For BM 1.4 VCAM1, culture expansion to later PDL led to a significant increase in expression compared to earliest PDL ($P<0.05$) and late PDL ($P<0.01$). Culture expansion led to a significant ($P<0.001$) decrease in MSX2 expression at both late and later PDLs compared to earliest and mid PDLs. The third marker expression, MCAM, decreased expression at later PDL significantly

compared to mid PDL ($P<0.05$) and later PDL ($P<0.01$). For BM 2.6, VCAM1 expression had a significant ($P<0.001$) increase at mid and late PDLs compared to earliest PDL, while continued culture expansion led to a significant ($P<0.001$) decrease at later PDL. MSX2 expression had a significant ($P<0.001$) decrease from earliest PDL compared to all other PDLs, while later PDL was expressed at a significantly ($P<0.001$) higher level compared to mid and late PDLs. MCAM marker expression had no significant changes due to extremely low expression levels. BM 3.1 expression of MSX2 had an extremely significant ($P<0.001$) decrease in a time-dependent manner, from earliest PDL compared to all other PDLs. In addition, all MSX2 PDLs had a statistically significant ($P<0.05$) decrease compared to the previous PDL. MCAM marker expression had no significant changes due to extremely low expression levels, and VCAM1 was not expressed. For DP 2.7, VCAM1 expression had a significant ($P<0.001$) decrease from earliest PDL compared to mid, late, and later PDLs. During culture expansion MSX2 expression had a significant ($P<0.001$) increase at mid PDL compared to earliest PDL, and compared to mid PDL, MSX2 expression significantly decreased at late PDL ($P<0.05$) and later PDL ($P<0.01$). MCAM marker expression had no significant changes due to extremely low expression levels. For DP E11, MSX2 expression had a significant ($P<0.05$) decrease from earliest to mid PDL, while late and later PDLs displayed a non-significant increase in expression. VCAM1 was not expressed and MCAM marker expression had no significant changes due to extremely low expression levels. For DP F2, MSX2 expression had a significant ($P<0.05$) increase from earliest to mid PDL, and compared to mid

PDL, MSX2 expression significantly decreased at late PDL ($P<0.05$) and later PDL ($P<0.01$). Again VCAM1 was not expressed, and neither was MCAM.

For bone marrow progenitors, the fastest proliferating clone BM 1.4 (PDL 42 in 96 days), expressed the highest level of MSX2 up to 4%. Clones BM 2.6 (PDL 40 in 136 days) and BM 3.1 (PDL 42 in 128 days) had similar proliferation rates, but BM 2.6 MSX2 was expressed three and a half times greater than BM 3.1. Likewise for dental pulp progenitors, the fastest proliferating clone DP F2 (PDL 42 in 129 days), expressed the highest level of MSX2 up to 24%. The next fastest proliferating clone DP 2.7 (PDL 42 in 128 days), expressed MSX2 up to 0.5%, and the slowest proliferating clone, of all dental pulp clones, DP E11 (PDL 42 in 224 days) expressed MSX2 up to 14%. Thus, each individual clone displayed a unique profile, with clones from the same tissue source and between the two tissue sources having distinct marker expressions.

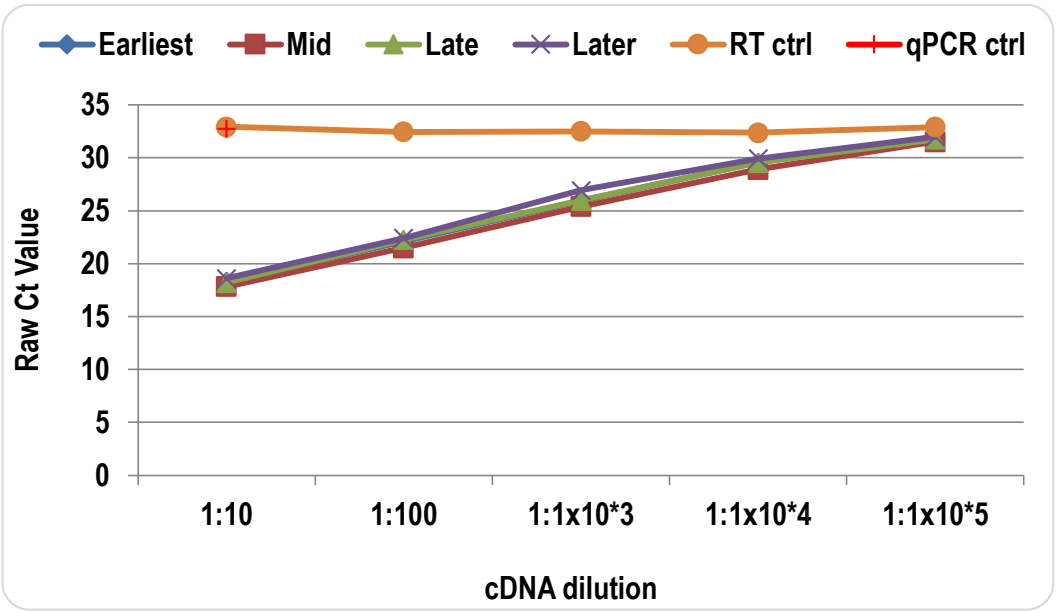

Figure 3.17A: Reference gene β-actin cDNA dilution assay. qPCR was amplified at 55°C for 40 cycles, with cDNA diluted ten fold from 1:10 to 1:1x10^5, for earliest, mid, late, and later PDLs. Raw Ct values overlapped and increased proportionally with dilution at each time-point, which indicated that age and dilution were not limiting factors. The RT and qPCR cDNA controls showed no expression. At 1:1x10^5 diluted cDNA (>30 Ct), no expression was observed. β-actin reference gene proved reliable. See gel products below.

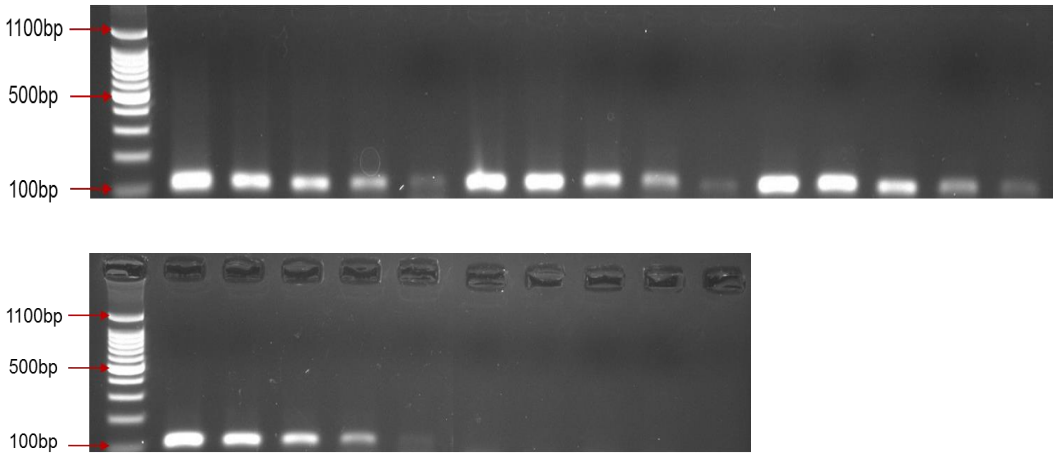

Figure 3.17B: Reference gene β-actin cDNA dilution assay products agarose gel. As cDNA dilution increased, the band intensity decreased. qPCR was amplified at 55°C for 40 cycles, with cDNA diluted ten fold from 1:10 to 1:1x10^5, for earliest (top lanes 2-6), mid (top lanes 7-11), late (top lanes 12-16), and later (bottom lanes 2-6) PDLs. Diluted RT sample (bottom lanes 7-11) showed no bands. The working dilution chosen for analyses was 1:10. β-actin product, 108bp.

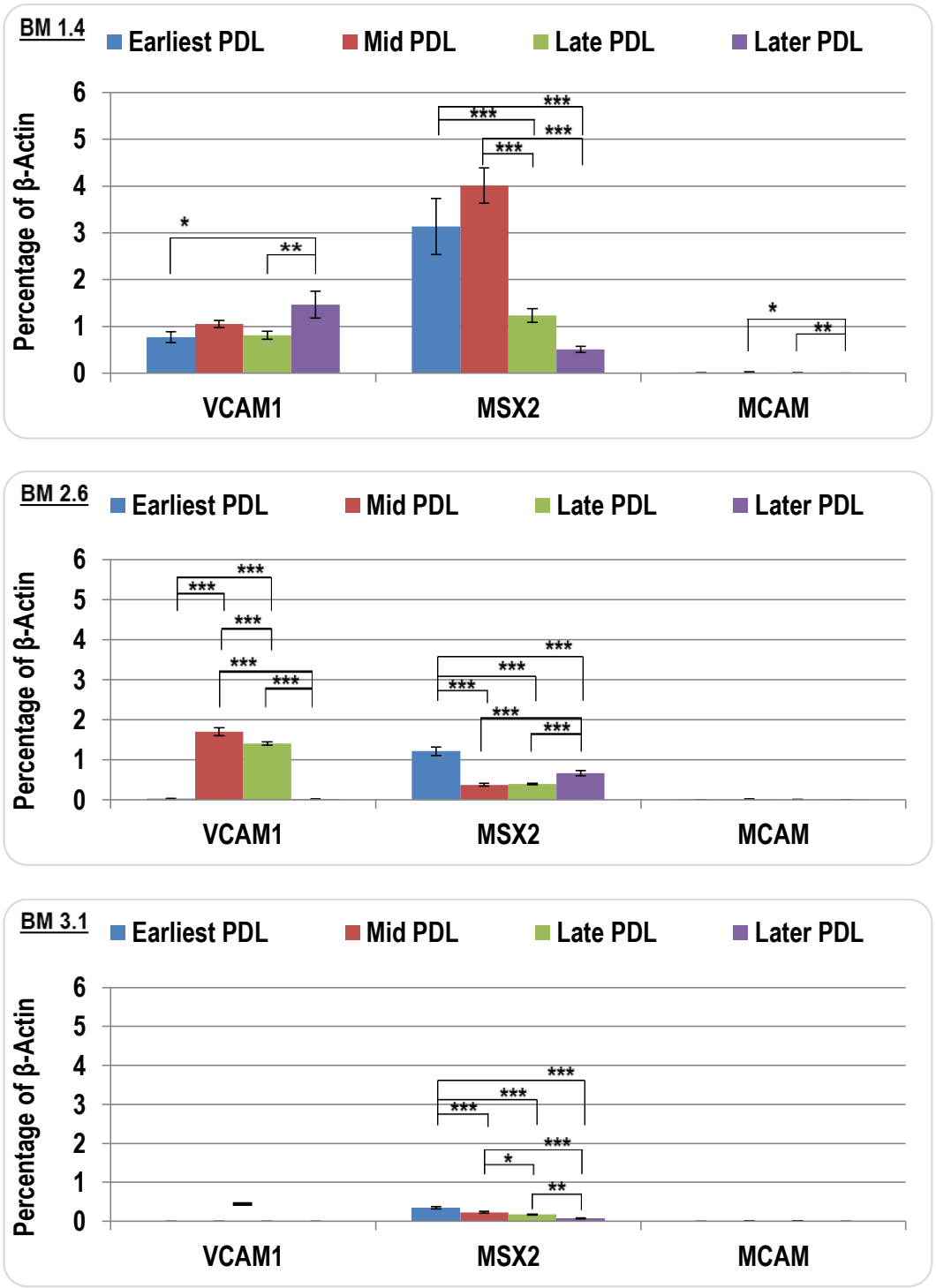

Figure 3.18: Bone marrow progenitor clones expression levels of MSC gene markers during *in vitro* culture expansion. VCAM1 and MSX2 gave unique expression profiles for each clone. VCAM1 had up- and down-regulation in BM 1.4 and BM 2.6, but was not expressed in BM 3.1. MSX2 gave a general trend of decreased expression with *in vitro* culture. MCAM marker expression was extremely low and only had significance in BM 1.4. Mean±SD. * = P<0.05, ** = P<0.01, *** = P<0.001. PDL, population doubling level (see table 2.1). (-) indicates not expressed.

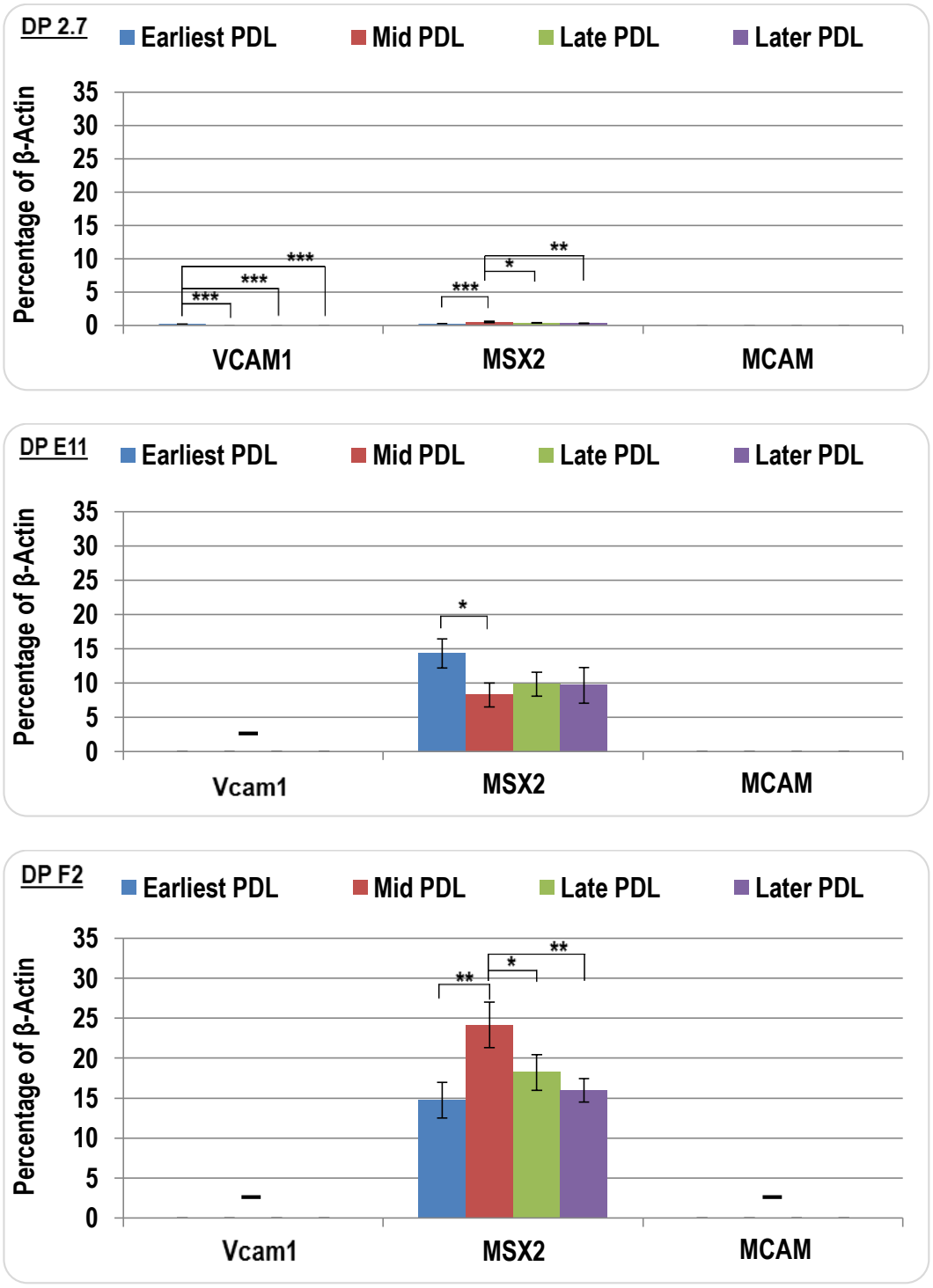

Figure 3.19: Dental progenitor clones expression levels of MSC gene markers during *in vitro* culture expansion. VCAM1 and MSX2 gave unique expression profiles for each clone. From earliest PDL, VCAM1 was downregulated in DP 2.7 significantly. MSX2 gave a general trend of decreased expression with *in vitro* culture. MCAM marker expression had no significant changes due to negligible expression levels. VCAM1 was not expressed by DP E11 and DP F2, and MCAM not by DP F2. Mean±SD. * = P<0.05, ** = P<0.01, *** = P<0.001. PDL, population doubling level (see table 2.1). (-) is not expressed.

3.4 Discussion

This chapter presents the first comprehensive and rigorous comparison of proliferative ability and quantification of MSC gene expression profiles, for progenitor clones from bone marrow and dental pulp tissue sources. Dental pulp progenitors formed fibronectin-adherent colonies at a rate on average twelve times greater than bone marrow. The bone marrow progenitors, however, proliferated approximately 1.5 times faster than dental pulp progenitors, and showed less variation in proliferation. Such findings shed light onto the cells that are contained within each tissue and highlights the stem cell hierarchy. Further analysis, revealed unique gene expression profiles of mesenchymal stem cell markers by each clone from both tissue sources, and elucidated that quantified MSC marker profiles are not able to identify a suitable and ideal progenitor clone for tissue engineering. These data lead the way to setting and defining culture conditions of progenitor clones for use in regenerative medicine.

Neural crest cells contribute to the origins of dental pulp (Lumsden, 1988, Chai et al., 2000), and bone marrow progenitor cells (Komada et al., 2012), which possibly have a neuro-ectodermal relationship (Pierret et al., 2006). Quantitative analyses suggested that colony-forming units of dental pulp originate from neural crest cells entirely, whereas bone marrow composed 57% neural crest-derived cells (Komada et al., 2012). Here, bone marrow progenitors formed colonies twice the size of dental pulp progenitors, and had a higher and less variable PDL capacity. As such, it appears that dental pulp are lineage-restricted stromal cells referred to as TA cells, which couples

proliferation and maturation (Potten and Loeffler, 1990). It has been proposed, large highly proliferative cell-dense colonies that are few in number, derive from the mother stem cell and closely-related progenitor cells, similar to BMSCs that displayed high proliferation and low CFE. While small colonies that are higher in number, derive from lineage-mature TA cells, which are committed to differentiate following a finite division number (see Chapter 1, figure 1.1) (Chan et al., 2004), similar to DPSCs that displayed a high CFE and lower more variable proliferation. This was akin to fibroblastic large colonies that possessed a high proliferation capacity compared to slow-replicating cells that formed small colonies (Smith et al., 1978). As such, the progenitors appeared to mimic their native microenvironment tissue source functions. For example, *in vivo*, resident dormant dental pulp stromal cells are proposed to only respond to trauma or damage (Smith et al., 1995) and so rarely divide or replace within the tissue, if at all. Whereas, bone marrow progenitors are constantly replenished from the stem cell population, due to continual bone -turnover and -remodeling during life-span (Parfitt, 1984).

Due to the heterogeneous nature of human cell populations, the vital recognition for examining the replicative behavior of single-cell clones, has long been suggested (Smith et al., 1978). The CFE of DPSCs was significantly greater than BMSCs, as reported by others for human (Gronthos et al., 2000) and rat (Alge et al., 2010), with a twelve fold difference. One reason for CFE differences between tissues, could be isolation and seeding of other mono-nucleate cells within the bone marrow Histopaque preparation *e.g.* haematopoietic stem cells (HSCs), monocytes, and leukocytes. Conversely,

Gronthos *et al.* (2000) state that from their unpublished observations, hematopoietic-free and collagenase-treated bone marrow increased the CFE by 10-fold to a similar level as dental pulp. Isolation and successful propagation of BMSCs was ~54%, which was similar to that reported using more technical methods on the basis of cell sorting (Gronthos et al., 2003), and BMSCs formed colonies twice the size as dental pulp. Such differences in colony size, was likely a contributing factor for the initial success in expanding and propagating BMSC colonies, compared to DPSCs with <10% propagated. Similarly, others report <20% of dental pulp clones successfully propagated during *in vitro* culture (Gronthos et al., 2002, Gronthos et al., 2003). Here, only two clones, DP 2.7 and DP E11, were isolated and initially propagated using a seeding density of 4000 cells/cm^2 in 20% serum. Hence, an alternative method of doubling surface area was adopted for DPSC clones (Breyer et al., 2006, Janebodin et al., 2011) by expanding in a single well of sequential 96-, 48-, 24-, 12-, and 6- well plates. After which point, clones were seeded at the normal $4x10^3$ cells/cm^2 density, having achieved sufficient cells numbers. This increased the success of propagated clones to ~50%, a level similar to bone marrow. Thus, while the fibronectin technique is simplistic, the cloning efficiency was very effective and has good basis to use by preferentially binding more primitive progenitor cells (Jones et al., 1995, Gandarillas and Watt, 1997, Zhu et al., 1999), rather than lineage-mature TA cells (Adams and Watt, 1991, Jones and Watt, 1993). In addition, the binding of fibronectin to α5β1 integrin, inhibits terminal differentiation (Watt et al., 1993).

For the first time, these results demonstrated proliferation of clonal progenitors from bone marrow and dental pulp tissues over an extended period, and provided high through-put techniques for successful isolation and propagation of approximately 50% of clonal progenitors up to 40 PDLs for both tissues. Reports state colony clones were difficult to obtain (d'Aquino et al., 2007), and 80% of clones propagated less than 20 PDLs for DPSCs (Gronthos et al., 2002) and BMSCs (Gronthos et al., 2003). Discrepancies are likely due to different employed protocols for progenitor isolation and propagation *e.g.* enzymatic dissociation (Gronthos et al., 2000), tissue explants (Lizier et al., 2012), extremely high-density ($1x10^6$ cells/cm^2) (Kern et al., 2006), and age (Stenderup et al., 2003). While others observe no significant differences in cloning efficiency of human bone marrow progenitors from different aged donors (Oreffo et al., 1998, Muraglia et al., 2000). The proliferative ability of BMSC progenitors was less variable and on average 1.5 times greater compared to DPSC progenitors. This is opposed to a report using donor-matched heterogeneous populations from rat bone marrow and dental pulp, which showed DPSC doubling time was significantly less and 1.5 times faster than BMSC (Alge et al., 2010). This observation, however, used a single rat and simple cell-count over three days at passage 3, unlike the extensive analysis with multiple animals here. Bone marrow clones proliferated a minimum 40 PDLs and up to 61 PDLs by passage 45, which was twice that of other literature reports for heterogeneous populations of <4-32 PDLs between 7-24 passages, irrespective of specimen age (Bruder et al., 1997, Duggal and Brinchmann, 2011, Zhang et al., 2011, Zou et al., 2012, Jin et al., 2013). In relation to time, heterogeneous BMSC populations that did reach 40 PDLs

required >200 days (Shibata et al., 2007) and up to 300-400 days *in vitro* culture (Stenderup et al., 2003), which was over twice as long as the slowest BMSC clone to reach 40 PDLs here. Concerning DPSCs, there are literature reports on the high clonogenic and proliferative nature of human molar DPSCs, but these were calculated from colony counts of BrdUrd incorporation over a twenty-four-hour period (Gronthos et al., 2000), and cell dilution assays over a three week period (Laino et al., 2006, d'Aquino et al., 2007), which was not a comparison to the culture period up to 248 days here. There are no reports that present long-term propagation data of heterogeneous populations to determine population doubling, as rigorously demonstrated here, despite claims of DPSC culture up to seven months with no senescence (Laino et al., 2005, Laino et al., 2006). In addition, other reports stated heterogeneous molar DPSC progenitor populations achieved a PDL of 20-30 (Gronthos et al., 2002), and PDL of ~120 (Miura et al., 2003), but they did not explain isolation or calculation protocols, which highlights the lack of protocol precedent within the literature for culture of progenitor cells. Stem cells from human exfoliated deciduous teeth (SHED), are reported to be maintained for only fifteen passages (Lizier et al., 2012), and goes some way to elucidating the proliferation ability of tooth stem cells, yet was half the passage number that DPSC clones achieved here. Of note, inter-species differences must be considered, as heterogeneous populations of mouse and rat bone marrow progenitors were capable of 120 PDLs within ~325 days and 100 PDLs in ~350 days, respectively, and single-cell populations, can expand for 120 and 80 PDLs, respectively (Jiang et al., 2002). In addition, cryopreservation of bone marrow progenitors, up to 20 months, and dental pulp progenitors, up to 5

months, displayed minimal effect on progenitor clones due to their reproducible proliferation growth curves (Bruder et al., 1997) in αMEM supplemented medium (Lizier et al., 2012), which lends support to reliability of the clones' growth profiles and highlights heterogeneity within total cell populations.

Within the literature, reports state hallmarked cellular senescence upon halted proliferation, which included: mitotic cessation, stressed morphology, >50% positive β-galactosidase, marked up-regulation of senescent proteins (p53, p21, and p16), and eventual apoptosis (Bruder et al., 1997, Jin et al., 2013). Here, clones did not senesce and showed no signs of stressed morphology or high β-galactosidase over 40 PDLs. Others, however, state that cell division potential primarily determines *in vitro* life-span (Dell'Orco et al., 1974), with a PDL rate of <0.5 per week defined as senescent (Stephens et al., 2003), and as such clones here during plateau-phase would be classed senescent, which was not the case. Hence, the importance of studying progenitor cells at a single-cell clone level, to isolate the potentially distinct clonal phenotypes that contribute the 20-30% multipotent progenitors, within a heterogeneous population (Abdallah and Kassem, 2012). The majority of clones had a unique plateau phase before linear growth, as seen elsewhere in rodent cell-sourced dental pulp progenitors (Waddington et al., 2009), and during early passage, up to P10 (Martin-Piedra et al., 2013). Similarly here, it was following the initial ten passages that the majority of clones increased their cell numbers substantially, up to 65 PDLs, which surpasses the somatic-cell proliferative limitation of 50 PDLs (Hayflick, 1989). An important consideration, however, is that upon reaching a plateau phase, progenitor cells are widely regarded as

senescent, with reports basing senescence on population doubling alone (Zhang et al., 2011) and when it is analysed with an additional parameter *e.g.* senescence marker, explanation is still lacking due to maintenance of telomeres (Franco et al., 2001). Thus, the scientific community could be over-looking cell populations. A hypothesis for this plateau-phase, is that while an isolated colony by definition is a single-cell derived clone (Dowthwaite et al., 2004), the stem cell hierarchy involves mother and progenitor stem cells, including more lineage restricted TA cells following further cell-divisions (Chan et al., 2004). Mother stem and daughter progenitor cells undergo a few divisions (initial PDL growth phase), to produce TA cells that are eventually rendered terminal and do not contribute to the progenitor-population (plateau phase). With no contribution from TA cells, mother stem cell and daughter progenitor cells adapt to culture conditions and may become engaged in continuous mitotic events (linear-like growth phase) to produce mass progenitor cell-numbers. Similarly ascribed during stromal bone marrow *in vitro* culture (Mets and Verdonk, 1981, Bruder et al., 1997), based on the terminal differentiation theory (Martin et al., 1974).

End-point PCR identified possible genes that were differentially expressed *e.g.* noticeably for VCAM1 and MCAM, which were then analysed *via* qPCR (see below). Interestingly, SOX2 was the only gene expressed by BMSC progenitors and not by DPSCs. Lack of expression may go some way to supporting the view that DPSCs are from a more mature and committed TA cells, compared to a more primitive bone marrow progenitor, as SOX2 is a critical transcription factor that regulated stem cell pluripotency (Takahashi et

al., 2007). Overall, expression of MSC markers was much like that previously shown by immuno-phenotype (Gronthos et al., 2000) and microarray analysis, which showed >4000 genes similarly expressed between bone marrow and dental pulp progenitors (Shi et al., 2001). As such, gene expression characteristics of these tissue sources was extremely similar, and isolation of preferential clones by phenotype for tissue engineering, is as yet unidentifiable (Abdallah and Kassem, 2012). Similarly, clonal quantification of such gene expression, was lacking within the literature, and is reported for the first time within this chapter.

The qPCR data revealed clearly distinguishable and unique profile "fingerprints" for each MSC clone at four defined PDLs, from both bone marrow and dental pulp tissue sources. VCAM1 was expressed by half of the clones, and likewise with MCAM, a clear expression pattern was only evident from qPCR compared to end-point PCR. The adhesion markers, MCAM (CD146) and VCAM1 (CD106), are two of the most reported MSC-phenotypes for bone marrow and dental pulp progenitors (Gronthos et al., 2000). Still, much is unknown concerning attributes of these markers to MSC progenitors. Clones DP 2.7 and DP E11 had negligible MCAM expression and DP F2 did not express MCAM, and showed 12-fold greater CFE than bone marrow. Yet, a report stated that MSC progenitors negative for MCAM did not form colonies, and that MCAM-positive progenitors contributed 96% of colonies formed (Shi and Gronthos, 2003). In addition, MCAM has been implicated to identify a progenitor perivascular niche due to localisation with blood vessel walls (Shi and Gronthos, 2003). As such, the clones isolated here could have identified

another niche within the mileu of bone marrow and dental tissues, of which there are a few proposed (Sloan and Waddington, 2009).

The close relationship of VCAM1-positive MSCs with endothelium also lends support to a possible resident niche of MSCs being peri-vascular (Ruster et al., 2006). With VCAM1 suggested to be involved in cell trafficking between bone marrow and vasculature (Jacobsen et al., 1996). In addition, a major advantage of VCAM1-positive MSCs is that they modulate immune suppression and response, in part due to inhibition of T-cell proliferation by BMSCs (Di Nicola et al., 2002) and monocyte proliferation by DPSCs (Wada et al., 2009). Here, BM 2.6 expressed the highest VCAM1, which altered during culture expansion. Similarly, VCAM1 was majorly expressed by BMSCs and down-regulated during culture (Qian et al., 2012), which could be due to *in vivo* environment priming before extraction and isolation (Shimizu et al., 1990). As such, expression of VCAM1 by MSCs appears to be sensitive to the microenvironment in which it finds itself. In addition, the progeny of higher proliferative clones, over 20 PDLs, have a VCAM1-positive characteristic (Gronthos et al., 2003), but BM 2.6 only achieved an average-mean proliferation rate.

MSX2 may act as a regulator in odontogenesis and osteogenesis (Shi et al., 2001), as enhanced MSX2 expression stimulated cell proliferation (Liu et al., 1999). End-point PCR showed MSX2 was consistent, but qPCR displayed MSX2 decrease during culture expansion, and yet proliferation rate was at its highest during later PDL. As such, expression of homeobox factor MSX2 may act to promote and facilitate proliferation of progenitors, when required during *in vitro* culture. Similarly as VCAM1, MSX2 expression appeared dependent

on microenvironment cues, and thus MSC marker quantification will probably not highlight an “ideal” progenitor for tissue engineering that is highly proliferative and multipotent (see next chapter).

In summary, bone marrow and dental pulp tissues can be acknowledged as heterogeneous populations, as displayed by unique growth profiles of single-cell derived colony clones. Isolating single colony clones on the basis of their β1 integrin receptor expression by fibronectin-adherence provided a reliable technique for progenitor cell isolation, with high colony formation and proliferation. While others report that isolated clones have limited proliferation capacity, with 80% of clones with a PDL of <20 (Gronthos et al., 2002), bone marrow clones here displayed higher proliferation rates and less variable growth patterns compared to dental pulp clones. Such shorter culture time combined with generation of sufficient population cell numbers, is beneficial for clinical applications (Jin et al., 2013). In addition, continued propagation following plateau, led to linear-like growth phase, and underlined that progenitor populations could be being overlooked by the scientific community. As such, rigorous and combined methodology is lacking in the literature for successful isolation of clonal populations from bone marrow and dental pulp tissues. From phenotypic MSC gene expression, the SOX2 marker appeared beneficial in highlighting preferential clones for isolation. To better understand the cell-phenotypes of these tissues, more research is required at a single-cell clone level if they are to be successfully applied within translational medicine.

Chapter 4

Differentiation Capacity of Bone Marrow and Dental Pulp Mesenchymal Stromal Cell Clones

4.1 Introduction

A critical criterion in the characterisation and utilisation of MSCs in tissue engineering is the multi-differentiation potential. The whole cell population of bone marrow and dental pulp tissues are relatively heterogeneous, and clonal analysis suggested only 20-30% of the total cell population was truly multipotent and the remaining population represents bi- or uni- potential, despite the identical expression of MSC markers (Abdallah and Kassem, 2012). Tri-differentiation capacity of MSC heterogeneous populations along adipogenic, chondrogenic, and osteogenic lineages was reported in human bone marrow (Pittenger et al., 1999, Zhang et al., 2011), rodent dental pulp (Janebodin et al., 2011) and human dental pulp (Zhang et al., 2006). While BMSC clones have proved pluripotent in their differentiation ability (Jiang et al., 2002), individual DPSC clones have thus far not been reported multipotent (Gronthos et al., 2000, Gronthos et al., 2002).

Human bone marrow sheds light on the nature of the whole cell population, as analysis on clonal populations revealed their tri-potent capacity, with all clones being osteogenic, and simultaneously being 80% adipogenic, and 30% chondrogenic (Pittenger et al., 1999). Individual multipotent colony clones reported by Pittenger *et al*., (1999) are opposed to the notion of bone marrow tissue harboring several committed progenitor cell-types each forming bone,

cartilage, and adipose tissues (Dennis and Caplan, 1996a). The study of clonal and heterogeneous populations is important for regenerative medicine, to best understand tissue and cell source efficacy for mineralised clinical applications, such as bone repair and tooth caries (Dennis and Caplan, 1996b). Elsewhere, 17% of primary human BMSC clones are reported tri-potent, with 80% as chondro-osteogenic, and 3% as osteogenic only, with no other uni- or bi-potent combination clones observed, which may indicate a hierarchical differentiation pathway, with tri-potent cells considered early progenitor MSCs that sequentially lose lineage potential to render osteogenic progenitors only (Muraglia et al., 2000). Others have attempted to isolate a preferential progenitor population for differentiation based on STRO-1^{+}/VCAM1^{+} cells, however, tri-lineage capacity was limited to clones at 20 PDLs, with clones >25 PDLs displaying differentiation inability (Gronthos et al., 2003). No reports, however, compare tri-lineage differentiation of clonal populations from bone marrow and dental pulp simultaneously, and within this chapter is the first presentation of such data.

Within this research chapter, the focus and aims are to simultaneously assess adipo-chondro-osteogenic differentiation capacity of three BMSC and three DPSC clonal populations (characterised in Chapter 3), and relate ability to their potential stem cell hierarchy, in order to compare efficacy of bone marrow and an alternative dental pulp progenitor source for use in tissue engineering applications. Differentiation capacity was analysed by *in vitro* assays with tissue-specific staining and quantitative gene-expression markers.

4.2 Materials and Methods

The differentiation potential of three clonal populations from bone marrow and dental pulp at mid PDL (see table 2.1) was investigated, each for three lineages: adipocytes, chondrocytes, and osteoblasts. Briefly, each clone for adipogenesis was seeded at $10x10^3/cm^2$ until >95% confluent and exposed to dexamethasone, 3-isobutyl-1-methylxanthine (IBMX), insulin, and indomethacin for 21 days (see 2.7.1 Adipogenic Differentiation Media). On day 21, total RNA was extracted for adipose-specific gene expression analysis (table 2.4) by qPCR (see 2.7.2 Adipogenic Differentiation Marker Expression Analysis), and presence of neutral lipids was assessed using LipidTOX™ stain (2.7.3 Adipogenic Differentiation Neutral Lipid Detection). For chondrogenesis, $2.5x10^5$ clonal cells were exposed to StemMACS ChondroDiff Media (Miltenyi Biotech Ltd.) as per manufacturer protocol for 24 days (see 2.7.4 Chondrogenic Differentiation Media). Formed pellets were sectioned by microtomy (see 2.7.5 Chondrogenic Differentiation Pellet Tissue Histology) and assessed for: haematoxylin and eosin staining, and collagen II synthesis by immunolocalisation (mouse CIIC1) (see 2.7.6 Chondrogenic Differentiation Immunohistological Analysis). For osteogenesis, clones were seeded at $4x10^3/cm^2$ for 5 days and exposed to dexamethasone and β-glycerophosphate (see 2.7.7 Osteogenic Differentiation Media) for 23 days. On day 23, total RNA was extracted and analysed for osteogenic-specific gene expression (table 2.5) by qPCR (see 2.6 Quantitative-Polymerase Chain Reaction of Colony Clones), and in addition was assessed for calcium deposition by alizarin red stain (see 2.7.9 Osteogenic Differentiation Alizarin Red Staining), and

osteopontin (P-18) protein production by immunolocalisation (see 2.7.10 Osteogenic Differentiation Immunocytochemistry).

4.3 Results

4.3.1 Adipogenic Differentiation of Characterised Progenitor Clones

Adipogenesis was successful in all three bone marrow clones (figures 4.1) and DP 2.7 clone, but not in DP E11 and DP F2 clones (figure 4.2). Adipocytes were seen to form intra-cellular lipid vesicles, which was confirmed by presence of neutral lipids using LipidTOX^{TM} fluorescent stain (figure 4.3), but was absent in non-adipogenic dental pulp clones. An adipocyte morphology of intracellular lipid vesicles was apparent for all adipogenic clones by day 7, and adipocytes increased in number and size by day 21 with concomitant increase in lipid vesicle size. BM 1.4 adipocytes observed very small lipid vesicles, some of which increased considerably by day 21 to large lipid vesicles. BM 2.6 adipocytes had small to medium size lipid vesicles and increased uniformly in adipocyte number by day 21. BM 3.1 adipocytes had small lipid vesicles, which increased substantially over 21 days to extremely large lipid vesicles. Although BM 1.4 had several larger lipid vesicles by day 21, they were not as numerous as BM 3.1. For DP 2.7, a single adipocyte with a few very small lipid vesicles was observed on day 7, which increased to a few adipocytes with medium size lipid vesicles by day 21. Morphology of all clones in non-adipogenic medium remained unchanged over the 21 days and only observed more compact cells due to proliferation (figures 4.1 and 4.2) compared to start of differentiation media (not shown).

For the three bone marrow clones, qPCR analysis revealed significant up-regulation in five of six adipogenic markers (figure 4.4). Mature adipogenic genes, FABP4 and LPL, were most markedly upregulated in bone marrow clones, up to 200% and 100% of reference gene expression, respectively. For

BM 1.4 and BM 3.1, adipsin, adiponectin, and FABP4 were only expressed in 21 day adipogenic treatment, with CEBPα and LPL showing a significant ($P<0.001$) increase in expression compared to 0- and 21- day non-adipogenic medium controls. BM 2.6 had expression only in 21 day adipogenic treatment, for adipsin, adioponectin, FABP4, and LPL. CEBPα and PPARγ did not significantly change, however, the expression pattern for 21 day treatment was of increase compared to 0- and 21- day non-adipogenic.

DP 2.7 showed significant upregulation in two adipogenic markers, but less than 20% (figure 4.5). Adipogenic treatment led to a significant ($P<0.001$) increase of CEBPα compared to 0- and 21- day non-adipogenic medium. LPL had a significant ($P<0.001$) increase compared to 0-day non-adipogenic medium, however, 21 day non-adipogenic medium and adipogenic treatment showed no difference in expression between them. PPARγ was only expressed in 21 day adipogenic treatment. DP E11 and DP F2 clones did not form adipocytes and qPCR showed no discernible pattern in adipogenic gene expression. The reliable marker LPL, showed no upregulation. For DP E11, PPARγ was only present in 21 day adipogenic treatment, and DP F2 showed significant ($P<0.001$) differences in transcription factor CEBPα, but were less than 4% (figure 4.5). Adipsin, adiponectin and FABP4 were not expressed for all three dental pulp clones.

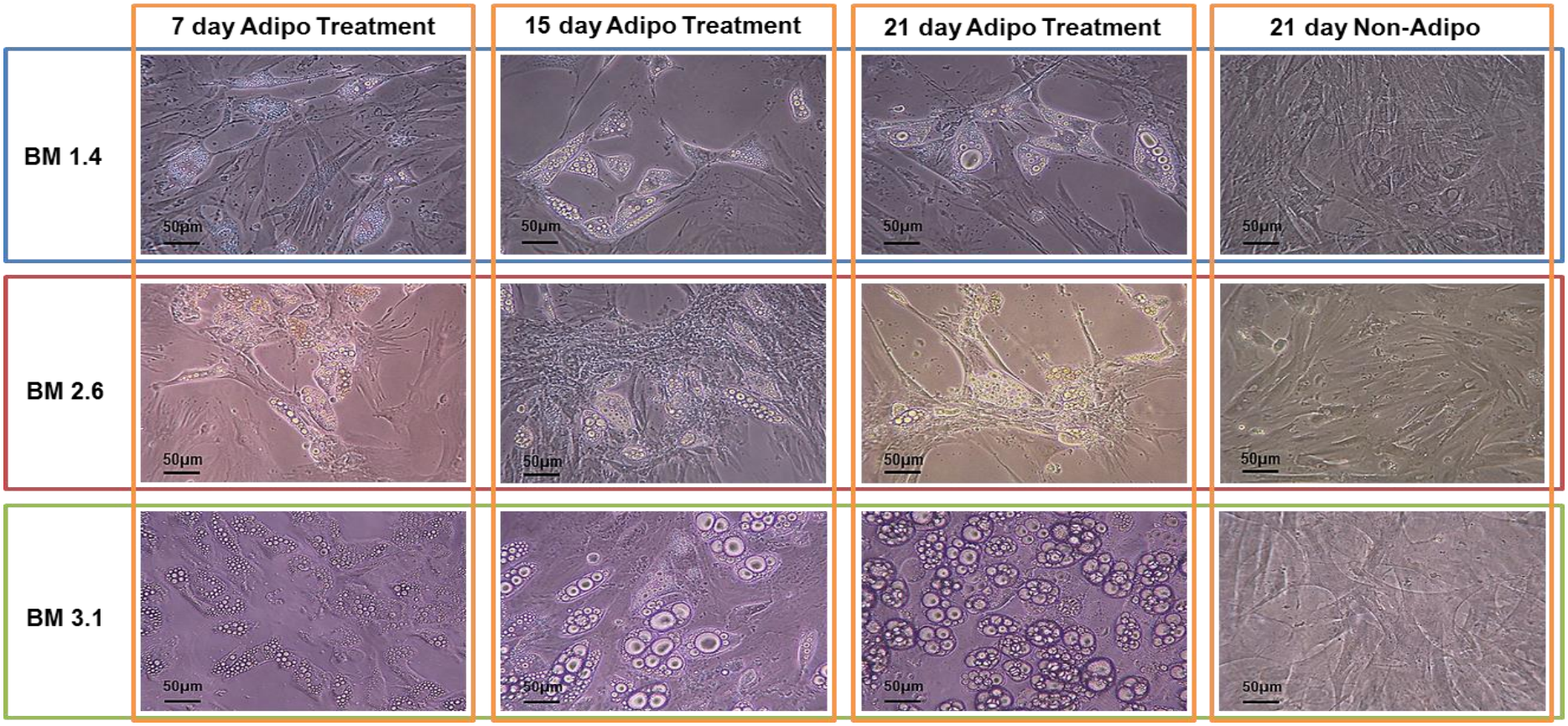

Figure 4.1: Adipogenic differentiation of progenitor clones BM 1.4, BM 2.6, and BM 3.1, over 21 days at mid PDL. Adipogenesis was observed from 7 days with formation of lipid vesicles in treatment. Up to 21 days, lipid vesicles increased considerably in number and size. Morphology of non-adipogenic medium remained unchanged by day 21. Scale bar, 50µm (20x objective).

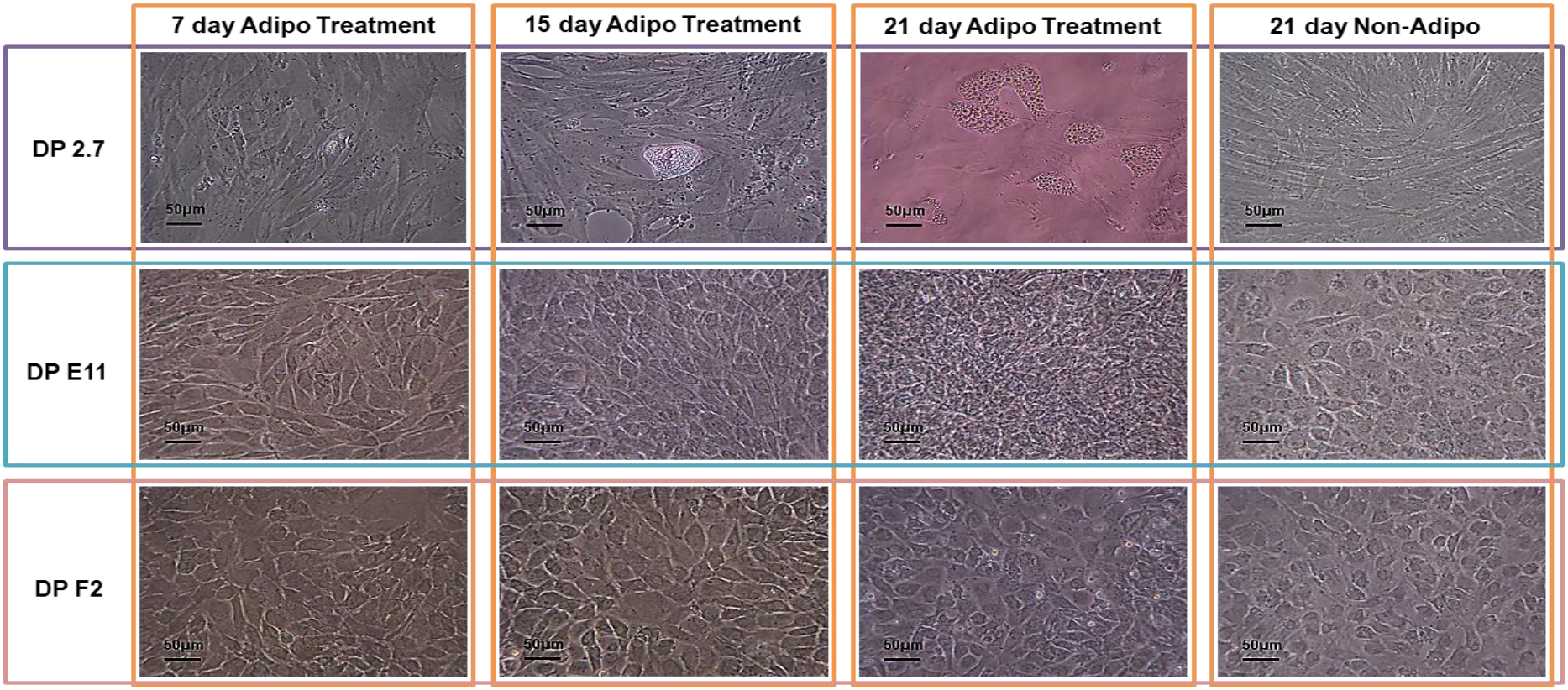

Figure 4.2: Adipogenic differentiation of progenitor clones DP 2.7, DP E11, and DP F2, over 21 days at mid PDL. In DP 2.7 adipogenic treatment, a single adipocyte with a few very small lipid vesicles was observed on day 7, which increased to a few adipocytes with medium size lipid vesicles by day 21. DP E11 and F2 formed no adipocytic lipid vesicles. Morphology of non-adipogenic medium remained unchanged by day 21. Scale bar 50µm (20x objective).

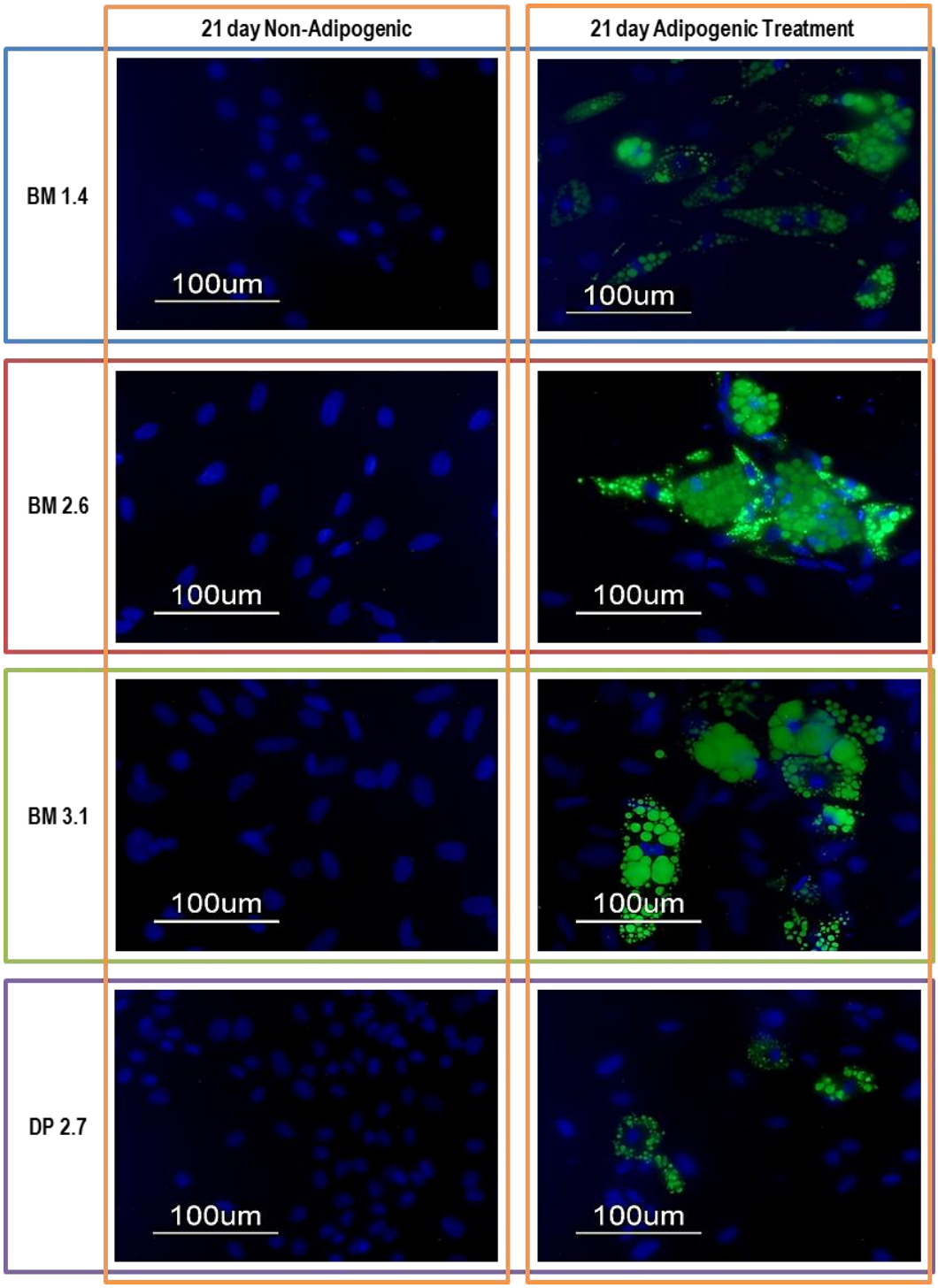

Figure 4.3: Adipogenesis of progenitor clones BM 1.4, BM 2.6, BM 3.1, and DP 2.7, on day 21 at mid PDL. Green fluorescence indicated presence of neutral lipid vesicles in adipogenic treatment only. Non-adipogenic medium had no lipid vesicles. DAPI nuclei stain (blue). Scale bar, 100µm (40x objective).

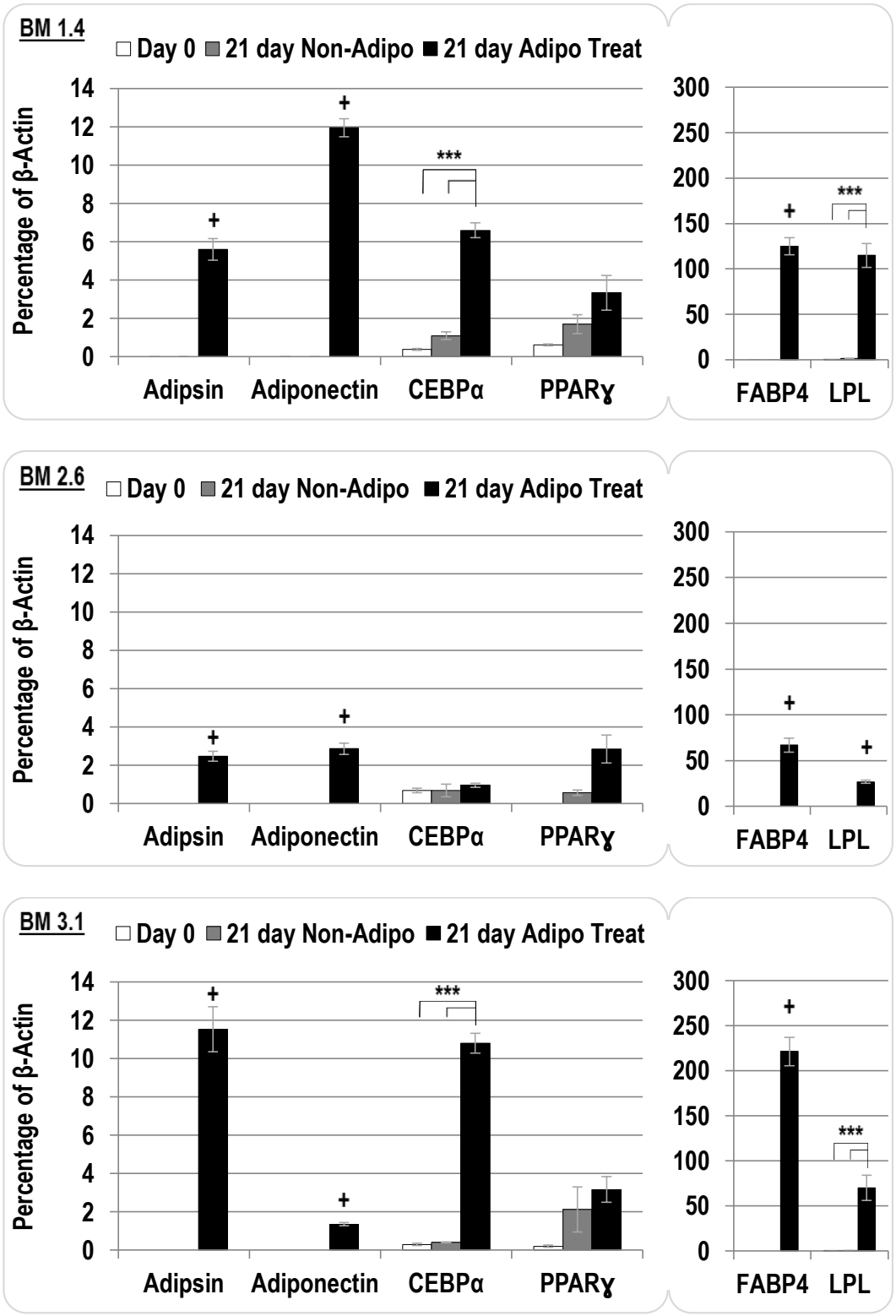

Figure 4.4: Bone marrow progenitor clones expression levels of adipose-related genes following *in vitro* adipogenic differentiation for 21 days. The three BM clones expressed all six adipogenic genes analysed. At 21 days adipogenic treatment, FABP4 and LPL were most markedly upregulated up to 200% and 100%, respectively. Mean±SD. *** = P<0.001. (+) indicates expression in adipogenic treatment only.

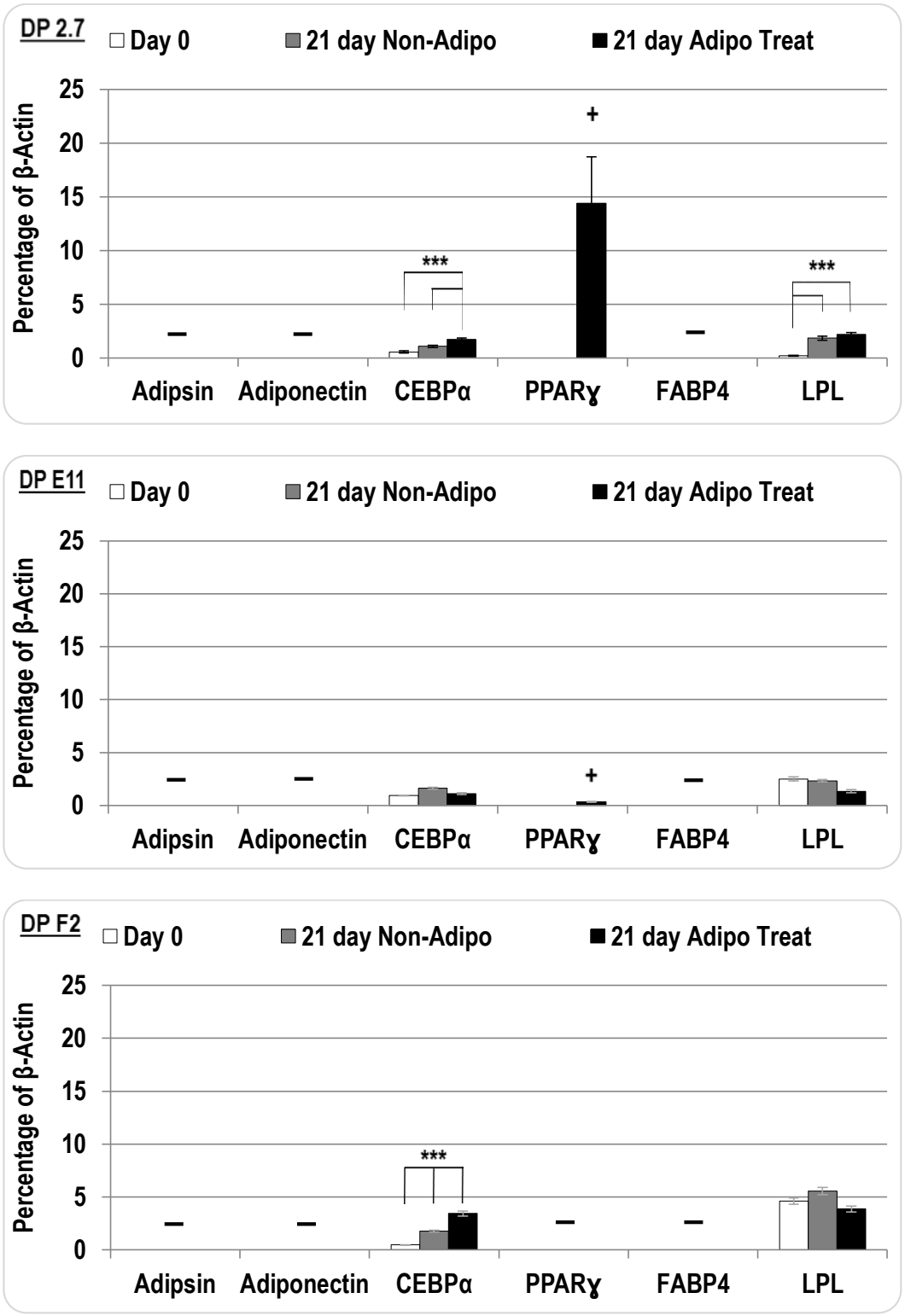

Figure 4.5: Dental pulp progenitor clones expression levels of adipose-related genes following *in vitro* adipogenic differentiation for 21 days. Only a maximum of three genes were expressed out of six adipogenic genes analysed. Only DP 2.7 adipogenic treatment formed adipocytes and correspondingly increased adipogenic gene expression. DP E11 and DP F2 failed to form adipocytes. Mean±SD. *** = P<0.001. (+) indicates expression in adipogenic treatment only; (-) indicates not expressed.

4.3.2 Chondrogenic Differentiation of Characterised Progenitor Clones

Chondrogenic pellets were formed by all bone marrow clones (figure 4.6) and DP F2 only, while DP 2.7 and DP E11 did not form spherical pellets but disk-like tissues that were not recoverable (figure 4.7). Chondrogenesis was evident in all bone marrow clones, with haematoxylin and eosin staining revealing cell-devoid areas where extracellular matrix had been produced in chondrogenic treatment but not in non-chondrogenic medium (figure 4.8). The higher cell numbers in treatment than non-chondrogenic are likely responsible for the production of extracellular matrix. Chondrogenic matrix was confirmed by cartilage marker collagen type II, which was abundant in clones BM 2.6 and BM 3.1 treatment, but equally present in BM 1.4 non-chondrogenic and chondrogenic treatment (figure 4.9). The chondrogenic pellet of DP F2 contained mostly cells with some matrix formation visible at its centre (figure 4.8), and collagen type II staining was minimal (figure 4.10). Isotype and antibody exclusion controls were negative for collagen II.

Chondrogenic differentiation was assessed on two separate occasions, and the least chondrogenic clones, BM 1.4 and DP F2, failed to form pellets on one of these occasions. Due to the diminutive pellets formed no RNA could be recovered for PCR analysis.

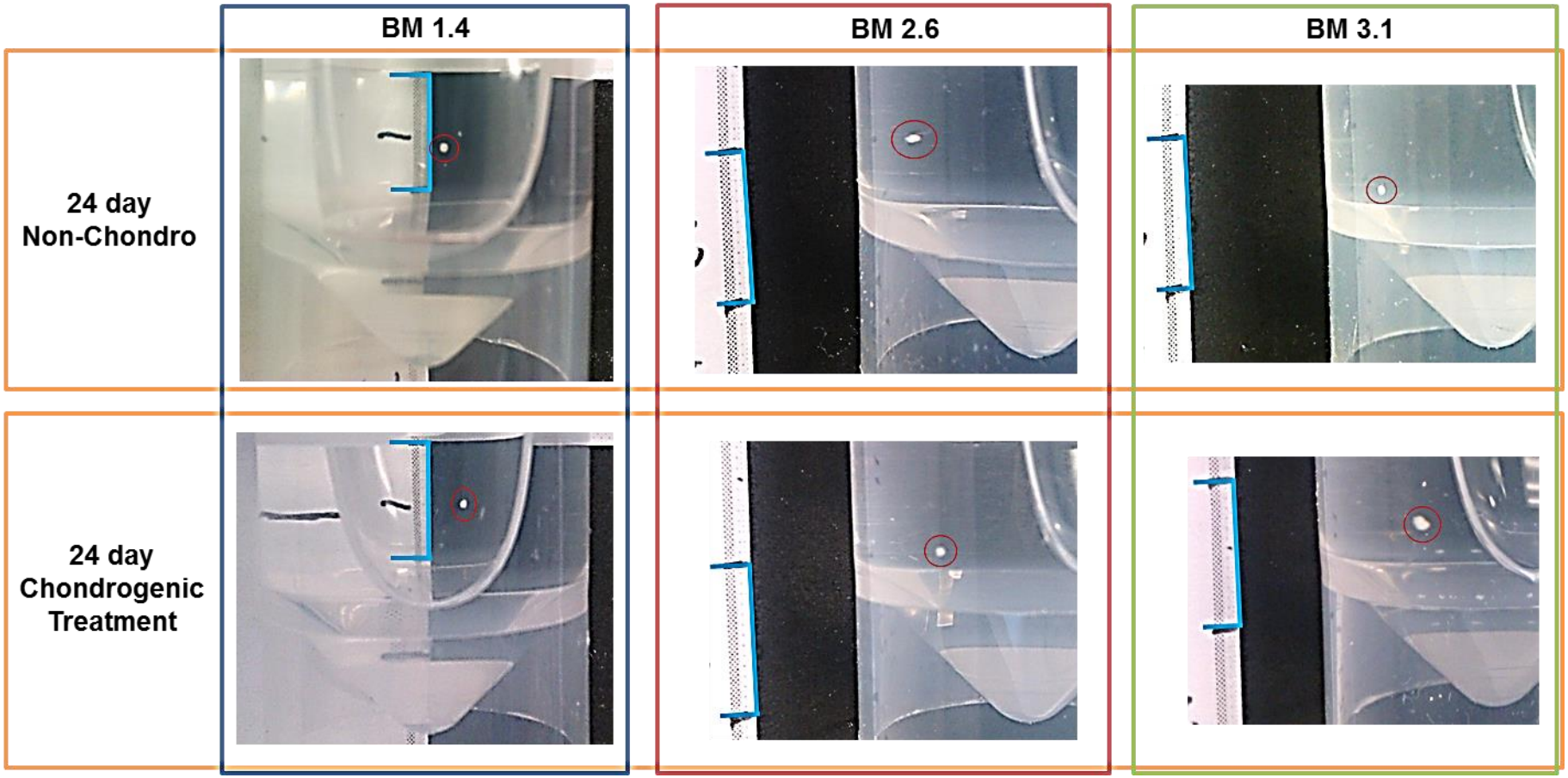

Figure 4.6: Photographs of bone marrow progenitor clones following 24 days culture in non-chondrogenic and chondrogenic treatment media. All clones for both non-chondrogenic and chondrogenic media formed pellets, which are encircled red. Scale bar (light blue), 1cm.

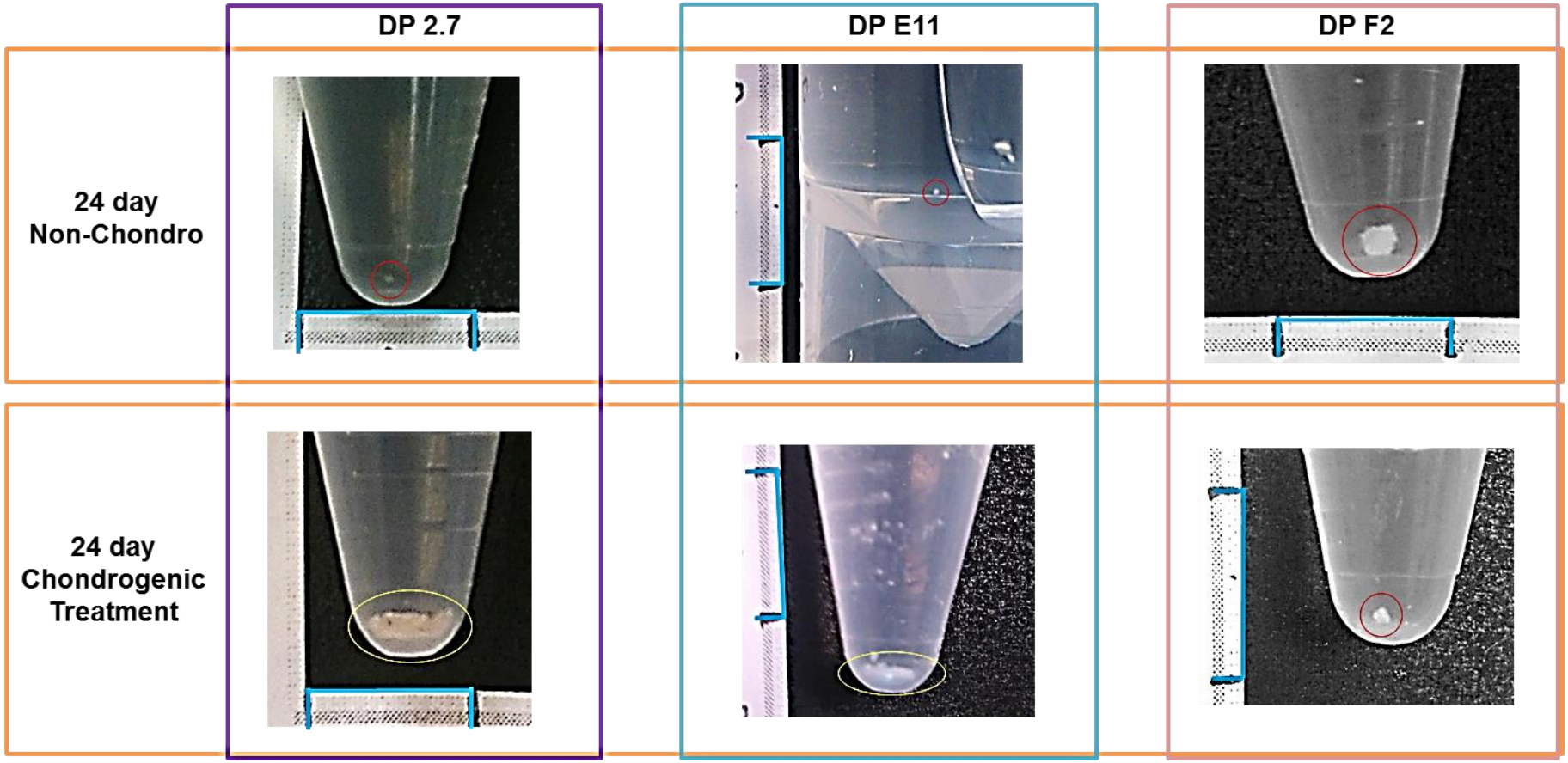

Figure 4.7: Photographs of dental pulp progenitor clones following 24 days culture in non-chondrogenic and chondrogenic treatment media. Formed pellets are encircled red, and chondrogenic treatment that formed a tissue-like disk only with no spherical pellet are encircled yellow. Scale bar (light blue), 1cm.

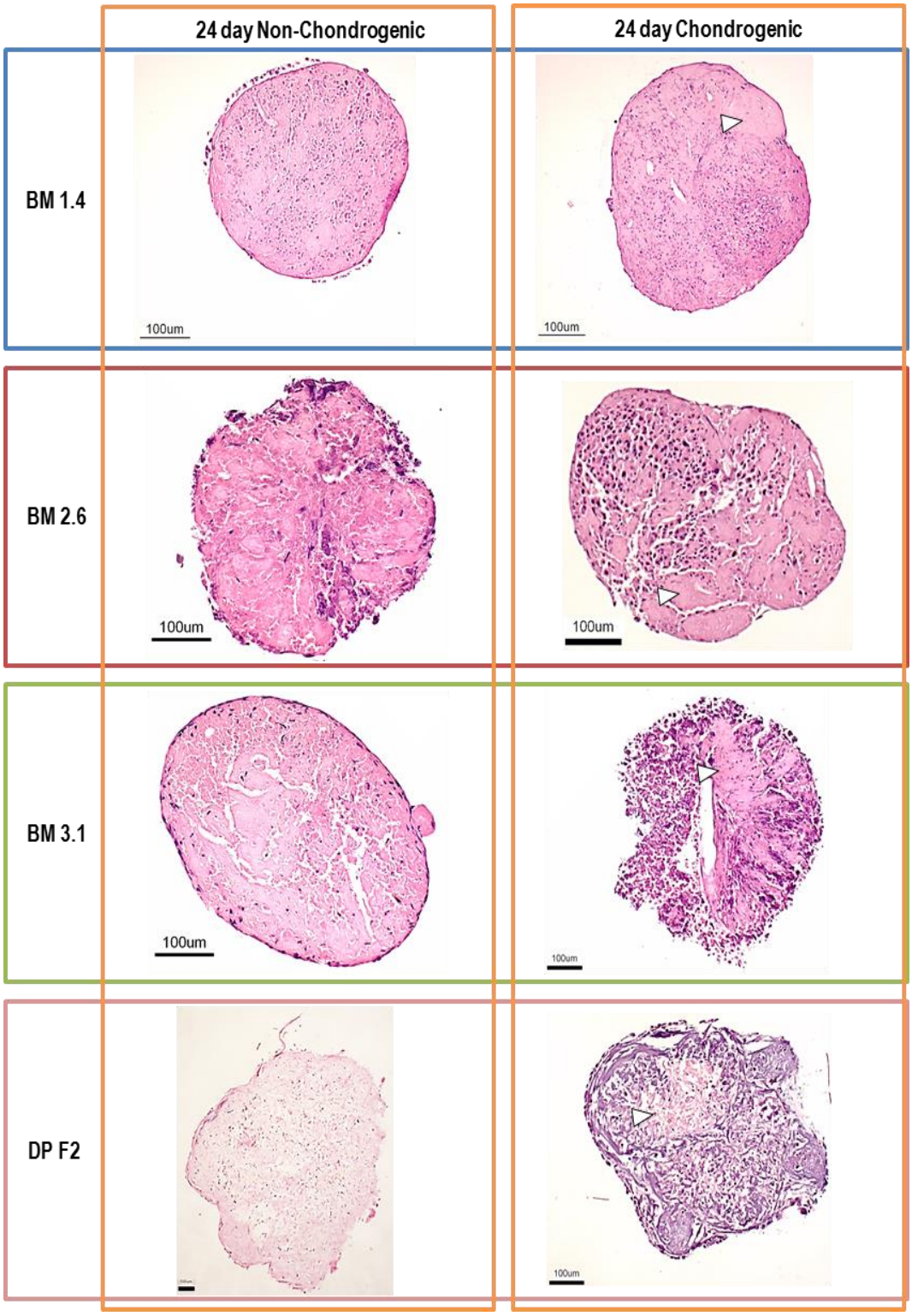

Figure 4.8: Bone marrow and dental pulp progenitor clones on day 24 chondrogenic differentiation *in vitro*, at mid PDL. Haematoxylin and eosin (H & E) staining showed a higher number of cells in chondrogenic treatment than non-chondrogenic medium, and chondrogenic treatment produced areas of extracellular matrix (white arrow-head) devoid of cells.

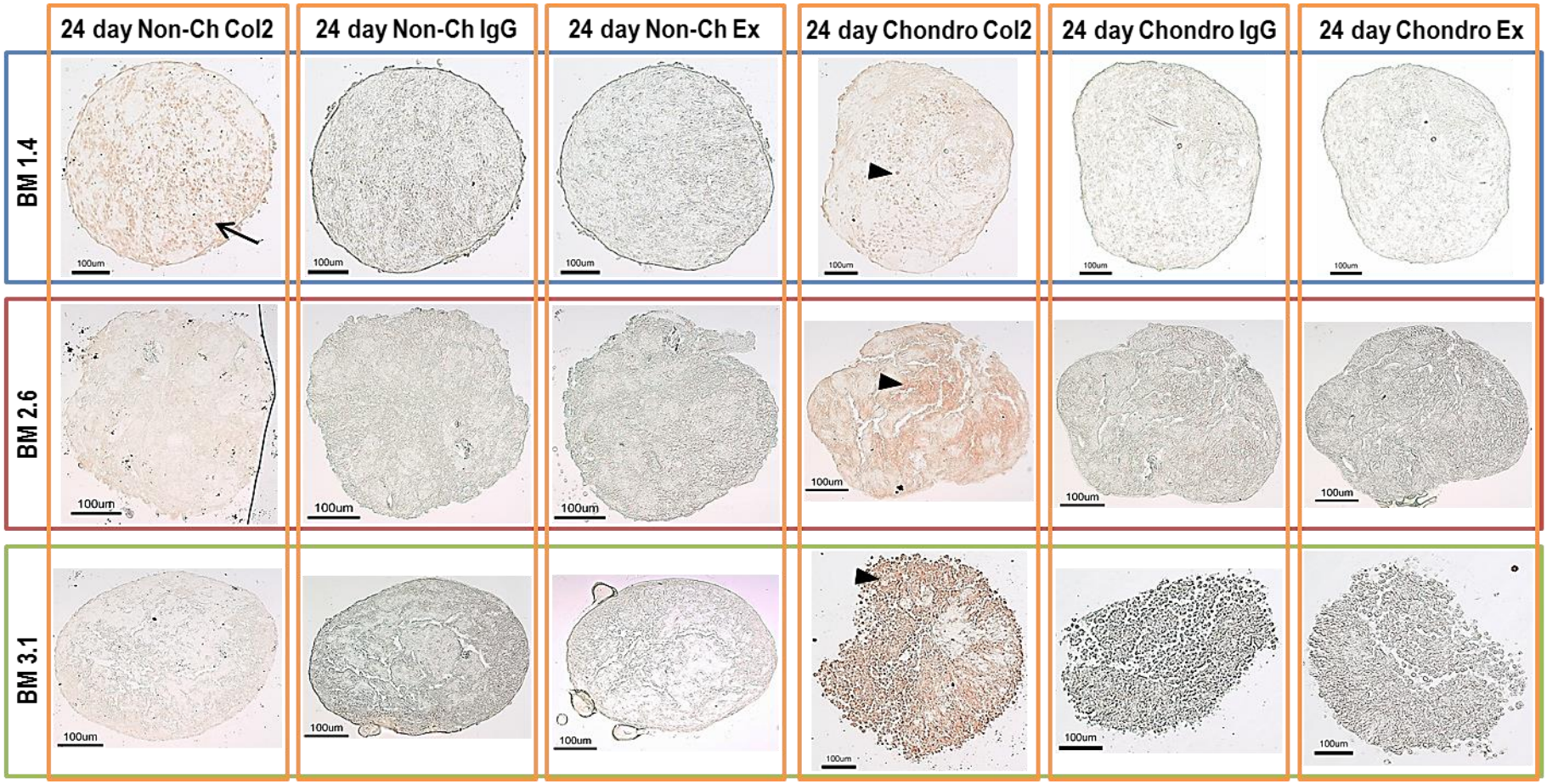

Figure 4.9: Bone marrow progenitor clones on day 24 chondrogenic differentiation *in vitro*, at mid PDL. Production of collagen II (Col2) was seen as brown staining (black arrow-head) in all chondrogenic (Chondro) treatment, and also in non-chondrogenic (Non-Ch) medium for BM 1.4 (black arrow). Isotype (IgG) and exclusion (Ex) antibody controls were negative. Scale bar, 100µm.

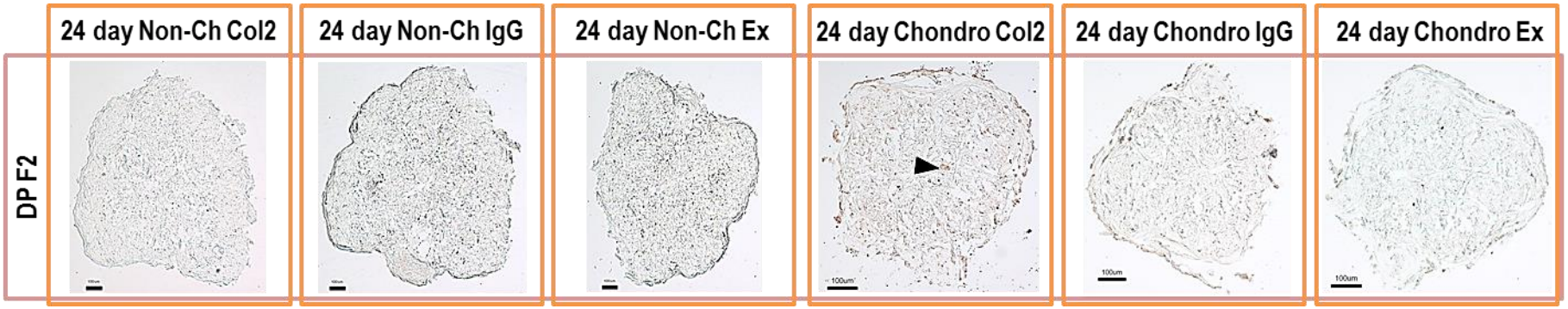

Figure 4.10: Progenitor clone DP F2 on day 24 chondrogenic differentiation *in vitro*, at mid PDL. The non-chondrogenic (Non-Ch) medium pellet was extremely large and approximately four times the size of the chondrogenic (Chondro) treatment pellet. Production of collagen II (Col2) was minimal in chondrogenic treatment, brown staining (black arrow-head). No collagen II was visible in non-chondrogenic. Isotype (IgG) and exclusion (Ex) antibody controls were negative. Scale bar, 100µm.

4.3.3 Osteogenic Differentiation of Characterised Progenitor Clones

Osteogenesis was evident in all clones from bone marrow and dental pulp. The morphology majorly differed between tissues, whereby bone marrow clones formed spherical nodules and dental pulp formed a more diffuse extracellular matrix. Calcification of these laid-down matrices was confirmed by intense alizarin red staining (figures 4.11 and 4.12). qPCR analysis showed all bone marrow clones and DP 2.7 clone significantly ($P<0.001$) increased their osteopontin expression, while all other markers showed no discernible pattern (figures 4.13 and 4.14). Upregulation of osteopontin was confirmed by immuolocalisation (figures 4.15 and 4.16). While mature markers BSP and osteocalcin were expressed by DP E11 and DP F2, which showed the most diffuse and intense alizarin red stain, 23 day treatment was not significantly upregulated compared to 23 day non-osteogenic control. Transcription factors RUNX2 was detected in all bone marrow and dental pulp clones at all time-points, while osterix was only detected in dental pulp clones at all time-points. For BM 1.4, levels of bone-related gene expression at 23 day osteogenic treatment had a significant ($P<0.001$) decrease in osteonectin and increase in osteopontin, compared to 0- and 23- day non-osteogenic medium. For BM 2.6, osteopontin significantly ($P<0.001$) increased at 23 day osteogenic treatment compared to 0- and 23- day non-osteogenic medium. For BM 3.1, osteopontin significantly ($P<0.001$) increased between each time-point and group, and osteonectin was significantly ($P<0.001$) higher at 23 day non-osteogenic medium compared to 0 day non-osteogenic and 23 day osteogenic media but showed no discernible pattern.

DP 2.7 had a significant ($P<0.001$) increase in osteonectin at 23 day non-osteogenic medium and 23 day osteogenic treatment compared to 0 day non-osteogenic, and increase in osteopontin at 23 day osteogenic treatment compared to 0- and 23- day non-osteogenic medium. For DP E11, BSP at 23 day non-osteogenic and 23 day osteogenic treatment led to a significant ($P<0.001$) increase compared to 0 day non-osteogenic. Osteopontin was significantly ($P<0.001$) lower at 23 day non-osteogenic medium compared to 0 day non-osteogenic and 23 day osteogenic media, but as with osteocalcin and osteonectin there was no discernible expression pattern. For DP F2, BSP was significantly ($P<0.001$) higher at 23 day non-osteogenic medium compared to 0 day non-osteogenic and 23 day osteogenic media, osteocalcin was significantly ($P<0.001$) higher at 0 day non-osteogenic medium compared to 23 day non-osteogenic and osteogenic media, and osteonectin was significantly ($P<0.001$) different between each time-point and group, however, there was no discernible gene expression patterns.

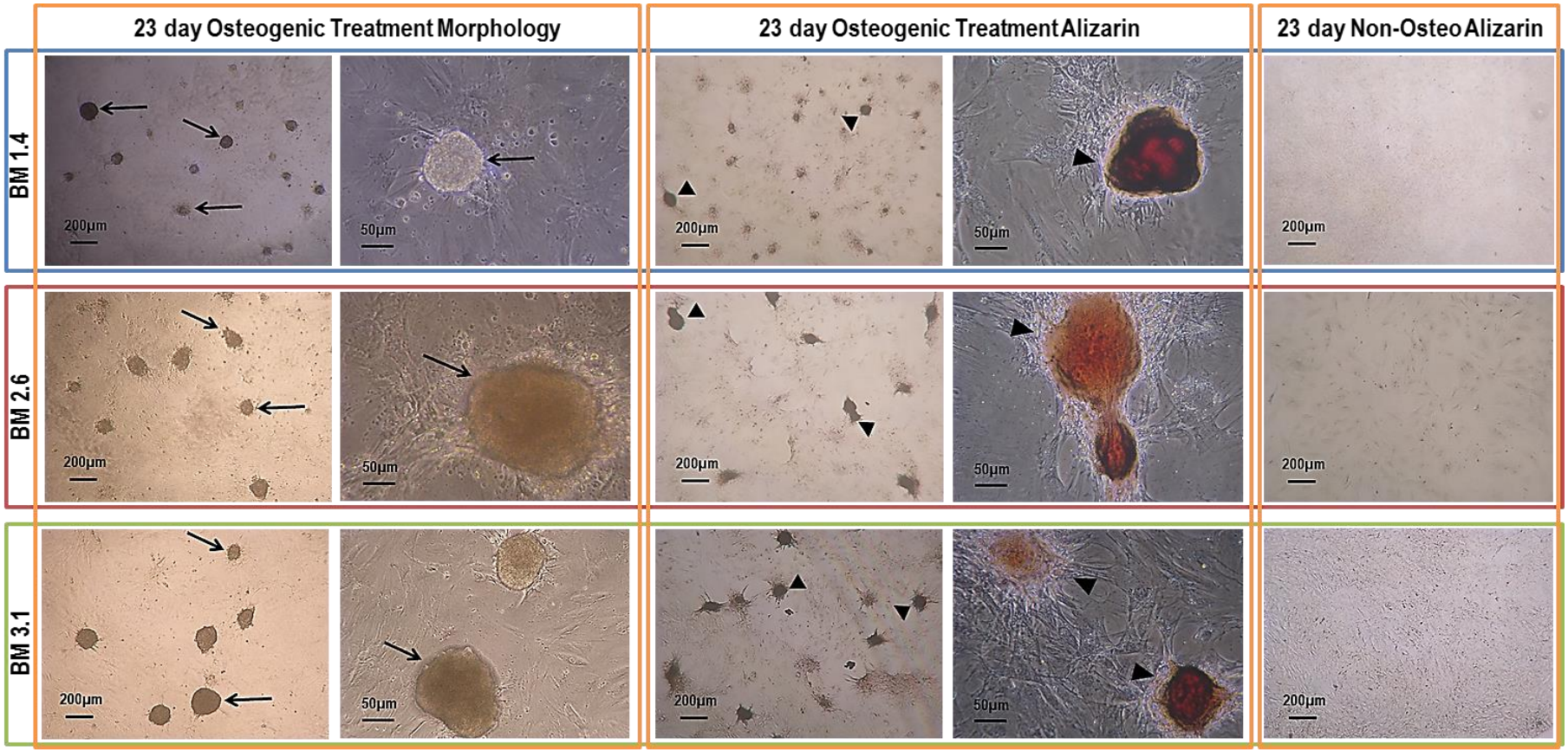

Figure 4.11: At mid PDL, osteogenic differentiation of progenitor clones BM 1.4, BM 2.6, and BM 3.1, on day 23 promoted medium, large, and extremely large dense spherical nodules respectively (arrows). Alizarin red stained calcium deposits within the extracellular matrix of osteogenic treatment (arrow-head). Morphology of non-osteogenic medium for all clones remained unchanged with no alizarin red staining. Scale bars: 4x and 20x objectives.

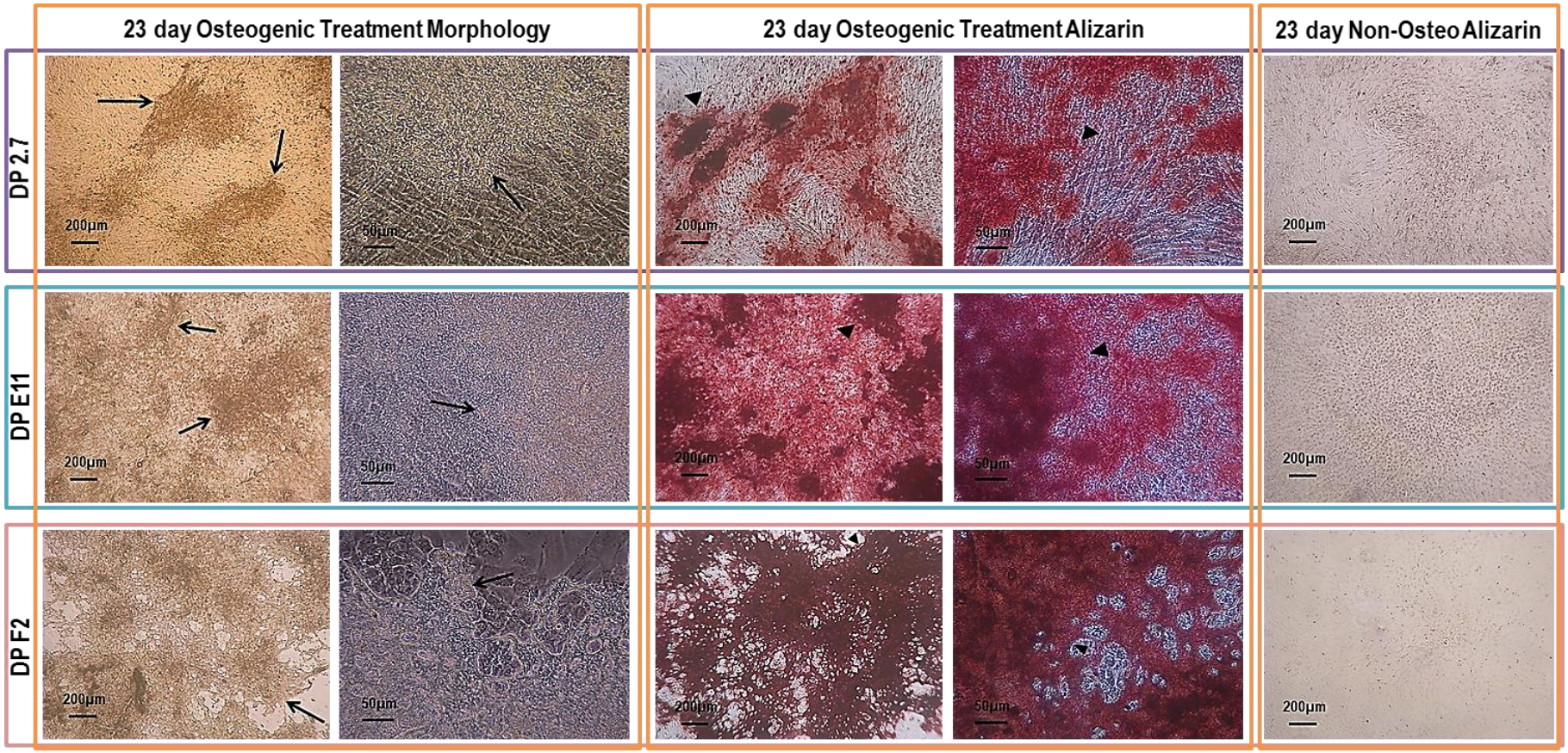

Figure 4.12: Osteogenic differentiation of progenitor clones DP 2.7, DP E11, and DP F2, on day 23 at mid PDL, promoted dark and dense accumulates (arrows). Alizarin red stained diffuse calcium deposits within the extracellular matrix of osteogenic treatment (arrow-head). Morphology of non-osteogenic medium for all clones remained unchanged with no alizarin red staining. Scale bars: 4x and 20x objectives.

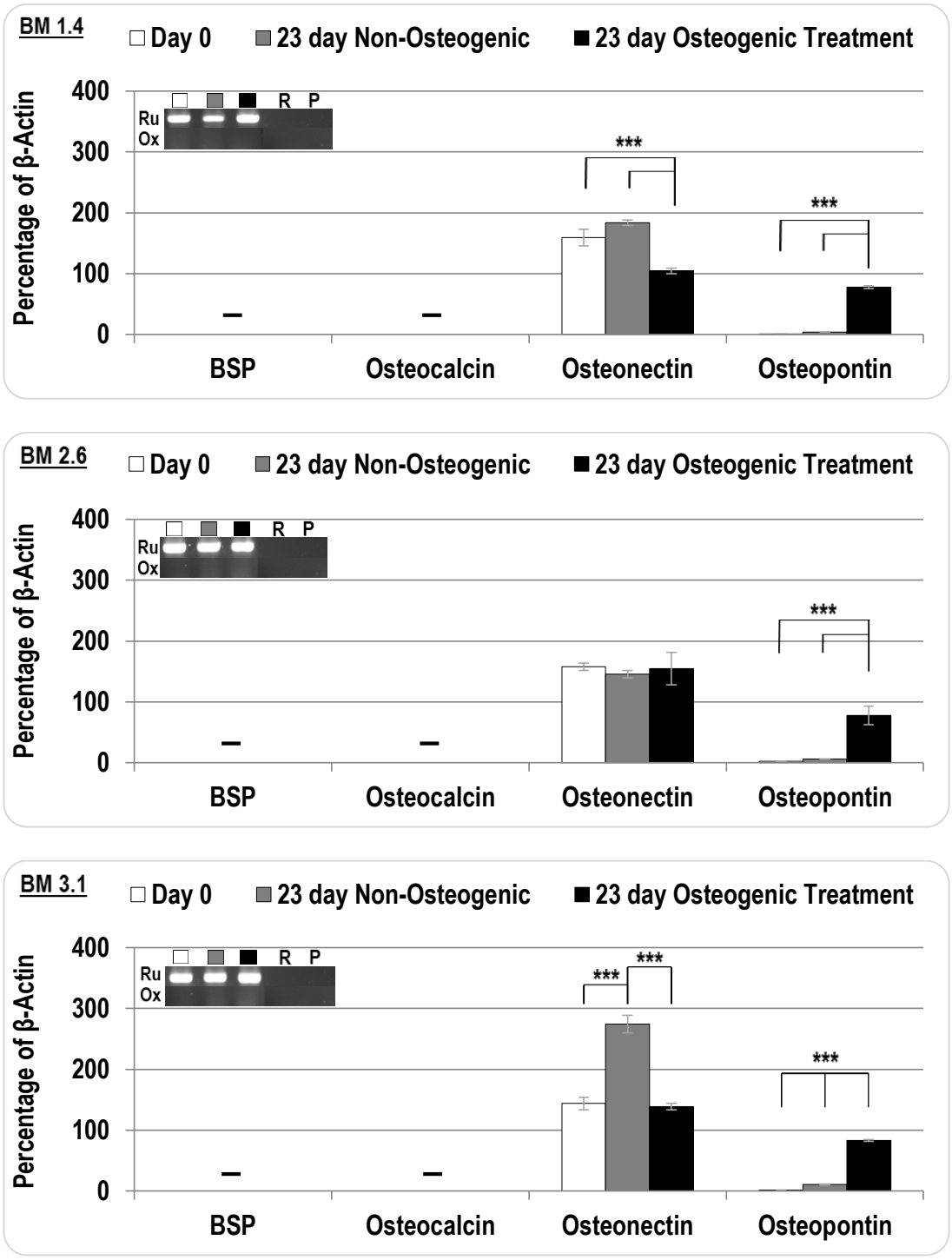

Figure 4.13: Progenitor clones BM 1.4, BM 2.6, and BM 3.1, expression levels of bone-related genes following *in vitro* osteogenic differentiation for 23 days. Osteogenic treatment lead to a significant increase in osteopontin for all bone marrow clones. Osteonectin showed a significant decrease for BM 1.4 only, with no discernible pattern for BM 2.6 and BM 3.1. Transcription factor RUNX (Ru) was present all at three time-points but osterix (Ox) was absent (end-point PCR inset). R = RT and P = PCR internal controls. Mean±SD. *** = P<0.001. (-) indicates not expressed.

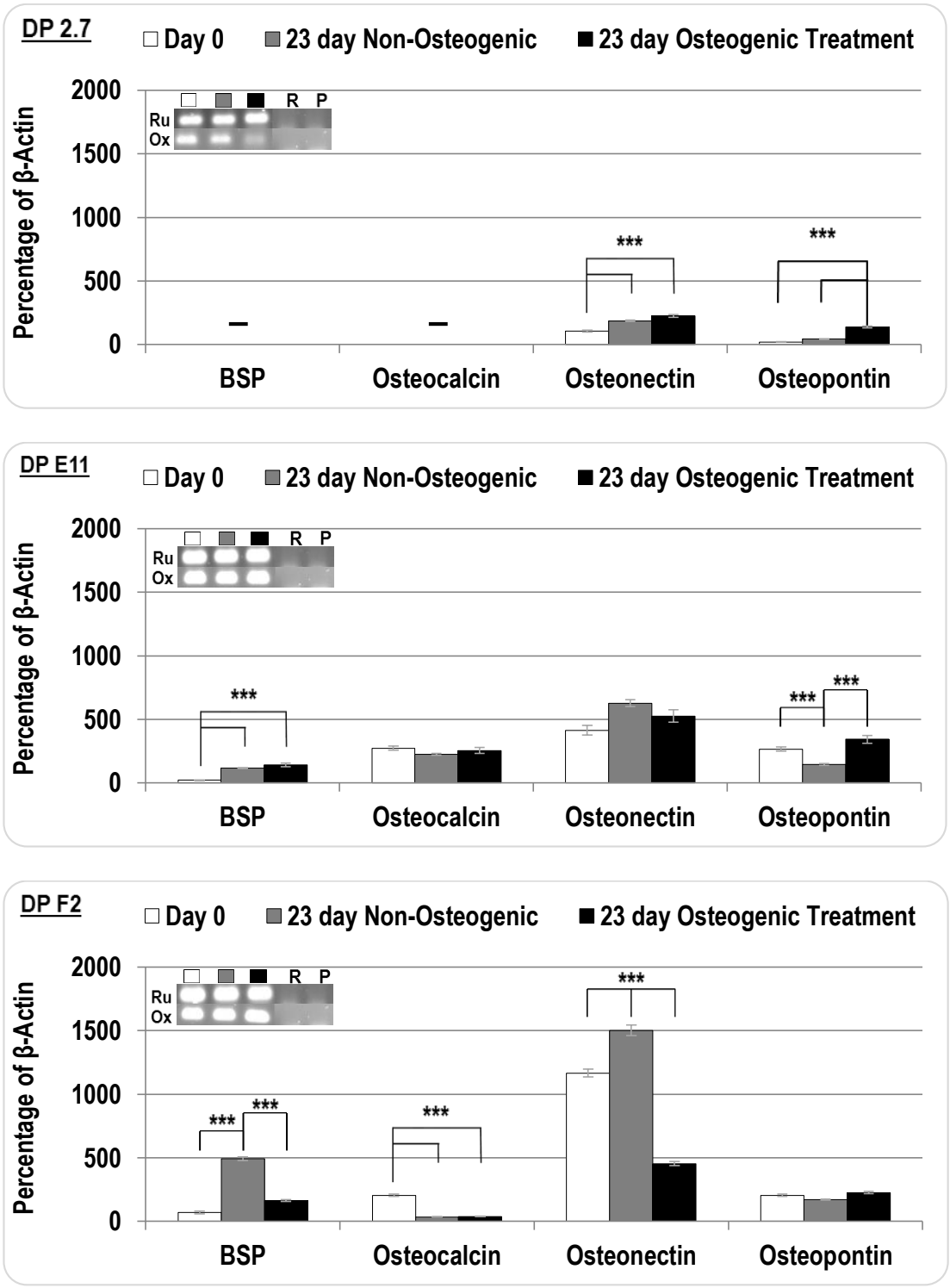

Figure 4.14: Progenitor clones DP 2.7, DP E11, and DP F2, expression levels of bone-related genes following *in vitro* osteogenic differentiation for 23 days. Osteogenic treatment lead to a significant increase in osteonectin and osteopontin for DP 2.7. DP E11 and DP F2 showed no osteogenic-treatment related gene expression patterns. Transcription factors RUNX (Ru) and osterix (Ox) were present all at three time-points (end-point PCR inset). R = RT and P = PCR internal controls. Mean±SD. *** = P<0.001.

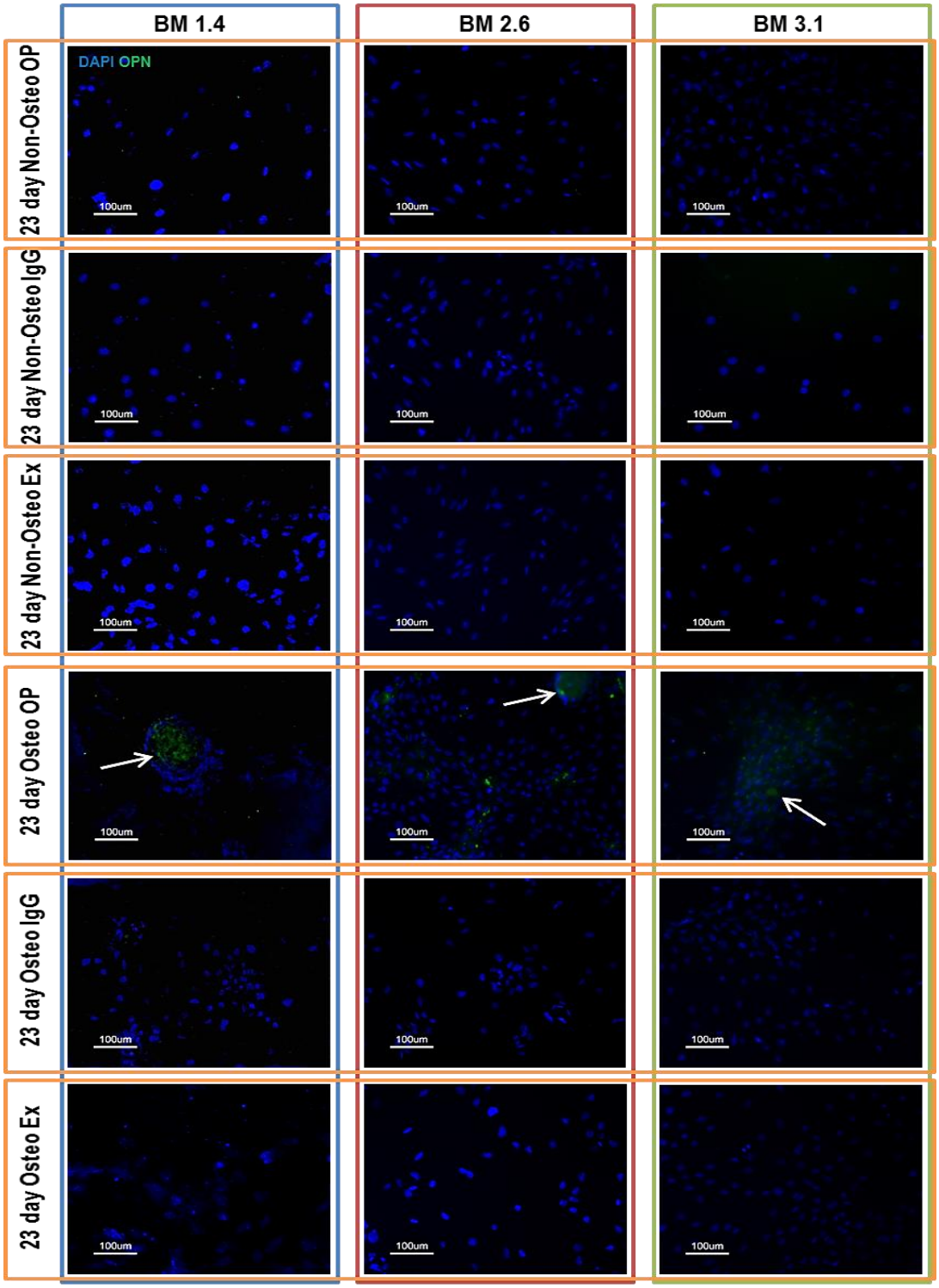

Figure 4.15: Osteogenic differentiation of progenitor clones BM 1.4, BM 2.6, and BM 3.1, on day 23 at mid PDL. Osteopontin (OPN) production in osteogenic (Osteo) treatment (white arrow) was confirmed by green-FITC, as indicated by upregulated gene expression using qPCR. No osteopontin expression was seen in non-osteogenic (Non-Osteo) medium. Isotype (IgG) and exclusion (Ex) antibody controls were negative. Equal exposure time for each clone. DAPI nuclei stain (blue). Scale bar 100µm (20x objective).

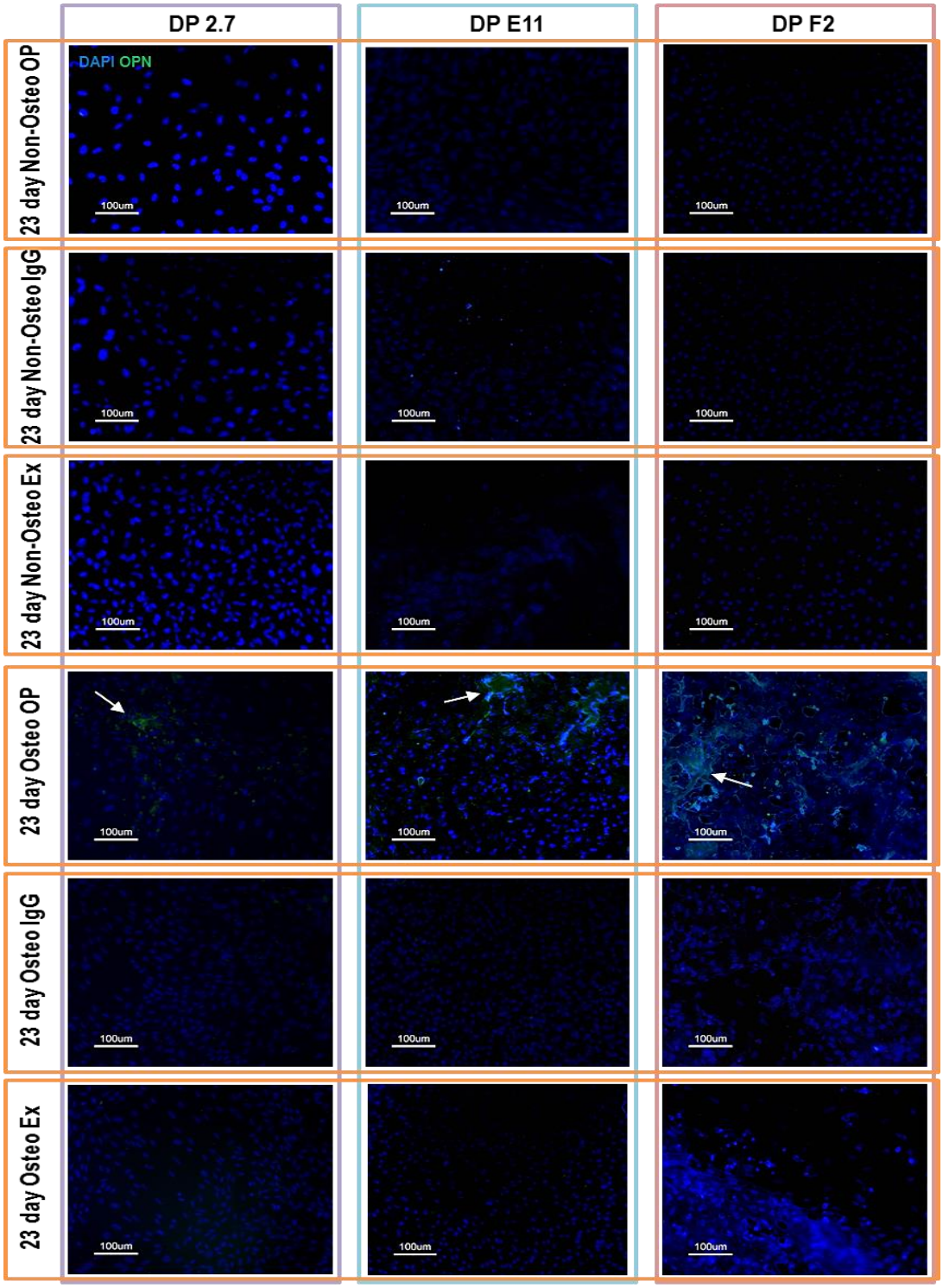

Figure 4.16: Osteogenic differentiation of progenitor clones DP 2.7, DP E11, and DP F2, on day 23 at mid PDL. Osteopontin (OPN) production in osteogenic (Osteo) treatment (white arrow) was confirmed by green-FITC, as indicated by upregulated gene expression using qPCR. No osteopontin expression was seen in non-osteogenic (Non-Osteo) medium. Isotype (IgG) and exclusion (Ex) antibody controls were negative. Equal exposure time for each clone. DAPI nuclei stain (blue). Scale bar 100µm (20x objective).

4.4 Discussion

As a continuation of the previous chapter, this chapter pioneered to simultaneously compare the multi-differentiation potential of clones from bone marrow and dental pulp tissues, in order to comprehensively characterise clonal variations of MSCs. All three bone marrow clones were capable of tri-lineage differentiation *i.e.* adipogeneis, chondrogenesis, and osteogensis. Whereas, dental pulp clones where uni- or bi- potent, which highlighted clonal variation. Bone marrow clones formed: adipocytes with the largest lipid vesicles and highest adipogenic-genes expression levels, chondrogenic spherical pellets with extensive extracellular matrix and collagen II production, and calcified extracellular nodules with the highest osteopontin expression change. Dental pulp clone DP 2.7 was bi-potent (adipogenic and osteogenic), DP E11 was uni-potent (osteogenic), and DP F2 was bi-potent (chondrogenic and osteogenic). Dental pulp clones, however, formed the most diffuse alizarin red calcified extracellular matrix, and was likely due to lineage restriction, as underlined in chapter 3 clonal characterisation, whereby DPSCs are lower hierarchy TA cells and more committed compared to BMSCs that are closely related to the mother stem cell. In addition, in conjunction with the previous chapter findings, the SOX2 marker appeared beneficial in the differentiation capacity of BMSCs.

The findings of this chapter lends support to the previous observations of the clones, whereby bone marrow clones are true stem cell progenitors and dental pulp stromal cells are more committed transit-amplifying (TA) cells. These results highlight that stem cells exist within a hierarchy (see Chapter 1, figure

1.1) (Chan et al., 2004), and that differentiation capacity was lost along the hierarchy to generate uni-potent osteogenic precursors (Muraglia et al., 2000). Dental pulp clones formed the most diffuse calcium extracellular matrix, which may represent precursors with osteogenic potential (Kuznetsov et al., 1997) due to mineralisation ability. Much debate surrounds the use of tissue clones *vs.* heterogeneous populations and none more so than concerning differentiation, in part due to reported limited proliferative ability of BMSC progenitor clones (Gronthos et al., 2003); with less than a third of the total cell population thought to be truly multipotent (Abdallah and Kassem, 2012). Dental pulp heterogeneous populations are reported to have greater multi-potent differentiation capacity compared to clones for odontoblasts, chondrocytes, adipocytes, neurons, and smooth muscles (Janebodin et al., 2011), which is opposed to bone marrow clones that display pluripotency (Jiang et al., 2002) and a high frequency for tri-potent differentiation (Muraglia et al., 2000). Lack of differentiation capacity lends support to limited potency of DPSC clones and possibly low numbers within the tissue, and hence for dental pulp sourced MSCs, a mixed heterogeneous cell population was likely required for multipotency.

Variation in differentiation capacity of human bone marrow clones has been reported, with all clones undergoing osteogenesis, 80% undergoing adipogenesis, and 30% undergoing chondrogenesis (Pittenger et al., 1999). In addition, limited bi-potency in human bone marrow clones has been reported for chondro-osteo but not for adipo-osteo (Muraglia et al., 2000), as seen here in DP F2 and DP 2.7, respectively. Interestingly, decreased bone formation

associated with age, was suggested to be due to lower cell numbers rather than decreased proliferative capacity or loss of function (Stenderup et al., 2003). Similarly, lack of multipotent differentiation capacity by DPSC clones could be due to proposed different progenitor populations, which were isolated based on neural crest marker low affinity nerve growth factor receptor (LANGFR) and β1 integrin expression (Sloan and Waddington, 2009), although both show propensity for adipogenic, chondrogenic, and osteogenic lineages (Waddington et al., 2009).

Adipocytes are derived from multipotent MSCs (Rosen and MacDougald, 2006). While all adipogenic clones formed multiple small lipid vacuoles characteristic of brown immature adipose tissue, BM 3.1 displayed large singular lipid vesicle sizes up to 25μm that engorged the adipocyte, which is characteristic of mature white adipose tissue (Saely et al., 2012). In addition, BM 1.4 and BM 2.6 displayed enlarging lipid droplets during adipogenic culture indicating maturing adipocytes that may have developed to white tissue as BM 3.1 if allowed to differentiate longer in culture. All droplets in DP 2.7 were <10μm and characteristic of immature brown adipose (Silva et al., 2014). The most marked upregulation during adipogenesis was seen by metabolic markers FABP4, a vital protein for solubilisation of fatty acids, their transport and storage (Marr et al., 2006), and LPL that hydrolyses triglyceride lipoproteins to form free fatty acids (Eckel, 1989). FABP4 upregulation was largest in BM 3.1 clones, and could be associated with formation of largest vesicles (unreported). There was no significant upregulation in transcription factor PPARγ, which could be due to its known early expression following

adipogenic induction (Ayala-Sumuano et al., 2008). Transcription factor CEBPα played a pivotal role in terminal adipogenic differentiation and halting proliferation (Freytag and Geddes, 1992), and was significantly upregulated in clones BM 1.4, BM 3.1, DP 2.7, and DP F2, however, DP F2 did not form adipocytes. Adipsin is a serine protease indicated in lipid metabolism (Cook et al., 1987, Miner et al., 2001) and adiponectin is an adipocytokine thought to be involved in insulin sensitisation (Okada-Iwabu et al., 2013). Both aforementioned markers were only expressed in adipogenic treatment culture for bone marrow clones and supports these truly multipotent MSCs as having committed fully to adipocytes, as displayed in mature white adipose (Ronti et al., 2006).

Chondrogenesis was successful in all BMSC clones and only DP F2 clone, as displayed by haematoxylin and eosin pellet morphology, and collagen type II expression. Collagen type II is classical of cartilage matrix (Oesser and Seifert, 2003) and the most reliable marker of chondrocytes (Lefebvre et al., 1997). Cartilage was the tissue type least formed by MSCs (Pittenger et al., 1999), which highlighted multipotency of BMSCs and confounds their true primitive stem cell hierarchy. While RNA was un-obtainable for gene expression comparison, elsewhere immunocytochemical analysis reports that un-stimulated DPSC and BMSC clones are negative for collagen type II (Gronthos et al., 2000).

Progenitors from the mesenchymal lineage are responsible for forming osteoblasts that once fully mature undergo either apoptosis, or proceed as

quiescent bone-lining cells, or entombed osteocytes (Delany and Hankenson, 2009). Osteogenic transcription factors RUNX2 and osterix are master regulators of osteogenic commitment, and RUNX2 was detected in all BMSC and DPSC clones for both non-osteogenic and osteogenic treatment cultures, as reported elsewhere (Gronthos et al., 2003). Expression level of RUNX2 was consistent during osteoblast differentiation (Mizuno and Kuboki, 2001), and knock-out arrested osteoblast differentiation (Ducy, 2000). The presence of RUNX2 was likely an indicator of a cells ability to undergo osteogenesis. Osterix is downstream of RUNX2 and specifically expressed by osteoblasts, and was essential for commitment of pre-osteoblasts to mature osteoblasts (Iohara et al., 2009, Zhang, 2012), which supports the notion of lineage-restricted DPSCs as BMSCs did not express osterix. Concerning bone-associated markers, osteopontin was present in osteoprogenitors indicating progenitor differentiation and was upregulated during matrix maturation (Lian and Stein, 1995), which was prior to BSP and subsequently osteocalcin (Liu et al., 1994) that bind hydroxyapatite and nucleates crystal formation (Ogata, 2008). Osteopontin is a phosphorylated glycoprotein expressed by osteoblasts restricted to endosteal and periosteal bone surfaces, and had a role in mineralised bone formation (Chen et al., 1993, Nilsson et al., 2005). Conversely, osteopontin was present on cells and involved in other processes such as cell adhesion, migration, and survival (Sodek et al., 2000). Here, osteopontin was significantly upregulated in all BMSC clones and DP 2.7, and likely indicated these clones were more primitive and non-committed, compared to DP E11 and DP F2 that expressed twice as much osteopontin with no significant upregulation and yet the most diffuse extracellular matrix

calcium deposition, which potentially indicated their lineage-commitment. BSP was reported to be expressed in pre-osteoblasts through to mineralisation stage, whereas osteocalcin was only seen in mature osteoblasts up to mineralisation after which expression was lost (Liu et al., 1994, Aubin et al., 1995). BSP and osteocalcin were evident at day 0 in both DP E11 and DP F2 for non-osteogenic and osteogenic treatment, which again supported the notion of lineage-commitment in these clones. Elsewhere, osteocalcin has been reported to be expressed in progenitors following a minimum of 28-35 days in osteogenic culture (Gronthos et al., 2003), and was not upregulated for up to 28 days alongside non-osteogenic (Neumann et al., 2008). Likewise, BSP did not upregulate expression between non-osteogenic and osteogenic treatment, as previously reported (Janebodin et al., 2011), which may suggest osteogenic imprinting and restricted differentiation potential in unstimulated cells (Satomura et al., 2000). Indeed, DP F2 formed the densest and deepest alizarin red and had decreased BSP and osteocalcin in 23 day osteogenic treatment, likely due to completion of mineralisation phase and thus lacked need of said gene-expression. All bone marrow clones and DP 2.7 lacked osteocalcin and BSP, and was likely due to their lesser matrix maturation and earlier-stage mineralisation. Interestingly, osteocalcin was reportedly expressed by dental pulp populations and only a subset within bone marrow, while BSP was not expressed in dental pulp but is within a subset of bone marrow cells (Gronthos et al., 2000), which is opposed to expression seen here. As a side note, osteonectin-null mice are osteopenic and display decreased bone formation (Delany et al., 2000), but osteonectin is also present in many other tissues at sites of turnover, and injury and disease, contributing

to matrix organisation (Bradshaw and Sage, 2001). As such, osteonectin is critical in bone remodelling (Delany and Hankenson, 2009), but appears to not undergo predictive changes in expression during *in vitro* osteogenesis.

As mentioned previously, all bone marrow clones and DP 2.7 significantly increased osteopontin expression, which was reported first to be expressed during osteoblastic differentiation and bind calcium within the matrix, and likely accounted for alizarin red staining, albeit binding was to a lesser extent than BSP (Chen et al., 1992). Conversely, osteopontin was proposed to inhibit hydroxyapatite formation controlling the size of crystals formed (Hunter et al., 1996). All clones analysed underwent osteogenesis, however, dental pulp clones formed the most diffuse and extensive calcified extracellular matrix compared to bone marrow clones. The two dental pulp clones that formed the most calcified matrix, DP E11 and DP F2, were the only clones to express the mature osteogenic genes BSP and osteocalcin in non-differentiation, which likely underlined their committed lineage restriction without need for osteogenic promoting medium (Kuznetsov et al., 1997), and suggested a "default" osteo-differentiation pathway in confluent DPSC cultures (Janebodin et al., 2011), unlike the more primitive BMSC progenitor clones that required osteogenic-promotion for increased osteopontin gene expression and protein level. In addition, absence of mature osteo-markers, BSP and osteocalcin by DP 2.7, could be due to its lack of commitment and thus adipogenic capability. Thus, it is likely that DPSCs are "primed" for differentiation and gave greater mineralisation within the same time-period than BMSCs. This is due to their *in vivo* role whereby BMSCs are constantly remodelling bone, and DPSCs require a rapid-response within the tooth following damage/injury, and hence

these MSC cell-soucres are at different stages of and have different time-scales for mineralisation.

A consideration of *in vitro* studies is their limitations and that *in vivo* models offer genuine predictive tissue regenerative ability (Gronthos et al., 2003), with evidence that serum source significantly affected cultured cells (Zheng et al., 2006) and their differentiation ability (Duggal and Brinchmann, 2011). *In vitro* attempts have failed to characterise and distinguish multi-potent clones based on cell morphology and growth rate (Kuznetsov et al., 1997, Kuznetsov et al., 2001), and cell surface marker expression (Shi et al., 2001, Gronthos et al., 2003). In support, the data presented within this chapter suggested that phenotype is likely not useful in predicting a cells' differentiation ability, as no specific MSC gene marker was highlighted as beneficial to differentiation capacity. Others have reported isolation of multipotent DPSC progenitors from monopotent clones by differential expression of minimal criteria MSC marker CD90, where the multipotent clone expressed CD90 at <5% of the population (Lacerda-Pinheiro et al., 2012), which would be opposite to that expected. Likewise, a second minimal criteria MSC marker CD105 was shown to be inversely correlated with differentiation ability in umbilical cord-MSCs (Jin et al., 2009). Ambiguity in MCAM has also been reported, where an $MCAM^+$ subpopulation of periodontal ligament MSCs showed higher proliferative potential and osteogenic capacity than $MCAM^-$ cells (Zhu et al., 2013), while a subpopulation of $MCAM^-/CD31^-$ DPSCs regenerated capillary and neuronal networks in amputated pulp *in vivo* (Iohara et al., 2009). Another adhesion molecule VCAM1 displayed tri-lineage capacity in $STRO\text{-}1^+/VCAM1^+$ cells, but

was limited to clones at PDL 20, as clones >25 PDLs displayed differentiation inability (Gronthos et al., 2003). Interestingly, $VCAM1^+$ BMSCs were preferentially adipogenic (Fukiage et al., 2008), and of the three DPSC clones only the $VCAM1^+$ clone, DP 2.7, was adipogenic. Hence, $VCAM1^-$ progenitors could be preferable for osteogenesis, as DP E11 and DP F2 (see Chapter 3, figure 3.19). In addition, Msx2 was reported to prevent osteoblast differentiation (Dodig et al., 1999), while elsewhere Msx2 was reported to promote osteogenic differentiation of MSCs by enhancing Wnt signalling important for osteogenesis (Cheng et al., 2008). Although the most osteogenic clones DP E11 and DP F2 expressed the highest MSX2, MSX2 expression was not associated with BMSC clone osteogenic capacity.

The only marker with any apparent relevance to differentiation capacity was SOX2. While SOX2 was reported to be expressed by heterogeneous DPSCs (Karaoz et al., 2011), single-cell populations weakly expressed (Janebodin et al., 2011), and here DPSC clones were negative (see Chapter 3, figure 3.16). This supported the notion that DPSC clones are lineage-restricted and -committed, as DPSCs lost SOX2 upon commitment unlike Nanog (Nozaki and Ohura, 2011), which is a non-defining factor for pluripotency in somatic-induced stem cells (Takahashi and Yamanaka, 2006). Nanog was expressed by all BMSC and DPSC clones analysed, and thus SOX2 was suggested a better predictor of differentiation capacity (Nozaki and Ohura, 2011). In addition, $SOX2^-$ DPSC clones only displayed uni- or bi-potent differentiation capacities, inclusive of osteogenesis. Hence, the pool of “truly” multipotent MSCs in dental pulp may be lower compared with bone marrow, as all BMSC clones expressed SOX2 and proved tri-potent differentiation.

To summarise, in support of the previous chapter findings, BMSC clones formed few and large sized colonies with a high and less varied proliferation rate beyond 20 PDLs, which was characteristic of cells higher in the stem cell hierarchy and closely related to the mother stem cell. This chapter highlighted high frequency and multipotent capacity of BMSC clones as a true indicator of their primitive stem cell nature. Whereas, in the previous chapter DPSCs formed many small colonies with more variable proliferation rates characteristic of lower stem cell hierarchy lineage committed TA cells, and in this chapter DPSCs displayed limited differentiation capacity with uni- and bi-potent clones. However, dental pulp tissue clones appear preferential for bone formation, and are potentially a reliable alternative source to bone marrow, advancing tissue engineering in pulpal regeneration and craniofacial bone regenerative medicine (Miura et al., 2006).

Chapter 5

Influence of Bone and Tooth Matrix Extracts on Proliferation and Osteogenesis of Bone Marrow and Dental Pulp Mesenchymal Stromal Cell Clones

5.1 Introduction

The tissue regenerative capabilities of bone marrow was introduced in the early 1970's, by way of so termed stromal stem cells (Patt and Maloney, 1975), although it was not until the early 1990's that use of MSCs in regenerative medicine was conducted. In addition, the recognition of extracted bone matrix on osteogenesis was introduced in 1965, *via* a process proposed as "autoinduction", due to migration and proliferation of immature host cells into decalcified bone matrix implants, which formed new osteoblasts (Urist, 1965). This followed a report the same year that suggested organic bone matrix determines osteoclasis (Irving and Migliore, 1965). Then, the late 1980's and early 1990's saw use of implantable scaffolds for tissue engineering (based on literature report dates). Followed by use of bone mineralised-tissue protein extracts due to contained bioactive components *e.g.* BMPs (Boden, 1999). More recently, is the idea of de-cellularised tissue protein matrices for use in re-cellularisation with specific cells, to precisely control and direct differentiation (Hoganson et al., 2014). Thus, while several applications exist to promote tissue regeneration, they all involve use of cells or proteins or biomaterial scaffolds, and it is the view here that an ideal cell-type source combined with a protein scaffold, would be optimal for translational regenerative medicine.

Regarding proteins within the extracellular matrix, research as early as the 1980's implicated proteoglycans (PGs) and their glycosaminoglycan (GAG) chains in sequestration of growth factors produced within the bone marrow microenvironment by *e.g.* stromal cells, and subsequent presentation in a biologically active form to *e.g.* haematopoietic progenitor cells. The functional result of GAG depletion is a 50% decrease in colony-forming unit number, which indicates influence of GAGs on cell replication (Gordon et al., 1987). In addition, research on the haematopoietic environment, shows the GAG hyaluronan regulates cytokine production *e.g.* IGF-1 (involved in proliferation and growth-promotion) *via* TNFα, and IL-1β (involved in inflammation, proliferation, differentiation, and apoptosis) (Noble et al., 1993), which are likely important processes in tissue regeneration (Goncharova et al., 2012). Other PGs within the extracellular matrix include biglycan and decorin, and their GAG chains dermatan and chondroitin sulfate. These PGs are highly expressed and display spatially restricted gene expression patterns and localisation during bone (Bianco et al., 1990) and tooth development (Matsuura et al., 2001). Consequently, extracellular matrix proteins are no longer considered as a structural contribution only, but a protein that directly and/or indirectly influences cellular behaviour.

Both bone and tooth tissues express proteins involved in mineralisation and calcification *e.g.* BSP, bone-acidic glycoprotein-75 (BAG-75) (Bronckers et al., 1993), and more tooth-associated dentin sialoprotein/dentin phosphoprotein (DSP/DPP) and dentin matrix protein-1 (DMP1) (Hu et al., 2006). While

research has uncovered bone associated proteins that are expressed in tooth, there are tooth restricted proteins found within the enamel *e.g.* amelogenins, amelobastins, enamelins and tuftelins (Robey, 1996), which are proposed as essential in bio-mineralisation and formation of hard tissues (Lyngstadaas et al., 2009).

In addition to the potential of an individual MSC clone, it has become evident that the extracellular matrix mircro-environment in which they find themselves, has a major influence on their behaviour; with biomaterial scaffolds providing a template structure and simultaneous cell signals for promotion of proliferation and differentiation (O'Brien, 2011). With characterisation and differentiation capacity of MSC clones being defined in the previous two chapters, the next focus was the influence of whole-protein matrix extracts of the MSC-clone niche from rat bone and tooth, on clonal proliferation and differentiation, specifically the capacity for osteogenic mineralisation. This research chapter aimed to assess the influence of whole-protein matrix extracts on *in vitro* clone viability, morphology, expansion, and osteoinduction, and to visualise protein profiles of extracted matrices.

5.2 Materials and Methods

The metabolism assay was used as a measure of cell viability for BMSC and DPSC clones over a 7 day period, to choose clones for further analysis (see 2.13 Metabolism Assay with Thiazolyl Blue Tetrazolium Bromide (MTT)). Cells were seeded in 10% culture medium at $2.8x10^3/cm^2$, $5.7x10^3/cm^2$, $11.4x10^3/cm^2$, $17.1x10^3/cm^2$, and $22.8x10^3/cm^2$. Whole-proteins from matrices were extracted from long bones and tooth incisors, referred to bone matrix extract (BME) and tooth matrix extract (TME), respectively (see 2.11 Mineralised Tissue Whole-Protein Extraction and Dialysis), and were each measured for protein concentration by assay (see 2.12 Bicinchoninic Acid (BCA) Protein Assay). One clone from each source was taken for further analysis without and with protein at 0.1µg/mL, 0.5µg/mL, 1µg/mL, and 2µg/mL, using an optimal seeding density of $5.7x10^3$ cells per cm^2. Morphological effects of BME and TME on cells was visually observed and assessed by cell size, appearance and thickness of stress-fibres. Growth expansion was assessed in presence of matrix extracts for 0.1µg/mL, 0.5µg/mL, and 1µg/mL protein concentrations, by successively passaging cells every 3-4 days up to day 30. The optimal protein concentration of 0.5µg/mL was then set for both extracts and was exposed to each clone for a period of 23 days, and assessed for alizarin red stain (see 2.7.9 Osteogenic Differentiation Alizarin Red Staining) and bone-related gene expression using qPCR (table 2.5) (see 2.6 Quantitative-Polymerase Chain Reaction of Colony Clones). In addition, BME and TME whole-protein extracts (10µg) underwent SDS-PAGE to identify protein band profiles (see 2.14 Sodium Dodecyl Sulphate – Polyacrylamide Gel Electrophoresis), by coomassie blue and silver staining.

5.3 Results

5.3.1 Cell Viability of MSC Clones from Bone Marrow and Dental Pulp

The number of viable cells of BM 2.6 and BM 3.1 peaked at day three, and BM 1.4 activity peaked at day five, and all plateaued thereafter (figure 5.1). The highest activity rate was that of BM 3.1, which displayed the most distinct relationship between seeding density and viability. By day 7, BM 3.1 cells seeded at $2.8x10^3/cm^2$ had a significantly lower viability compared to cells seeded at $11.4x10^3/cm^2$, $17.1x10^3/cm^2$, and $22.8x10^3/cm^2$. Although the viability of BM 3.1 was twice that of BM 1.4, by day 7, BM 1.4 also showed cells seeded at $2.8x10^3/cm^2$ had a significantly lower viability than cells seeded at $11.4x10^3/cm^2$, $17.1x10^3/cm^2$, and $22.8x10^3/cm^2$, and additionally viability of cells seeded at $5.7x10^3/cm^2$ was significantly lower than $17.1x10^3/cm^2$. For clone BM 2.6, cells seeded at the lowest density $2.8x10^3/cm^2$ only had a significantly lower viability compared to cells seeded at the highest density $22.8x10^3/cm^2$ (figure 5.1).

Viability of DPSC clones peaked later than BMSC clones. DP 2.7 and DP E11 peaked at day five and decreased thereafter, whereas DP F2 increased up to day seven and gave the highest number of viable cells, displaying the most distinct relationship between viability and seeding density (figure 5.2). By day 7, DP F2 clone viability at each seeding density was significantly different to the other, with exception of no difference between $2.8x10^3/cm^2$ and $5.7x10^3/cm^2$, and so viability correlated well with cell seeding density. DP E11 cells seeded at $2.8x10^3/cm^2$ had a significantly lower viability than all higher seeding densities, and at $5.7x10^3/cm^2$ viability was significantly lower than

$17.1x10^3/cm^2$ and $22.8x10^3/cm^2$. DP 2.7 cells seeded at $2.8x10^3/cm^2$ only had a significantly lower viability than $17.1x10^3/cm^2$.

Consequently, BM 3.1 and DP F2 were taken on for further analysis with whole-protein matrix extracts.

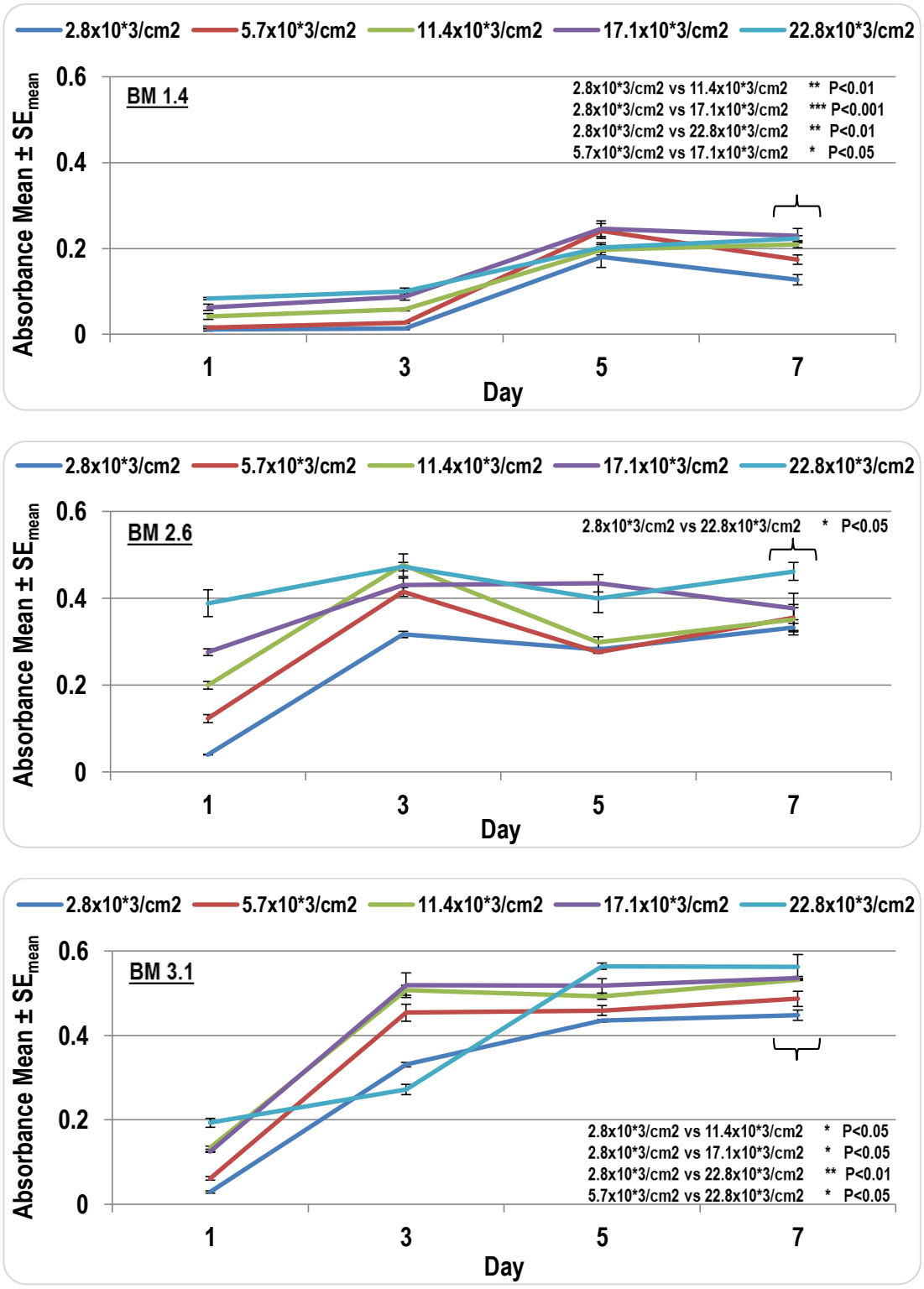

Figure 5.1: Progenitor clones BM 1.4, BM 2.6, and BM 3.1, viability in culture for seven days. BM 1.4 activity peaked at day five, and BM 2.6 and BM 3.1 peaked at day three, and all plateaued thereafter. BM 3.1 gave highest activity rate and displayed most distinct relationship between viability and seeding density, as seen from day 7 statistics (inset). Seeding density stated as cell number (x10^3 per cm^2). Mean±SE_{mean}. *n*=1 (triplicate).

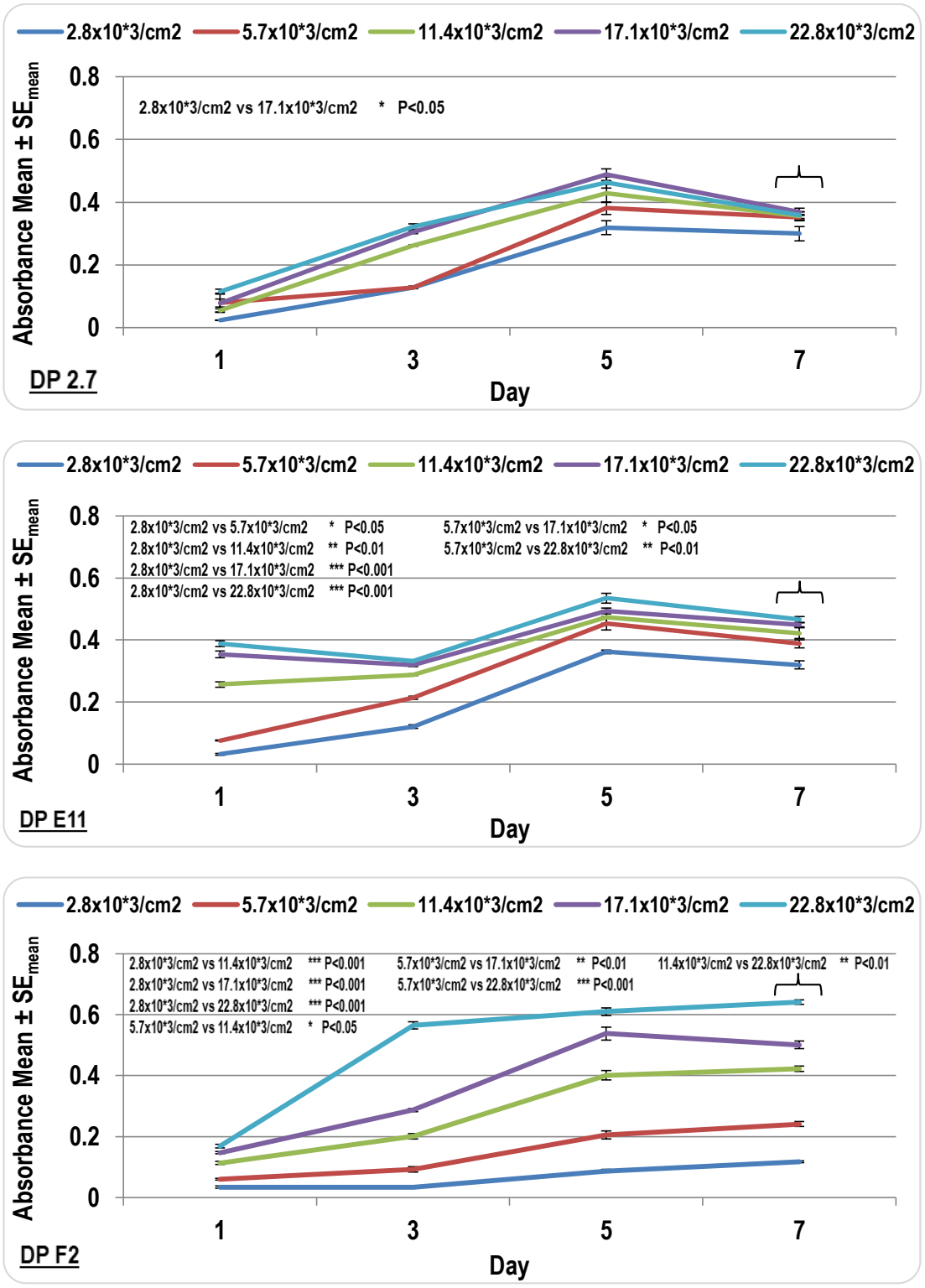

Figure 5.2: Progenitor clones DP 2.7, DP E11, and DP F2, viability in culture for seven days. DP 2.7 and DP E11 activity peaked at day five and decreased thereafter. DP F2 activity increased up to day seven. DP F2 gave highest activity rate and displayed most distinct relationship between viability and seeding density, as seen from day 7 statistics (inset). Seeding density stated as cell number (x10^3 per cm^2). Mean± SE_{mean}. *n*=1 (triplicate).

5.3.2 Viability and Morphology of Selected MSC Clones in Whole-Protein Matrix Extracts

From the cell viability of bone marrow and dental pulp clones, the most highly active clone from each source that displayed significant differences between seeding densities was chosen for further analysis *i.e.* BM 3.1 and DP F2. These two clones had their viability and cell expansion ability assessed in the presence of whole-protein matrix extracts from rat long-bones, termed bone matrix extract (BME), and rat incisor tooth, termed tooth matrix extract (TME).

The viability of clone BM 3.1 with 2μg/mL BME was significantly ($P<0.01$) decreased by day three (figure 5.3), which was probably due to a too high concentration of protein as no viable cells were visualised in the cell culture (figure 5.5). No-extract control and other protein concentrations were not significantly decreased, but at 1μg/mL the viability was below that of lower protein concentrations (figure 5.3) and the cultured cells appeared larger in size with a stressed-like morphology (figure 5.5).

In the presence of TME, BM 3.1 displayed more varied effects in viability by day three (figure 5.3). Similarly as BME by day three, 2μg/mL of TME significantly ($P<0.01$) decreased viability, and cells were few in number and morphologically appeared with thick aligned stress-fibres (figure 5.6). A second group of TME protein concentrations (0.5μg/mL and 1μg/mL) significantly ($P<0.05$) decreased viability compared to no-extract control and 0.1μg/mL (figure 5.3).

For the majority, both BME and TME proteins displayed no influence on DP F2 viability, with exception that 2μg/mL TME significantly ($P<0.05$) decreased activity on day three (figure 5.4). Likewise, the morphological appearance of DP F2 remained relatively unchanged, with only few enlarged cells with thin stress-fibres in 2μg/mL BME and TME (figures 5.7 and 5.8).

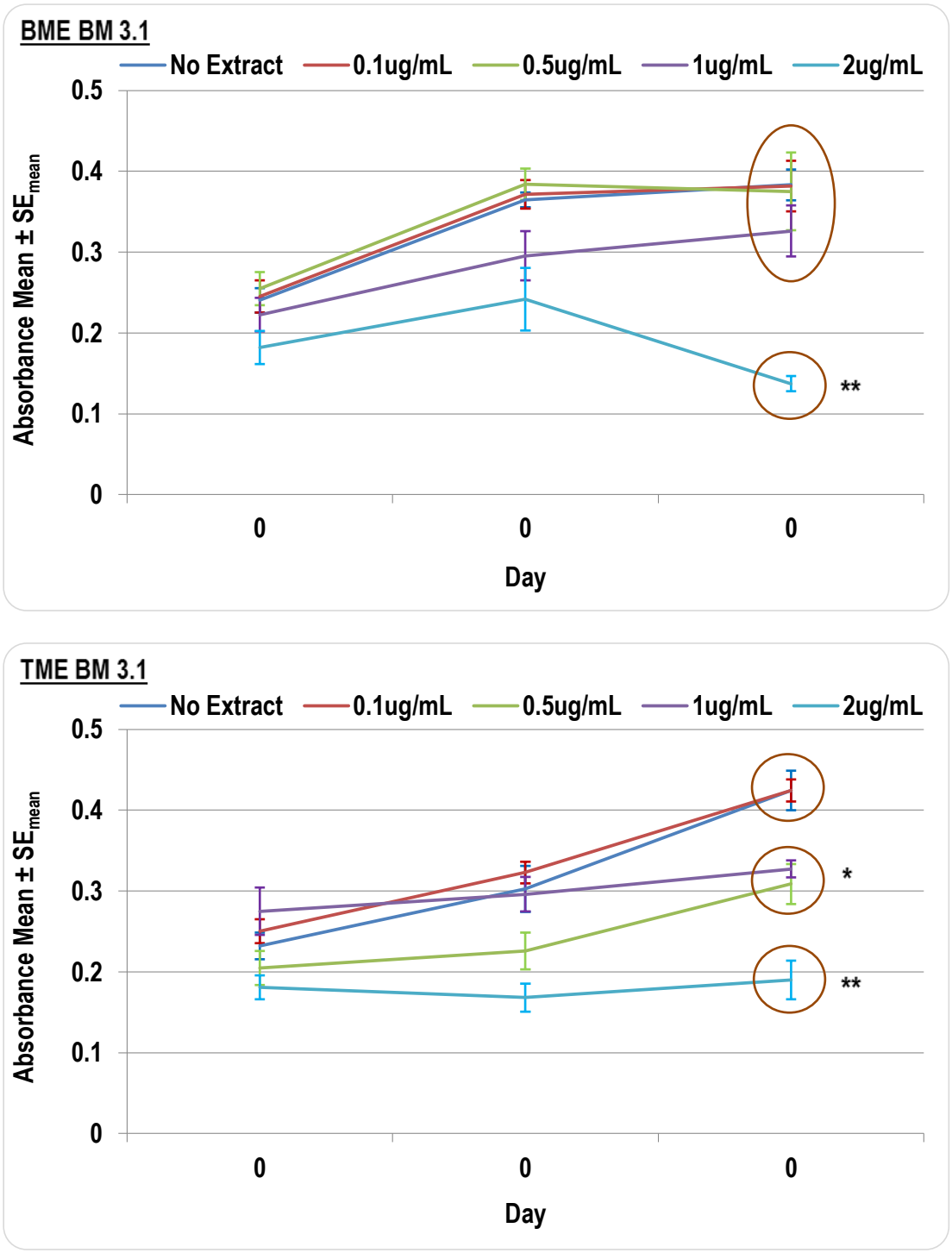

Figure 5.3: Viability of BM 3.1 in BME and TME proteins for three days. At day three, protein concentrations were grouped and encircled (brown) having been found statistically different from another concentration. BME and TME at 2µg/mL caused a significant ($P<0.01$) decrease in viability compared to no-extract and all other protein concentrations. TME at 0.5µg/mL and 1µg/mL, had significantly ($P<0.05$) lower viability than no-extract and 0.1µg/mL. Seeding density was $5.7x10^3$ cells per cm^2. *n*=2 (triplicate). Mean± SE_{mean}. ** = $P<0.01$, * = $P<0.05$.

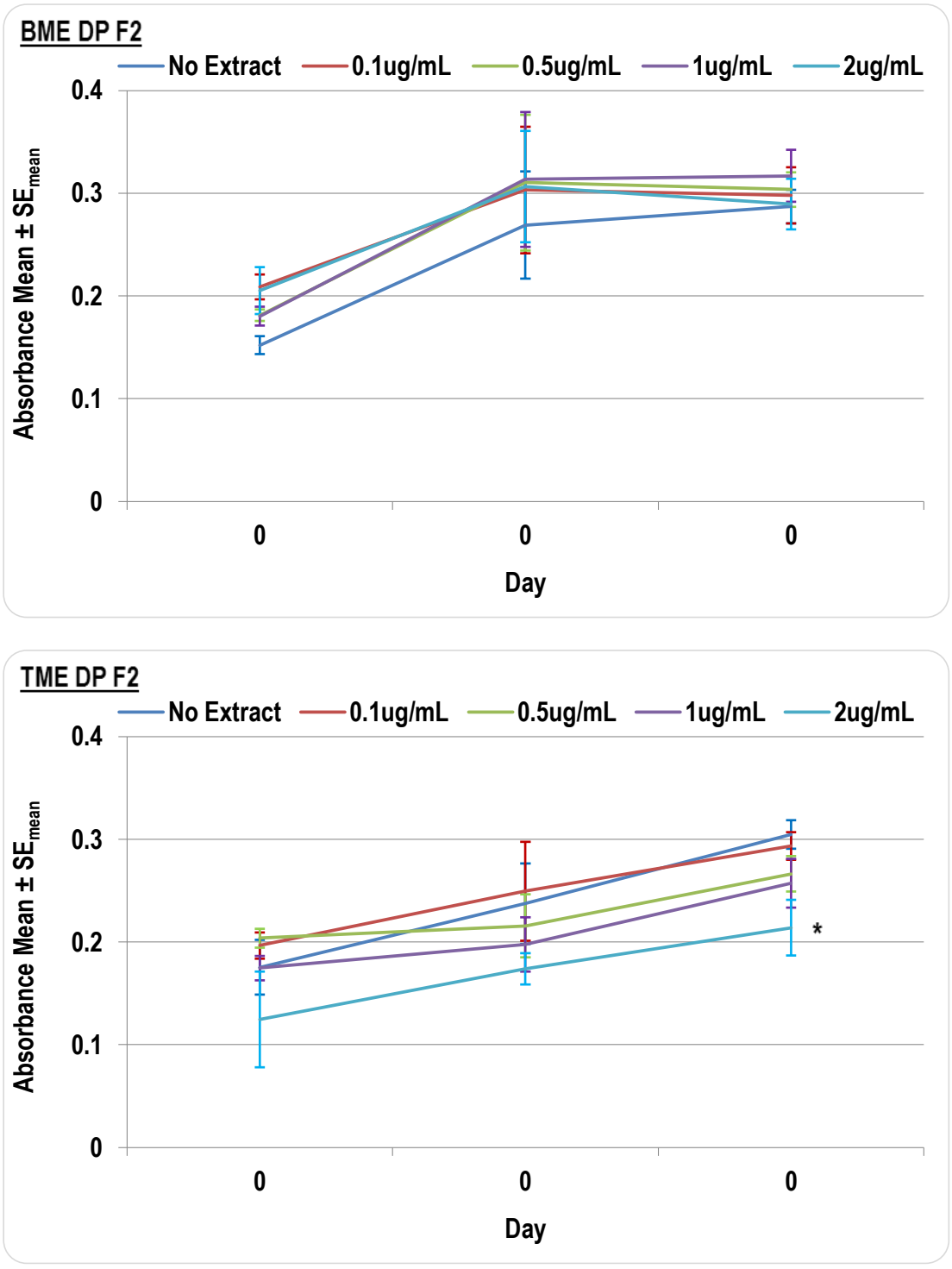

Figure 5.4: Viability of DP F2 in BME and TME proteins for three days. BME activity plateaued following day two, and in TME activity increased up to day three. For BME, no differences in viability were seen between protein concentrations, and only 2µg/mL TME was found to significantly ($P<0.05$) decrease viability compared to no-extract. Seeding density was $5.7x10^3$ cells per cm^2. *n*=2 (triplicate). Mean± SE_{mean}. * = $P<0.05$.

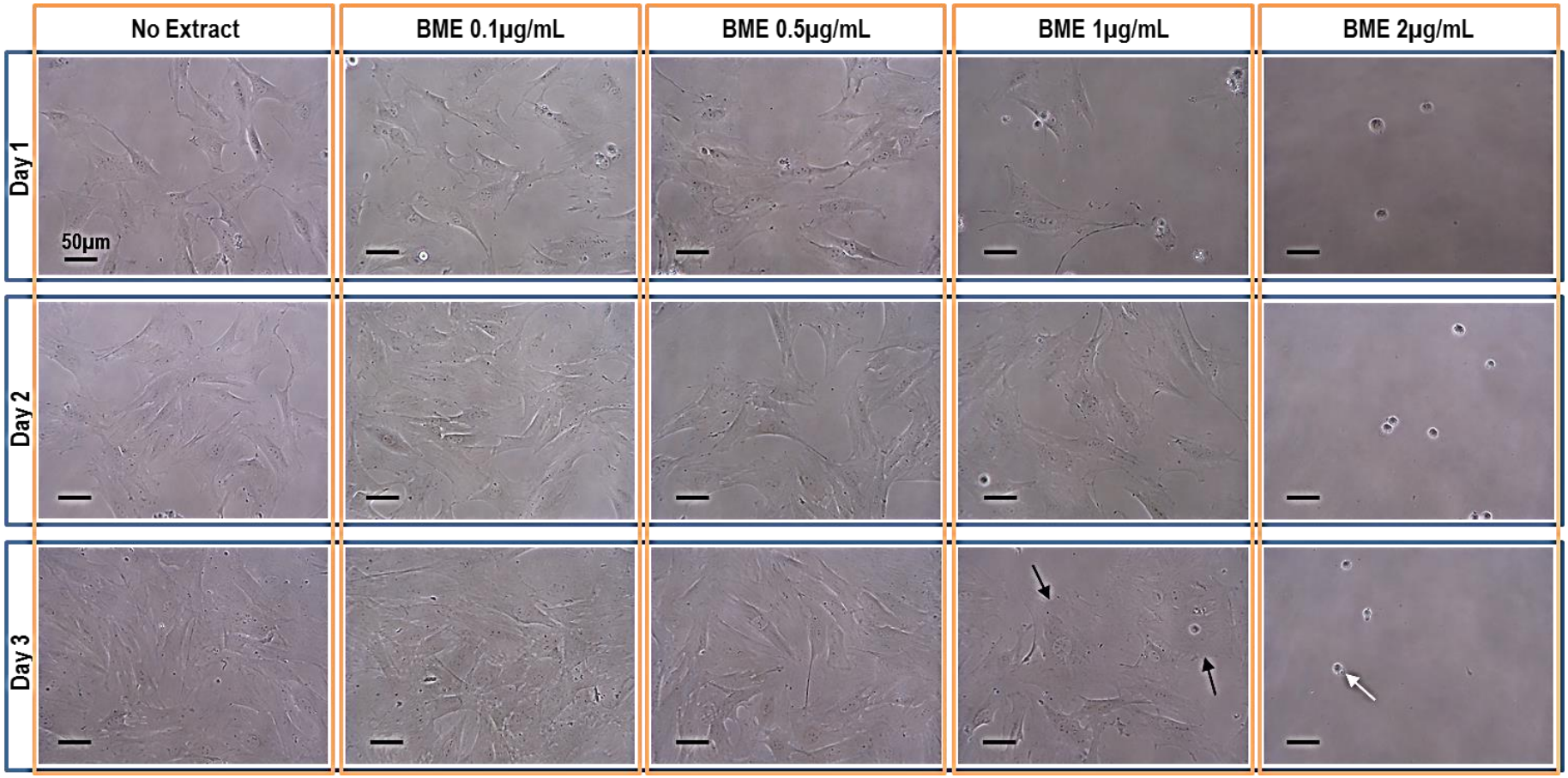

Figure 5.5: Progenitor clone BM 3.1 morphology exposed to BME protein over three days. By day three, morphology of cells with 0.1µg/mL and 0.5µg/mL protein remained unchanged compared with no-extract. While 1µg/mL had larger cells with stressed-like morphology (black arrow), and 2µg/mL had no viable cells (white arrow). Scale bar: 20x objective.

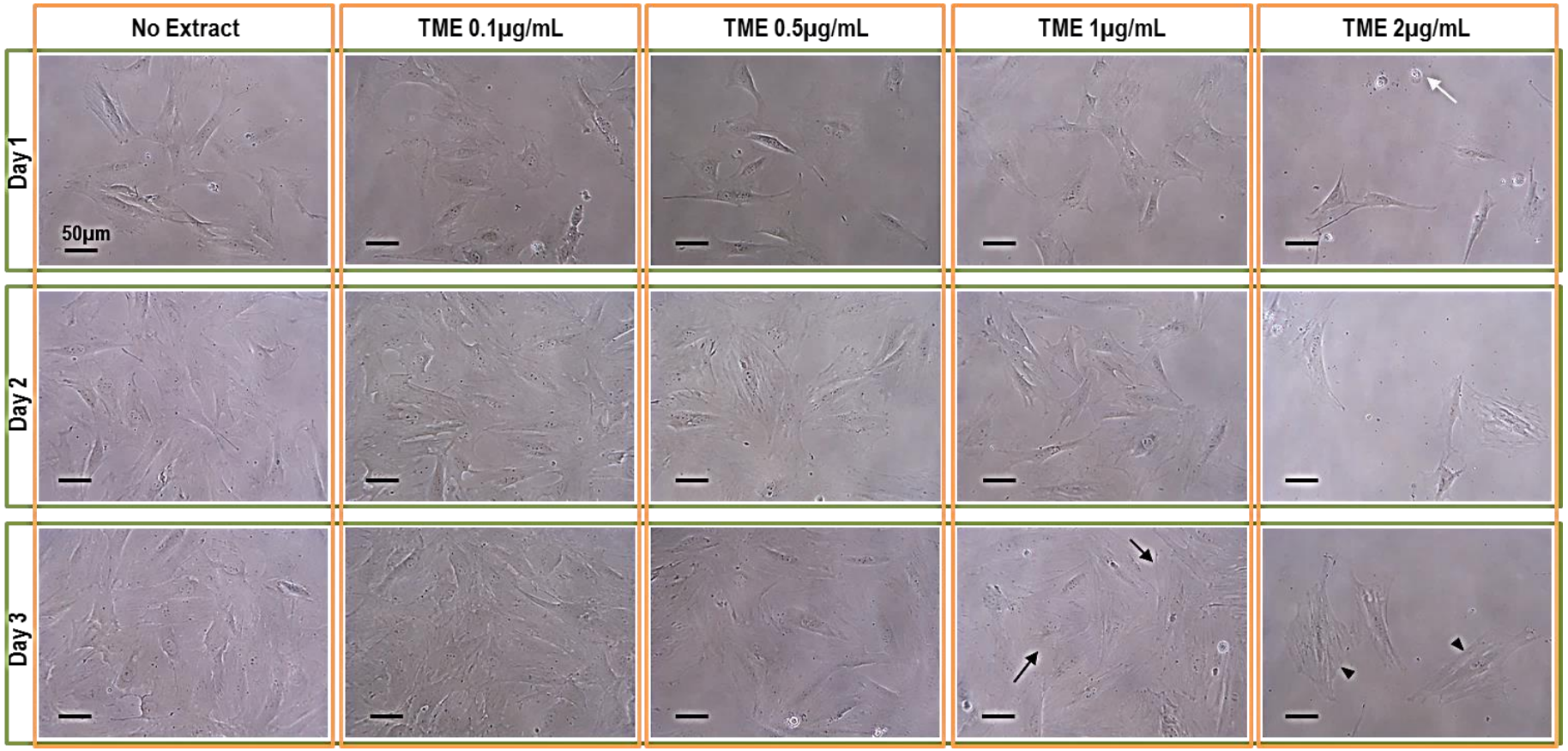

Figure 5.6: Progenitor clone BM 3.1 morphology exposed to TME protein over three days. Over three days, morphology of cells with 0.1µg/mL and 0.5µg/mL protein remained unchanged compared with no-extract. By day three, 1µg/mL had a larger cell morphology with thin stress-fibres (black arrow). On day one, 2µg/mL had some non-viable cells (white arrow), and by day three the few cells present had thick aligned stress-fibres (black arrow-head). Scale bar: 20x objective.

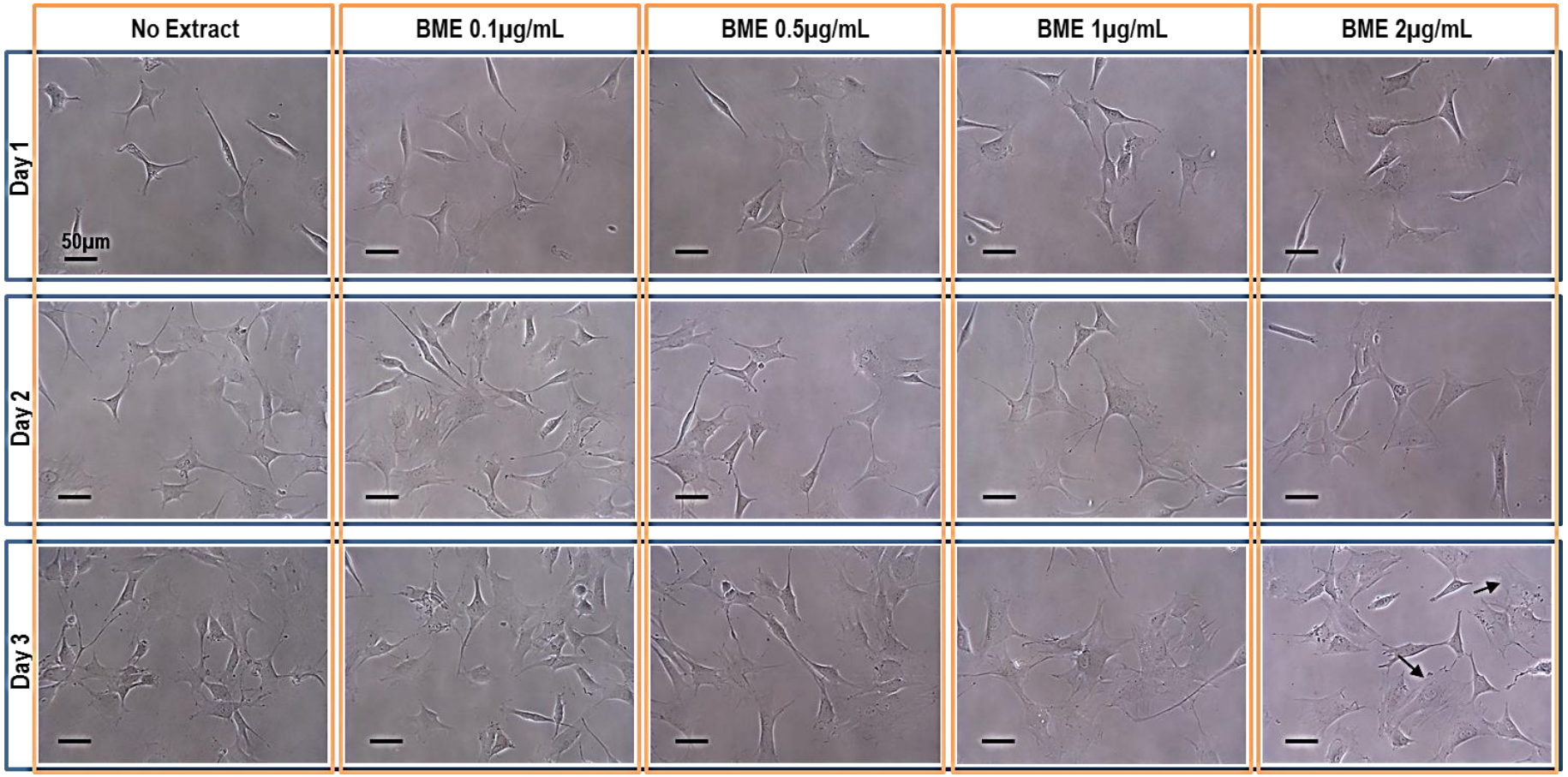

Figure 5.7: Progenitor clone DP F2 morphology exposed to BME protein over three days. Morphology of cells with 0.1µg/mL, 0.5µg/mL, and 1µg/mL protein remained relatively unchanged compared to no-extract. By day three, 2µg/mL had a few enlarged cells with thin stress-fibres (black arrow). Scale bar: 20x objective.

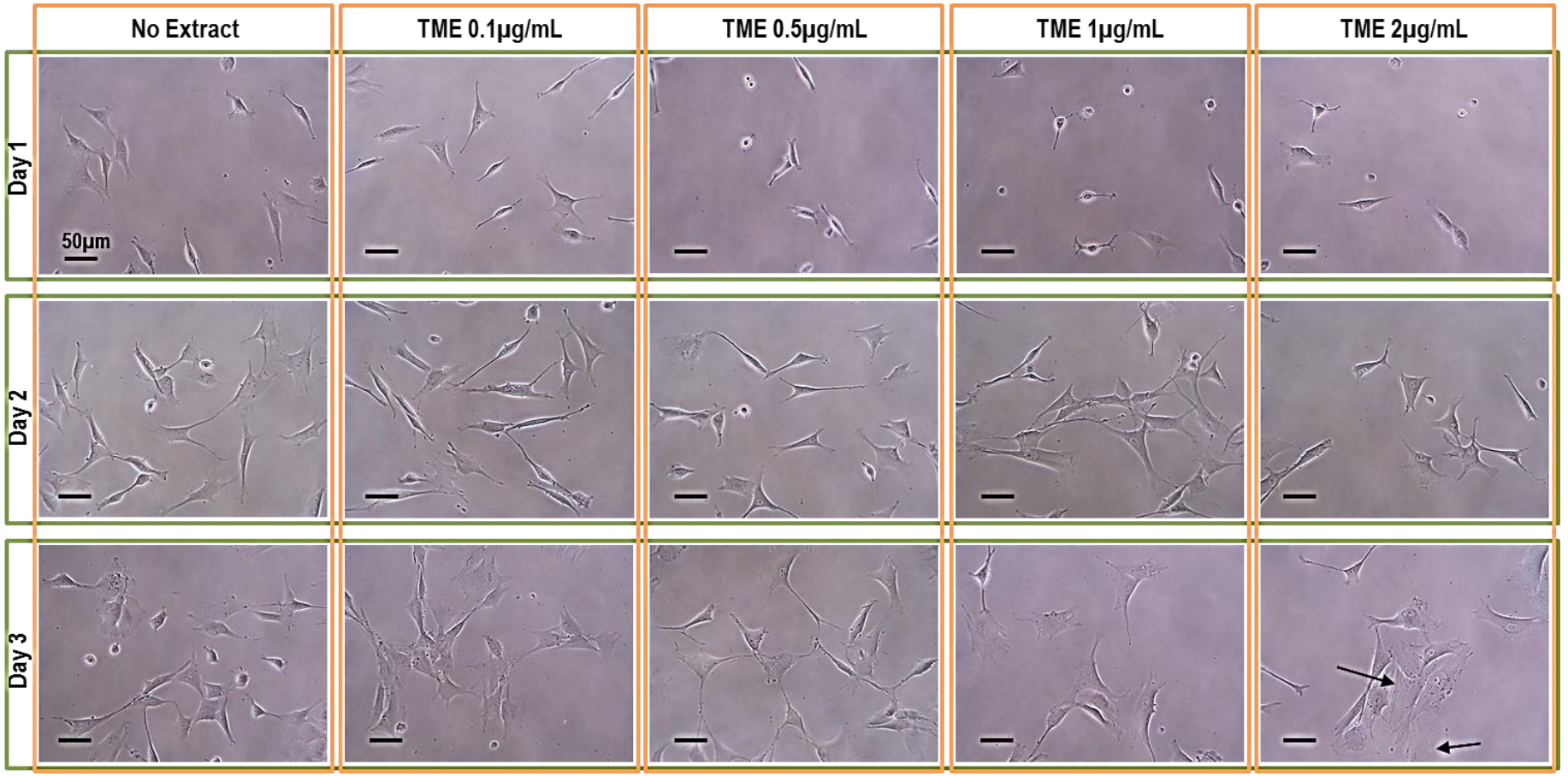

Figure 5.8: Progenitor clone DP F2 morphology exposed to TME protein over three days. Morphology of cells with 0.1µg/mL, 0.5µg/mL, and 1µg/mL protein remained relatively unchanged compared to no-extract. By day three, 2µg/mL had a few enlarged cells with thin stress-fibres (black arrow). Scale bar: 20x objective.

5.3.3 Growth Profile of Selected MSC Clones with Whole-Protein Matrix Extracts

From the viability assays, 2μg/mL protein concentration was excluded for further analysis due to its deleterious effects on cell-stress and number of viable cells, and MSC characteristics. All other protein concentrations were further assessed during extended clonal expansion by the population doubling level growth profile.

For BM 3.1 during the 32 day culture period, compared to no-extract control at 13.9 PDLs, all BME concentrations marginally decreased cell expansion and achieved PDLs of 13.4 in 0.5μg/mL, 12.8 in 0.1μg/mL and 1μg/mL (figure 5.9). While TME decreased cell expansion in a protein concentration-dependent manner, and achieved PDLs of 12.1 in 0.1μg/mL, 11.1 in 0.5μg/mL, and 10.4 in 1μg/mL (figure 5.9).

For DP F2, extended expansion in BME protein was unaffected up to day 16. After day 16, compared to no-extract control at 14.3 PDLs, cell expansion in BME decreased up to day 32 achieving PDLs of 13.4, 13.2, and 11.6 for 0.1μg/mL, 0.5μg/mL and 1μg/mL. Unlike BM 3.1, TME proteins decreased cell expansion in a protein concentration-independent manner, which achieved PDLs of 12.2 in 0.1μg/mL and 0.5μg/mL, and 11.5 in 1μg/mL (figure 15.9).

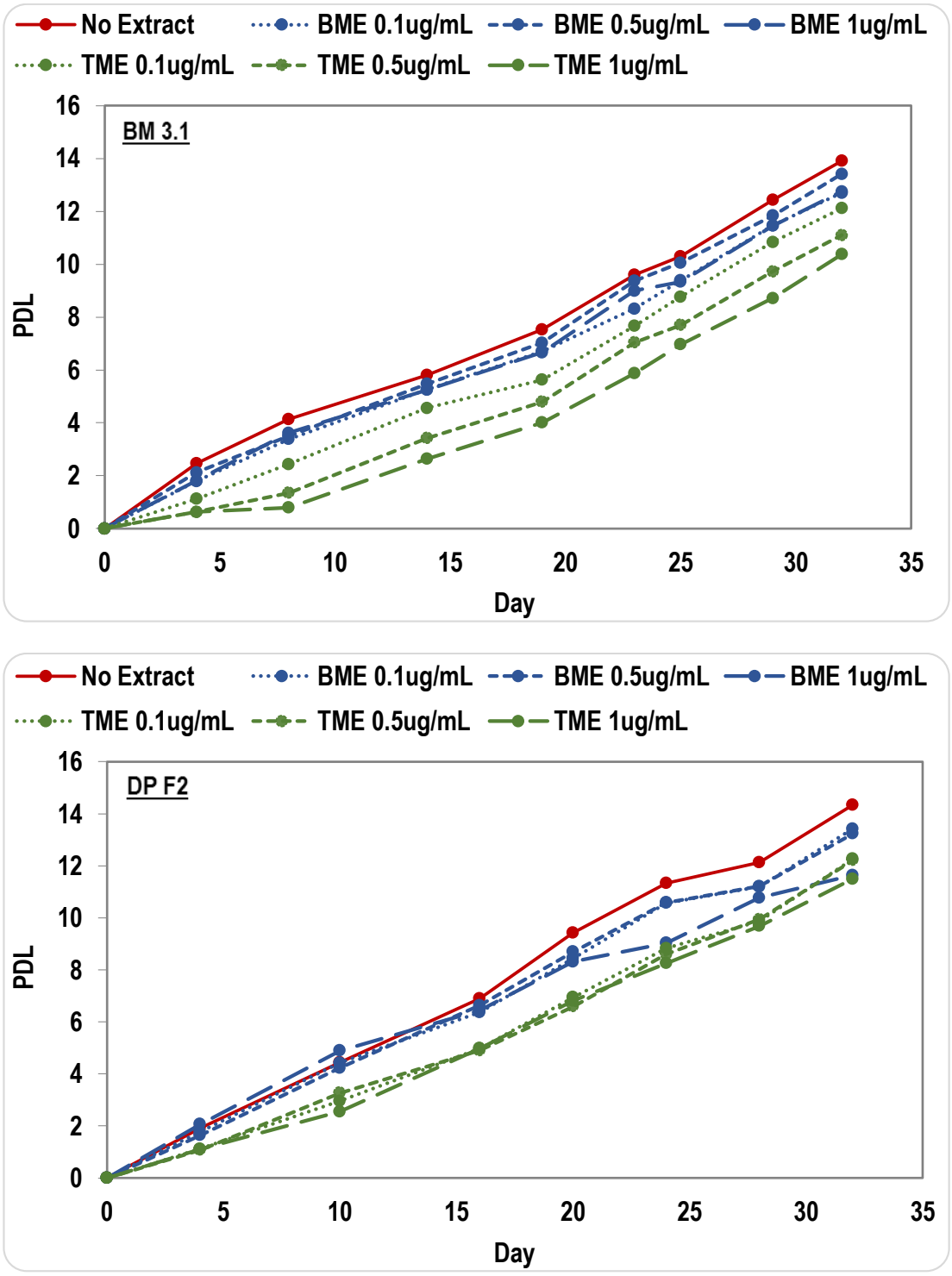

Figure 5.9: Progenitor clones BM 3.1 and DP F2 growth expansion in BME and TME proteins for 32 days. BME effects upon BM 3.1 cell expansion was minimal, but TME decreased expansion in a concentration-dependent manner. For DP F2, BME decreased cell number half way through culture time, while all TME concentrations decreased expansion equally over the culture period.

5.3.4 Mineralising Effects of Whole-Protein Matrix Extracts on Selected MSC Clones

From the previous viability and growth expansion assays on BM 3.1 and DP F2 clones, a final protein concentration of 0.5µg/mL was chosen to assess the mineralising effects of the whole-protein matrix extracts on the clones over 23 days (period for normal osteogenic differentiation). The 0.5µg/mL protein concentration was decided as the optimal concentration due to the similar viability and morphological appearance compared to no-extract control, and 0.5µg/mL concentration displayed decreased population doubling level, which potentially indicated cellular differentiation.

After 23 days *in vitro* culture, BM 3.1 did not synthesise a mineralised matrix when exposed to BME protein as seen from absence of nodule morphology and no alizarin red stain for extracellular matrix calcium deposits. On the other hand, TME promoted nodule formation that stained red with alizarin for extracellular matrix calcium (figure 5.10), similarly as osteogenic promotion (see Chapter 4, figure 4.10). No-extract control did not show mineral synthesis or alizarin red staining (figures 5.10). At day 23, BM 3.1 osteonectin gene expression in BME and TME was significantly decreased compared to no-extract control ($P<0.01$), and TME was very significantly decreased compared to BME ($P<0.01$). Gene expression levels of osteopontin, however, did not show any significant changes (figure 5.12). In addition, BSP and osteocalcin was not expressed in BM 3.1, similarly as in osteo-inductive medium (figure 4.13).

After 23 days *in vitro* culture, DP F2 synthesised a mineralised matrix in both BME and TME, and promoted areas of dense accumulates that stained brown with alizarin for calcium deposits within the extracellular matrix. No-extract control did not show mineral synthesis or alizarin red staining (figure 5.11). Compared to no-extract control at day 23, BSP was significantly higher in TME ($P<0.05$), osteocalcin was significantly higher in BME and TME ($P<0.001$) and BME was significantly higher than TME ($P<0.01$), and osteopontin was significantly higher in BME and TME ($P<0.05$) (figure 5.12). Osteonectin showed no significant changes.

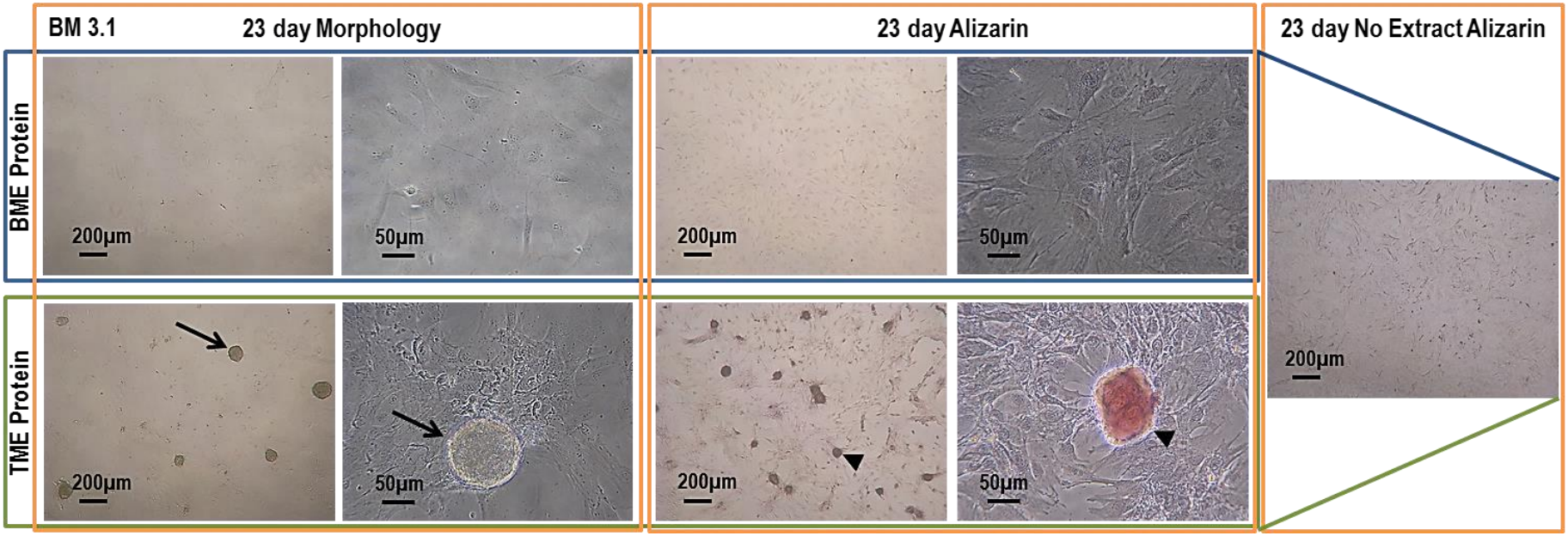

Figure 5.10: Progenitor clone BM 3.1 mineral synthesis exposed to BME and TME proteins, at day 23. BME exposure did not promote calcium deposits. TME promoted dense spherical nodules (arrows), with alizarin red stained calcium deposits within the extracellular matrix (arrow-head). Morphology of no-extract medium remained unchanged and showed no alizarin red stain. Scale bars: 4x and 20x objectives.

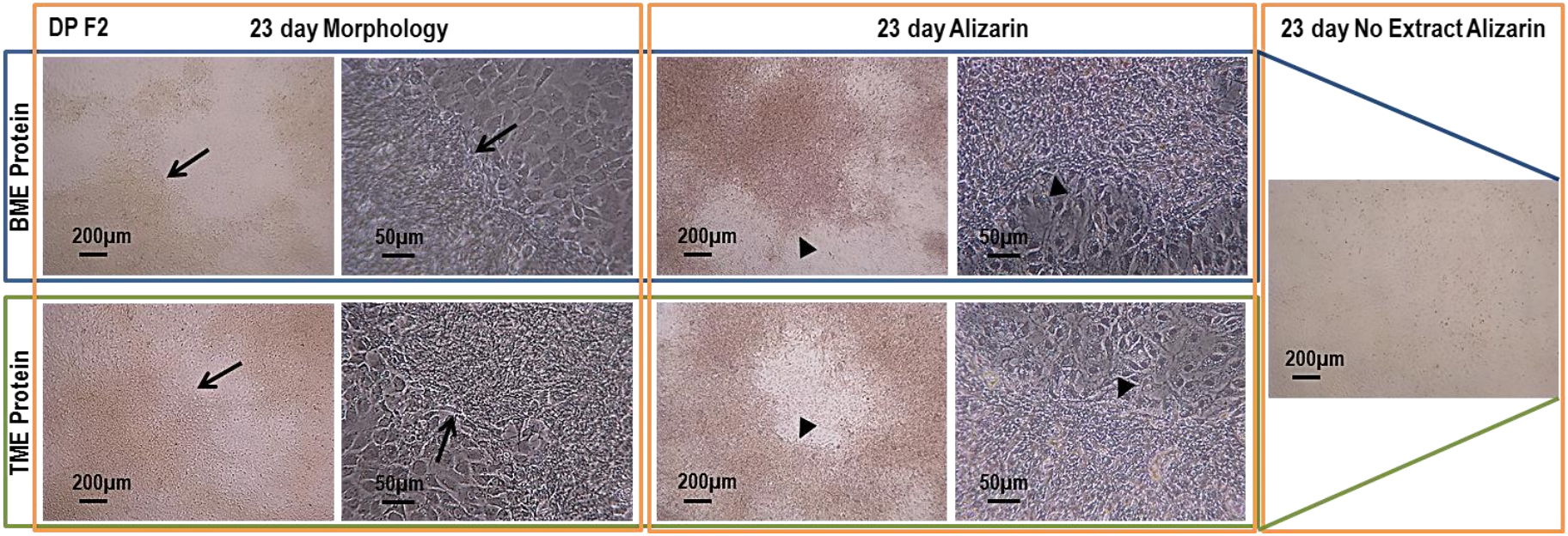

Figure 5.11: Progenitor clone DP F2 mineral synthesis exposed to BME and TME proteins, at day 23. BME and TME promoted areas of dense accumulates (arrows), with alizarin red stained calcium deposits within the extracellular matrix (arrow-head). Morphology of no-extract medium remained unchanged and showed and showed no alizarin red stain. Scale bars: 4x and 20x objectives.

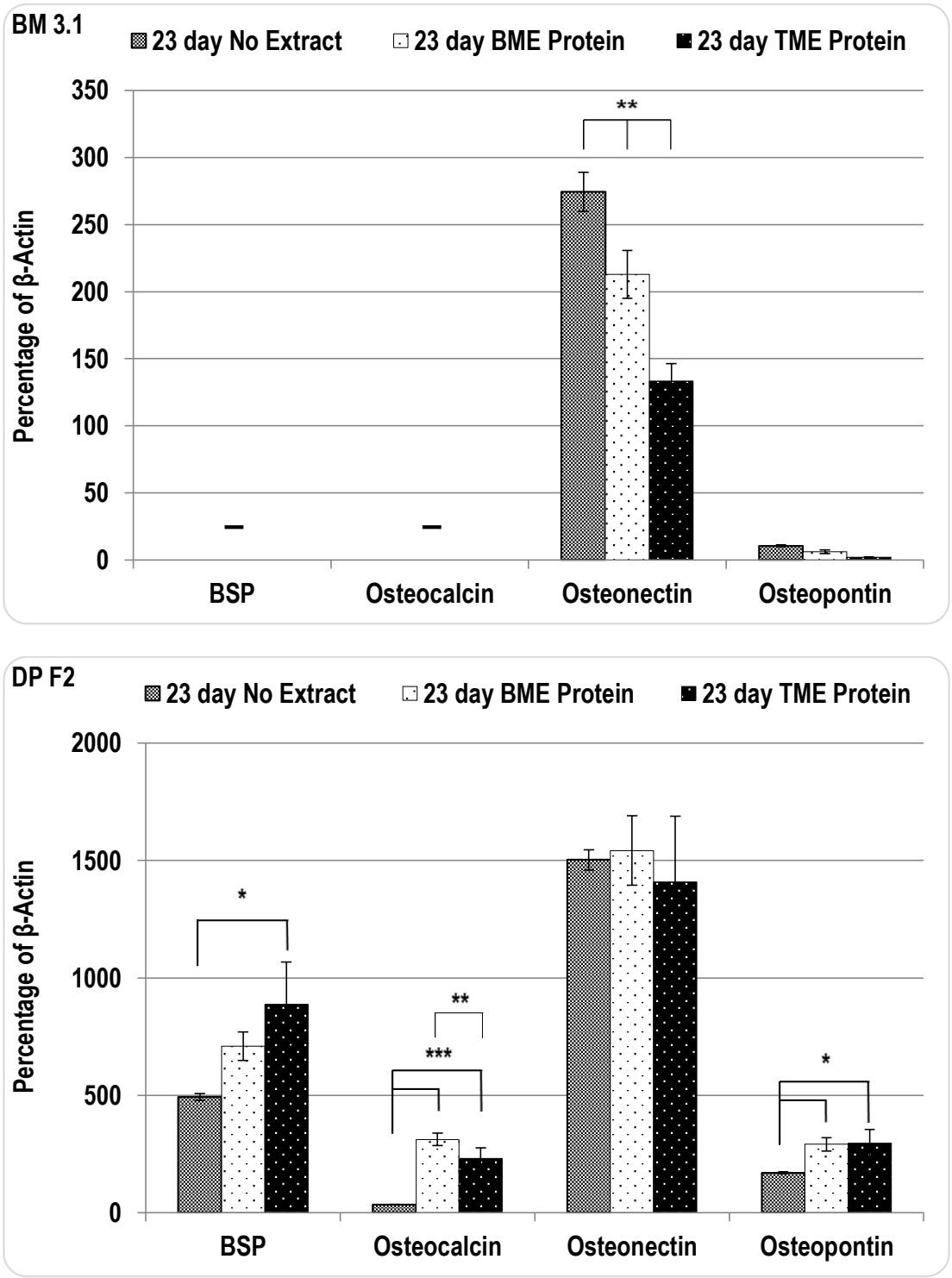

Figure 5.12: Progenitor clones BM 3.1 and DP F2 expression levels of bone-related genes following *in vitro* exposure to BME and TME proteins for 23 days. BM 3.1 osteonectin expression in BME and TME was very significantly lower than no-extract, but osteopontin was not significant. For DP F2, BSP was significantly higher in TME, and osteocalcin and osteopontin were significantly higher in BME and TME. DP F2 osteonectin was not significant. Mean±SD. * = P<0.05, ** = P<0.01, *** = P<0.001.

5.3.5 Separation of Whole-Protein Matrix Extracts from Bone and Tooth

SDS-PAGE separation of BME and TME protein extracts showed three identical bands with coomassie brilliant blue staining between 38KDa and 82KDa at apparent 65KDa, 70KDa and 75KDa. On further analysis with a protein-sensitive (<100ng) silver stain, additional proteins were uniquely observed in BME extract between 114-204KDa, and TME extract between 82-114KDa (figure 5.13).

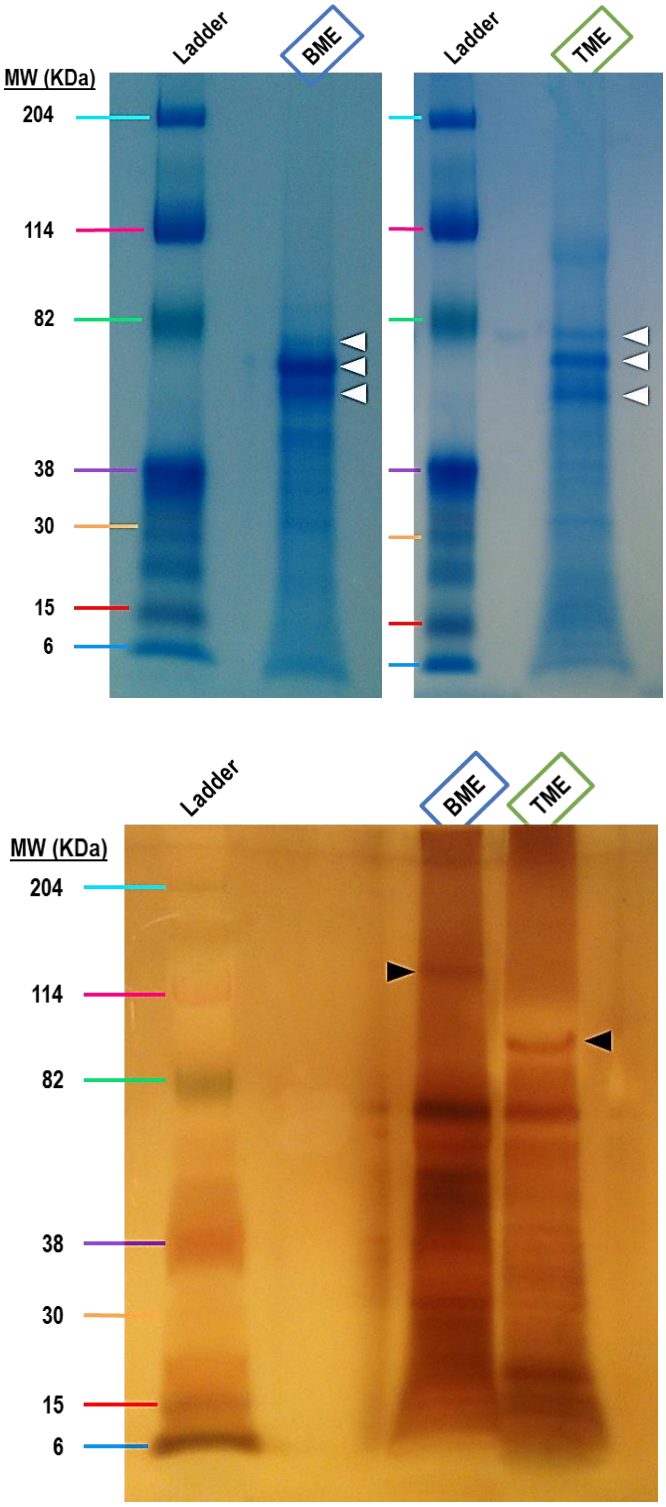

Figure 5.13: Separation of whole-protein matrix extracts from rat bone (BME) and rat tooth (TME) by SDS-PAGE. In coomassie brilliant blue (top), three main bands are evident in both protein extracts between 38KDa and 82KDa, at apparent 65KDa, 70KDa and 75KDa (white arrow heads). Other bands (black arrow heads) appear unique to each extract when observed by the protein-sensitive silver stain (bottom). 10µg protein each sample.

5.4 Discussion

This chapter highlights two important points often questioned in tissue engineering and regenerative medicine *i.e.* what is the best tissue-sourced cells to use? And what is the optimal mircro-environment support needed? *E.g.* protein and/or scaffold. These two points shed light to preferentially use DPSCs and tooth protein extract. Due to, the effects of BME and TME on DPSCs was protein concentration-independent, as cell viability, growth-expansion, and cell morphology was maintained, and that TME was successful at promoting mineralisation in BMSCs and DPSCs.

Viability of BM 3.1 was significantly effected in a concentration-dependent manner so that with increased protein concentration the viability decreased, and was concomitant with the appearance of thick cytoskeletal fibres that are indicative of stress in rigid and non-motile cells (Tojkander et al., 2012). Such thick stress-fibres were seen in BM 3.1 with higher protein matrix-extract concentrations, which suggested the MSC clone experienced cytotoxic stress-induced morphological changes when in presence of too high extracellular matrix protein concentration. DP F2 was for the majority unaffected by higher protein concentrations and displayed similar viability and morphology, which could be accounted for as DPSCs are reported as more resistant to external oxidative-stress factors than BMSCs (Alraies, 2013). Concerning growth expansion, BME displayed minimal effect, unlike that which as may be expected due to the plethora of mineral and calcium promoting extracellular matrix proteins present in bone *e.g.* proteoglycans biglycan and decorin (Bianco et al., 1990), and BSP and BAG-75 (Bronckers et al., 1993). Such

proteins, however, while having ability to promote mineralisation, also have the ability to promote a state of proliferation *e.g.* biglycan (Chen et al., 2002, Waddington et al., 2003a) (see Chapter 1, sections Proteoglycans Regulate Cellular Behaviour, and Biglycan Regulates Cellular Proliferation and Differentiation). TME decreased proliferation, with BM 3.1 growth expansion decreased in a concentration-dependent manner, while DP F2 growth expansion marginally decreased in a concentration-independent manner. This growth expansion decrease could well be due to the array of additional proteins within the tooth that constitute the extracellular matrix and promote mineralisation *e.g.* amelogenin and enamelin (reviewed (Goldberg and Smith, 2004)), compared to bone. In addition, as to why BME promoted mineralisation in DP F2 and not BM 3.1 could well be related to the hierarchical position of these MSCs, with BMSCs proposed as a progenitor closely related to the mother stem cell higher up the hierarchy, and so may need longer and more sustained periods for differentiation promotion. Whereas, DPSCs are proposed lineage-restricted transit-amplifying (TA) cells that are partially committed and so may require less time for mineralisation within the correct micro-environment. This can be related to the *in vivo* role of DPSCs, which requires rapid cell number amplification, followed by immediate odontoblast-like cell formation for tertiary dentin production, after trauma/injury and death to the original odontoblast cell layer (Smith et al., 1995). Reparative tertiary dentinogenesis involved recruitment of DPSCs from the pulp (of which several niches are proposed) to allow dentin bridge formation at pulp-exposed sites, as well as ectopic bone formation (Goldberg and Smith, 2004), due to BMP activity (Butler et al., 1977), and as such DPSCs within pulp are likely “primed”

for mineralisation roles such as odontogenesis and osteogenesis. Interestingly, following extrusion trauma of rat incisor, osteopontin was highly expressed in reparative dentine and shared structural characteristics of primary bone (Aguiar and Arana-Chavez, 2007). As such, with a supportive micro-environment DPSCs were able to acutely form proteins associated with osteogenic mineralisation, seen by significant increases in BSP, osteocalcin, and osteopontin compared with no-extract. The expression of BSP in DPSCs exposed to both BME and TME was evidently higher than osteocalcin. This may suggest that DPSCs are in a state associated with the initial phase of mineralisation as BSP peaks before osteocalcin, which disappeared following completion of mineralisation (Aubin et al., 1995), and possibly why alizarin stain was brown and not deep red in colour as within osteo-inductive medium (see Chapter 4, figure 4.12). In addition, dense accumulates were evident in the extracellular matrix of cell-culture with matrix-extract protein, which were not present in the no-extract control medium culture stained with alizarin.

While bone harbours ten-fold BSP and osteopontin than in tooth (Fujisawa et al., 1993), only TME promoted mineralised nodules by BM 3.1. Although BM 3.1 exposed to TME did not see any upregulation in osteopontin (as in osteogenic treatment, see 4.3.3 Osteogenic Differentiation of Characterised Progenitor Clones), other mineralisation-specific proteins that were not analysed here could be responsible for alizarin red stained calcium-binding within the extracellular matrix *e.g.* BAG-75 (Gorski et al., 1996), which was enriched at mineralisation-foci within developing bone (Gorski et al., 2004). In addition, when in barrier-restricted oral epithlium co-culture, BMSCs are

promoted to produce odontogenic genes such as DMP1, Pax9, and DSPP that facilitate mineralisation (Li et al., 2007, Mashhadi Abbas et al., 2013), which may be comparable in effect to exposing BMSC clone to TME proteins. This is supported by evidence that conditioned-medium from tooth-germ cells stimulated DMP1 and DPP protein expression, and mineralised nodule formation by umbilical-cord MSCs (Li et al., 2013), and by DPSCs, creating a potent odontogenic micro-environment (Yu et al., 2006). Interestingly, in an approach to secondary dentinogenesis, canine dentin and bone matrix extracts were implanted into pulpal sites, and reported that dentin matrix promoted dentin histogenesis and odontoblast-like cell differentiation, whereas bone matrix promoted tertiary reparative dentin only (Tziafas and Kolokuris, 1990). This highlights that TME is potentially more potent than BME due to some constituent proteins in TME that are not present in BME.

Many proteins associated with mineralisation and calcification are present in both skeletal bone and tooth tissues (reviewed (Staines et al., 2012)), which include majorly osteopontin, BSP, BAG-75 (Bronckers et al., 1993), and more dentin-primary DSP/DPP and DMP1 (Hu et al., 2006). Proteins specific to tooth are those within the enamel *e.g.* amelogenins, amelobastins, enamelins and tuftelins (Robey, 1996), which are suggested to contribute extensively to bio-mineralisation and formation of hard tissues (Lyngstadaas et al., 2009). The main protein bands present in BME and TME may represent full-length osteopontin at 65KDa (Kim and Shin, 2007) and BSP at 70 KDa (Wuttke et al., 2001). These bands were more concentrated in BME than TME and was probably due to ten-times concentration of BSP and osteopontin within bone

than dentin (Fujisawa et al., 1993) (importance of proteins discussed in Chapter 4, section 4.4 Discussion). For example, BSP-null mice displayed tooth root and alveolar bone resorption (Foster et al., 2013), and delayed bone growth and mineralisation (Malaval et al., 2008). While ostepontin null-mice are reported to display hyper-mineralised bone matrix (Boskey et al., 2002) and reduced tooth resorption due to decreased odontoclastic cells following orthodontic tooth force (Chung et al., 2008).

The distinct protein band seen in the TME between 82-114KDa could belong to tooth-associated proteins DSP (Bronckers et al., 1993), and DPP and/or full-length DMP1 that co-elute together, all of which reported a 95KDa protein band in SDS-PAGE (Sun et al., 2011). These proteins were vital to tooth development and mineralisation, which led to dentinogenesis imperfecta and the disease-associated phenotype in mice with DSP/DPP and DMP1 mutations, respectively (Ye et al., 2004). Other extracellular matrix proteins highly expressed in bone and tooth are SLRPs, decorin and biglycan, which are becoming increasingly evident as important in mineralisation processes (Sugars et al., 2003) (see Chapter 1, section Proteoglycans Regulate Cellular Behaviour). These SLRPs were probably within the smear of protein bands seen above 38KDa, accounting for the core proteins and *in vivo* degradation of (Waddington et al., 2003b), as these glycosylated proteins are of a larger 100-350KDa range (see Chapter 1, figure 1.4). Biglycan and decorin were differentially and spatially expressed during bone (Bianco et al., 1990) and tooth development (Matsuura et al., 2001), and during tooth resorption (Benedetto et al., 2013), due to their proposed distinct *in vivo* roles. Biglycan has been reported to initiate apatite formation (Boskey et al., 1997) while

decorin inhibited mineralisation and rather contributed to collagen fibril assembly (Hoshi et al., 1999). Within the tooth, these functions suggested that decorin influenced dentin formation by associating with type I collagen fibrils to regulate its mineralisation, and that biglycan was potentially involved in differentiation of odontoblasts and ameloblasts, and consequently enamel formation (Matsuura et al., 2001). The presence of such specific proteins and glycosaminoglycans, however, needs to be further elucidated and confirmed *via* Western blot analyses on SDS-PAGE of separated matrix extracts.

In summary, DPSCs were able to undergo mineral synthesis when exposed to BME and TME, likely due to their lineage-commitment related to their position within the stem cell hierarchy, and the niche micro-environment in which they are maintained *in vivo*. Whereas the HSC environment of BMSCs is highly complex and is able to compartmentalise progenitors of many systemic cell-types (Morrison and Scadden, 2014) not limited to mineralised tissues, which may keep them in a state that is higher up the stem cell hierarchy. Therefore, BMSCs probably needed additional time in the presence of BME, but exposure to TME-proteins promoted such osteogenic differentiation and maturation. In addition, DPSC viability and growth expansion was higher compared to BMSCs in the presence whole-protein matrix extracts. Thus, preferential use of DPSCs and its tissue-sourced protein-extracts could potentially be an advantage to tissue regenerative medicine, by preferential capacity for bio-mineralisation applications.

Chapter 6

Proliferation and Differentiation of Bone Marrow and Dental Pulp Mesenchymal Stromal Cell Clones on Bone and Tooth Tissue Slabs

6.1 Introduction

Study of osseointegration and endosseous healing processes in bone grafting and dental implants, has led to better understand the biological cascade as three distinct phases: 1) osteoconduction, cell recruitment through blood clotting, 2) *de novo* bone formation, mineralised interfacial matrix as observed in cementum and primary bone, and 3) bone remodeling, exquisite highly-organised microarchitecture (Davies, 2003). Thus, investigations on identifying the most efficacious source of MSCs and protein matrix extract to mimic an optimal microenvironment for mineralisation, is of utmost importance to tissue engineering and improvement in regenerative medicine applications.

Human BMSCs and DPSCs were capable of attachment and proliferation on lyophilized bovine bone grafts up to 7 days in culture (Weszl et al., 2012). *In vivo* research into use of DPSCs as an alternative cell-source, revealed potential of tooth-tissue scaffolds as a suitable microenvironment to support cell differentiation for tissue engineering and has been suggested for clinical dental therapeutic purposes (Batouli et al., 2003), as the dentin-pulp complex does not re-model but supports reparative dentin formation by DPSCs that differentiate to odontoblast-like cells following injury to protect the pulp (Smith et al., 1995). On the other hand, BMSCs did not form dentinogenic tissue in response to tooth-tissue scaffolds and was suggested to be due to distinct

regulatory mechanisms controlling mineralisation and consequently different organisation of the mineralised tissue (Batouli et al., 2003). Interestingly, reparative dentine formed by odotoblast-like cells following DPSC recruitment from the pulp, was strongly immunoreactive for osteopontin, similarly to primary bone, and these osteopontin-forming odontoblast-like cells resembled osteoblasts rather than odontoblasts (Aguiar and Arana-Chavez, 2007). In addition, osteopontin was found to initiate bone remodeling *via* osteocyte expression (Terai et al., 1999), and be highly enriched at regions of bone resorption, to attract and bind osteoclasts and precursors, and subsequently act as an anchor for osteoclasts (Reinholt et al., 1990). Likewise, osteopontin was observed along newly formed tooth cementum following applied force, and was suggested to play a role in osteogenic differentiation (Kim et al., 2012).

Following on from *in vitro* characterisation and differentiation of bone marrow and dental pulp MSC clones, the behaviour of MSC clones on both bone and tooth tissue-slabs was investigated, in an organotypic culture model, to represent an *in vivo* micro-environment of tissue trauma and injury *e.g.* fracture and caries, respectively. Scanning electron microscopy (SEM) detected cell attachment and morphology, and proliferating cell nuclear antigen (PCNA) stained the growth expansion of clones on tissue-slabs.

6.2 Materials and Methods

Rat long-bones from femur, tibia, and fibula, and tooth lower and upper incisors were dissected and cleaned of all attached soft-tissues. Extracted bones and teeth were sectioned longitudinally and cut two or three times to produce tissue-slabs of 4-5mm length. BMSC and DPSC clones were seeded onto tissue-slabs at $16x10^3$ cells/cm^2 in culture medium (see 2.8 Mineralised Tissue-Slab Preparation and Culture). Following two days incubation, cell-seeded tissue-slabs were fixed with glutaraldehyde, and observed for morphology by scanning by electron microscopy (SEM), and for a marker of proliferation, proliferating cell nuclear antigen (PCNA). Control tissue-slabs had no cells seeded with culture medium. PCNA detection used HRP-conjugated secondary antibody and TMB-substrate development to a blue colour (see 2.9 Mineralised Tissue-Slab Antibody Detection). SEM involved specimen dehydration in a series of increasing alcohol concentrations and drying with HMDS chemical agent overnight. Tissue-slab samples were affixed to aluminium stubs with carbon adhesive tape and gold sputter-coated for viewing under SEM (see 2.10 Mineralised Tissue-Slab Scanning Electron Microscopy).

6.3 Results

6.3.1 Scanning Electron Microscopy of Bone Marrow and Dental Pulp MSC Clone Attachment to Bone and Tooth Tissue Slabs

BM 3.1 attached to bone slab but no cells were visible on tooth slab. On bone, BM 3.1 had many extensions that interacted with other attached cells (figure 6.1, black arrow-head) as well as the tissue environment haversian canals (figure 6.1, black arrow). DP F2 attached to both bone and tooth slabs, and similar to BM 3.1, had many extensions interacting with other cells and its environment. BM 3.1 cells on bone slab and DP F2 cells on tooth slab were rather flattened with a large surface area and spread morphology, whereas DP F2 on bone slab was more rounded with extensive filopodia (figure 6.1). DP F2 cells also appeared to produce their own organic matrix (figure 6.1, white arrow). All attached cells appeared to align themselves in a single and parallel direction. Bone haversian canals and tooth tubules were evident across tissue slabs (figure 6.1, yellow asterisks) and at higher magnification collagen fibrils were clearly distinguished (figure 6.1, yellow arrows).

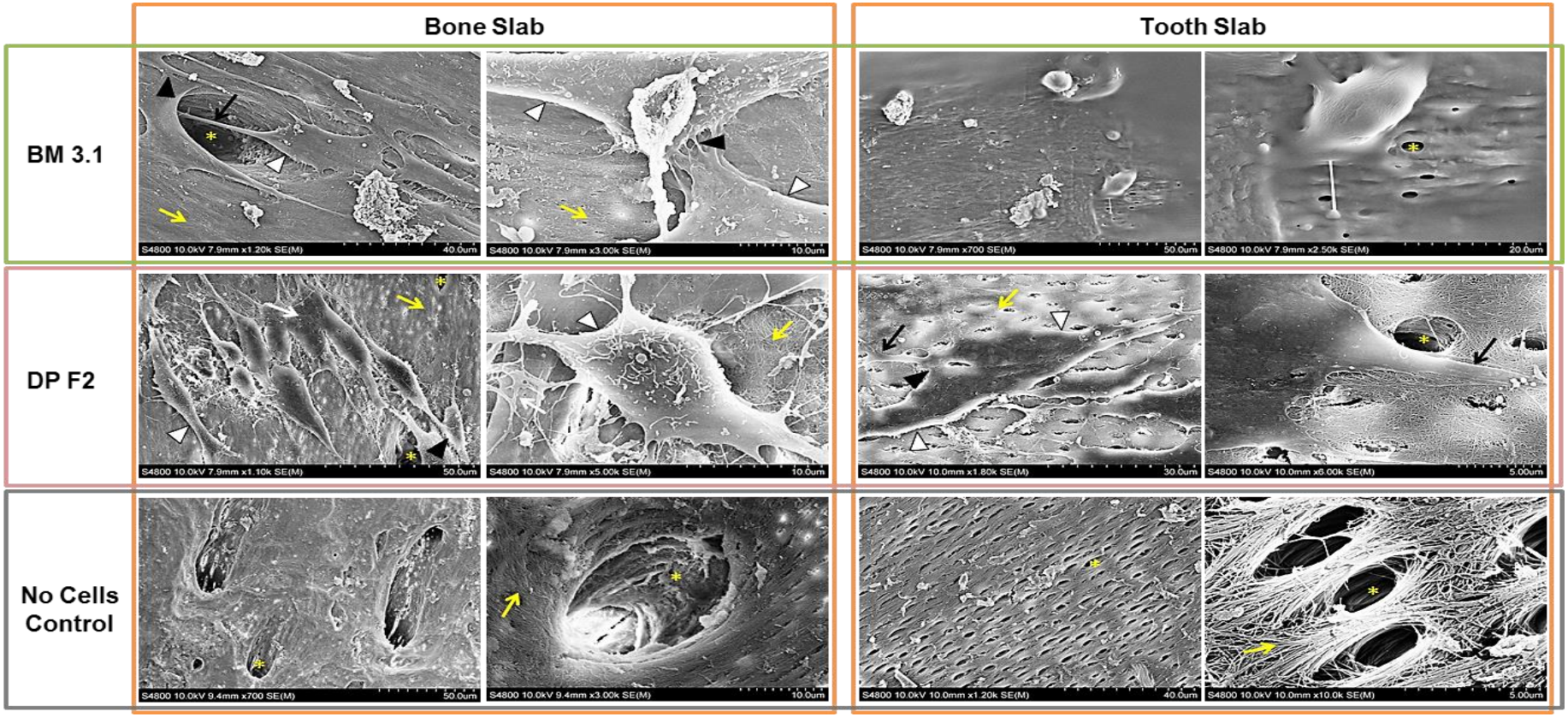

Figure 6.1: Scanning electron microscopy (SEM) of progenitor clones BM 3.1 and DP F2 following two days *in vitro* culture on bone and tooth slabs, at mid PDL. BM 3.1 attached to bone slab but no cells were visible on tooth slab, while DP F2 attached to both bone and tooth slabs. MSCs (white arrow-head) had many extensions interacting with other cells (black arrow-head) and its environment (black arrow). MSCs also appeared to produce their own matrix (white arrow). Bone haversian canals and tooth tubules (yellow asterisks), and collagen fibrils (yellow arrows). Magnification and scale bar inset.

6.3.2 Proliferation of Bone Marrow and Dental Pulp MSC Clone on Bone and Tooth Tissue Slabs

MSC clones, BM 3.1 and DP F2, seeded on bone slab had visible areas of proliferation indicated by the blue staining for PCNA, with DP F2 showing larger areas of blue compared to BM 3.1 (figure 6.2). On tooth slabs, however, PCNA bound non-cellular elements, as BM 3.1 tooth slab (no visibly attached cells with SEM analysis) colour was similar to the control tissue slab with no cells (figure 6.2). Despite cross-reactive blue staining, DP F2 displayed a deeper blue PCNA stain, potentially indicating active cell proliferation. All IgG isotype antibody controls showed no blue staining.

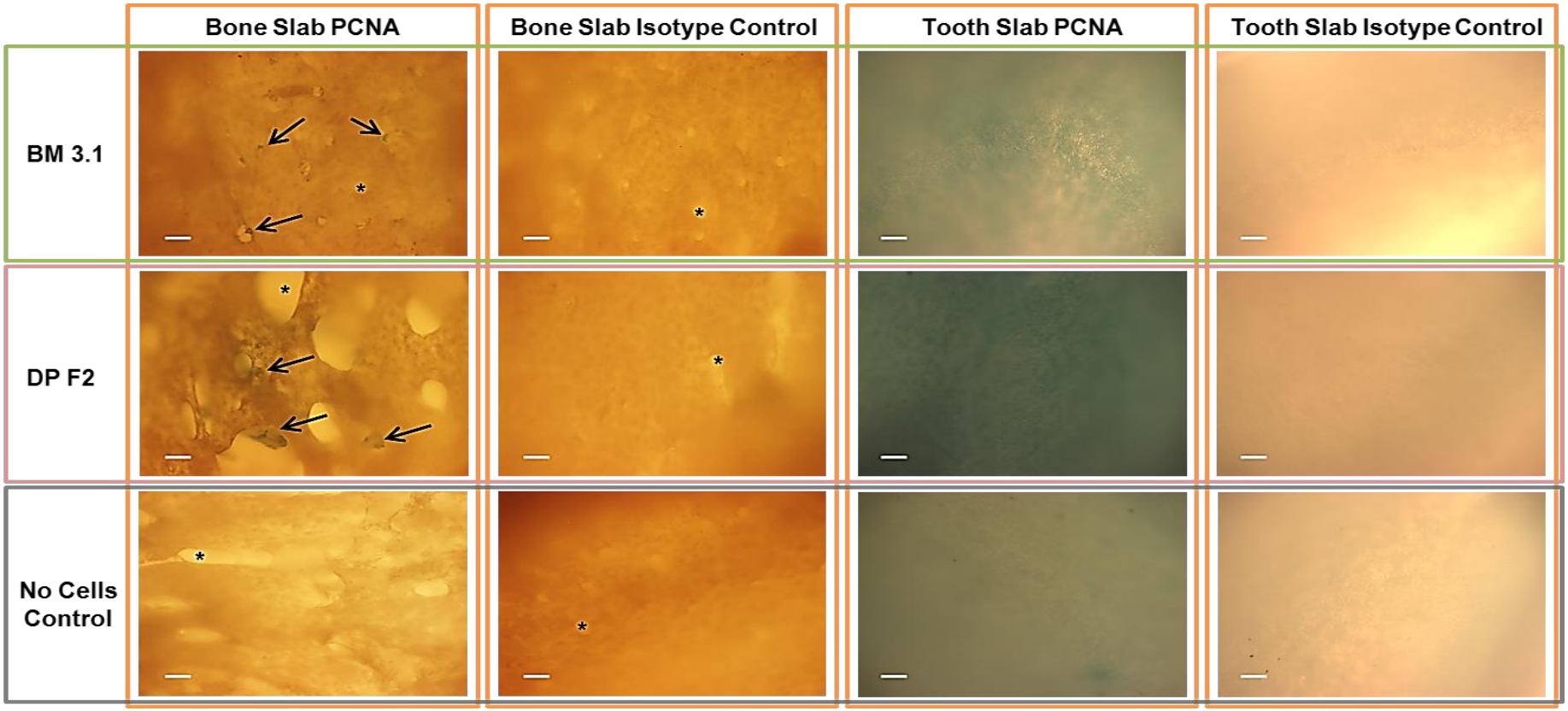

Figure 6.2: Proliferation of MSC clones BM 3.1 and DP F2 following two days culture in vitro on bone and tooth slabs, at mid PDL. BM 3.1 and DP F2 seeded on bone slab had visible areas of proliferation indicated by blue staining for PCNA (black arrow). On tooth slab, BM 3.1 PCNA stained non-specific blue, similarly as control tissue slab with no cells. DP F2, however, stained deeper blue for PCNA, potentially indicating active cell proliferation. IgG isotype antibody controls showed no staining. Equal light intensity and exposure for tissue samples. Bone haversian canal (black asterix). Magnification x10, scale bar = 100μm.

6.4 Discussion

Critical to *in vitro* primary research investigations on optimal progenitor and protein sources for tissue regeneration, is relating and interpreting its findings to clinical applications such as bone grafting and dental implants, in order to better understand osseointegration and endosseous healing processes. As such, use of tissue-slabs can mimic and represent an *in vivo* micro-environment of trauma and injury. Here, DPSC clone DP F2 attached to bone and tooth tissue-slab surfaces, whereas BMSC clone BM 3.1 only showed attachment to bone tissue-slab, and both clones indicated proliferation and potential differentiation.

Proliferation of BM 3.1 and DP F2 was evident on bone slab following two days culture, and human BMSCs and DPSCs were capable of attachment and proliferation on lyophilized bovine bone grafts up to 7 days in culture (Weszl et al., 2012). On tooth slab, proliferation was only evident in DP F2, as no BM 3.1 cells were attached to tooth slab. In addition, control tooth slab with no cells showed similar levels of blue TMB-substrate as BM 3.1 tooth slab (no cells attached), which indicated that PCNA was cross-reactive to a non-cellular structure, possibly to a protein within the pre-dentin layer, and that alternative antibodies for proliferation should be tested *e.g.* Ki-67. From the morphology of cells under SEM, it was interesting to hypothesize that rounded cells were actively proliferating, as displayed by DP F2 on bone slab, while flattened cells were undergoing differentiation, as displayed by BM 3.1 on bone slab and DP F2 on tooth slab. As after 2 days culture, human MSCs and fibroblasts are reported to have prominent spindle shapes, and that murine osteoblasts

exhibit a branched structure with increased focal adhesion points, suggesting proliferation and differentiation, respectively (Lavenus et al., 2011). On bone tissue-slabs, BM 3.1 morphology displayed flat cells with lower PCNA, while DP F2 morphology displayed rounded cyto-types with higher PCNA. Oppositely to bone slab, on tooth tissue DP F2 was flattened and similar to BM 3.1 on bone slab, potentially indicating differentiation. DP F2 PCNA staining was not area-specific for tooth slab and was judged on depth of colour alone comparative to the no-cells control, with DP F2 displaying increased PCNA staining. Morphology of cells can be indicative of their cell-cycle state, whereby actively proliferating cells were considered rounded with filopodia and a clearly visible cell-border, whilst non-proliferating cells are largely spread flattened cells (Gonzalez et al., 2009). Human MSCs are said to exhibit two distinct morphologies termed rapidly self-renewing cells (RS), and flat cells (FC) that had a very low proliferation rate. Flat cells had a larger surface area and the cell-specific flatness could be correlated with higher level of focal adhesions (Docheva et al., 2008). In addition, the role of focal adhesion kinase (FAK) in osteogenic differentiation was purported important (Mathieu and Loboa, 2012), with FAK knock-down reported to diminish osteocalcin secretion (Chen et al., 2013). As seen during *in vitro* culture, however, BM 3.1 cells are of a more cobble-stone shape compared to DP F2 with a defined dendritic cell-shape (see Chapter 3, figures 3.14 and 3.15), and so additional immunocytochemical analyses are required to confirm differentiation *e.g.* anti-FAK, osteopontin, BSP, and osteocalcin. Interestingly, DP F2 on bone slab for two days displayed a round-like morphology along with apparent organic-matrix production, and it was reported that during proliferation phases, bone stromal cells expressed

dermatan-sulfated biglycan, which peaked and was highly expressed at two days culture (Waddington et al., 2003b).

SEM analysis of calf pulp-derived cells spread and flatten following 7 days culture to form cell-cell contact on dentin, similarly as here after 2 days culture, and following 14 days cells became multilayered (Schmalz et al., 2001), with human pulpal-cells surviving for periods of up to 16 days on dentin surfaces (Huang et al., 2006a). Elsewhere, human dental pulp cells are reported to proliferate minimally, unlike 3T3 fibroblasts, on a dentin surface compared to culture plastic using trypsinized cell-counts (Huang et al., 2006b). As seen here with BM 3.1 on tooth slab, no cells were visible and at higher magnification only debris could be seen similar to that seen in Huang *et al*., 2006b, which was likely due to SEM processing. Absence of dental pulp cells on dentin surface would account for the discrepancy of apparent low cell numbers when Huang *et al*., 2006b compared cell number of dental pulp cells and fibroblasts during tissue culture plastic expansion and proliferation with collagen gel scaffold matrix, which gave similar cell growth profiles. In addition, dental pulp cells are reported to interact with open dentin tubules following 2 days (Shao et al., 2011), 7 days (Schmalz et al., 2001), and 16 days (Huang et al., 2006a), which exhibited odontoblast behaviour. Here, however, no specific association between MSCs and dentin tubules or bone haversian canals was evident. Interestingly, actin filaments of multilayered human DPSCs on human dentin discs aligned in a parallel fashion as early as day 2, and was highly organised by day 10 culture, which was also characteristic of odontoblasts (Shao et al., 2011). Such alignment of cells was displayed in

attached bone marrow and dental pulp clones on both bone slab and tooth slab, and was indicative of micro-environment influence on cell behaviour and that study of *in vivo* native injury micro-environments can potentially provide beneficial in understanding interaction between MSCs and their environment for tissue engineering in orthopaedic and dental regenerative medicine. Interestingly, human dentin surfaces have provided a scaffold onto which seeded DPSCs were able to undergo dentinogenesis and produce a reparative dentin-like tissue matrix (Batouli et al., 2003)

BMSCs and DPSCs are suggested to undergo organogenesis and replicate their own niche of origin *i.e.* bone and tooth, respectively, which highlights inherent tissue "memory'' that may be pivotal for cell therapy and tissue engineering applications (Janebodin et al., 2011). In support, distinct regulation mechanisms between BMSCs and DPSCs have been suggested, which may lead to different organisation of mineralised tissues (Batouli et al., 2003). Within an organotypic model, attachment of DPSCs to both bone and tooth tissue slabs, and their proliferation and apparent differentiation within two days culture, suggests dental pulp is potentially a better source of MSCs for mineralised tissue engineering purposes, which is a therapy lacking in craniofacial medicine (Miura et al., 2006).

Chapter 7

General Discussion

The term mesenchymal stem cell was highlighted as being misused in the literature, to classify unfractionated and multipotent plastic adherent cells *in vitro*, and until their characterisation such cells should be referred to as mesenchymal stromal cells (MSCs) (Horwitz et al., 2005). Here, the MSC criteria met were i) uniform population forming colony units (fibronectin-adherent clones) ii) long-term self-renewal (population doubling level) iii) specific surface marker expression (PCR analyses) and iv) multipotent differentiation (adipogenic, chondrogenic, and osteogenic), as set out by The International Society for Cellular Therapy position statement (Dominici et al., 2006).

Our results showed that dental pulp stromal cells had a higher colony forming efficiency compared to bone marrow stromal cells as found by Gronthos *et al*., 2000 in human molars, and Alge *et al*., 2010 in rat. Gronthos *et al*., 2000 suggest this was due to basic composition differences, where dental pulp was largely fibrous and bone marrow majorly constituted haematopoietic cells (>99.9%). They indicated that when bone marrow is free of haematopoietic cells and subjected to collagenase treatment, colony forming efficiency increased 10-fold compared to whole aspirates of bone marrow. The authors stated that the 10-fold increase were unpublished observations, and that the numbers of colony forming units from connective tissue without haematopoietic cells were similar to dental pulp. As in our methodology,

however, we employed cell separation using histopaque and β1-integrin adhesion assay to isolate the representative population of bone marrow progenitor stromal cells from haematopoietic stem cells, and showed that even without haematopoietic stem cells, the bone marrow progenitors had a lower colony forming efficiency. The significant differences between the number of colonies formed likely relates to the hierarchical theory that large colonies formed by the bone marrow MSC progenitors are closely related to the mother stem cell, whereas the small colonies formed by dental pulp MSCs are lineage restricted transit-amplifying cells (Chan et al., 2004). This hypothesis is supported by SOX2 expression in BMSC clones and lack of expression by DPSC clones. As SOX2 is vital for embryonic development and was expressed by pluripotent ESCs, and overexpression of which increased proliferation, as well as adipogenic and osteogenic differentiation in porcine BMSCs (Fan et al., 2013b). Likewise, all BMSC clones proved tri-potent adipo-chondro-osteo capacity that represented progenitor stem cells, while DPSC clones only proved uni- or bi- potent (osteo-inclusive) capacity that represented lineage-committed transit-amplifying cells.

The developmental origins of DPSC colony-forming units were reported as entirely neural crest derived, and BMSC colony-forming units as 43% neural crest derived (Komada et al., 2012). This indicated that DPSCs are not contributed to beyond developmental stages into adulthood, whereas 57% of BMSCs are contributed to by mesenchyme-derived and other as yet unknown cells. BMSCs compose part of the haematopoietic microenvironment that supports compartmentalised HSCs, BMSCs, and lymphoid and myeloid

progenitor niches (Morrison and Scadden, 2014), providing a vast diversity of cells from erythrocytes to specialised lymphocytes, which involves delicate transcription and growth factor balance to robustly sustain stem cell hierarchy dynamics, and health to the whole body (Maclean et al., 2014). Within this haematopoietic environment BMSCs are likely kept in a progenitor-state, until needed for bone remodelling that occurs during adulthood (Parfitt, 1984). Whereas, the dental pulp microenvironment is much less complex, but still of vital importance to maintain in the adult. The sole known *in vivo* role of DPSCs is formation of odontoblast-like cells that produce reparative tertiary dentin after trauma/injury and death to original odontoblasts, to limit pulpal destruction (Smith et al., 1995). Such replacement with odontoblast-like cells, probably requires rapid amplification of cell numbers and immediate differentiation following recruitment from the pulp tissue, where there are several niches proposed (Sloan and Waddington, 2009), In addition, evidence showed genetic lineage tracing (Cre/LacZ) of neural crest-derived DPSCs to the sub-odontoblastic and perivascular regions (Janebodin et al., 2011). Hence, all DPSC clones underwent mineralised osteoblastic differentiation, which likely relates to their *in vivo* role described above and thus their lack of multipotentiality. This may indicate that DPSCs are lineage committed due to loss of stem cell characteristics and gain of a more differentiated and mature progeny (as reviewed (Alison et al., 2002)). In addition, it is interesting to propose that due to lineage-restriction of DPSCs that dental pulp is a more heterogeneous population when undergoing differentiation stimulation, compared to whole bone marrow that proved multipotent at a single-cell clonal level. In opposition to lineage-restriction, others reported gain of adipo- and

chondro- capacity in erupted murine molars, compared to unerupted molars that were not capable of adipo- and chondro- differentiation, and displayed significantly reduced osteo-dentinogenic potential (Balic et al., 2010).

Another crux to tissue engineering, in conjunction with the ideal cell source, is an appropriate scaffold for the survival of cells and promotion of specified differentiation. As described above, BMSCs are within the haematopoietic microenvironment sustaining a progenitor-state, with the DPSC niche harbouring cells until recruitment from the pulp, which likely involves an extracellular matrix that promotes odontoblast-like cell differentiation. Proteins within the tooth extracellular matrix included proteoglycans decorin and biglycan (Rahemtulla et al., 1984) that are involved in processes of mineralisation (Ameye and Young, 2002, Waddington et al., 2003b). While these proteoglycans were present in bone, additional proteins unique to tooth are likely major factors to potentially contributing towards DPSC lineage-commitment *e.g.* amelogenins, amelobastins, enamelins and tuftelins (Robey, 1996) that are suggested to contribute extensively to bio-mineralisation and formation of hard tissues (Lyngstadaas et al., 2009). Here, only exposure to tooth-matrix extract caused BMSC clone mineralisation, whereas both bone- and tooth- matrix extracts promoted DPSC clone mineralisation, which again highlighted potent influence of tooth proteins on the BMSC progenitor clone and thus lineage-commitment of DPSC clone due to mineralisation by bone proteins, within the given time-frame. Similarly, a versatile DPSC clone DP F2 attached, and displayed expansion and potentially differentiation, on bone and tooth tissue slabs. Interestingly, enamel matrix protein combined with natural

bone mineral are being investigated for their influence, which showed enhanced speed of newly formed bone in rodent (Miron et al., 2014), and significant primate periodontal regeneration (Cochran et al., 2003), which sheds light on their potential clinical application. Currently, treatment of dental-diseases *e.g.* periodontitis involves grafting of bone and/or guided tissue regeneration (GTR) (Feng and Lengner, 2013). Due to varied and unpredictable success of current dental treatments, potential regenerative medicine applications such as combined cell with protein scaffold/biomaterial is becoming increasingly popular, particularly alternative autologous cell-sources like dental pulp. Interestingly, as of August 2013, patient recruitment started on a clinical trial using deciduous dental pulp MSCs, with collagen and hydroxyapatite biomaterial for alveolar bone defect tissue engineering in cleft lip/palate patients (Bueno, 2013).

While scientists strive for a “holy grail” marker-phenotye representing an ideal and preferential MSC for use in tissue engineering and regenerative medicine, still much is yet unknown as to the specific roles of individual markers. For example, the minimal MSC triplicate markers (CD73, CD90 and CD105) are stated paramount for definition of an MSC, admittedly along with other criteria, but the roles of the markers are undefined. CD73 and CD105 are reported as unspecific for MSCs, as fibroblasts (human fetal lung) express this phenotypic markers but lack colony and differentiation capacity (Alt et al., 2011). In addition, SOX2 is an important transcription factor in embryogenesis and adult progenitor maintenance, and specifically in mouse during odontogenesis (Zhang et al., 2012). Human third molars, however, contain two distinct

populations of cells that showed SOX2^{+} DPSCs lack CD73 and *vice versa* (Atari et al., 2012), as presented here whereby CD73^{+} DPSC clones did not express SOX2. Although each clone analysed by qPCR gave a unique expression profile, unfortunately this did not relate to the multipotential capacity of MSCs. Likewise, MSX2 was implicated in the maintenance of cell proliferation (Dodig et al., 1999, Liu et al., 1999), however, quantitative analyses did not relate expression to proliferative ability, here. As such, the reliable marker for multipotent differentiation proved to be embryonic transcription factor SOX2.

Since discovery over a decade ago, DPSCs hold much potential as an alternative and easily accessible source of MSCs for tissue engineering and regenerative medicine (Gronthos et al., 2000), still more research and analysis is required; with BMSCs having been studied for almost half a decade. The focus, here, was how standard-use BMSCs and alternative-sourced DPSCs compared in contributing to bone-tissue regeneration, specifically for the orofacial region due to congenital abnormality and following trauma or tumor resection, which is an unmet clinical need (as reviewed (Mao and Prockop, 2012)). Due to their lineage-commitment, DPSCs provide a viable alternative source of MSCs for mineralised tissue formation, which lends support to cryo-banking of such tissues for translational-medicine and importantly standardisation of cell culture methods, as is becoming more recognised by the scientific community (Stacey, 2012). As such, fundamental to stem- and progenitor- cell classification is continuous and repeated assessment during *in vitro* culture, and perhaps more cumbersome *in vivo* studies. Concomitant with

such analysis is cell manipulation, which can include cell-transformation/immortalisation, and so continuous study of stem cell and progenitor cell biological-characteristics is important for determining therapeutic application of each cell-type (Seaberg and van der Kooy, 2003). In addition, long-term cryopreservation of progenitor cells from human bone marrow and dental pulp up to three and two years, respectively, was reported to maintain osteogenic differentiation capacity, which is an attractive feature with possibilities to tailor patient therapy (Kotobuki et al., 2005, Papaccio et al., 2006). Such differentiation ability following cryopreservation was capable along five separate lineages for primary human heterogeneous dental pulp progenitors (Zhang et al., 2006). Cryo-injury, however, is a multifaceted issue (Gao and Critser, 2000), and karyotyping was suggested to be regularly conducted alongside cryo-storage to ensure normal cytogenetics (Breyer et al., 2006).

Thus, bone marrow clonal cells can be categorised as primitive stem cells, closely related to the mother stem cell, due to their forming of few and large colonies, and dental pulp clones referred to as transit-amplifying cells, due to formation of many small colonies (Chan et al., 2004). In addition, bone marrow cells showed less variable proliferation and would likely be considered a more homogeneous tissue source, while dental pulp cells showed more variable proliferative potential and could be considered more heterogeneous in nature, properties of stem cells and transit-amplifying cells, respectively (Pellegrini et al., 1999). Such a classification may be fitting, due to the multipotent differentiation ability of bone marrow, and lineage restricted differentiation of

the dental pulp, possibly as a result of loss of stem cell characteristics and progressive gain of a more differentiated committed mature progeny (as reviewed (Alison et al., 2002)). Hence, DPSCs may be beneficial to use if mineralised tissue is required, due to limited proliferation and potent differentiation capacity, as opposed to stem cells that may form non-specific tissues to the destination, due to rapid self-renewal and spontaneous differentiation characteristics (Seong et al., 2010).

In support of this thesis, clonal analysis revealed existence of multipotent colonies (Pittenger et al., 1999, Muraglia et al., 2000) and opposes the notion of a total cell tissue population harboring several committed progenitor cell-types that each forms *e.g.* bone, cartilage, or adipose (Dennis and Caplan, 1996a). Principal to tissue engineering and regenerative medicine is study of clonal cell populations, to best characterise and understand which tissue source is most efficacious for mineralised clinical applications such as bone repair and tooth caries (Dennis and Caplan, 1996b), which is particularly lacking for craniofacial therapy. Thus, preferential use of DPSCs and tissue-sourced tooth protein-extracts could potentially be advantageous to tissue regenerative medicine, due preferential capacity for bio-mineralisation. And perhaps more wider in wound-healing therapy (Nuschke, 2013) and pulpal treatment (Iohara et al., 2009), as BMSCs produce factors *e.g.* FGF2 and MMP-9 during *in vivo* osteogenesis that is critical in angiogenesis promotion (Batouli et al., 2003).

Chapter 8

Future Work

There is still much debate concerning use of clonal or heterogeneous MSC populations, as a heterogeneous BMSC population displayed propensity for chondrogenic differentiation *in vivo*, while clonal populations were only capable of adipogenic and osteogenic differentiation *in vitro* (Dennis and Caplan, 1996a). As such, “mixed” clonal populations may provide cytokine, trophic factor, and/or hormone support that is required for differentiation into *e.g.* cartilage tissue, for which TGFβ superfamily was essential (Wang et al., 2014). In addition, would “mixed” clonal populations have a synergistic effect on cell proliferation and gain-of differentiation capacity, with only one (DP F2) of three DPSC clones, here, capable of chondrogenesis. Likewise, would “mixing” clonal populations with different surface marker expressions, *e.g.* MCAM, have gain-of differentiation capacity, as an $MCAM^+$ subpopulation of periodontal ligament MSCs showed higher proliferative potential and osteogenic capacity than $MCAM^-$ cells (Zhu et al., 2013), while a subpopulation of $MCAM^-/CD31^-$ DPSCs regenerated capillary and neuronal networks in canine amputated pulp *in vivo* (Iohara et al., 2009) with angiogenesis and innervation being crucial for pulpal regeneration. Issues highlighted by the International Society for Cellular Therapy, is *in vivo* demonstration of self-renewal capacity and multi-lineage differentiation as during *in vitro* culture (Horwitz et al., 2005), and clonal *in vivo* differentiation pattern could be observed against their known *in vitro* capacity, as a “true” measure of potential.

The potential clinical use of whole-protein bone- and tooth- matrix extracts for tissue engineering needs to be further analysed using immunodepletion against unique proteins highlighted in each extract to observe for loss-of differentiation capacity, in order to identify those proteins vital in mineralisation *e.g.* against proteoglycans biglycan and decorin. In addition, inhibiting MSC cell-surface integrins such as α2β1, which is a major collagen receptor (Watson and Gibbins, 1998), by snake venom rhodocytin (Suzuki-Inoue et al., 2006), can uncover those integrins important for cell migration and attachment (Ganguly et al., 2013), and spatial positioning within a stem cell niche that play a key role in niche maintenance (Riquelme et al., 2008). Additionally, the effects on change in MSC morphology can be observed, as other integrin ligands *e.g.* fibronectin can inhibit terminal differentiation (Watt et al., 1993) and potentially promote migration and proliferation at injury sites.

Lastly, to follow on from the organotypic tissue-slab experiments as a bridge from *in vivo*, the use of a Cre/Lac Z reporter system could label and track the destination of MSC clones in an *in vivo* injury model at sites of damage *e.g.* fracture or caries, and potentially determine MSC proliferative potential and differentiation capacity to uncover their role in healing processes.

References

ABDALLAH, B. M. & KASSEM, M. 2012. New factors controlling the balance between osteoblastogenesis and adipogenesis. *Bone,* 50**,** 540-5.

ADAMS, J. C. & WATT, F. M. 1990. Changes in keratinocyte adhesion during terminal differentiation: reduction in fibronectin binding precedes alpha 5 beta 1 integrin loss from the cell surface. *Cell,* 63**,** 425-35.

ADAMS, J. C. & WATT, F. M. 1991. Expression of beta 1, beta 3, beta 4, and beta 5 integrins by human epidermal keratinocytes and non-differentiating keratinocytes. *J Cell Biol,* 115**,** 829-41.

AGUIAR, M. C. & ARANA-CHAVEZ, V. E. 2007. Ultrastructural and immunocytochemical analyses of osteopontin in reactionary and reparative dentine formed after extrusion of upper rat incisors. *J Anat,* 210**,** 418-27.

AKITA, K., VON HOLST, A., FURUKAWA, Y., MIKAMI, T., SUGAHARA, K. & FAISSNER, A. 2008. Expression of multiple chondroitin/dermatan sulfotransferases in the neurogenic regions of the embryonic and adult central nervous system implies that complex chondroitin sulfates have a role in neural stem cell maintenance. *Stem Cells,* 26**,** 798-809.

ALGE, D. L., ZHOU, D., ADAMS, L. L., WYSS, B. K., SHADDAY, M. D., WOODS, E. J., GABRIEL CHU, T. M. & GOEBEL, W. S. 2010. Donor-matched comparison of dental pulp stem cells and bone marrow-derived mesenchymal stem cells in a rat model. *J Tissue Eng Regen Med,* 4**,** 73-81.

ALISON, M. R., POULSOM, R., FORBES, S. & WRIGHT, N. A. 2002. An introduction to stem cells. *J Pathol,* 197**,** 419-23.

ALRAIES, A. 2013. *Characterisation of Clonal Dental Pulp Progenitors and the Effects of In Vitro Expansion and Hydrogen Peroxide* PhD Thesis, Cardiff University.

ALT, E., YAN, Y., GEHMERT, S., SONG, Y. H., ALTMAN, A., VYKOUKAL, D. & BAI, X. 2011. Fibroblasts share mesenchymal phenotypes with stem cells, but lack their differentiation and colony-forming potential. *Biol Cell,* 103**,** 197-208.

AMEYE, L. & YOUNG, M. F. 2002. Mice deficient in small leucine-rich proteoglycans: novel in vivo models for osteoporosis, osteoarthritis, Ehlers-Danlos syndrome, muscular dystrophy, and corneal diseases. *Glycobiology,* 12**,** 107R-16R.

ARVIDSON, K., ABDALLAH, B. M., APPLEGATE, L. A., BALDINI, N., CENNI, E., GOMEZ-BARRENA, E., GRANCHI, D., KASSEM, M., KONTTINEN, Y. T., MUSTAFA, K., PIOLETTI, D. P., SILLAT, T. & FINNE-WISTRAND, A. 2011. Bone regeneration and stem cells. *J Cell Mol Med,* 15**,** 718-46.

ATARI, M., GIL-RECIO, C., FABREGAT, M., GARCIA-FERNANDEZ, D., BARAJAS, M., CARRASCO, M. A., JUNG, H. S., ALFARO, F. H., CASALS, N., PROSPER, F.,

FERRES-PADRO, E. & GINER, L. 2012. Dental pulp of the third molar: a new source of pluripotent-like stem cells. *J Cell Sci,* 125**,** 3343-56.

AUBIN, J. E., LIU, F., MALAVAL, L. & GUPTA, A. K. 1995. Osteoblast and chondroblast differentiation. *Bone,* 17**,** 77s-83s.

AYALA-SUMUANO, J. T., VELEZ-DEL VALLE, C., BELTRAN-LANGARICA, A., HERNANDEZ, J. M. & KURI-HARCUCH, W. 2008. Adipogenic genes on induction and stabilization of commitment to adipose conversion. *Biochem Biophys Res Commun,* 374**,** 720-4.

BAKSH, D., DAVIES, J. E. & ZANDSTRA, P. W. 2003. Adult human bone marrow-derived mesenchymal progenitor cells are capable of adhesion-independent survival and expansion. *Exp Hematol,* 31**,** 723-32.

BALIC, A., AGUILA, H. L., CAIMANO, M. J., FRANCONE, V. P. & MINA, M. 2010. Characterization of stem and progenitor cells in the dental pulp of erupted and unerupted murine molars. *Bone,* 46**,** 1639-51.

BARCZYK, M., CARRACEDO, S. & GULLBERG, D. 2010. Integrins. *Cell Tissue Res,* 339**,** 269-80.

BATOULI, S., MIURA, M., BRAHIM, J., TSUTSUI, T. W., FISHER, L. W., GRONTHOS, S., ROBEY, P. G. & SHI, S. 2003. Comparison of stem-cell-mediated osteogenesis and dentinogenesis. *J Dent Res,* 82**,** 976-81.

BENEDETTO, M. S., SIQUEIRA, F. M., MASCARO, M. B., ARAUJO, V. C. & BONECKER, M. J. 2013. Immunohistochemical expression of biglycan and decorin in the pulp tissue of human primary teeth during resorption. *Braz Oral Res,* 27**,** 438-44.

BI, Y., EHIRCHIOU, D., KILTS, T. M., INKSON, C. A., EMBREE, M. C., SONOYAMA, W., LI, L., LEET, A. I., SEO, B. M., ZHANG, L., SHI, S. & YOUNG, M. F. 2007. Identification of tendon stem/progenitor cells and the role of the extracellular matrix in their niche. *Nat Med,* 13**,** 1219-27.

BIANCO, P. & COSSU, G. 1999. Uno, nessuno e centomila: searching for the identity of mesodermal progenitors. *Exp Cell Res,* 251**,** 257-63.

BIANCO, P., FISHER, L. W., YOUNG, M. F., TERMINE, J. D. & ROBEY, P. G. 1990. Expression and localization of the two small proteoglycans biglycan and decorin in developing human skeletal and non-skeletal tissues. *J Histochem Cytochem,* 38**,** 1549-63.

BIANCO, P., RIMINUCCI, M., GRONTHOS, S. & ROBEY, P. G. 2001. Bone marrow stromal stem cells: nature, biology, and potential applications. *Stem Cells,* 19**,** 180-92.

BODEN, S. D. 1999. Bioactive factors for bone tissue engineering. *Clin Orthop Relat Res***,** S84-94.

BODO, M., BARONI, T., CARINCI, F., BECCHETTI, E., BELLUCCI, C., CONTE, C., PEZZETTI, F., EVANGELISTI, R., TOGNON, M. & CARINCI, P. 1999. A regulatory role of fibroblast growth factor in the expression of decorin, biglycan, betaglycan and

syndecan in osteoblasts from patients with Crouzon's syndrome. *Eur J Cell Biol,* 78**,** 323-30.

BOSKEY, A. L., SPEVAK, L., DOTY, S. B. & ROSENBERG, L. 1997. Effects of bone CS-proteoglycans, DS-decorin, and DS-biglycan on hydroxyapatite formation in a gelatin gel. *Calcif Tissue Int,* 61**,** 298-305.

BOSKEY, A. L., SPEVAK, L., PASCHALIS, E., DOTY, S. B. & MCKEE, M. D. 2002. Osteopontin deficiency increases mineral content and mineral crystallinity in mouse bone. *Calcif Tissue Int,* 71**,** 145-54.

BRADSHAW, A. D. & SAGE, E. H. 2001. SPARC, a matricellular protein that functions in cellular differentiation and tissue response to injury. *J Clin Invest,* 107**,** 1049-54.

BREYER, A., ESTHARABADI, N., OKI, M., ULLOA, F., NELSON-HOLTE, M., LIEN, L. & JIANG, Y. 2006. Multipotent adult progenitor cell isolation and culture procedures. *Exp Hematol,* 34**,** 1596-601.

BRONCKERS, A. L., D'SOUZA, R. N., BUTLER, W. T., LYARUU, D. M., VAN DIJK, S., GAY, S. & WOLTGENS, J. H. 1993. Dentin sialoprotein: biosynthesis and developmental appearance in rat tooth germs in comparison with amelogenins, osteocalcin and collagen type-I. *Cell Tissue Res,* 272**,** 237-47.

BRUDER, S. P., JAISWAL, N. & HAYNESWORTH, S. E. 1997. Growth kinetics, self-renewal, and the osteogenic potential of purified human mesenchymal stem cells during extensive subcultivation and following cryopreservation. *J Cell Biochem,* 64**,** 278-94.

BRUNNER, G., NGUYEN, H., GABRILOVE, J., RIFKIN, D. B. & WILSON, E. L. 1993. Basic fibroblast growth factor expression in human bone marrow and peripheral blood cells. *Blood,* 81**,** 631-8.

BUENO, D. F. 2013. *Use of Mesenchymal Stem Cells for Alveolar Bone Tissue Engineering for Cleft Lip and Palate Patients* [Online]. Available: http://clinicaltrials.gov/ct2/show/NCT01932164?term=dental+pulp+stem+cells&rank=1.

BUSSARD, K. M., GAY, C. V. & MASTRO, A. M. 2008. The bone microenvironment in metastasis; what is special about bone? *Cancer Metastasis Rev,* 27**,** 41-55.

BUTLER, W. T., MIKULSKI, A., URIST, M. R., BRIDGES, G. & UYENO, S. 1977. Noncollagenous proteins of a rat dentin matrix possessing bone morphogenetic activity. *J Dent Res,* 56**,** 228-32.

CARINCI, F., PAPACCIO, G., LAINO, G., PALMIERI, A., BRUNELLI, G., D'AQUINO, R., GRAZIANO, A., LANZA, V., SCAPOLI, L., MARTINELLI, M. & PEZZETTI, F. 2008. Comparison between genetic portraits of osteoblasts derived from primary cultures and osteoblasts obtained from human pulpar stem cells. *J Craniofac Surg,* 19**,** 616-25; discussion 626-7.

CARINCI, P., BECCHETTI, E., BARONI, T., CARINCI, F., PEZZETTI, F., STABELLINI, G., LOCCI, P., SCAPOLI, L., TOGNON, M., VOLINIA, S. & BODO, M. 2007. Extracellular

matrix and growth factors in the pathogenesis of some craniofacial malformations. *Eur J Histochem,* 51 Suppl 1**,** 105-15.

CASTRO-MALASPINA, H., GAY, R. E., RESNICK, G., KAPOOR, N., MEYERS, P., CHIARIERI, D., MCKENZIE, S., BROXMEYER, H. E. & MOORE, M. A. 1980. Characterization of human bone marrow fibroblast colony-forming cells (CFU-F) and their progeny. *Blood,* 56**,** 289-301.

CHAI, Y., JIANG, X., ITO, Y., BRINGAS, P., JR., HAN, J., ROWITCH, D. H., SORIANO, P., MCMAHON, A. P. & SUCOV, H. M. 2000. Fate of the mammalian cranial neural crest during tooth and mandibular morphogenesis. *Development,* 127**,** 1671-9.

CHAN, R. W., SCHWAB, K. E. & GARGETT, C. E. 2004. Clonogenicity of human endometrial epithelial and stromal cells. *Biol Reprod,* 70**,** 1738-50.

CHEN, D., ZHAO, M. & MUNDY, G. R. 2004a. Bone morphogenetic proteins. *Growth Factors,* 22**,** 233-41.

CHEN, J., SINGH, K., MUKHERJEE, B. B. & SODEK, J. 1993. Developmental expression of osteopontin (OPN) mRNA in rat tissues: evidence for a role for OPN in bone formation and resorption. *Matrix,* 13**,** 113-23.

CHEN, X. D., FISHER, L. W., ROBEY, P. G. & YOUNG, M. F. 2004b. The small leucine-rich proteoglycan biglycan modulates BMP-4-induced osteoblast differentiation. *Faseb J,* 18**,** 948-58.

CHEN, X. D., SHI, S., XU, T., ROBEY, P. G. & YOUNG, M. F. 2002. Age-related osteoporosis in biglycan-deficient mice is related to defects in bone marrow stromal cells. *J Bone Miner Res,* 17**,** 331-40.

CHEN, Y., BAL, B. S. & GORSKI, J. P. 1992. Calcium and collagen binding properties of osteopontin, bone sialoprotein, and bone acidic glycoprotein-75 from bone. *J Biol Chem,* 267**,** 24871-8.

CHEN, Y. J., SHIE, M. Y., HUNG, C. J., WU, B. C., LIU, S. L., HUANG, T. H. & KAO, C. T. 2013. Activation of focal adhesion kinase induces extracellular signal-regulated kinase-mediated osteogenesis in tensile force-subjected periodontal ligament fibroblasts but not in osteoblasts. *J Bone Miner Metab*.

CHENG, S. L., SHAO, J. S., CAI, J., SIERRA, O. L. & TOWLER, D. A. 2008. Msx2 exerts bone anabolism via canonical Wnt signaling. *J Biol Chem,* 283**,** 20505-22.

CHUNG, C. J., SOMA, K., RITTLING, S. R., DENHARDT, D. T., HAYATA, T., NAKASHIMA, K., EZURA, Y. & NODA, M. 2008. OPN deficiency suppresses appearance of odontoclastic cells and resorption of the tooth root induced by experimental force application. *J Cell Physiol,* 214**,** 614-20.

CIRUNA, B. & ROSSANT, J. 2001. FGF signaling regulates mesoderm cell fate specification and morphogenetic movement at the primitive streak. *Dev Cell,* 1**,** 37-49.

COCHRAN, D. L., JONES, A., HEIJL, L., MELLONIG, J. T., SCHOOLFIELD, J. & KING, G. N. 2003. Periodontal regeneration with a combination of enamel matrix proteins and autogenous bone grafting. *J Periodontol,* 74**,** 1269-81.

COLTER, D. C., CLASS, R., DIGIROLAMO, C. M. & PROCKOP, D. J. 2000. Rapid expansion of recycling stem cells in cultures of plastic-adherent cells from human bone marrow. *Proc Natl Acad Sci U S A,* 97**,** 3213-8.

COMOGLIO, P. M., BOCCACCIO, C. & TRUSOLINO, L. 2003. Interactions between growth factor receptors and adhesion molecules: breaking the rules. *Curr Opin Cell Biol,* 15**,** 565-71.

COOK, K. S., MIN, H. Y., JOHNSON, D., CHAPLINSKY, R. J., FLIER, J. S., HUNT, C. R. & SPIEGELMAN, B. M. 1987. Adipsin: a circulating serine protease homolog secreted by adipose tissue and sciatic nerve. *Science,* 237**,** 402-5.

COUCHMAN, J. R., CATERSON, B., CHRISTNER, J. E. & BAKER, J. R. 1984. Mapping by monoclonal antibody detection of glycosaminoglycans in connective tissues. *Nature,* 307**,** 650-2.

D'AQUINO, R., GRAZIANO, A., SAMPAOLESI, M., LAINO, G., PIROZZI, G., DE ROSA, A. & PAPACCIO, G. 2007. Human postnatal dental pulp cells co-differentiate into osteoblasts and endotheliocytes: a pivotal synergy leading to adult bone tissue formation. *Cell Death Differ,* 14**,** 1162-71.

D'SOUZA, R. N., ABERG, T., GAIKWAD, J., CAVENDER, A., OWEN, M., KARSENTY, G. & THESLEFF, I. 1999. Cbfa1 is required for epithelial-mesenchymal interactions regulating tooth development in mice. *Development,* 126**,** 2911-20.

DAVIES, J. E. 2003. Understanding peri-implant endosseous healing. *J Dent Educ,* 67**,** 932-49.

DAY, T. F., GUO, X., GARRETT-BEAL, L. & YANG, Y. 2005. Wnt/beta-catenin signaling in mesenchymal progenitors controls osteoblast and chondrocyte differentiation during vertebrate skeletogenesis. *Dev Cell,* 8**,** 739-50.

DELANY, A. M., AMLING, M., PRIEMEL, M., HOWE, C., BARON, R. & CANALIS, E. 2000. Osteopenia and decreased bone formation in osteonectin-deficient mice. *J Clin Invest,* 105**,** 915-23.

DELANY, A. M. & HANKENSON, K. D. 2009. Thrombospondin-2 and SPARC/osteonectin are critical regulators of bone remodeling. *J Cell Commun Signal,* 3**,** 227-38.

DELL'ACCIO, F., DE BARI, C., EL TAWIL, N. M., BARONE, F., MITSIADIS, T. A., O'DOWD, J. & PITZALIS, C. 2006. Activation of WNT and BMP signaling in adult human articular cartilage following mechanical injury. *Arthritis Res Ther,* 8**,** R139.

DELL'ORCO, R. T., MERTENS, J. G. & KRUSE, P. F., JR. 1974. Doubling potential, calendar time, and donor age of human diploid cells in culture. *Exp Cell Res,* 84**,** 363-6.

DELORME, B., RINGE, J., PONTIKOGLOU, C., GAILLARD, J., LANGONNE, A., SENSEBE, L., NOEL, D., JORGENSEN, C., HAUPL, T. & CHARBORD, P. 2009. Specific lineage-priming of bone marrow mesenchymal stem cells provides the molecular framework for their plasticity. *Stem Cells,* 27**,** 1142-51.

DENNIS, J. E. & CAPLAN, A. I. 1996a. Analysis of the developmental potential of conditionally immortal marrow-derived mesenchymal progenitor cells isolated from the H-2Kb-tsA58 transgenic mouse. *Connect Tissue Res,* 35**,** 93-9.

DENNIS, J. E. & CAPLAN, A. I. 1996b. Differentiation potential of conditionally immortalized mesenchymal progenitor cells from adult marrow of a H-2Kb-tsA58 transgenic mouse. *J Cell Physiol,* 167**,** 523-38.

DESCHASEAUX, F., SENSEBE, L. & HEYMANN, D. 2009. Mechanisms of bone repair and regeneration. *Trends Mol Med,* 15**,** 417-29.

DI NICOLA, M., CARLO-STELLA, C., MAGNI, M., MILANESI, M., LONGONI, P. D., MATTEUCCI, P., GRISANTI, S. & GIANNI, A. M. 2002. Human bone marrow stromal cells suppress T-lymphocyte proliferation induced by cellular or nonspecific mitogenic stimuli. *Blood,* 99**,** 3838-43.

DIMITRIOU, R., TSIRIDIS, E. & GIANNOUDIS, P. V. 2005. Current concepts of molecular aspects of bone healing. *Injury,* 36**,** 1392-404.

DING, C., LI, L., SU, Y. C., XIANG, R. L., CONG, X., YU, H. K., LI, S. L., WU, L. L. & YU, G. Y. 2013. Adiponectin increases secretion of rat submandibular gland via adiponectin receptors-mediated AMPK signaling. *PLoS One,* 8**,** e63878.

DOCHEVA, D., PADULA, D., POPOV, C., MUTSCHLER, W., CLAUSEN-SCHAUMANN, H. & SCHIEKER, M. 2008. Researching into the cellular shape, volume and elasticity of mesenchymal stem cells, osteoblasts and osteosarcoma cells by atomic force microscopy. *J Cell Mol Med,* 12**,** 537-52.

DODIG, M., TADIC, T., KRONENBERG, M. S., DACIC, S., LIU, Y. H., MAXSON, R., ROWE, D. W. & LICHTLER, A. C. 1999. Ectopic Msx2 overexpression inhibits and Msx2 antisense stimulates calvarial osteoblast differentiation. *Dev Biol,* 209**,** 298-307.

DOHERTY, M. J., ASHTON, B. A., WALSH, S., BERESFORD, J. N., GRANT, M. E. & CANFIELD, A. E. 1998. Vascular pericytes express osteogenic potential in vitro and in vivo. *J Bone Miner Res,* 13**,** 828-38.

DOMINICI, M., LE BLANC, K., MUELLER, I., SLAPER-CORTENBACH, I., MARINI, F., KRAUSE, D., DEANS, R., KEATING, A., PROCKOP, D. & HORWITZ, E. 2006. Minimal criteria for defining multipotent mesenchymal stromal cells. The International Society for Cellular Therapy position statement. *Cytotherapy,* 8**,** 315-7.

DOWTHWAITE, G. P., BISHOP, J. C., REDMAN, S. N., KHAN, I. M., ROONEY, P., EVANS, D. J., HAUGHTON, L., BAYRAM, Z., BOYER, S., THOMSON, B., WOLFE, M. S. & ARCHER, C. W. 2004. The surface of articular cartilage contains a progenitor cell population. *J Cell Sci,* 117**,** 889-97.

DUCY, P. 2000. Cbfa1: a molecular switch in osteoblast biology. *Dev Dyn,* 219**,** 461-71.

DUGGAL, S. & BRINCHMANN, J. E. 2011. Importance of serum source for the in vitro replicative senescence of human bone marrow derived mesenchymal stem cells. *J Cell Physiol,* 226**,** 2908-15.

ECKEL, R. H. 1989. Lipoprotein lipase. A multifunctional enzyme relevant to common metabolic diseases. *N Engl J Med,* 320**,** 1060-8.

ELLMAN, M. B., AN, H. S., MUDDASANI, P. & IM, H. J. 2008. Biological impact of the fibroblast growth factor family on articular cartilage and intervertebral disc homeostasis. *Gene,* 420**,** 82-9.

EMBERY, G., REES, S., HALL, R., ROSE, K., WADDINGTON, R. & SHELLIS, P. 1998. Calcium- and hydroxyapatite-binding properties of glucuronic acid-rich and iduronic acid-rich glycosaminoglycans and proteoglycans. *Eur J Oral Sci,* 106 Suppl 1**,** 267-73.

FAN, J., PARK, H., TAN, S. & LEE, M. 2013a. Enhanced osteogenesis of adipose derived stem cells with Noggin suppression and delivery of BMP-2. *PLoS One,* 8**,** e72474.

FAN, Y. X., GU, C. H., ZHANG, Y. L., ZHONG, B. S., WANG, L. Z., ZHOU, Z. R., WANG, Z. Y., JIA, R. X. & WANG, F. 2013b. Oct4 and Sox2 overexpression improves the proliferation and differentiation of bone mesenchymal stem cells in Xiaomeishan porcine. *Genet Mol Res,* 12**,** 6067-79.

FENG, R. & LENGNER, C. 2013. Application of Stem Cell Technology in Dental Regenerative Medicine. *Adv Wound Care (New Rochelle),* 2**,** 296-305.

FILSHIE, R. J., ZANNETTINO, A. C., MAKRYNIKOLA, V., GRONTHOS, S., HENNIKER, A. J., BENDALL, L. J., GOTTLIEB, D. J., SIMMONS, P. J. & BRADSTOCK, K. F. 1998. MUC18, a member of the immunoglobulin superfamily, is expressed on bone marrow fibroblasts and a subset of hematological malignancies. *Leukemia,* 12**,** 414-21.

FINKELMAN, R. D. 1992. Growth factors in bones and teeth. *J Calif Dent Assoc,* 20**,** 23-9.

FLEISCHMAJER, R., FISHER, L. W., MACDONALD, E. D., JACOBS, L., JR., PERLISH, J. S. & TERMINE, J. D. 1991. Decorin interacts with fibrillar collagen of embryonic and adult human skin. *J Struct Biol,* 106**,** 82-90.

FOSTER, B. L., SOENJAYA, Y., NOCITI, F. H., JR., HOLM, E., ZERFAS, P. M., WIMER, H. F., HOLDSWORTH, D. W., AUBIN, J. E., HUNTER, G. K., GOLDBERG, H. A. & SOMERMAN, M. J. 2013. Deficiency in acellular cementum and periodontal attachment in bsp null mice. *J Dent Res,* 92**,** 166-72.

FRANCO, S., MACKENZIE, K. L., DIAS, S., ALVAREZ, S., RAFII, S. & MOORE, M. A. 2001. Clonal variation in phenotype and life span of human embryonic fibroblasts (MRC-5) transduced with the catalytic component of telomerase (hTERT). *Exp Cell Res,* 268**,** 14-25.

FREYTAG, S. O. & GEDDES, T. J. 1992. Reciprocal regulation of adipogenesis by Myc and C/EBP alpha. *Science,* 256**,** 379-82.

FRIEDENSTEIN, A. J., GORSKAJA, J. F. & KULAGINA, N. N. 1976. Fibroblast precursors in normal and irradiated mouse hematopoietic organs. *Exp Hematol,* 4**,** 267-74.

FUCHS, E., TUMBAR, T. & GUASCH, G. 2004. Socializing with the neighbors: stem cells and their niche. *Cell,* 116**,** 769-78.

FUJISAWA, R., BUTLER, W. T., BRUNN, J. C., ZHOU, H. Y. & KUBOKI, Y. 1993. Differences in composition of cell-attachment sialoproteins between dentin and bone. *J Dent Res,* 72**,** 1222-6.

FUJITA, K. & JANZ, S. 2007. Attenuation of WNT signaling by DKK-1 and -2 regulates BMP2-induced osteoblast differentiation and expression of OPG, RANKL and M-CSF. *Mol Cancer,* 6**,** 71.

FUKIAGE, K., AOYAMA, T., SHIBATA, K. R., OTSUKA, S., FURU, M., KOHNO, Y., ITO, K., JIN, Y., FUJITA, S., FUJIBAYASHI, S., NEO, M., NAKAYAMA, T., NAKAMURA, T. & TOGUCHIDA, J. 2008. Expression of vascular cell adhesion molecule-1 indicates the differentiation potential of human bone marrow stromal cells. *Biochem Biophys Res Commun,* 365**,** 406-12.

GANDARILLAS, A. & WATT, F. M. 1997. c-Myc promotes differentiation of human epidermal stem cells. *Genes Dev,* 11**,** 2869-82.

GANGULY, K. K., PAL, S., MOULIK, S. & CHATTERJEE, A. 2013. Integrins and metastasis. *Cell Adh Migr,* 7**,** 251-61.

GAO, D. & CRITSER, J. K. 2000. Mechanisms of cryoinjury in living cells. *Ilar j,* 41**,** 187-96.

GEORGIOU, K. R., SCHERER, M. A., FAN, C. M., COOL, J. C., KING, T. J., FOSTER, B. K. & XIAN, C. J. 2012. Methotrexate chemotherapy reduces osteogenesis but increases adipogenic potential in the bone marrow. *J Cell Physiol,* 227**,** 909-18.

GIUSTINA, A., MAZZIOTTI, G. & CANALIS, E. 2008. Growth hormone, insulin-like growth factors, and the skeleton. *Endocr Rev,* 29**,** 535-59.

GOLDBERG, M., RAPOPORT, O., SEPTIER, D., PALMIER, K., HALL, R., EMBERY, G., YOUNG, M. & AMEYE, L. 2003. Proteoglycans in predentin: the last 15 micrometers before mineralization. *Connect Tissue Res,* 44 Suppl 1**,** 184-8.

GOLDBERG, M. & SMITH, A. J. 2004. CELLS AND EXTRACELLULAR MATRICES OF DENTIN AND PULP: A BIOLOGICAL BASIS FOR REPAIR AND TISSUE ENGINEERING. *Crit Rev Oral Biol Med,* 15**,** 13-27.

GONCHAROVA, V., SEROBYAN, N., IIZUKA, S., SCHRAUFSTATTER, I., DE RIDDER, A., POVALIY, T., WACKER, V., ITANO, N., KIMATA, K., ORLOVSKAJA, I. A., YAMAGUCHI, Y. & KHALDOYANIDI, S. 2012. Hyaluronan expressed by the hematopoietic microenvironment is required for bone marrow hematopoiesis. *J Biol Chem,* 287**,** 25419-33.

GONZALEZ, R. F., ALLEN, L. & DOBBS, L. G. 2009. Rat alveolar type I cells proliferate, express OCT-4, and exhibit phenotypic plasticity in vitro. *Am J Physiol Lung Cell Mol Physiol,* 297**,** L1045-55.

GORDON, M. Y., RILEY, G. P., WATT, S. M. & GREAVES, M. F. 1987. Compartmentalization of a haematopoietic growth factor (GM-CSF) by glycosaminoglycans in the bone marrow microenvironment. *Nature,* 326**,** 403-5.

GORSKI, J. P., KREMER, E. A. & CHEN, Y. 1996. Bone acidic glycoprotein-75 self-associates to form large macromolecular complexes. *Connect Tissue Res,* 35**,** 137-43.

GORSKI, J. P., WANG, A., LOVITCH, D., LAW, D., POWELL, K. & MIDURA, R. J. 2004. Extracellular bone acidic glycoprotein-75 defines condensed mesenchyme regions to be mineralized and localizes with bone sialoprotein during intramembranous bone formation. *J Biol Chem,* 279**,** 25455-63.

GOVINDASAMY, V., ABDULLAH, A. N., RONALD, V. S., MUSA, S., AB AZIZ, Z. A., ZAIN, R. B., TOTEY, S., BHONDE, R. R. & ABU KASIM, N. H. 2010. Inherent differential propensity of dental pulp stem cells derived from human deciduous and permanent teeth. *J Endod,* 36**,** 1504-15.

GRONTHOS, S., BRAHIM, J., LI, W., FISHER, L. W., CHERMAN, N., BOYDE, A., DENBESTEN, P., ROBEY, P. G. & SHI, S. 2002. Stem cell properties of human dental pulp stem cells. *J Dent Res,* 81**,** 531-5.

GRONTHOS, S., MANKANI, M., BRAHIM, J., ROBEY, P. G. & SHI, S. 2000. Postnatal human dental pulp stem cells (DPSCs) in vitro and in vivo. *Proc Natl Acad Sci U S A,* 97**,** 13625-30.

GRONTHOS, S., ZANNETTINO, A. C., HAY, S. J., SHI, S., GRAVES, S. E., KORTESIDIS, A. & SIMMONS, P. J. 2003. Molecular and cellular characterisation of highly purified stromal stem cells derived from human bone marrow. *J Cell Sci,* 116**,** 1827-35.

HALFON, S., ABRAMOV, N., GRINBLAT, B. & GINIS, I. 2011. Markers distinguishing mesenchymal stem cells from fibroblasts are downregulated with passaging. *Stem Cells Dev,* 20**,** 53-66.

HARRINGTON, J., SLOAN, A. J. & WADDINGTON, R. J. 2014. Quantification of clonal heterogeneity of mesenchymal progenitor cells in dental pulp and bone marrow. *Connect Tissue Res,* 55 Suppl 1**,** 62-7.

HAYFLICK, L. 1989. Antecedents of cell aging research. *Exp Gerontol,* 24**,** 355-65.

HILDEBRAND, A., ROMARIS, M., RASMUSSEN, L. M., HEINEGARD, D., TWARDZIK, D. R., BORDER, W. A. & RUOSLAHTI, E. 1994. Interaction of the small interstitial proteoglycans biglycan, decorin and fibromodulin with transforming growth factor beta. *Biochem J,* 302 (Pt 2)**,** 527-34.

HOGANSON, D. M., MEPPELINK, A. M., HINKEL, C. J., GOLDMAN, S. M., LIU, X. H., NUNLEY, R. M., GAUT, J. P. & VACANTI, J. P. 2014. Differentiation of human bone marrow mesenchymal stem cells on decellularized extracellular matrix materials. *J Biomed Mater Res A,* 102**,** 2875-83.

HOMBACH-KLONISCH, S., PANIGRAHI, S., RASHEDI, I., SEIFERT, A., ALBERTI, E., POCAR, P., KURPISZ, M., SCHULZE-OSTHOFF, K., MACKIEWICZ, A. & LOS, M. 2008. Adult stem cells and their trans-differentiation potential--perspectives and therapeutic applications. *J Mol Med,* 86**,** 1301-14.

HORWITZ, E. M., LE BLANC, K., DOMINICI, M., MUELLER, I., SLAPER-CORTENBACH, I., MARINI, F. C., DEANS, R. J., KRAUSE, D. S. & KEATING, A. 2005. Clarification of the nomenclature for MSC: The International Society for Cellular Therapy position statement. *Cytotherapy,* 7**,** 393-5.

HOSHI, K., KEMMOTSU, S., TAKEUCHI, Y., AMIZUKA, N. & OZAWA, H. 1999. The primary calcification in bones follows removal of decorin and fusion of collagen fibrils. *J Bone Miner Res,* 14**,** 273-80.

HOSOKAWA, R., URATA, M., HAN, J., ZEHNALY, A., BRINGAS, P., JR., NONAKA, K. & CHAI, Y. 2007. TGF-beta mediated Msx2 expression controls occipital somites-derived caudal region of skull development. *Dev Biol,* 310**,** 140-53.

HOTCHIN, N. A., GANDARILLAS, A. & WATT, F. M. 1995. Regulation of cell surface beta 1 integrin levels during keratinocyte terminal differentiation. *J Cell Biol,* 128**,** 1209-19.

HOU, S., MACCARANA, M., MIN, T. H., STRATE, I. & PERA, E. M. 2007. The secreted serine protease xHtrA1 stimulates long-range FGF signaling in the early Xenopus embryo. *Dev Cell,* 13**,** 226-41.

HU, B., UNDA, F., BOPP-KUCHLER, S., JIMENEZ, L., WANG, X. J., HAIKEL, Y., WANG, S. L. & LESOT, H. 2006. Bone marrow cells can give rise to ameloblast-like cells. *J Dent Res,* 85**,** 416-21.

HUANG, G. T., GRONTHOS, S. & SHI, S. 2009. Mesenchymal stem cells derived from dental tissues vs. those from other sources: their biology and role in regenerative medicine. *J Dent Res,* 88**,** 792-806.

HUANG, G. T., SHAGRAMANOVA, K. & CHAN, S. W. 2006a. Formation of odontoblast-like cells from cultured human dental pulp cells on dentin in vitro. *J Endod,* 32**,** 1066-73.

HUANG, G. T., SONOYAMA, W., CHEN, J. & PARK, S. H. 2006b. In vitro characterization of human dental pulp cells: various isolation methods and culturing environments. *Cell Tissue Res,* 324**,** 225-36.

HUANG, W., YANG, S., SHAO, J. & LI, Y. P. 2007. Signaling and transcriptional regulation in osteoblast commitment and differentiation. *Front Biosci,* 12**,** 3068-92.

HUNTER, G. K., HAUSCHKA, P. V., POOLE, A. R., ROSENBERG, L. C. & GOLDBERG, H. A. 1996. Nucleation and inhibition of hydroxyapatite formation by mineralized tissue proteins. *Biochem J,* 317 (Pt 1)**,** 59-64.

HUTTENLOCHER, A., WERB, Z., TREMBLE, P., HUHTALA, P., ROSENBERG, L. & DAMSKY, C. H. 1996. Decorin regulates collagenase gene expression in fibroblasts adhering to vitronectin. *Matrix Biol,* 15**,** 239-50.

INKSON, C. A., ONO, M., BI, Y., KUZNETSOV, S. A., FISHER, L. W. & YOUNG, M. F. 2009. The potential functional interaction of biglycan and WISP-1 in controlling differentiation and proliferation of osteogenic cells. *Cells Tissues Organs,* 189**,** 153-7.

IOHARA, K., ZHENG, L., ITO, M., ISHIZAKA, R., NAKAMURA, H., INTO, T., MATSUSHITA, K. & NAKASHIMA, M. 2009. Regeneration of dental pulp after pulpotomy by transplantation of CD31(-)/CD146(-) side population cells from a canine tooth. *Regen Med,* 4**,** 377-85.

IRVING, J. T. & MIGLIORE, S. A. 1965. CONNECTIVE TISSUE RESPONSES TO ALTERED COLLAGEN AND BONE IMPLANTS. *Am J Anat,* 117**,** 151-8.

JACKSON, A., VAYSSIERE, B., GARCIA, T., NEWELL, W., BARON, R., ROMAN-ROMAN, S. & RAWADI, G. 2005. Gene array analysis of Wnt-regulated genes in C3H10T1/2 cells. *Bone,* 36**,** 585-98.

JACKSON, W. M., LOZITO, T. P., DJOUAD, F., KUHN, N. Z., NESTI, L. J. & TUAN, R. S. 2011. Differentiation and regeneration potential of mesenchymal progenitor cells derived from traumatized muscle tissue. *J Cell Mol Med,* 15**,** 2377-88.

JACOB, A. L., SMITH, C., PARTANEN, J. & ORNITZ, D. M. 2006. Fibroblast growth factor receptor 1 signaling in the osteo-chondrogenic cell lineage regulates sequential steps of osteoblast maturation. *Dev Biol,* 296**,** 315-28.

JACOBSEN, K., KRAVITZ, J., KINCADE, P. W. & OSMOND, D. G. 1996. Adhesion receptors on bone marrow stromal cells: in vivo expression of vascular cell adhesion molecule-1 by reticular cells and sinusoidal endothelium in normal and gamma-irradiated mice. *Blood,* 87**,** 73-82.

JANEBODIN, K., HORST, O. V., IERONIMAKIS, N., BALASUNDARAM, G., REESUKUMAL, K., PRATUMVINIT, B. & REYES, M. 2011. Isolation and characterization of neural crest-derived stem cells from dental pulp of neonatal mice. *PLoS One,* 6**,** e27526.

JI, Y., LIU, J., WANG, Z., LIU, N. & GOU, W. 2009. PPARgamma agonist, rosiglitazone, regulates angiotensin II-induced vascular inflammation through the TLR4-dependent signaling pathway. *Lab Invest,* 89**,** 887-902.

JIANG, Y., JAHAGIRDAR, B. N., REINHARDT, R. L., SCHWARTZ, R. E., KEENE, C. D., ORTIZ-GONZALEZ, X. R., REYES, M., LENVIK, T., LUND, T., BLACKSTAD, M., DU, J., ALDRICH, S., LISBERG, A., LOW, W. C., LARGAESPADA, D. A. & VERFAILLIE, C. M. 2002. Pluripotency of mesenchymal stem cells derived from adult marrow. *Nature,* 418**,** 41-9.

JIN, H. J., BAE, Y. K., KIM, M., KWON, S. J., JEON, H. B., CHOI, S. J., KIM, S. W., YANG, Y. S., OH, W. & CHANG, J. W. 2013. Comparative analysis of human mesenchymal stem cells from bone marrow, adipose tissue, and umbilical cord blood as sources of cell therapy. *Int J Mol Sci,* 14**,** 17986-8001.

JIN, H. J., PARK, S. K., OH, W., YANG, Y. S., KIM, S. W. & CHOI, S. J. 2009. Down-regulation of CD105 is associated with multi-lineage differentiation in human umbilical cord blood-derived mesenchymal stem cells. *Biochem Biophys Res Commun,* 381**,** 676-81.

JOHNSTONE, B., MARKOPOULOS, M., NEAME, P. & CATERSON, B. 1993. Identification and characterization of glycanated and non-glycanated forms of biglycan and decorin in the human intervertebral disc. *Biochem J,* 292 (Pt 3)**,** 661-6.

JONES, P. H., HARPER, S. & WATT, F. M. 1995. Stem cell patterning and fate in human epidermis. *Cell,* 80**,** 83-93.

JONES, P. H. & WATT, F. M. 1993. Separation of human epidermal stem cells from transit amplifying cells on the basis of differences in integrin function and expression. *Cell,* 73**,** 713-24.

KAMURA, S., MATSUMOTO, Y., FUKUSHI, J. I., FUJIWARA, T., IIDA, K., OKADA, Y. & IWAMOTO, Y. 2010. Basic fibroblast growth factor in the bone microenvironment enhances cell motility and invasion of Ewing's sarcoma family of tumours by activating the FGFR1-PI3K-Rac1 pathway. *Br J Cancer,* 103**,** 370-81.

KARAOZ, E., DEMIRCAN, P. C., SAGLAM, O., AKSOY, A., KAYMAZ, F. & DURUKSU, G. 2011. Human dental pulp stem cells demonstrate better neural and epithelial stem cell properties than bone marrow-derived mesenchymal stem cells. *Histochem Cell Biol,* 136**,** 455-73.

KATO, M. V. 2000. A secreted tumor-suppressor, mac25, with activin-binding activity. *Mol Med,* 6**,** 126-35.

KAWASHIMA, R., MOCHIDA, S., MATSUI, A., YOULUTU, Z. Y., ISHIKAWA, K., TOSHIMA, K., YAMANOBE, F., INAO, M., IKEDA, H., OHNO, A., NAGOSHI, S., UEDE, T. & FUJIWARA, K. 1999. Expression of osteopontin in Kupffer cells and hepatic macrophages and Stellate cells in rat liver after carbon tetrachloride intoxication: a possible factor for macrophage migration into hepatic necrotic areas. *Biochem Biophys Res Commun,* 256**,** 527-31.

KERKIS, I., KERKIS, A., DOZORTSEV, D., STUKART-PARSONS, G. C., GOMES MASSIRONI, S. M., PEREIRA, L. V., CAPLAN, A. I. & CERRUTI, H. F. 2006. Isolation and characterization of a population of immature dental pulp stem cells expressing OCT-4 and other embryonic stem cell markers. *Cells Tissues Organs,* 184**,** 105-16.

KERN, S., EICHLER, H., STOEVE, J., KLUTER, H. & BIEBACK, K. 2006. Comparative analysis of mesenchymal stem cells from bone marrow, umbilical cord blood, or adipose tissue. *Stem Cells,* 24**,** 1294-301.

KETTUNEN, P., KARAVANOVA, I. & THESLEFF, I. 1998. Responsiveness of developing dental tissues to fibroblast growth factors: expression of splicing alternatives of FGFR1, -2, -3, and of FGFR4; and stimulation of cell proliferation by FGF-2, -4, -8, and -9. *Dev Genet,* 22**,** 374-85.

KIM, E. G., KWON, H. M., BURROW, C. R. & BALLERMANN, B. J. 1993. Expression of rat fibroblast growth factor receptor 1 as three splicing variants during kidney development. *Am J Physiol,* 264**,** F66-73.

KIM, J. Y., KIM, B. I., JUE, S. S., PARK, J. H. & SHIN, J. W. 2012. Localization of osteopontin and osterix in periodontal tissue during orthodontic tooth movement in rats. *Angle Orthod,* 82**,** 107-14.

KIM, S. & SHIN, T. 2007. Immunohistochemical study of osteopontin in boar testis. *J Vet Sci,* 8**,** 107-10.

KNOEPFFLER, N., SCHIPANSKI, D. & SORGNER, S. L. 2007. *Humanbiotechnology as Social Challenge: An Interdisciplinary Introduction to Bioethics*, Ashgate Publishing Limited.

KOKUDO, T., SUZUKI, Y., YOSHIMATSU, Y., YAMAZAKI, T., WATABE, T. & MIYAZONO, K. 2008. Snail is required for TGFbeta-induced endothelial-mesenchymal transition of embryonic stem cell-derived endothelial cells. *J Cell Sci,* 121**,** 3317-24.

KOMADA, Y., YAMANE, T., KADOTA, D., ISONO, K., TAKAKURA, N., HAYASHI, S. & YAMAZAKI, H. 2012. Origins and properties of dental, thymic, and bone marrow mesenchymal cells and their stem cells. *PLoS One,* 7**,** e46436.

KOMORI, T., YAGI, H., NOMURA, S., YAMAGUCHI, A., SASAKI, K., DEGUCHI, K., SHIMIZU, Y., BRONSON, R. T., GAO, Y. H., INADA, M., SATO, M., OKAMOTO, R., KITAMURA, Y., YOSHIKI, S. & KISHIMOTO, T. 1997. Targeted disruption of Cbfa1 results in a complete lack of bone formation owing to maturational arrest of osteoblasts. *Cell,* 89**,** 755-64.

KORKALAINEN, M., KALLIO, E., OLKKU, A., NELO, K., ILVESARO, J., TUUKKANEN, J., MAHONEN, A. & VILUKSELA, M. 2009. Dioxins interfere with differentiation of osteoblasts and osteoclasts. *Bone,* 44**,** 1134-42.

KOTOBUKI, N., HIROSE, M., MACHIDA, H., KATOU, Y., MURAKI, K., TAKAKURA, Y. & OHGUSHI, H. 2005. Viability and osteogenic potential of cryopreserved human bone marrow-derived mesenchymal cells. *Tissue Eng,* 11**,** 663-73.

KRAMPERA, M., PASINI, A., RIGO, A., SCUPOLI, M. T., TECCHIO, C., MALPELI, G., SCARPA, A., DAZZI, F., PIZZOLO, G. & VINANTE, F. 2005. HB-EGF/HER-1 signaling in bone marrow mesenchymal stem cells: inducing cell expansion and reversibly preventing multilineage differentiation. *Blood,* 106**,** 59-66.

KRATCHMAROVA, I., BLAGOEV, B., HAACK-SORENSEN, M., KASSEM, M. & MANN, M. 2005. Mechanism of divergent growth factor effects in mesenchymal stem cell differentiation. *Science,* 308**,** 1472-7.

KUMAR, A., SALIMATH, B. P., STARK, G. B. & FINKENZELLER, G. 2010. Platelet-derived growth factor receptor signaling is not involved in osteogenic differentiation of human mesenchymal stem cells. *Tissue Eng Part A,* 16**,** 983-93.

KUWABA, K., KOBAYASHI, M., NOMURA, Y., IRIE, S. & KOYAMA, Y. 2001. Elongated dermatan sulphate in post-inflammatory healing skin distributes among collagen fibrils separated by enlarged interfibrillar gaps. *Biochem J,* 358**,** 157-63.

KUWADA, S. K. & LI, X. 2000. Integrin alpha5/beta1 mediates fibronectin-dependent epithelial cell proliferation through epidermal growth factor receptor activation. *Mol Biol Cell,* 11**,** 2485-96.

KUZNETSOV, S. A., KREBSBACH, P. H., SATOMURA, K., KERR, J., RIMINUCCI, M., BENAYAHU, D. & ROBEY, P. G. 1997. Single-colony derived strains of human marrow stromal fibroblasts form bone after transplantation in vivo. *J Bone Miner Res,* 12**,** 1335-47.

KUZNETSOV, S. A., MANKANI, M. H., GRONTHOS, S., SATOMURA, K., BIANCO, P. & ROBEY, P. G. 2001. Circulating skeletal stem cells. *J Cell Biol,* 153**,** 1133-40.

LACERDA-PINHEIRO, S., DIMITROVA-NAKOV, S., HARICHANE, Y., SOUYRI, M., PETIT-COCAULT, L., LEGRES, L., MARCHADIER, A., BAUDRY, A., RIBES, S., GOLDBERG, M., KELLERMANN, O. & POLIARD, A. 2012. Concomitant multipotent and unipotent dental pulp progenitors and their respective contribution to mineralised tissue formation. *Eur Cell Mater,* 23**,** 371-86.

LAI, C. F. & CHENG, S. L. 2002. Signal transductions induced by bone morphogenetic protein-2 and transforming growth factor-beta in normal human osteoblastic cells. *J Biol Chem,* 277**,** 15514-22.

LAINO, G., D'AQUINO, R., GRAZIANO, A., LANZA, V., CARINCI, F., NARO, F., PIROZZI, G. & PAPACCIO, G. 2005. A new population of human adult dental pulp stem cells: a useful source of living autologous fibrous bone tissue (LAB). *J Bone Miner Res,* 20**,** 1394-402.

LAINO, G., GRAZIANO, A., D'AQUINO, R., PIROZZI, G., LANZA, V., VALIANTE, S., DE ROSA, A., NARO, F., VIVARELLI, E. & PAPACCIO, G. 2006. An approachable human adult stem cell source for hard-tissue engineering. *J Cell Physiol,* 206**,** 693-701.

LAVENUS, S., PILET, P., GUICHEUX, J., WEISS, P., LOUARN, G. & LAYROLLE, P. 2011. Behaviour of mesenchymal stem cells, fibroblasts and osteoblasts on smooth surfaces. *Acta Biomater,* 7**,** 1525-34.

LEE, H. T. & KAY, E. P. 2003. FGF-2 induced reorganization and disruption of actin cytoskeleton through PI 3-kinase, Rho, and Cdc42 in corneal endothelial cells. *Mol Vis,* 9**,** 624-34.

LEFEBVRE, V., HUANG, W., HARLEY, V. R., GOODFELLOW, P. N. & DE CROMBRUGGHE, B. 1997. SOX9 is a potent activator of the chondrocyte-specific enhancer of the pro alpha1(II) collagen gene. *Mol Cell Biol,* 17**,** 2336-46.

LI, T. X., YUAN, J., CHEN, Y., PAN, L. J., SONG, C., BI, L. J. & JIAO, X. H. 2013. Differentiation of mesenchymal stem cells from human umbilical cord tissue into odontoblast-like cells using the conditioned medium of tooth germ cells in vitro. *Biomed Res Int,* 2013**,** 218543.

LI, Y., LI, J., ZHU, S., LUO, E., FENG, G., CHEN, Q. & HU, J. 2012. Effects of strontium on proliferation and differentiation of rat bone marrow mesenchymal stem cells. *Biochem Biophys Res Commun,* 418**,** 725-30.

LI, Z. Y., CHEN, L., LIU, L., LIN, Y. F., LI, S. W. & TIAN, W. D. 2007. Odontogenic potential of bone marrow mesenchymal stem cells. *J Oral Maxillofac Surg,* 65**,** 494-500.

LIAN, J. B., JAVED, A., ZAIDI, S. K., LENGNER, C., MONTECINO, M., VAN WIJNEN, A. J., STEIN, J. L. & STEIN, G. S. 2004. Regulatory controls for osteoblast growth and differentiation: role of Runx/Cbfa/AML factors. *Crit Rev Eukaryot Gene Expr,* 14**,** 1-41.

LIAN, J. B. & STEIN, G. S. 1995. Development of the osteoblast phenotype: molecular mechanisms mediating osteoblast growth and differentiation. *Iowa Orthop J,* 15**,** 118-40.

LIU, F., MALAVAL, L., GUPTA, A. K. & AUBIN, J. E. 1994. Simultaneous detection of multiple bone-related mRNAs and protein expression during osteoblast differentiation: polymerase chain reaction and immunocytochemical studies at the single cell level. *Dev Biol,* 166**,** 220-34.

LIU, Y. H., TANG, Z., KUNDU, R. K., WU, L., LUO, W., ZHU, D., SANGIORGI, F., SNEAD, M. L. & MAXSON, R. E. 1999. Msx2 gene dosage influences the number of proliferative osteogenic cells in growth centers of the developing murine skull: a possible mechanism for MSX2-mediated craniosynostosis in humans. *Dev Biol,* 205**,** 260-74.

LIZIER, N. F., KERKIS, A., GOMES, C. M., HEBLING, J., OLIVEIRA, C. F., CAPLAN, A. I. & KERKIS, I. 2012. Scaling-up of dental pulp stem cells isolated from multiple niches. *PLoS One,* 7**,** e39885.

LOH, Y. H., WU, Q., CHEW, J. L., VEGA, V. B., ZHANG, W., CHEN, X., BOURQUE, G., GEORGE, J., LEONG, B., LIU, J., WONG, K. Y., SUNG, K. W., LEE, C. W., ZHAO, X. D., CHIU, K. P., LIPOVICH, L., KUZNETSOV, V. A., ROBSON, P., STANTON, L. W., WEI, C. L., RUAN, Y., LIM, B. & NG, H. H. 2006. The Oct4 and Nanog transcription network regulates pluripotency in mouse embryonic stem cells. *Nat Genet,* 38**,** 431-40.

LUMSDEN, A. G. 1988. Spatial organization of the epithelium and the role of neural crest cells in the initiation of the mammalian tooth germ. *Development,* 103 Suppl**,** 155-69.

LYNGSTADAAS, S. P., WOHLFAHRT, J. C., BROOKES, S. J., PAINE, M. L., SNEAD, M. L. & RESELAND, J. E. 2009. Enamel matrix proteins; old molecules for new applications. *Orthod Craniofac Res,* 12**,** 243-53.

MACLEAN, A. L., FILIPPI, S. & STUMPF, M. P. 2014. The ecology in the hematopoietic stem cell niche determines the clinical outcome in chronic myeloid leukemia. *Proc Natl Acad Sci U S A,* 111**,** 3883-8.

MALAVAKI, C., MIZUMOTO, S., KARAMANOS, N. & SUGAHARA, K. 2008. Recent advances in the structural study of functional chondroitin sulfate and dermatan sulfate in health and disease. *Connect Tissue Res,* 49**,** 133-9.

MALAVAL, L., WADE-GUEYE, N. M., BOUDIFFA, M., FEI, J., ZIRNGIBL, R., CHEN, F., LAROCHE, N., ROUX, J. P., BURT-PICHAT, B., DUBOEUF, F., BOIVIN, G., JURDIC, P., LAFAGE-PROUST, M. H., AMEDEE, J., VICO, L., ROSSANT, J. & AUBIN, J. E. 2008. Bone sialoprotein plays a functional role in bone formation and osteoclastogenesis. *J Exp Med,* 205**,** 1145-53.

MAO, J. J. & PROCKOP, D. J. 2012. Stem cells in the face: tooth regeneration and beyond. *Cell Stem Cell,* 11**,** 291-301.

MARR, E., TARDIE, M., CARTY, M., BROWN PHILLIPS, T., WANG, I. K., SOELLER, W., QIU, X. & KARAM, G. 2006. Expression, purification, crystallization and structure of human adipocyte lipid-binding protein (aP2). *Acta Crystallogr Sect F Struct Biol Cryst Commun,* 62**,** 1058-60.

MARTIN, G. M., SPRAGUE, C. A., NORWOOD, T. H. & PENDERGRASS, W. R. 1974. Clonal selection, attenuation and differentiation in an in vitro model of hyperplasia. *Am J Pathol,* 74**,** 137-54.

MARTIN-PIEDRA, M. A., GARZON, I., OLIVEIRA, A. C., ALFONSO-RODRIGUEZ, C. A., SANCHEZ-QUEVEDO, M. C., CAMPOS, A. & ALAMINOS, M. 2013. Average cell viability levels of human dental pulp stem cells: an accurate combinatorial index for quality control in tissue engineering. *Cytotherapy,* 15**,** 507-18.

MASHHADI ABBAS, F., SICHANI FALLAHI, H., KHOSHZABAN, A., MAHDAVI, N. & BAGHERI, S. S. 2013. Expression of odontogenic genes in human bone marrow mesenchymal stem cells. *Cell J,* 15**,** 136-41.

MATHIEU, P. S. & LOBOA, E. G. 2012. Cytoskeletal and focal adhesion influences on mesenchymal stem cell shape, mechanical properties, and differentiation down osteogenic, adipogenic, and chondrogenic pathways. *Tissue Eng Part B Rev,* 18**,** 436-44.

MATSUURA, T., DUARTE, W. R., CHENG, H., UZAWA, K. & YAMAUCHI, M. 2001. Differential expression of decorin and biglycan genes during mouse tooth development. *Matrix Biol,* 20**,** 367-73.

MECHAM, R. P. 2001. Overview of extracellular matrix. *Curr Protoc Cell Biol,* Chapter 10**,** Unit 10.1.

MERLINE, R., SCHAEFER, R. M. & SCHAEFER, L. 2009. The matricellular functions of small leucine-rich proteoglycans (SLRPs). *J Cell Commun Signal,* 3**,** 323-35.

METS, T. & VERDONK, G. 1981. In vitro aging of human bone marrow derived stromal cells. *Mech Ageing Dev,* 16**,** 81-9.

MINER, J. L., HAHN, K. J., SPURLOCK, M. E. & STATEN, N. R. 2001. Expression and complement d activity of porcine adipsin. *Protein Expr Purif,* 23**,** 14-21.

MIRON, R. J., WEI, L., BOSSHARDT, D. D., BUSER, D., SCULEAN, A. & ZHANG, Y. 2014. Effects of enamel matrix proteins in combination with a bovine-derived natural bone mineral for the repair of bone defects. *Clin Oral Investig,* 18**,** 471-8.

MIURA, M., GRONTHOS, S., ZHAO, M., LU, B., FISHER, L. W., ROBEY, P. G. & SHI, S. 2003. SHED: stem cells from human exfoliated deciduous teeth. *Proc Natl Acad Sci U S A,* 100**,** 5807-12.

MIURA, M., MIURA, Y., SONOYAMA, W., YAMAZA, T., GRONTHOS, S. & SHI, S. 2006. Bone marrow-derived mesenchymal stem cells for regenerative medicine in craniofacial region. *Oral Dis,* 12**,** 514-22.

MIZUNO, M. & KUBOKI, Y. 2001. Osteoblast-related gene expression of bone marrow cells during the osteoblastic differentiation induced by type I collagen. *J Biochem,* 129**,** 133-8.

MONTERO, A., OKADA, Y., TOMITA, M., ITO, M., TSURUKAMI, H., NAKAMURA, T., DOETSCHMAN, T., COFFIN, J. D. & HURLEY, M. M. 2000. Disruption of the

fibroblast growth factor-2 gene results in decreased bone mass and bone formation. *J Clin Invest,* 105**,** 1085-93.

MORRISON, S. J. & SCADDEN, D. T. 2014. The bone marrow niche for haematopoietic stem cells. *Nature,* 505**,** 327-34.

MORSCZECK, C., GOTZ, W., SCHIERHOLZ, J., ZEILHOFER, F., KUHN, U., MOHL, C., SIPPEL, C. & HOFFMANN, K. H. 2005. Isolation of precursor cells (PCs) from human dental follicle of wisdom teeth. *Matrix Biol,* 24**,** 155-65.

MURAGLIA, A., CANCEDDA, R. & QUARTO, R. 2000. Clonal mesenchymal progenitors from human bone marrow differentiate in vitro according to a hierarchical model. *J Cell Sci,* 113 (Pt 7)**,** 1161-6.

MURRAY, S. A., ORAM, K. F. & GRIDLEY, T. 2007. Multiple functions of Snail family genes during palate development in mice. *Development,* 134**,** 1789-97.

NAGANO, T., OIDA, S., ANDO, H., GOMI, K., ARAI, T. & FUKAE, M. 2003. Relative levels of mRNA encoding enamel proteins in enamel organ epithelia and odontoblasts. *J Dent Res,* 82**,** 982-6.

NAKASHIMA, K., ZHOU, X., KUNKEL, G., ZHANG, Z., DENG, J. M., BEHRINGER, R. R. & DE CROMBRUGGHE, B. 2002. The novel zinc finger-containing transcription factor osterix is required for osteoblast differentiation and bone formation. *Cell,* 108**,** 17-29.

NAKASHIMA, M., NAGASAWA, H., YAMADA, Y. & REDDI, A. H. 1994. Regulatory role of transforming growth factor-beta, bone morphogenetic protein-2, and protein-4 on gene expression of extracellular matrix proteins and differentiation of dental pulp cells. *Dev Biol,* 162**,** 18-28.

NEAME, P., J. & KAY, C., J. 2000. Small Leucine-Rich Proteoglycans. *In:* IOZZO, R., V. (ed.) *Proteoglycans Structure Biology and Molecular Interactions.* 1 ed. New York: Marcel Dekker, Inc.

NEUMANN, K., DEHNE, T., ENDRES, M., ERGGELET, C., KAPS, C., RINGE, J. & SITTINGER, M. 2008. Chondrogenic differentiation capacity of human mesenchymal progenitor cells derived from subchondral cortico-spongious bone. *J Orthop Res,* 26**,** 1449-56.

NILSSON, S. K., JOHNSTON, H. M., WHITTY, G. A., WILLIAMS, B., WEBB, R. J., DENHARDT, D. T., BERTONCELLO, I., BENDALL, L. J., SIMMONS, P. J. & HAYLOCK, D. N. 2005. Osteopontin, a key component of the hematopoietic stem cell niche and regulator of primitive hematopoietic progenitor cells. *Blood,* 106**,** 1232-9.

NOBLE, P. W., LAKE, F. R., HENSON, P. M. & RICHES, D. W. 1993. Hyaluronate activation of CD44 induces insulin-like growth factor-1 expression by a tumor necrosis factor-alpha-dependent mechanism in murine macrophages. *J Clin Invest,* 91**,** 2368-77.

NOZAKI, T. & OHURA, K. 2011. Gene expression profile of dental pulp cells during differentiation into an adipocyte lineage. *J Pharmacol Sci,* 115**,** 354-63.

NUSCHKE, A. 2013. Activity of mesenchymal stem cells in therapies for chronic skin wound healing. *Organogenesis.*

O'BRIEN, F. J. 2011. Biomaterials & scaffolds for tissue engineering. *Materials Today,* 14**,** 88-95.

OESSER, S. & SEIFERT, J. 2003. Stimulation of type II collagen biosynthesis and secretion in bovine chondrocytes cultured with degraded collagen. *Cell Tissue Res,* 311**,** 393-9.

OGATA, Y. 2008. Bone sialoprotein and its transcriptional regulatory mechanism. *J Periodontal Res,* 43**,** 127-35.

OKADA-IWABU, M., YAMAUCHI, T., IWABU, M., HONMA, T., HAMAGAMI, K., MATSUDA, K., YAMAGUCHI, M., TANABE, H., KIMURA-SOMEYA, T., SHIROUZU, M., OGATA, H., TOKUYAMA, K., UEKI, K., NAGANO, T., TANAKA, A., YOKOYAMA, S. & KADOWAKI, T. 2013. A small-molecule AdipoR agonist for type 2 diabetes and short life in obesity. *Nature,* 503**,** 493-9.

ONISHI, T., KINOSHITA, S., SHINTANI, S., SOBUE, S. & OOSHIMA, T. 1999. Stimulation of proliferation and differentiation of dog dental pulp cells in serum-free culture medium by insulin-like growth factor. *Arch Oral Biol,* 44**,** 361-71.

OREFFO, R. O., BORD, S. & TRIFFITT, J. T. 1998. Skeletal progenitor cells and ageing human populations. *Clin Sci (Lond),* 94**,** 549-55.

ORNITZ, D. M. 2005. FGF signaling in the developing endochondral skeleton. *Cytokine Growth Factor Rev,* 16**,** 205-13.

OTTO, F., THORNELL, A. P., CROMPTON, T., DENZEL, A., GILMOUR, K. C., ROSEWELL, I. R., STAMP, G. W., BEDDINGTON, R. S., MUNDLOS, S., OLSEN, B. R., SELBY, P. B. & OWEN, M. J. 1997. Cbfa1, a candidate gene for cleidocranial dysplasia syndrome, is essential for osteoblast differentiation and bone development. *Cell,* 89**,** 765-71.

OWEN, M. & FRIEDENSTEIN, A. J. 1988. Stromal stem cells: marrow-derived osteogenic precursors. *Ciba Found Symp,* 136**,** 42-60.

PAPACCIO, G., GRAZIANO, A., D'AQUINO, R., GRAZIANO, M. F., PIROZZI, G., MENDITTI, D., DE ROSA, A., CARINCI, F. & LAINO, G. 2006. Long-term cryopreservation of dental pulp stem cells (SBP-DPSCs) and their differentiated osteoblasts: a cell source for tissue repair. *J Cell Physiol,* 208**,** 319-25.

PARFITT, A. M. 1984. The cellular basis of bone remodeling: the quantum concept reexamined in light of recent advances in the cell biology of bone. *Calcif Tissue Int,* 36 Suppl 1**,** S37-45.

PATT, H. M. & MALONEY, M. A. 1975. Bone marrow regeneration after local injury: a review. *Exp Hematol,* 3**,** 135-48.

PELLEGRINI, G., GOLISANO, O., PATERNA, P., LAMBIASE, A., BONINI, S., RAMA, P. & DE LUCA, M. 1999. Location and clonal analysis of stem cells and their differentiated progeny in the human ocular surface. *J Cell Biol,* 145**,** 769-82.

PENC, S. F., POMAHAC, B., ERIKSSON, E., DETMAR, M. & GALLO, R. L. 1999. Dermatan sulfate activates nuclear factor-kappab and induces endothelial and circulating intercellular adhesion molecule-1. *J Clin Invest,* 103**,** 1329-35.

PENC, S. F., POMAHAC, B., WINKLER, T., DORSCHNER, R. A., ERIKSSON, E., HERNDON, M. & GALLO, R. L. 1998. Dermatan sulfate released after injury is a potent promoter of fibroblast growth factor-2 function. *J Biol Chem,* 273**,** 28116-21.

PENG, L., JIA, Z., YIN, X., ZHANG, X., LIU, Y., CHEN, P., MA, K. & ZHOU, C. 2008. Comparative analysis of mesenchymal stem cells from bone marrow, cartilage, and adipose tissue. *Stem Cells Dev,* 17**,** 761-73.

PIERRET, C., SPEARS, K., MARUNIAK, J. A. & KIRK, M. D. 2006. Neural crest as the source of adult stem cells. *Stem Cells Dev,* 15**,** 286-91.

PITTENGER, M. F., MACKAY, A. M., BECK, S. C., JAISWAL, R. K., DOUGLAS, R., MOSCA, J. D., MOORMAN, M. A., SIMONETTI, D. W., CRAIG, S. & MARSHAK, D. R. 1999. Multilineage potential of adult human mesenchymal stem cells. *Science,* 284**,** 143-7.

POTTEN, C. S. & LOEFFLER, M. 1990. Stem cells: attributes, cycles, spirals, pitfalls and uncertainties. Lessons for and from the crypt. *Development,* 110**,** 1001-20.

PRISELL, P. T., EDWALL, D., LINDBLAD, J. B., LEVINOVITZ, A. & NORSTEDT, G. 1993. Expression of insulin-like growth factors during bone induction in rat. *Calcif Tissue Int,* 53**,** 201-5.

PROCKOP, D. J. 1997. Marrow stromal cells as stem cells for nonhematopoietic tissues. *Science,* 276**,** 71-4.

QIAN, H., LE BLANC, K. & SIGVARDSSON, M. 2012. Primary mesenchymal stem and progenitor cells from bone marrow lack expression of CD44 protein. *J Biol Chem,* 287**,** 25795-807.

QIN, C., BRUNN, J. C., CADENA, E., RIDALL, A., TSUJIGIWA, H., NAGATSUKA, H., NAGAI, N. & BUTLER, W. T. 2002. The expression of dentin sialophosphoprotein gene in bone. *J Dent Res,* 81**,** 392-4.

RAHEMTULLA, F., PRINCE, C. W. & BUTLER, W. T. 1984. Isolation and partial characterization of proteoglycans from rat incisors. *Biochem J,* 218**,** 877-85.

REINHOLT, F. P., HULTENBY, K., OLDBERG, A. & HEINEGARD, D. 1990. Osteopontin--a possible anchor of osteoclasts to bone. *Proc Natl Acad Sci U S A,* 87**,** 4473-5.

REN, G., ZHAO, X., ZHANG, L., ZHANG, J., L'HUILLIER, A., LING, W., ROBERTS, A. I., LE, A. D., SHI, S., SHAO, C. & SHI, Y. 2010. Inflammatory cytokine-induced intercellular adhesion molecule-1 and vascular cell adhesion molecule-1 in mesenchymal stem cells are critical for immunosuppression. *J Immunol,* 184**,** 2321-8.

REYA, T., MORRISON, S. J., CLARKE, M. F. & WEISSMAN, I. L. 2001. Stem cells, cancer, and cancer stem cells. *Nature,* 414**,** 105-11.

RIQUELME, P. A., DRAPEAU, E. & DOETSCH, F. 2008. Brain micro-ecologies: neural stem cell niches in the adult mammalian brain. *Philos Trans R Soc Lond B Biol Sci,* 363**,** 123-37.

ROBEY, P. G. 1996. Vertebrate mineralized matrix proteins: structure and function. *Connect Tissue Res,* 35**,** 131-6.

RONTI, T., LUPATTELLI, G. & MANNARINO, E. 2006. The endocrine function of adipose tissue: an update. *Clin Endocrinol (Oxf),* 64**,** 355-65.

ROSEN, E. D. & MACDOUGALD, O. A. 2006. Adipocyte differentiation from the inside out. *Nat Rev Mol Cell Biol,* 7**,** 885-96.

RUSTER, B., GOTTIG, S., LUDWIG, R. J., BISTRIAN, R., MULLER, S., SEIFRIED, E., GILLE, J. & HENSCHLER, R. 2006. Mesenchymal stem cells display coordinated rolling and adhesion behavior on endothelial cells. *Blood,* 108**,** 3938-44.

SAELY, C. H., GEIGER, K. & DREXEL, H. 2012. Brown versus white adipose tissue: a mini-review. *Gerontology,* 58**,** 15-23.

SATOKATA, I. & MAAS, R. 1994. Msx1 deficient mice exhibit cleft palate and abnormalities of craniofacial and tooth development. *Nat Genet,* 6**,** 348-56.

SATOMURA, K., KREBSBACH, P., BIANCO, P. & GEHRON ROBEY, P. 2000. Osteogenic imprinting upstream of marrow stromal cell differentiation. *J Cell Biochem,* 78**,** 391-403.

SCHMALZ, G., SCHUSTER, U., THONEMANN, B., BARTH, M. & ESTERBAUER, S. 2001. Dentin barrier test with transfected bovine pulp-derived cells. *J Endod,* 27**,** 96-102.

SEABERG, R. M. & VAN DER KOOY, D. 2003. Stem and progenitor cells: the premature desertion of rigorous definitions. *Trends Neurosci,* 26**,** 125-31.

SEARFOSS, G. H., JORDAN, W. H., CALLIGARO, D. O., GALBREATH, E. J., SCHIRTZINGER, L. M., BERRIDGE, B. R., GAO, H., HIGGINS, M. A., MAY, P. C. & RYAN, T. P. 2003. Adipsin, a biomarker of gastrointestinal toxicity mediated by a functional gamma-secretase inhibitor. *J Biol Chem,* 278**,** 46107-16.

SELL, S. 2004. *Stem Cells Handbook,* Totowa, New Jersey, Humana Press.

SEO, B. M., MIURA, M., GRONTHOS, S., BARTOLD, P. M., BATOULI, S., BRAHIM, J., YOUNG, M., ROBEY, P. G., WANG, C. Y. & SHI, S. 2004. Investigation of multipotent postnatal stem cells from human periodontal ligament. *Lancet,* 364**,** 149-55.

SEONG, J. M., KIM, B. C., PARK, J. H., KWON, I. K., MANTALARIS, A. & HWANG, Y. S. 2010. Stem cells in bone tissue engineering. *Biomed Mater,* 5**,** 062001.

SHAO, M. Y., FU, Z. S., CHENG, R., YANG, H., CHENG, L., WANG, F. M. & HU, T. 2011. The presence of open dentinal tubules affects the biological properties of dental pulp cells ex vivo. *Mol Cells,* 31**,** 65-71.

SHI, S. & GRONTHOS, S. 2003. Perivascular niche of postnatal mesenchymal stem cells in human bone marrow and dental pulp. *J Bone Miner Res,* 18**,** 696-704.

SHI, S., ROBEY, P. G. & GRONTHOS, S. 2001. Comparison of human dental pulp and bone marrow stromal stem cells by cDNA microarray analysis. *Bone,* 29**,** 532-9.

SHIBA, H., FUJITA, T., DOI, N., NAKAMURA, S., NAKANISHI, K., TAKEMOTO, T., HINO, T., NOSHIRO, M., KAWAMOTO, T., KURIHARA, H. & KATO, Y. 1998. Differential effects of various growth factors and cytokines on the syntheses of DNA, type I collagen,

laminin, fibronectin, osteonectin/secreted protein, acidic and rich in cysteine (SPARC), and alkaline phosphatase by human pulp cells in culture. *J Cell Physiol,* 174**,** 194-205.

SHIBATA, K. R., AOYAMA, T., SHIMA, Y., FUKIAGE, K., OTSUKA, S., FURU, M., KOHNO, Y., ITO, K., FUJIBAYASHI, S., NEO, M., NAKAYAMA, T., NAKAMURA, T. & TOGUCHIDA, J. 2007. Expression of the p16INK4A gene is associated closely with senescence of human mesenchymal stem cells and is potentially silenced by DNA methylation during in vitro expansion. *Stem Cells,* 25**,** 2371-82.

SHIMIZU, Y., VAN SEVENTER, G. A., HORGAN, K. J. & SHAW, S. 1990. Roles of adhesion molecules in T-cell recognition: fundamental similarities between four integrins on resting human T cells (LFA-1, VLA-4, VLA-5, VLA-6) in expression, binding, and costimulation. *Immunol Rev,* 114**,** 109-43.

SHIMIZU-HIROTA, R., SASAMURA, H., KURODA, M., KOBAYASHI, E., HAYASHI, M. & SARUTA, T. 2004. Extracellular matrix glycoprotein biglycan enhances vascular smooth muscle cell proliferation and migration. *Circ Res,* 94**,** 1067-74.

SHIRAKIHARA, T., HORIGUCHI, K., MIYAZAWA, K., EHATA, S., SHIBATA, T., MORITA, I., MIYAZONO, K. & SAITOH, M. 2011. TGF-beta regulates isoform switching of FGF receptors and epithelial-mesenchymal transition. *Embo J,* 30**,** 783-95.

SILVA, F. J., HOLT, D. J., VARGAS, V., YOCKMAN, J., BOUDINA, S., ATKINSON, D., GRAINGER, D. W., REVELO, M. P., SHERMAN, W., BULL, D. A. & PATEL, A. N. 2014. Metabolically active human brown adipose tissue derived stem cells. *Stem Cells,* 32**,** 572-81.

SLOAN, A. J. & WADDINGTON, R. J. 2009. Dental pulp stem cells: what, where, how? *Int J Paediatr Dent,* 19**,** 61-70.

SMITH, A. J., CASSIDY, N., PERRY, H., BEGUE-KIRN, C., RUCH, J. V. & LESOT, H. 1995. Reactionary dentinogenesis. *Int J Dev Biol,* 39**,** 273-80.

SMITH, J. R., PEREIRA-SMITH, O. M. & SCHNEIDER, E. L. 1978. Colony size distributions as a measure of in vivo and in vitro aging. *Proc Natl Acad Sci U S A,* 75**,** 1353-6.

SODEK, J., CHEN, J., NAGATA, T., KASUGAI, S., TODESCAN, R., JR., LI, I. W. & KIM, R. H. 1995. Regulation of osteopontin expression in osteoblasts. *Ann N Y Acad Sci,* 760**,** 223-41.

SODEK, J., GANSS, B. & MCKEE, M. D. 2000. Osteopontin. *Crit Rev Oral Biol Med,* 11**,** 279-303.

SONOYAMA, W., LIU, Y., FANG, D., YAMAZA, T., SEO, B. M., ZHANG, C., LIU, H., GRONTHOS, S., WANG, C. Y., WANG, S. & SHI, S. 2006. Mesenchymal stem cell-mediated functional tooth regeneration in swine. *PLoS One,* 1**,** e79.

SPRADLING, A., DRUMMOND-BARBOSA, D. & KAI, T. 2001. Stem cells find their niche. *Nature,* 414**,** 98-104.

STACEY, G. 2012. Banking stem cells for research and clinical applications. *Prog Brain Res,* 200**,** 41-58.

STAINES, K. A., MACRAE, V. E. & FARQUHARSON, C. 2012. The importance of the SIBLING family of proteins on skeletal mineralisation and bone remodelling. *J Endocrinol,* 214**,** 241-55.

STENDERUP, K., JUSTESEN, J., CLAUSEN, C. & KASSEM, M. 2003. Aging is associated with decreased maximal life span and accelerated senescence of bone marrow stromal cells. *Bone,* 33**,** 919-26.

STEPHENS, P., COOK, H., HILTON, J., JONES, C. J., HAUGHTON, M. F., WYLLIE, F. S., SKINNER, J. W., HARDING, K. G., KIPLING, D. & THOMAS, D. W. 2003. An analysis of replicative senescence in dermal fibroblasts derived from chronic leg wounds predicts that telomerase therapy would fail to reverse their disease-specific cellular and proteolytic phenotype. *Exp Cell Res,* 283**,** 22-35.

SU, N., DU, X. & CHEN, L. 2008. FGF signaling: its role in bone development and human skeleton diseases. *Front Biosci,* 13**,** 2842-65.

SUGARS, R. V., MILAN, A. M., BROWN, J. O., WADDINGTON, R. J., HALL, R. C. & EMBERY, G. 2003. Molecular interaction of recombinant decorin and biglycan with type I collagen influences crystal growth. *Connect Tissue Res,* 44 Suppl 1**,** 189-95.

SUN, Y., LU, Y., CHEN, L., GAO, T., D'SOUZA, R., FENG, J. Q. & QIN, C. 2011. DMP1 processing is essential to dentin and jaw formation. *J Dent Res,* 90**,** 619-24.

SUZUKI, S., LI, A. J., IKEMOTO, M. & IMAMURA, T. 2002. Expression of tenascin-C long isoforms is induced in the hypothalamus by FGF-1. *Neuroreport,* 13**,** 1041-5.

SUZUKI-INOUE, K., FULLER, G. L., GARCIA, A., EBLE, J. A., POHLMANN, S., INOUE, O., GARTNER, T. K., HUGHAN, S. C., PEARCE, A. C., LAING, G. D., THEAKSTON, R. D., SCHWEIGHOFFER, E., ZITZMANN, N., MORITA, T., TYBULEWICZ, V. L., OZAKI, Y. & WATSON, S. P. 2006. A novel Syk-dependent mechanism of platelet activation by the C-type lectin receptor CLEC-2. *Blood,* 107**,** 542-9.

TAKAHASHI, K., TANABE, K., OHNUKI, M., NARITA, M., ICHISAKA, T., TOMODA, K. & YAMANAKA, S. 2007. Induction of pluripotent stem cells from adult human fibroblasts by defined factors. *Cell,* 131**,** 861-72.

TAKAHASHI, K. & YAMANAKA, S. 2006. Induction of pluripotent stem cells from mouse embryonic and adult fibroblast cultures by defined factors. *Cell,* 126**,** 663-76.

TAMAMA, K., FAN, V. H., GRIFFITH, L. G., BLAIR, H. C. & WELLS, A. 2006. Epidermal growth factor as a candidate for ex vivo expansion of bone marrow-derived mesenchymal stem cells. *Stem Cells,* 24**,** 686-95.

TAMAMA, K., KAWASAKI, H. & WELLS, A. 2010. Epidermal growth factor (EGF) treatment on multipotential stromal cells (MSCs). Possible enhancement of therapeutic potential of MSC. *J Biomed Biotechnol,* 2010**,** 795385.

TEN CATE, A., R. 1994. *Oral Histology,* USA, Mosby- Year Book, Inc.

TERAI, K., TAKANO-YAMAMOTO, T., OHBA, Y., HIURA, K., SUGIMOTO, M., SATO, M., KAWAHATA, H., INAGUMA, N., KITAMURA, Y. & NOMURA, S. 1999. Role of

osteopontin in bone remodeling caused by mechanical stress. *J Bone Miner Res,* 14**,** 839-49.

THEOCHARIS, A. D., KARAMANOS, N. K., PAPAGEORGAKOPOULOU, N., TSIGANOS, C. P. & THEOCHARIS, D. A. 2002. Isolation and characterization of matrix proteoglycans from human nasal cartilage. Compositional and structural comparison between normal and scoliotic tissues. *Biochim Biophys Acta,* 1569**,** 117-26.

TOJKANDER, S., GATEVA, G. & LAPPALAINEN, P. 2012. Actin stress fibers--assembly, dynamics and biological roles. *J Cell Sci,* 125**,** 1855-64.

TOKUNAGA, A., OYA, T., ISHII, Y., MOTOMURA, H., NAKAMURA, C., ISHIZAWA, S., FUJIMORI, T., NABESHIMA, Y., UMEZAWA, A., KANAMORI, M., KIMURA, T. & SASAHARA, M. 2008. PDGF receptor beta is a potent regulator of mesenchymal stromal cell function. *J Bone Miner Res,* 23**,** 1519-28.

TROKOVIC, N., TROKOVIC, R., MAI, P. & PARTANEN, J. 2003. Fgfr1 regulates patterning of the pharyngeal region. *Genes Dev,* 17**,** 141-53.

TURNBULL, J. E., FERNIG, D. G., KE, Y., WILKINSON, M. C. & GALLAGHER, J. T. 1992. Identification of the basic fibroblast growth factor binding sequence in fibroblast heparan sulfate. *J Biol Chem,* 267**,** 10337-41.

TZIAFAS, D. & KOLOKURIS, I. 1990. Inductive influences of demineralized dentin and bone matrix on pulp cells: an approach of secondary dentinogenesis. *J Dent Res,* 69**,** 75-81.

URIST, M. R. 1965. Bone: formation by autoinduction. *Science,* 150**,** 893-9.

VETTER, U., VOGEL, W., JUST, W., YOUNG, M. F. & FISHER, L. W. 1993. Human decorin gene: intron-exon junctions and chromosomal localization. *Genomics,* 15**,** 161-8.

VINCENT, T., HERMANSSON, M., BOLTON, M., WAIT, R. & SAKLATVALA, J. 2002. Basic FGF mediates an immediate response of articular cartilage to mechanical injury. *Proc Natl Acad Sci U S A,* 99**,** 8259-64.

WADA, N., MENICANIN, D., SHI, S., BARTOLD, P. M. & GRONTHOS, S. 2009. Immunomodulatory properties of human periodontal ligament stem cells. *J Cell Physiol,* 219**,** 667-76.

WADDINGTON, R. J., HALL, R. C., EMBERY, G. & LLOYD, D. M. 2003a. Changing profiles of proteoglycans in the transition of predentine to dentine. *Matrix Biol,* 22**,** 153-61.

WADDINGTON, R. J., ROBERTS, H. C., SUGARS, R. V. & SCHONHERR, E. 2003b. Differential roles for small leucine-rich proteoglycans in bone formation. *Eur Cell Mater,* 6**,** 12-21; discussion 21.

WADDINGTON, R. J., YOUDE, S. J., LEE, C. P. & SLOAN, A. J. 2009. Isolation of distinct progenitor stem cell populations from dental pulp. *Cells Tissues Organs,* 189**,** 268-74.

WAN, M. & CAO, X. 2005. BMP signaling in skeletal development. *Biochem Biophys Res Commun,* 328**,** 651-7.

WANG, W., RIGUEUR, D. & LYONS, K. M. 2014. TGFbeta signaling in cartilage development and maintenance. *Birth Defects Res C Embryo Today,* 102**,** 37-51.

WATSON, S. P. & GIBBINS, J. 1998. Collagen receptor signalling in platelets: extending the role of the ITAM. *Immunol Today,* 19**,** 260-4.

WATT, F. M., KUBLER, M. D., HOTCHIN, N. A., NICHOLSON, L. J. & ADAMS, J. C. 1993. Regulation of keratinocyte terminal differentiation by integrin-extracellular matrix interactions. *J Cell Sci,* 106 (Pt 1)**,** 175-82.

WEBER, C. K., SOMMER, G., MICHL, P., FENSTERER, H., WEIMER, M., GANSAUGE, F., LEDER, G., ADLER, G. & GRESS, T. M. 2001. Biglycan is overexpressed in pancreatic cancer and induces G1-arrest in pancreatic cancer cell lines. *Gastroenterology,* 121**,** 657-67.

WELLS, A. 1999. EGF receptor. *Int J Biochem Cell Biol,* 31**,** 637-43.

WESTENDORF, J. J., KAHLER, R. A. & SCHROEDER, T. M. 2004. Wnt signaling in osteoblasts and bone diseases. *Gene,* 341**,** 19-39.

WESZL, M., SKALICZKI, G., CSELENYAK, A., KISS, L., MAJOR, T., SCHANDL, K., BOGNAR, E., STADLER, G., PETERBAUER, A., CSONGE, L. & LACZA, Z. 2012. Freeze-dried human serum albumin improves the adherence and proliferation of mesenchymal stem cells on mineralized human bone allografts. *J Orthop Res,* 30**,** 489-96.

WUTTKE, M., MULLER, S., NITSCHE, D. P., PAULSSON, M., HANISCH, F. G. & MAURER, P. 2001. Structural characterization of human recombinant and bone-derived bone sialoprotein. Functional implications for cell attachment and hydroxyapatite binding. *J Biol Chem,* 276**,** 36839-48.

XU, T., BIANCO, P., FISHER, L. W., LONGENECKER, G., SMITH, E., GOLDSTEIN, S., BONADIO, J., BOSKEY, A., HEEGAARD, A. M., SOMMER, B., SATOMURA, K., DOMINGUEZ, P., ZHAO, C., KULKARNI, A. B., ROBEY, P. G. & YOUNG, M. F. 1998. Targeted disruption of the biglycan gene leads to an osteoporosis-like phenotype in mice. *Nat Genet,* 20**,** 78-82.

XUAN, D., SUN, X., YAN, Y., XIE, B., XU, P. & ZHANG, J. 2010. Effect of cleidocranial dysplasia-related novel mutation of RUNX2 on characteristics of dental pulp cells and tooth development. *J Cell Biochem,* 111**,** 1473-81.

YE, L., MACDOUGALL, M., ZHANG, S., XIE, Y., ZHANG, J., LI, Z., LU, Y., MISHINA, Y. & FENG, J. Q. 2004. Deletion of dentin matrix protein-1 leads to a partial failure of maturation of predentin into dentin, hypomineralization, and expanded cavities of pulp and root canal during postnatal tooth development. *J Biol Chem,* 279**,** 19141-8.

YOSHIDA, A., ANAND-APTE, B. & ZETTER, B. R. 1996. Differential endothelial migration and proliferation to basic fibroblast growth factor and vascular endothelial growth factor. *Growth Factors,* 13**,** 57-64.

YU, J., DENG, Z., SHI, J., ZHAI, H., NIE, X., ZHUANG, H., LI, Y. & JIN, Y. 2006. Differentiation of dental pulp stem cells into regular-shaped dentin-pulp complex induced by tooth germ cell conditioned medium. *Tissue Eng,* 12**,** 3097-105.

ZHANG, C. 2012. Molecular mechanisms of osteoblast-specific transcription factor Osterix effect on bone formation. *Beijing Da Xue Xue Bao,* 44**,** 659-65.

ZHANG, L., YUAN, G., LIU, H., LIN, H., WAN, C. & CHEN, Z. 2012. Expression pattern of Sox2 during mouse tooth development. *Gene Expr Patterns,* 12**,** 273-81.

ZHANG, W., WALBOOMERS, X. F., SHI, S., FAN, M. & JANSEN, J. A. 2006. Multilineage differentiation potential of stem cells derived from human dental pulp after cryopreservation. *Tissue Eng,* 12**,** 2813-23.

ZHANG, X., HIRAI, M., CANTERO, S., CIUBOTARIU, R., DOBRILA, L., HIRSH, A., IGURA, K., SATOH, H., YOKOMI, I., NISHIMURA, T., YAMAGUCHI, S., YOSHIMURA, K., RUBINSTEIN, P. & TAKAHASHI, T. A. 2011. Isolation and characterization of mesenchymal stem cells from human umbilical cord blood: reevaluation of critical factors for successful isolation and high ability to proliferate and differentiate to chondrocytes as compared to mesenchymal stem cells from bone marrow and adipose tissue. *J Cell Biochem,* 112**,** 1206-18.

ZHENG, X., BAKER, H., HANCOCK, W. S., FAWAZ, F., MCCAMAN, M. & PUNGOR, E., JR. 2006. Proteomic analysis for the assessment of different lots of fetal bovine serum as a raw material for cell culture. Part IV. Application of proteomics to the manufacture of biological drugs. *Biotechnol Prog,* 22**,** 1294-300.

ZHU, A. J., HAASE, I. & WATT, F. M. 1999. Signaling via beta1 integrins and mitogen-activated protein kinase determines human epidermal stem cell fate in vitro. *Proc Natl Acad Sci U S A,* 96**,** 6728-33.

ZHU, W., TAN, Y., QIU, Q., LI, X., HUANG, Z., FU, Y. & LIANG, M. 2013. Comparison of the properties of human CD146+ and CD146- periodontal ligament cells in response to stimulation with tumour necrosis factor alpha. *Arch Oral Biol,* 58**,** 1791-803.

ZOU, C., CHOU, B. K., DOWEY, S. N., TSANG, K., HUANG, X., LIU, C. F., SMITH, C., YEN, J., MALI, P., ZHANG, Y. A., CHENG, L. & YE, Z. 2012. Efficient derivation and genetic modifications of human pluripotent stem cells on engineered human feeder cell lines. *Stem Cells Dev,* 21**,** 2298-311.

ZUK, P. A., ZHU, M., ASHJIAN, P., DE UGARTE, D. A., HUANG, J. I., MIZUNO, H., ALFONSO, Z. C., FRASER, J. K., BENHAIM, P. & HEDRICK, M. H. 2002. Human adipose tissue is a source of multipotent stem cells. *Mol Biol Cell,* 13**,** 4279-95.